SALES, MARCELO

AN NMR STUDY OF THE INCLUSION GEOMETRIES OF STEROID-CYCLODEXTRIN COMPLEXES

MSc UP 1997

An NMR study of the inclusion geometries of steroid-cyclodextrin complexes

A dissertation submitted by

Marcelo Sales

In partial fulfilment of the requirements for the degree

Magister Scientiae

In the Faculty of Science
University of Pretoria
Pretoria

January 1997

An NMR study of the inclusion geometries of steroid-cyclodextrin complexes

Candidate: **Marcelo Sales**

Promoter: **Professor P.L. Wessels**

Department of Chemistry, University of Pretoria

Degree: **Magister Scientiae**

Summary

The inclusion geometries formed by the three water insoluble steroids (cyproterone acetate, ethynyl oestradiol and danazol) with β- and γ-cyclodextrin were determined with the use of NMR experiments and molecular modelling. Observed intermolecular nuclear Overhauser effects (NOE's) were used to obtain qualitative distance constraints between the protons of the steroid and cyclodextrin. The inclusion geometries of the complexes were modelled using these distance constraints.

The steroid-cyclodextrin complexes were prepared in D_2O by a kneading and a sonication method. Both methods afforded equivalent concentrations of complex. The concentration of steroid-cyclodextrin complex is independant of the method of preparation. The concentration is only dependant on the stability constant K which is a measure of the tendency of a complex to dissociate in the presence of water. The concentrations of the cyproterone acetate- and danazol-β-cyclodextrin and the cyproterone acetate- and ethynyl oestradiol-γ-cyclodextrin complexes facilitated an NMR study. The ethynyl oestradiol-β-cyclodextrin complex was poorly water soluble and this complex with a stoichiometry of 1:2 (steroid:cyclodextrin) was isolated. The poor solubility of the ethynyl oestradiol-β-cyclodextrin complex in D_2O prevented a thorough NMR investigation. The concentration of this complex was increased by preparing it in a 1:2 (v/v) mixture of DMSO-d_6 and D_2O. The observation of NOE's between the proton atoms of ethynyl oestradiol and β-cyclodextrin proved that ethynyl oestradiol-β-cyclodextrin complex exists in the 1:2 mixture despite the fact that pure DMSO-d_6 prevents complex formation. The

danazol-γ-cyclodextrin complex was water insoluble. The concentration of this complex is increased when it is prepared in a 1:2 mixture of DMSO-d_6 and D_2O.

Two different inclusion geometries were identified for all the steroid-cyclodextrin complexes. One geometry has the A-ring of the steroid inserted into the cyclodextrin cavity and the other has the D-ring inserted into the cavity. The inclusion of the A-ring results in the formation of a binary complex. The formation of this binary complex is postulated as the solubilising step. The inclusion geometry where the D-ring is inserted into the cavity is most likely obtained from a ternary complex where the A- and D-rings are both capped by a cyclodextrin.

γ-Cyclodextrin solubilised a larger amount of cyproterone acetate than β-cyclodextrin. This increase in solubility occured alongside an increase in the depth of insertion of the A-ring of cyproterone acetate into the γ-cyclodextrin cavity relative to the insertion into β-cyclodextrin cavity.

The fact that γ-cyclodextrin solubilised ethynyl oestradiol better and that the danazol-γ-cyclodextrin complex exists in a mixture which contains the destabilising DMSO-d_6 solvent proves that both the ethynyl oestradiol- and danazol-γ-cyclodextrin complexes are stable. This stability is attributed to favourable entropic contributions towards complex formation which arise as a result of the high mobilites which ethynyl oestradiol and danazol have within the γ-cyclodextrin cavity.

Samevatting

Die insluitingsgeometrië van die komplekse gevorm deur die drie nie water oplosbare steroïde (siproteroonasetaat, etynielestradiol en danasol) met β- en γ-siklodekstrien is bepaal met behulp van KMR eksperimente en molekulêre modelering. Waargeneemde intermolekulêre kern Overhauser effekte is gebriuk om kwalitatiewe afstandsbeperkings tussen die protone van die steroïed en siklodekstrien te bepaal. Die insluitingsgeometrië van die komplekse is gemodelleer deur van hierdie afstandsbeperkings gebruik te maak.

Die steroïed-siklodekstrien komplekse is in D_2O met behulp van n knie en 'n sonikasie metode berei. Dieselfde konsentrasies kompleks is vanaf albei metodes verkry. Die konsentrasie van die steroïed-siklodekstrien komplekse in D_2O is onafhanklik van die voorbereidingsmetode en slegs van die stabiliteitskonstante, K, afhanklik. Die stabiliteitskonstante is 'n maatstaf vir die neiging van 'n kompleks om in water te dissosieer. Die konsentrasies van die siproteroonasetaat- en danasol-β-siklodekstrien en die siproteroonasetaat- en etynielestradiol-γ-siklodekstrien komplekse was voldoende oplosbaar in D_2O om 'n deeglike KMR studie te bevorder. Die etyniel oestradiol-β-siklodekstrien kompleks is swak water oplosbaar en die kompleks, met a stoichiometrie van 1:2 (steroïed:siklodekstrien), is geïsoleer. Die swak oplosbaarheid van die etyniel oestradiol-β-siklodekstrien kompleks maak 'n deeglike KMR ondersoek onmoontlik. Die konsentrasie van hierdie kompleks is verhoog deur dit in 'n 1:2 (v/v) mengsel van DMSO-d_6 en D_2O te berei. Die waarneming van kern Overhauser effekte tussen die proton atome van etyniel en β-siklodekstrien bewys dat die etyniel oestradiol-β-siklodekstrien kompleks wel in hierdie mengsel bestaan ten spyte van die feit dat suiwer DMSO-d_6 kompleks vormasie verhoud. Die danasol-γ-siklodekstrien kompleks is water onoplosbaar. Die konsentrasie van hierdie kompleks verhoog deur dit in 'n 1:2 mengsel van DMSO-d_6 en D_2O te berei.

Twee verskillende insluitingsgeometrië is vir die steroïed-siklodekstrien komplekse geïdentifiseer. In een geometrie voeg die A-ring van die steroïed in die siklodekstrien holte in en in die ander geometrie voeg die D-ring in die holte in. Die invoeging van die A-ring veroorsaak die vorming van 'n binêre kompleks. Die vorming van die binêre kompleks is gepostuleer as die oplossings-stap. Die insluitingsgeometrie waar die D-ring in die siklodekstrien holte ingevoeg is, word waarkynlik verkry vanaf 'n tersiêre kompleks waar albei die A- en

D-ringe met 'n siklodekstrien gekomplekseerd is.

γ-Siklodekstrien het 'n groter oplosbaarheidsvermoë vir siproteroonasetaat as β-siklodekstrien. Hierdie verhoging in oplosbaarheid gaan gepaard met 'n verhoging in die diepte van invoeging van die A-ring van siproteroonasetaat in die holte van γ-silkodekstrien in vergelyking met invoeging in die holte van β-siklodekstrien.

Die feit dat γ-siklodekstrien meer etynielestradiol oplos en dat die danasol-γ-siklodekstrien kompleks nogsteeds bestaan in 'n oplossing wat die destabiliserende DMSO-d_6 bevat bewys dat albei die etyniel oestradiol- en danasol-γ-siklodekstrien komplekse stabiel is. Hierdie stabiliteit is as gevolg van voordelige entropie bydrae tot kompleks vorming veroorsaak deur die hoë beweeglikheid van etyniel oestradiol en danasol binne-in die groter holte van γ-siklodekstrien.

Acknowledgements

I would like to express my gratitude to the following people who helped make this contribution possible:

To Julius my loving mother, to Helio my inspiring father and to Clara my grandmother who taught me discipline.

My Promoter, Professor P.L. Wessels for helping me overcome the phobia of NMR spectroscopy and most importantly for teaching a systematic approach towards problem solving.

To Mr. E.R. Palmer for teaching the zen of shimming.

To Dr. L.J. Penkler for his enthusiastic input.

To the Foundation for Research and Development, to the University of Pretoria and to South African Druggists for the use of their resources and financial support.

To the rest of my family and closest friends for their words of encouragement.

Marcelo

January 1997

The Nightingale and the Lark

What can one say to those writers who blithely fly far above the heads of most of their readers? The same, surely, as the nightingale said to the lark: My friend, are you soaring so high in order that your song cannot be heard?

Gotthold Ephraim Lessing

Contents

		Page
1	**Introduction**	
1.1	General introduction	1
1.2	The cyclodextrins	4
1.3	The driving forces of complex formation	6
1.4	The topology of inclusion complexes	8
1.5	Methods used to study inclusion complexes	12
1.5.1	The Calorimetric method	12
1.5.2	Nuclear Magnetic Resonance Spectroscopic methods	14
1.5.2.1	Determination of the stoichiometry of complexation	15
1.5.2.2	The use of Complexation Induced Shift (CIS) values to determine inclusion geometry	16
1.5.2.3	The use of the NOE to determine inclusion geometry	23
1.5.3	The use of computer molecular modelling to determine inclusion geometry	26
1.6	The aim and approach for the study of the steroid-cyclodextrin complexes	29
2	**Principle of two-dimensional NMR spectroscoy**	
2.1	Introduction	31
2.2	The mechanism of the 2-D NMR experiment	32
2.3	Heteronuclear shift-correlated NMR spectroscopy	36
2.4	Homonuclear shift-correlated NMR spectroscopy	41
2.5	The nuclear Overhauser effect	44
2.5.1	A 1-D NOE experiment	44
2.5.2	The 2-D NOESY experiment	50
2.5.3	The 2-D ROESY experiment	51
3	**The steroid assignments**	
3.1	Introduction	55
3.2	The assignment strategy	56

3.2.1	The Heteronuclear Multiple-Quantum Correlation (HMQC) experiment	58
3.2.2	The phase sensitive DQF-COSY experiment	59
3.2.3	Iterative spin-system analysis	61
3.2.4	The stereochemical assignments	61
3.2.4.1	Stereochemical assignments using coupling constants	62
3.2.4.2	Stereochemical assignments using the nuclear Overhauser effect	63
3.3	A complete assignment of the proton resonances of cyproterone acetate	65
3.3.1	The connectivity assignments	65
3.3.2	The stereochemical assignments	73
3.3.3	The assignment of the resonances to the protons of the methylene bridge	78
3.4	A summary	82
4	**The results of the NMR study of the steroid-cyclodextrin complexes**	
4.1	Introduction	91
4.2	A solubility study of the steroid-cyclodextrin complexes	91
4.2.1	Cyproterone acetate-β-cyclodextrin complex	93
4.2.2	Cyproterone acetate-γ-cyclodextrin complex	95
4.2.3	Ethynyl oestradiol-β-cyclodextrin complex	95
4.2.4	Ethynyl oestradiol-γ-cyclodextrin complex	98
4.2.5	Danazol-β-cyclodextrin complex	98
4.2.6	Danazol-γ-cyclodextrin complex	99
4.2.7	A comparison of the kneading and sonication methods	100
4.3	The chemical shift determination of the steroid-cyclodextrin complexes	101
4.4	The intermolecular NOE values of the steroid-cyclodextrin complexes	104
4.4.1	Cyproterone acetate-β-cyclodextrin complex	109
4.4.2	Cyproterone acetate-γ-cyclodextrin complex	114

4.4.3	Ethynyl oestradiol-β-cyclodextrin complex	116
4.4.4	Ethynyl oestradiol-γ-cyclodextrin complex	117
4.4.5	Danazol-β-cyclodextrin complex	117
4.4.6	Danazol-γ-cyclodextrin complex	118
4.5	Summary	131
5	**Modelling of the steroid-cyclodextrin complexes**	
5.1	Introduction	134
5.2	Modelling of the complexes using the intermolecular nuclear Overhauser effects	136
5.2.1	Cyproterone acetate-β-cyclodextrin complex	140
5.2.2	Cyproterone acetate-γ-cyclodextrin complex	144
5.2.3	Ethynyl oestradiol-β-cyclodextrin complex	146
5.2.4	Ethynyl oestradiol-γ-cyclodextrin complex	151
5.2.5	Danazol-β-cyclodextrin complex	159
5.2.6	Danazol-γ-cyclodextrin complex	161
5.3	The causes for the Δ chemical shift values	165
5.3.1	The Δ values of the cyproterone acetate-cyclodextrin complexes	166
5.3.2	The Δ values of the ethynyl oestradiol- and danazol-cyclodextrin complexes	168
5.4	Conclusion	170
5.4.1	Cyproterone acetate-cyclodextrin complexes	171
5.4.2	Ethynyl oestradiol- and danazol-cyclodextrin complexes	172
5.5	Future prospects	176
6	**Experimental**	
6.1	Materials	178
6.2	Sample preparation	178
6.2.1	The preparation of the steroid samples in $CDCl_3$	178
6.2.2	The preparation of the steroid-cyclodextrin complexes using the kneading method	178
6.2.2.1	The isolation procedure for obtaining a water-insoluble	179

	complex	
6.2.3	The preparation of the steroid-cyclodextrin complexes using sonication	180
6.3	Nuclear Magnetic Resonance Experiments	181
6.4	The Molecular Modelling methods	183
	References	185

1 Introduction

1.1 General introduction

The first evidence for the inclusion of a guest within the intramolecular cavity of a host was first reported in 1938. At that time, Freudenburg and Meyer-Delius[1] proposed that the formation of an adduct between iodine and cyclodextrins was a result of the inclusion of the iodine molecule into the cavity formed by the cyclodextrin ring. During his habilitation with Freudenburg at the end of the forties to the beginning of the fifties, Cramer[2] pioneered the research area which is now known as host-guest chemistry or molecular recognition. At that time he undertook the first systematic studies on the cavity inclusion complexation between cyclodextrins and organic guests in aqueous solution and in the solid state.

As one of the pioneers of molecular recognition, Cramer had to fight as a young man for his ideas and beliefs. Recently, Cramer[3] related the strength of opposition he met in 1948 as a young scientist when he first proposed the idea that a molecule even in solution can envelop another molecule, and more specifically, the conjecture that cyclodextrins form inclusion compounds even in solution. He reflected almost forty years later in 1987, 'When I presented my results for the first time at a meeting in Lindau, Lake Konstanz, I met fierce opposition from some parts of the establishment. One of my older (and very important) colleagues even stated publicly and bluntly in the discussion that he would try to remove a young man with such crazy ideas from the academic scene. But there was also a good number of supporters, so I finally made it'.[3]

The isolation and investigation of the properties of the cyclodextrins were the first experiments which laid down the foundations for host-guest chemistry. The cyclodextrins were first isolated in 1891 by Villiers[4] as degradation products of starch and they were characterised as cyclic oligosaccharides in 1904 by Schardinger[5]. It is for this reason that cyclodextrins (cycloamyloses) are described by some authors, especially in the older literature, as Schardinger dextrins. In 1938 Freudenburg et al[1] reported that cyclodextrins are constructed from $\alpha(1\rightarrow4)$-linked glucose units.

Later, Freudenburg[6] recognised that cyclodextrins could form inclusion compounds. The formation of cyclodextrin guest complexes was then systematically studied by Cramer et al[7]. He also discovered that cyclodextrins have a catalytic action in some reactions and described racemate resolution with cyclodextrins.[8]

The most important property of inclusion compunds is that a host molecule can allow guest molecules to enter its cavity without covalent bonds being formed. The study of inclusion compounds in fundamental research furnishes information about non-covalent, intermolecular forces and that they also serve as models for studying topochemical problems and the mode of action of enzymes. On the other hand, inclusion compounds are also utilised as ion exchangers, as catalysts in chemical reactions, or for microencapsulation of sensitive, active and aromatic substances. Crown ethers[9], cyclophanes[10] and cyclodextrins[11] are a few examples of organic host molecules. The crown ethers and cyclophanes are toxic. The considerably lower toxicity of cyclodextrins increases the pharmacological importance of these complexating agents relative to the other organic host molecules.

The inability to generate water-soluble parenteral formulations has limited the application and development of many drug substances. Parenteral administration is the term used to denote intravenous as well as intramuscular administration of a formulation. A further problem is that successful parenteral systems must be non-toxic and stable. There is a general lack of delivery approaches which would provide these beneficial attributes. Traditional methods improving aqueous solubility of drugs include the use of organic co-solvents, such as ethanol and propylene glycol, and non-ionic surfactants such as Tween or Cremaphor®.[12] Unfortunately these materials can induce local irritation when administered intravenously and they can be systematically toxic. Cremaphor®, for example, is thought to be involved in histamine release from mast cells after parenteral administration, a circumstance which can precipitate anaphylactiod (non-immune) shock.[13] New approaches for providing safe formulations for parenteral administration include the use of emulsions and liposomes.[14] However, there are still dangers involved concerning the use of these formulations. Technical problems which arise in the large scale production of these microparticulate formulations prevent a consistent size for the lipid bodies. A large particle size for these lipid bodies may be inappropriately targeted to the lung, liver or reticulo-endothelial

system.

The use of cyclodextrins may circumvent these mentioned obstacles. Cyclodextrins are able to form inclusion complexes with drugs.[15] Safe cyclodextrin formulations containing drugs for parenteral administration are in use. For example, two products which are currently marketed are Ono's prostaglandin $F_{2\alpha}$ and a piroxicam-β-cyclodextrin complex from Chiesi Farmaceutici (Italy) which are used as abortifacients and anti-inflammatory agents, respectively.

Oral administration of cyclodextrins does not result in acute toxicity, and long-term administration leads to no significant change in the vital organs.[16] Parenteral administration of cyclodextrins has completely different consequences. The intramuscular administration of β-cyclodextrin results in ulcerations, and its intravenous administration has nephrotoxic and haemolytic effects. Probably due to its better water solubilty, γ-cyclodextrin is not so nephrotoxic as β-cyclodextrin and it is less heamolytic.[16] This means that β- and γ-cyclodextrins can be used for oral administration. The use of β-cyclodextrin for parenteral administration is not recommended without taking due care of the dose administered. γ-Cyclodextrin may be used parenterally as it is easiliy metabolised.

The advantageous properties which cyclodextrins can confer to guest molecules were reviewed by Duchene and Wouessidjewe.[16] The encapsulation of a guest molecule in a cyclodextrin cavity can normally lead to an *improvement in stability of the guest molecule from environmental factors* such as heat, light and oxygen. Methylparathion, an insecticide, is a non-volatile contact poison which decomposes rapidly. Inclusion in β-cyclodextrin not only improves its stability but, as a consequence, enables the reduction of the dose in plant treatment. Furthermore, inclusion can also *protect the surrounding medium from undesirable side effects from the guest molecule.* Non-steroidal anti-inflammatory substances are often aggressive for the stomach mucosa. For example, the inclusion of phenylbutazone in β-cyclodextrin reduces its irritating power. The cyclodextrins are hydrophobic inside their cavity and they are hydrophilic outside. As a result from an inclusion by the cavity of a hydrophillic molecule the cyclodextrin is able to 'hide' the hydrophobic molecule from the aqueous environment. The complex which forms from this inclusion is on many occasions water-soluble, and in this way *cyclodextrins can be used as*

solubilising agents for hydrophobic molecules. This property can be used to increase the ability of insoluble substances to be absorbed through various membranes. The inclusion of Melphalan, an anticancer drug, increases its water solubility and stability.[16]

Since the cyclodextrins are versatile complexating agents they were the chosen host molecules with which to make the inclusion complexes relevant to this study. A further description of these host molecules is therefore warranted.

1.2 The cyclodextrins

Cyclodexrins are a natural product made from the enzymatic degradation of starch by cyclodextrin glucosyl transferases (CGTases). These enzymes are of bacterial origin, for example from Bacillus macerans and alcaliphilic bacilli.[17] Cyclodextrins are cyclic oligomers of amylose (amylose = D-glucopyranose). The three oligomers α-, β- and γ-cyclodextrin consist of 6, 7 and 8 units of α 1,4-linked D-glucopyranose residues, respectively (fig 1.1).

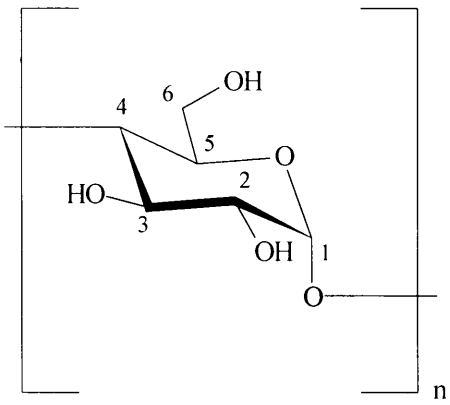

Figure 1.1 An amylose monomer of cyclodextrin. n = 6, 7, 8 for α-, β- and γ-cyclodextrin, respectively.

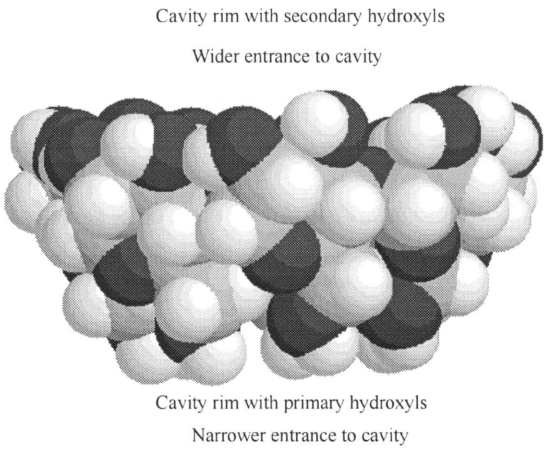

Figure 1.2 A side view of β-cyclodextrin.

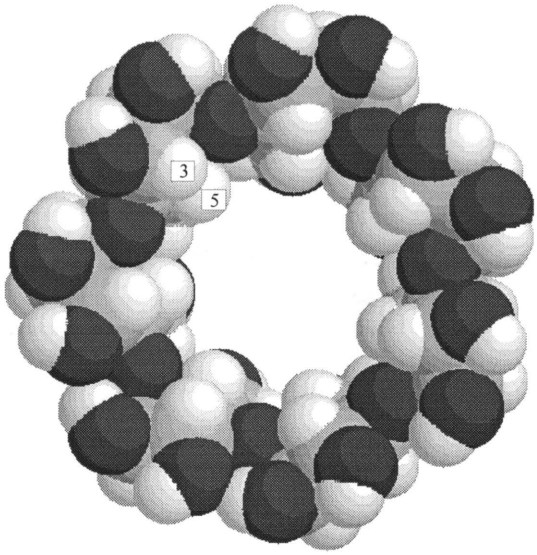

Figure 1.3 β-Cyclodextrin as seen from the secondary hydroxyl side.

The structures of the cyclodextrins have been determined by X-ray crystallography and neutron diffraction (α-CD[18], β-CD[19], γ-CD[20]). These crystal structures reveal that all the cyclodextrin molecules resemble a hollow truncated cone (torus) and have an approximate C_n symmetry (figures 1.2 and 1.3). The secondary hydroxyl (2°-OH) groups bonded to carbon-two and -three are located on the broader side of the cone and the primary hydroxyl (1°-OH) groups attached to carbon six are on the narrower side. In this study the 1°-OH rim of the cyclodextrin is defined as an imaginary rim which passes through carbon five of each amylose monomer of the cyclodextrin. In the same way, the 2°-OH rim is an imaginary rim which passes through carbon three of each amylose monomer.

The height for all the α-, β- and γ- cyclodextrin rings is 7.9-8.0Å which is measured with the aid of the space-filling Corey-Pauling-Koltun (CPK) models. The α-, β- and γ-cyclodextrins have cavity diameters of 4.7-5.2 Å, 6.0-6.4 Å and 7.5-8.3 Å, respectively.[11] These values are measured from CPK models where the smaller value is for the ring of hydrogen atoms (proton 5) bonded to carbon five and the larger value is for the ring of hydrogen atoms (proton 3) bonded to

carbon three. All the amylose building blocks exist in a $^4C_1$ chair conformation. Although the torus is stabilised by intramolecular hydrogen bonds between the secondary hydroxyls, it is still flexible enough to permit considerable deviation from the regular toroidal shape. However, the time-averaged structure has C_n symmetry which is supported by the observation that the resonances of the different proton and carbon-13 nuclei of all the amylose monomers are chemically equivalent in ^1H and ^{13}C NMR spectroscopy. Complete rotation of an amylose unit about the C(1)-O-C(4') bonds is not possible for steric reasons. Thus, the protons situated on carbon-three and -five (protons 3 and 5) are always situated within the cavity (fig 1.3) and the protons on carbon-one, -two and -four (protons 1, 2 and 4) always point outwards. The 2°-OH's are involved in hydrogen bonding to stabilise the conformation. The 1°- and 2°-OH's contribute towards the hydrophilic nature of the cavity.

The water solubilities for the α-, β- and γ-cyclodextrins are 14.5g/100ml, 1.85g/100ml and 23.2g/100ml respectively. γ-Cyclodextrin is the most soluble and β-cyclodextrin is the least soluble of the three different oligomers of amylose.[11]

The concepts of stoichiometry and inclusion geometry which are necessary to understand the topology of cyclodextrin inclusion complexes are introduced under the heading that follows.

1.3 The driving forces of complex formation

The consistent projection of the protons 3 and 5 as well as the glycosidic oxygen 4 towards the inside confers hydrophobicity to the cyclodextrin cavity.[21] This property of the cavity surrounded by the hydrophilic secondary and primary hydroxyls is the reason for the behaviour of cyclodextrins as host molecules in aqueous solution. The host-guest complexes result from non-covalent interactions between two or more molecules.[22] It is known that several forces act simultaneously to promote complex formation.[23] The most important of these forces are discussed below.

The dependance of complex formation binding constants on substrate polarisability indicates that in general, the attractive van der Waals forces between the atoms of the host and guest molecules are the dominating forces involved in complex formation.[24] Hydrophobic interactions between host and guest molecules are also involved in the complex formation.[25] On inclusion within the cyclodextrin cavity the guest molecule must expel the molecules already present and strip off its own hydration sphere. The liberated water molecules are taken up by the bulk water. These expelled water molecules gain degrees of freedom and contribute to the stability of the complex caused by the resulting increase in entropy. Hydrogen bonding between the guest atoms and the hydroxyl groups of the cyclodextrin is also a driving force leading to complex formation.[26]

As inclusion can be largely independant of the chemical properties of the guest molecule, it has been suggested that forces inherent in the cyclodextrin contribute to association. The water enclosed in the 'empty' cyclodextrin cavity could exert such a force. This water is in an unfavourable, hydrophobic environment and it cannot satiate its tetrahedral hydrogen bond potential and is thus 'activated'.[25] On expulsion, complex formation is favoured by a gain in entropy as well as by a gain in potential energy.[24]

The six amylose units of uncomplexed α-cyclodextrin are strained.[18] Energy is lowered when the strain is relieved on complex formation. This favourable lowering occurs only with α-cyclodextrin as the uncomplexed β- and γ-cyclodextrin are not significantly strained.[19]

Although recent experiments[25] have shown that van der Waals forces and hydrophobic interactions probably dominate in complex formation, the other forces previously mentioned which are inherent in the 'empty' cyclodextrin water complex may also be involved. The extent to which these forces contribute depends on the nature of the enclosed guest molecule. The inherent ring structure of the cyclodextrin is decisive as inclusion complex formation is favoured if there is a good spatial fit between the guest and host components.[23]

The concepts of stoichiometry and inclusion geometry which are necessary to understand the topology of cyclodextrin inclusion complexes are introduced under the heading that follows.

1.4 The topology of inclusion complexes

Cyclodextrins can form adducts with guest molecules in an aqueous solution.[11] These adducts are termed *inclusion compounds* according to the nomenclature proposed by Cramer[27]. On the other hand, if the guest molecule lies outside the cavity, the compounds are referred to as *association compounds.* The packing of the cyclodextrin adducts is determined predominantly by the dimensions of the guest relative to those of the cavity. Examples of the packing of these adducts can be found in figure 1.4. The guest can be either completely or partially surrounded by the host molecule. A rod-like guest can form an axial inclusion compound, whereas a disc-like guest can form a partially included structure. In general, the stability of cyclodextrin inclusion compounds increases with the extent to which the cavity is filled by the hydrophobic part of the guest. The stoichiometries of the inclusion compounds are denoted by a ratio written as *x:y* where *x* is the number of guest molecules and *y* is the number of host molecules that are involved in the formation of the adduct. The stoichiometries of the complexes in figure 1.4 are as follows: a), b) and c) are all 1:1 inclusion complexes which illustrate total, axial and partial inclusion respectively, d) is a 1:2 inclusion complex e) is 2:1 and f) is a 2:2 complex. The adduct (g) is an association compound with a stoichiometry of 1:1.

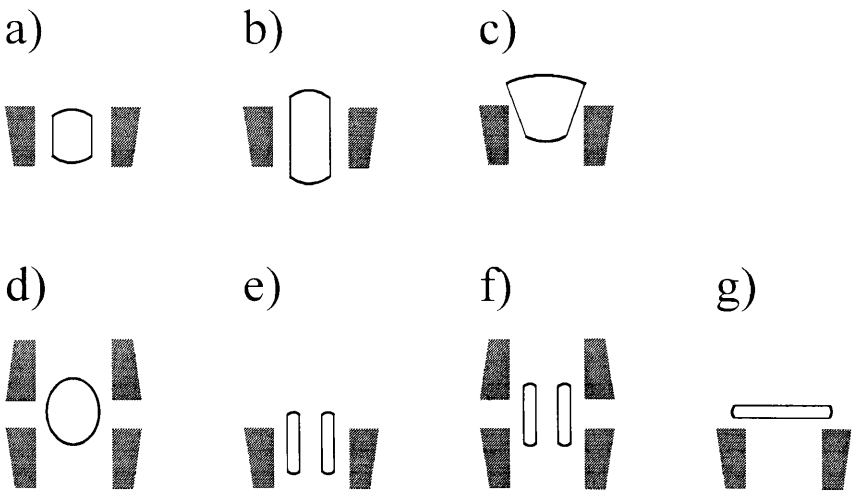

Figure 1.4 Various topologies of cyclodextrin adducts.

A factor which will effect the formation of inclusion complexes is the topology of the guest molecule. Albers and Müller[28] carried out phase solubility studies of steroids in a solution of β-cyclodextrin to determine the dependance of the solubilising power of the β-cyclodextrin molecule with regard to the structure of the steroid guest molecule. The method used to obtain the phase solubility diagram involved placing excessive amounts of steroid in a vial. To this vial standardised solutions of β-cyclodextrin were added and this solution of steroid and cyclodextrin was then sonicated for an extended period of time to ensure that complex formation had reached equilibrium. The sonicated solutions were filtered through 0.22-μm membrane filters. The concentration of steroid in the filtered solutions was then determined with high-performance liquid chromatography along with standardised solutions of steroid. Theobtained phase solubility diagram of cyproterone acetate with β-cyclodextrin is illustrated in figure 1.5.

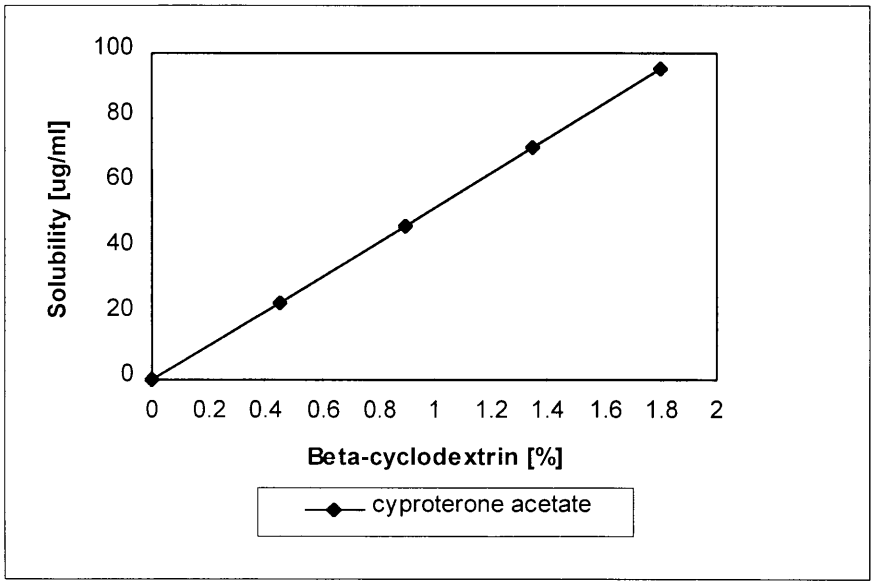

Figure 1.5 The phase solubility diagram of cyproterone acetate with β-cyclodextrin.

The percentages on the x-axis for the β-cyclodextrin solutions are weight by volume. For clarity sake, a percentage of 1% is an amount of 1.0g of β-cyclodextrin dissolved in 100.0ml of water. The results clearly show that the greater the amount of dissolved β-cyclodextrin the higher will be the concentration of cyproterone acetate.

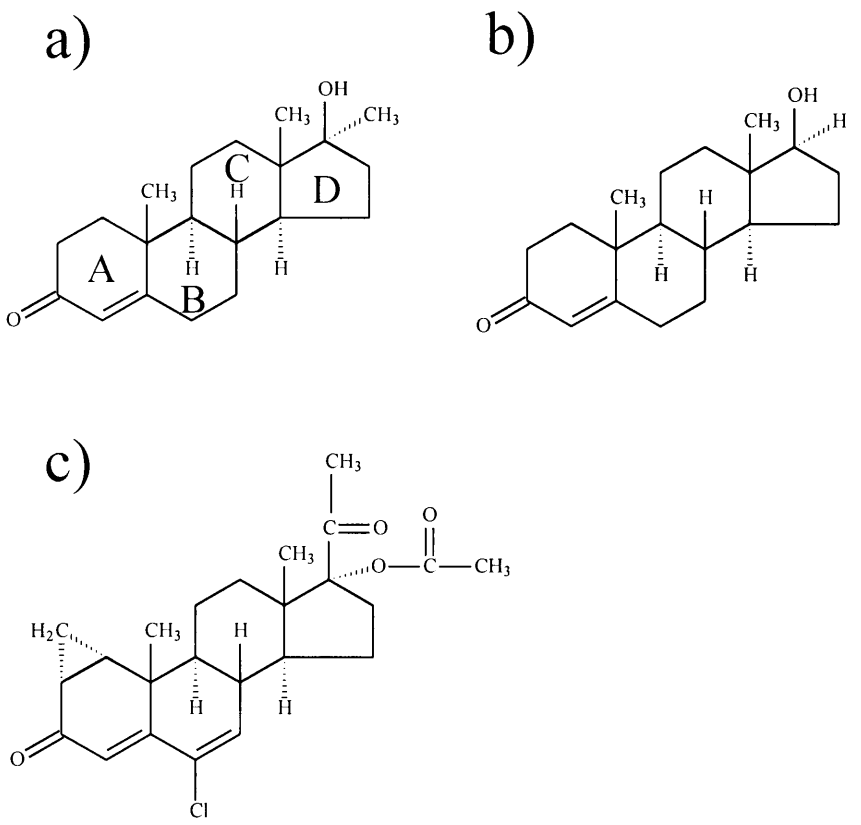

Figure 1.6 The chemical structures of a) methyl testosterone b) testosterone c) cyproterone acetate.

Amongst the steroids in the study of Albers and Müller[28], the solubilization of the three steroids methyl testosterone, testosterone and cyproterone acetate with β-cyclodextrin decrease in the following order :

methyl testosterone > testosterone > > cyproterone acetate

The chemical structure of methyl testosterone, illustrated in figure 1.6, reveals the labelling convention used for the rings of the steroid carbon-framework. The A-, B- and C-rings are six-membered and the D-ring is a five-membered ring. A conclusion was that interactions with cyclodextrins are massively reduced by the introduction of bulky or polar groups into the steroid structure.[28] This is exemplified in cyproterone acetate by the methylene bridge on the A-ring and the chlorine substituent on the B-ring.

Cyclodextrin inclusion compounds are usually prepared in water. Other solvents such as dimethyl sulphoxide (DMSO) are less suitable than water, since the stability of the inclusion

complex in this solvent is much lower.[29] Even the addition of small amounts of short-chain alcohols lowers the stability of the inclusion complex considerably.[30] In heterogeneous systems, where the host is water-soluble and the guest is not, the rate of host-guest complex formation is determined by the rate of dissolution of the water-insoluble guest molecule. In homogeneous systems where both the guest and host molecules are water soluble the inclusion complexes form very quickly, generally within micro- or milliseconds.[31]

In the study of Albers and Müller[28] cyproterone acetate and dissolved β-cyclodextrin form a heterogeneous system. Cyproterone acetate is water-insoluble and before sonication, all of this steroid was in the solid state. As mentioned earlier, the rate of formation of the cyproterone acetate-β-cyclodextrin complex is determined by the rate of dissolution of cyproterone acetate. Since β-cyclodextrin linearly increases the amount of cyproterone acetate solubilised with increasing β-cyclodextrin concentrations, it is well established that the mechanism for solubilisation is solution complex formation. From the phase solubility diagram of the cyproterone acetate-β-cyclodextrin complex (see fig 1.5) the stoichiometry is assumed to be 1:1 due to the linearity of the curve. The real question of the present study is the mode of inclusion. The determination of the mode of inclusion of the complex might reveal whether the lower solubility of cyproterone acetate in the presence of dissolved β-cyclodextrin is as a result of a partial inclusion of this steroid into the cavity (see fig 1.4 complex c.). The inclusion geometry determines the topology of the complex as it describes which part of the guest molecule is included. For a steroid-cyclodextrin complex the geometry of inclusion will determine which end of the steroid molecule is included into the cavity. For example, whether it is the end nearest the A-ring or the end nearest the D-ring. The inclusion geometry can also reveal the relative depth of insertion of the included end.

Solubility studies, such as those obtained by Albers and Müller[28] are frequently used to determine the stoichiometry of inclusion. However, such phase solubility studies cannot determine the inclusion geometry of the complex that is being formed. Knowledge of the inclusion geometry is essential to the growimg understanding of the inclusion process. Various methods which are used to obtain these properties are discussed in the paragraphs that follow.

1.5 Methods used to study inclusion complexes

1.5.1 The Calorimetric method

Calorimetric measurements are used to determine energies of complexation between host and guest molecules in solution. In these studies only the changes in enthalpy, **Δ**H, and entropy, ΔS, are determined. Although these macroscopic changes indicate that some chemical event has taken place in the microscopic (molecular) level this is not conclusive evidence that inclusion of the guest molecule by the host has taken place. There are many other factors in solution which can also contribute towards changes in enthalpy and entropy. Various attempts have been made to ascribe the enthalpy and entropy changes to the hydrophobic and van der Waals driving forces present during complex formation. From a study of the association of bulk alcohols such as 2,2-dimethyl-1-propanol and cyclohexanol with α- and β-cyclodextrin, Matsui et al [32] concluded that the van der Waals interactions between these host and guest molecules are accompanied by a negative enthalpy change (ΔH < 0). One particular example worthy of mention is the study of the adamantane carboxylate-cyclodextrin complexes (fig 1.7).[22,33] The energies of complexation obtained from the calorimetric study are given in table 1.1.

Table 1.1 Energy of complexation (kJ.mol^{-1}) in H_2O for the complexation of adamantane-1-carboxylate with α-, β- and γ- cyclodextrins, respectively

	α	β	γ
cavity diameter/ Å	5.0	6.9	8.5
ΔH	-13.5	-20.3	5.0
TΔS	-0.3	4.3	25.1
ΔG	-13.2	-24.6	-20.1

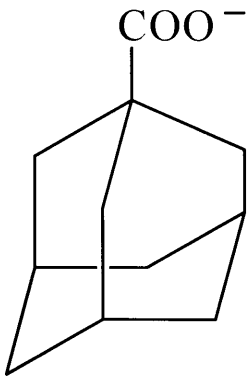

Figure 1.7 Chemical structure of adamantane carboxylate.

The $\Delta H°$ values for the adamantane carboxylate-α- and β-cyclodextrin complexes are -13.5kJ.mol^{-1} and -20.3kJ.mol^{-1}, respectively. The smaller negative $\Delta H°$ value for the adamantane carboxylate-α-cyclodextrin complex is as a result of a lower contribution from van der Waals contacts. This is expected since adamantane carboxylate is too large to completely penetrate the α-cyclodextrin cavity resulting in a small area of contact between host and guest. Adamantane carboxylate, with a diameter of 7.0Å if considered as a spherical molecule, when complexed to β-cyclodextrin with a diameter of 6.9Å will produce a snug-fit. There are more opportunities for van der Waals interactions due to the large surface area contact between host and guest molecules. This is reflected in the larger negative $\Delta H°$ value of -20.3kJ.mol^{-1} for the adamantane carboxylate-β-cyclodextrin complex.

There are negligibly small entropy contributions from the complexes of α- and β-cyclodextrin with adamantane carboxylate. The γ-cyclodextrin cavity is 1-2Å larger than the diameter of the adamantyl group. The endothermic $\Delta H°$ of 5.0kJ.mol^{-1} can be attributable to the critical distance dependance of the van der Waals forces and the fact that the ligand is only able to touch a small portion of the internal cavity at a time. The large entropy contribution of 25.1kJ.mol^{-1} is also contributed by the larger degree of rotational freedom experienced by the included adamantyl group when complexed to γ-cyclodextrin as compared to α- and β-cyclodextrin.

These rationale to explain the origins of the $\Delta H°$ and $\Delta S°$ values as used by Cromwell et al[33], whilst of interest for understanding the driving forces involved in complexation, are speculative. Other factors such as the partial collapse of the cyclodextrins to provide a snug-fit as well as the displacement of high energy water from the cyclodextrin cavity will influence the enthalpy and entropy changes. Water molecules enclosed within the uncomplexed cyclodextrin cannot satiate its tetrahedral hydrogen bond potential owing to interference from the amylose ring of cyclodextrin, thus making them enthalpy rich. The expulsion of these enthalpy rich molecules into the bulk water upon substrate inclusion results in a negative enthalpy change, together with a negative entropy change.[32,34] Nevertheless it is still possible to interpret the $\Delta G°$ for these complexes in terms of the varying cavity size of the cyclodextrin molecule. The stability of the adamantane carboxylate-cyclodextrin complexes are in the following order β- > γ- >> α-cyclodextrin. The trend indicates that an optimum matching between the size of the

cyclodextrin cavity and the size of the ligand leads to optimum binding. This is in accordance to the lock-and-key principle which states that optimum binding will occur when host and guest molecules have complementary shapes. This complementarity will ensure that the atoms of the host and guest can come close to each other to promote the opportunity for van der Waals contacts.[35] What is contrary to the lock-and-key principle is the favourable Gibb's energy of complexation of -20.1kJ.mol^{-1} for the adamantane carboxylate-γ-cyclodextrin complex. The large cavity size of γ-cyclodextrin relative to α- and β-cyclodextrin make it unsuitable for effective van der Waals contacts. Entropy factors in γ-cyclodextrin complexes must therefore be an important consideration when predicting the strength of γ-cyclodextrin complexes with guest molecules that do not give a tight fit.

1.5.2 Nuclear Magnetic Resonance Spectroscopic methods

To characterise the inclusion phenomenon of cyclodextrins on the molecular level, accurate structures of inclusion complexes in solution have to be determined. The insertion of a guest molecule into the cavity of a cyclodextrin is clearly reflected by changes in NMR parameters such as the NMR chemical shift and the nuclear Overhauser effect (NOE). The use of the changes in the chemical shifts of the proton resonances of the host and guest molecules will be discussed to illustrate how the stoichiometry and in some cases the inclusion geometry of the host-guest complexes can be obtained. Modern pulse NMR spectroscopy enables the NOE between the protons of the guest and host molecules to be detected. The magnitude of this observed NOE is a function of the intermolecular distance between the guest and host protons. The inclusion geometry of the host-guest complex can be obtained by proposing a mode of inclusion which will account for the magnitudes of the NOE's. The modelling of the complexes according to the NOE often leads to the discovery that a solution actually contains a complex which has more than one type of inclusion geometry.[36] In these instances more than one mode of complexation has to be proposed to account for all the NOE's.

1.5.2.1 Determination of the stoichiometry of complexation

The chemical shifts of protons are influenced by the chemical environments of the protons and it follows that changes in chemical environment of these protons should be reflected as changes in their chemical shift.[37] It is expected that the protons of host and guest molecules undergo changes in chemical shift upon complexation. This change in chemical shift is a function of the concentrations of the host and guest present in solution. With the continuous variation method (Job Plot)[38,39,40] it is possible to determine the stoichiometry of inclusion. The method involves keeping the total concentration of host and guest constant ([host] + [guest]), while the ratio r = [guest]/([host]+[guest]) is varied between 0 to 1. The quantity $\Delta\delta\times$[guest] is plotted against the ratio r. The $\Delta\delta$ is the difference between the chemical shift of a guest proton in the uncomplexed state and the observed value for the shift of this guest proton in the presence of a specific host concentration according to the ratio r. The r value at the turning point of the plot is used to determine the stoichiometry of complexation. A continuous variation plot was obtained by Ganza-Gonzalez et al[41] for the naproxen-β-cyclodextrin complex. This plot was symmetrical and had a turning point at r = 0.5. A value of r = 0.5 is indicative of a 1:1 guest-host complex. Complexes which have stoichiometries other than 1:1 will lead to asymmetric continuous variation plots which can be caused by the competitive formation of other types of stoichiometries.

A limitation of determining the stoichiometry of complexation is that the guest molecule must be soluble to the extent that large r values can be obtained. An excess of the guest compound must be soluble in the presence of a relatively low concentration of host compound.

In the case where the formed host-guest complex is insoluble in an aqueous medium and precipitates upon formation, the continuous variation method cannot be employed. Some steroid-β-cyclodextrin complexes are highly water-insoluble and have precipitated upon formation. An example of such a complex is the cholesterol-β-cyclodextrin complex.[39] These water insoluble β-cyclodextrin complexes have proven to be insoluble in diethyl ether as well. Isolation of these insoluble complexes according to the method of Djedaïni et al[39] involves the following steps:

i) Formation of the complex in aqueous medium.

ii) Washing of the precipitated complex with water to remove excess uncomplexed β-cyclodextrin.

iii) Step (ii) is followed by washing of the precipitated complex with diethyl ether to remove any uncomplexed steroid.

After these three steps only the pure complex should remain. Most steroids and all the α-, β-, γ-cyclodextrins are soluble in dimethyl sulphoxide. The stoichiometry of complexation is determined by dissolving the isolated complex in DMSO-d_6 and recording the ^{1}H NMR spectrum. The ^{1}H NMR resonances of the steroid and β-cyclodextrin protons are integrated to derive the molecular ratio. The determined molecular ratio of steroid to β-cyclodextrin will be equivalent to the stoichiometry of complexation. Djedaïni et al[39] used the above method to obtain the stoichiometry of complexation of 1:1 for the water insoluble cholesterol-β-cyclodextrin complex.

The solvent DMSO-d_6 is preferred since it solvates the cyclodextrin cavity resulting in removal of the complexed steroid from the cavity. The basis for proving desinclusion is the observation that there is no change in the chemical shift of the steroid protons in the absence or presence of β-cyclodextrin in DMSO-d_6 medium.[39] The absence of chemical shift changes between the steroid protons in the presence and absence of β-cyclodextrin normally proves that there is no change in the chemical environment to these protons which can arise as a result of inclusion of the steroid into the cyclodextrin cavity.

1.5.2.2 The use of Complexation Induced Shift (CIS) values to determine inclusion-geometry

The changes in chemical shifts of the protons of the guest and host molecules are dependant on the concentration of these two species in solution. Complex formation is a dynamic process and the observed chemical shifts of the guest and host protons will be an average of the chemical shifts of these protons in the complexed as well as the uncomplexed state. To obtain the chemical shift of a guest proton in the fully complexed state use is made of the Benesi-Hildebrand

method (eqn. 1.1).[42]

$$\frac{[\,CD\,]_t}{\Delta\delta_{obs}} = \frac{[\,CD\,]_t}{\Delta\delta_c} + \frac{1}{K\,\Delta\delta_c} \qquad [1.1]$$

$[\,CD\,]_t$ is the total concentration of cyclodextrin present in solution.

$\Delta\delta_{obs}$ is the observed chemical shift difference between the resonance of the guest proton in the presence of a standardised concentration of cyclodextrin and the resonance of the guest proton in the free uncomplexed state.

$\Delta\delta_c$ is the chemical shift difference between the resonance of a guest proton which is 100% complexed and the guest proton in the free uncomplexed state.

K is the equilibrium stability constant for host-guest complex formation.

A prerequisite for the Benesi-Hildebrand method is that the guest molecule must be water soluble so that the $\Delta\delta_{obs}$ and $\Delta\delta_c$ values can be calculated. In other words, the guest molecule must be soluble in water in the absence of cyclodextrin to determine the ^{1}H NMR chemical shifts of the proton resonances of the uncomplexed molecule.

The complexation induced shift (CIS) value is defined as the chemical shift difference between the resonance of a proton in the fully complexed state and the uncomplexed state. The CIS value is identical to $\Delta\delta_c$ (eqn 1.1).

From equation 1.1, the slope of the plot of $[\,CD\,]_t / \Delta\delta_{obs}$ against $[\,CD\,]_t$ is equal to $1 / \Delta\delta_c$. This plot can be used to obtain the CIS value. The data for the plot is experimentally obtained as follows. A number of vials are prepared where the concentration of the guest molecule is kept constant. In each vial a different concentration of cyclodextrin is added, therefore each vial has a different $[\,CD\,]_t$ value. In this manner a dilution series of the complexating agent is made where the concentration ranges from that of the guest to at least two orders greater. The ^{1}H NMR spectra of each vial are then recorded. From the resonances of a guest proton in each spectrum the $\Delta\delta_{obs}$ values can be obtained.

Unlike the calorimetric method, NMR spectroscopy can unambiguously determine whether or not inclusion has occured. Large chemical shift changes for the cyclodextrin protons 3 and 5 situated inside the hydrophobic cavity will clearly prove inclusion. These changes can only arise from a change in the chemical environment of the cyclodextrin cavity which are caused by the included guest molecule. On the same basis, the protons of the included guest molecule also undergo chemical shift changes as a result of a change in their chemical environment.

A brief discussion of the causes for changes in NMR chemical shift of the resonances of the carbon-13 and proton nuclei found in cyclodextrin inclusion complexes follows. Models based on the solvent effect have been proposed to explain the chemical shifts of the carbon-13 nuclei of included guest molecules.[23] In these models the guest compound is equated with the solute and the cyclodextrin cavity is equated with the solvent. Carbon-13 NMR studies of α-cyclodextrin inclusion complexes with benzoic acid, p-nitrophenol and p-nitrophenolate led to the discovery that the carbon-13 nuclei of the guest that were included into the cyclodextrin cavity experiences upfield shifts and the carbon-13 nuclei at the exposed 2°-OH rim of the cavity experienced downfield shifts (see fig 1.8).[43,44]

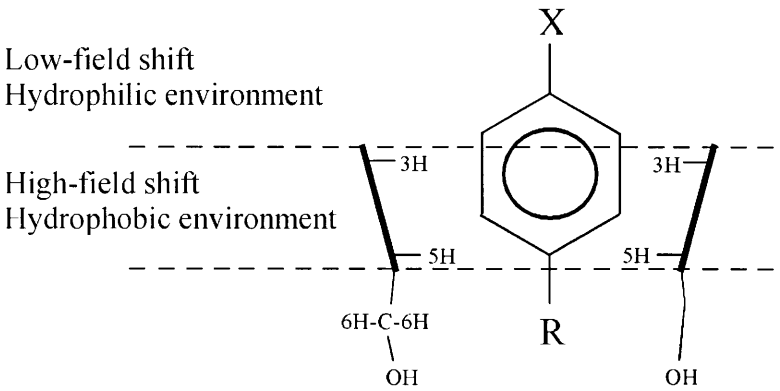

Figure 1.8 The 'double-layer' model used for explaining guest ^{13}C NMR chemical shift changes induced by complexation with α-cyclodextrin.

By taking this trend into account , the 'bilayer model' was constructed in which the included carbon-13 nuclei experienced upfield shifts as a result of being close to the walls of the cavity and subjected to a hydrophobic environment, and the downfield shifts of the carbon-13 nuclei at the 2°-OH rim of the cavity is caused by exposure to the hydrophilic environment. This model

is supported by the observation that when these aromatic guest molecules complex with α-cyclodextrin in an aqueous solution, the included guests show UV spectral changes almost identical with that observed when the guest compounds are moved from an aqueous to a dioxane solution. This result suggests that the carbon-13 chemical shift changes of the included aromatic guests arise from the changes in environment from a highly polar one (water) to a more apolar one (dioxane).

It is established that solvent effects (polar or apolar) can cause changes in chemical shift. In a review written by Y. Inoue[23], the causes for these solvent effects were attributed to van der Waals effects, neighbour anisotropic susceptibility and electric field effects. H-J. Schneider et al[45] modelled the causes for the chemical shifts of the proton nuclei found in cyclohexane, methyl cyclohexane and n-butane. The approach used attributed the origin for the differences in chemical shift to electric field effects, the anisotropy effect and sterically induced polarisation effects.

In the study by H-J. Schneider et al[45] the contribution from the *electric field effects* was calculated by the Buckingham approach[46]. The method calculates the degree of longitudinal polarisation of a bond with a polarisability P by a charge q at a distance r and an angle Θ between the field gradient and bond. The contribution for the *anisotropy effects* was calculated using the McConell equation.[45] The *sterically induced polarisation* was calculated with the use of a force-field derived function.[45]

In most cases (possible exceptions can be found in the study by Schneider and Weigand[47]) the steric forces acting on the C-H bonds will push electrons towards the carbon atom, and since the non-bonded steric force is exponential in the distance r between the C-H bond and the interacting atom, the effect is difficult to differentiate from the deshielding effects of nearby van der Waals forces which have a distance dependance of r^{-6}. As a consequence, steric effects on proton shielding have usually been disregarded since they have previously been ascribed to van der Waals forces. However, the existence of sterically induced polarisation was verified by a study of the chemical shifts of steroid protons by H-J. Schneider et al.[48] This study showed that the shielding of the axial protons increases with the number of other axial C-H bonds. This effect was shown to be attributed to sterically induced polarisations and not to the electric field effects

of the diaxial C-H dipoles which was previously considered to be the origin of the chemical shift variations of the axial protons.

When all the possible causes for the changes in chemical shift are taken into account it can be concluded that the cyclodextrin host molecule possesses many factors which can change the chemical shifts of the proton resonances of the included guest molecule. For example, the oxygen atoms of the 1°- and 2°-OH's can be regarded as negative point charges (q) which can polarise a bond of an included guest molecule. The π-electron rich glycosidic oxygen atoms (cyclodextrin oxygen 4's) can be a source of anisotropy which will influence the chemical shifts of the guest protons. The cyclodextrin protons 3 and 5 which are situated within the cavity can be a source of sterically induced polarisation for the atoms of the included guest.

For cyclodextrins, it cannot as yet be theoretically predicted whether their will be a resultant upfield or downfield shift in the proton resonance of an included guest proton upon taking the possible causes of polarisation into account. At this stage, the only recourse is to experimentally obtain CIS values of included guest protons and determine whether any trends in these CIS values can be found. In the study of the naproxen-β-cyclodextrin, Ganza-Gonzalez observed trends in the CIS values of the protons of the included naproxen.[41] These trends in the CIS values were used by Ganza-Gonzalez to model the inclusion geometry of the naproxen-β-cycylodextrin complex. The results of this study follows.

According to Ganza-Gonzalez et al[41] an upfield shift of a guest proton resonance indicates that this proton is close to a cyclodextrin atom which is rich in π electrons. The hydroxyl groups on the 1°-OH and 2°-OH rims of the cyclodextrin cavity are π electron rich environments as a result of the oxygen atoms. A guest proton with an upfield shift will have a negative CIS value. A guest proton with a downfield shift indicates a deshielding effect due to van der Waals forces. The protons 3 and 5 within the cyclodextrin cavity provide opportunities for van der Waals contacts to guest protons. A guest proton with a downfield shift will have a positive CIS value. The CIS values of the protons of naproxen were used by Gonza-Gonzalez et al[41] to obtain the proposed inclusion geometry of the naproxen-β-cyclodextrin complex as shown in figure 1.9.

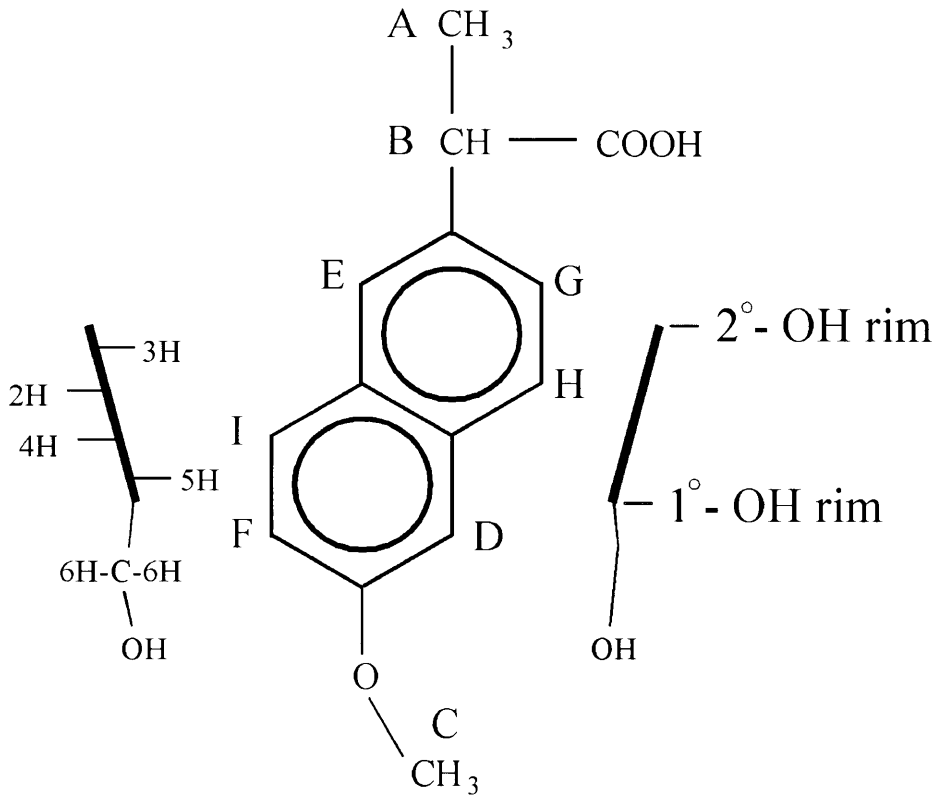

Figure 1.9 A representation of the naproxen-β-cyclodextrin complex (transverse cross-sectional view) showing the orientation of the drug with respect to the primary and secondary hydroxyl rims of the cavity.

The complexation induced shift (CIS) values of the naproxen protons A-I were determined with the Benesi-Hildebrand method. The naproxen protons E, D, G and F were displaced upfield and they have the CIS values of -0.1164ppm, -0.0530ppm, -0.0566ppm and -.0556ppm, respectively. These upfield displacements place these protons close to the π electron rich oxygen atoms of the hydroxyl groups located at the rims of the β-cyclodextrin cavity (see fig 1.9). The protons H and I were displaced downfield and they have CIS values of 0.0389ppm and 0.1775ppm, respectively. These positive CIS values are caused by the increased van der Waals interactions of protons H and I to the β-cyclodextrin cavity protons 3 and 5. The large positive sign of the CIS value of I indicates that this proton is located at some distance away from the hydroxyl groups on the β-cyclodextrin rims and close to the cyclodextrin protons 3 and 5 to promote van der Waals contacts. The smaller magnitude of the CIS value of H compared to the CIS value of I can be explained by a masked upfield displacement from the interactions with H from π electron rich oxygen atoms.

The naproxen proton C shows only a slight downfield shift of 0.0018ppm, since its van der Waals interaction with the proton 6's of β-cyclodextrin is partly counteracted with the freely rotating π electron rich terminal secondary hydroxyl groups. The slight downfield shift of proton A of 0.0291ppm cannot be due to van der Waals interactions in the interior of the cavity since proton A is positioned outside the cavity. According to Ganza-Gonzalez et al[41] this downfield displacement may be due to steric perturbation by the primary hydroxyl groups of the cyclodextrin molecule, or to a delocalisation of charge into the aromatic ring of naproxen occuring as a result of inclusion. The CIS value of naproxen proton B could not be obtained since this proton resonance overlapped with those of the β-cyclodextrin protons.

Further evidence in support of the proposed inclusion geometry illustrated in figure 1.9 can be obtained from the interpretation of the CIS values of the β-cyclodextrin protons. The CIS values of the β-cyclodextrin protons 3-H, 5-H and 6-H are -0.1408ppm, -0.2811ppm and -0.1441ppm, respectively. These values are all upfield shifts which indicate that these β-cyclodextrin protons are all close to π electron rich guest protons. These CIS values of the β-cyclodextrin protons demonstrate that the entire aromatic naproxen ring is included into the cavity.

Ganza-Gonzalez simplistically attributes the downfield shifts to van der Waals forces present in the cavity and the upfield shifts to the π-electrons of the 1°- and 2°-OH's and fails to consider the other possible causes for changes in chemical shift studied by H-J. Schneider.[45,48] However, this failure by Ganza-Gonzalez does not diminish the validity of the trend that guest protons close to the walls of the cavity experience downfield shifts and protons near the 1°- and 2°-OH's experience upfield shifts. This same trend was also observed in the study of the ibuproxam-β-cyclodextrin complex by Mulinacci et al[49] (see 1.5.3).

In a similar manner that the 'bilayer model' was proposed to explain the chemical shifts of included carbon-13 nuclei, it can be proposed that the accumulative effect of all the causes for proton chemical shifts of guest molecule when complexed to the cyclodextrin will result in a downfield shift (positive CIS value) if the guest proton is close to the cavity walls and an upfield shift (negative CIS value) if the proton is close to either the 1°- or 2°-OH rim.

1.5.2.3 The use of the NOE to determine inclusion geometry

Since the magnitude of the NOE's are dependant on distance these effects have been utilised as a tool to obtain solution conformations of host-guest complexes. The study of the complexes of 1-anilino-8-naphthalenesulphonate (ANS) with β- and γ-cyclodextrin by Schneider et al[36] is used as an example to illustrate the effectiveness of using the NOE to obtain the inclusion geometry. The ANS molecule contains both phenyl and naphthyl units. The object of this study was to discover which inclusion modes for the ANS-β-cyclodextrin and ANS-γ-cyclodextrin complexes are favoured. Will the phenyl unit be the included portion in the cyclodextrin cavity or will the naphthyl unit be favoured?

Predictions by Schneider et al[36] were made on the assumption that the inclusion mode which promotes the most opportunity for van der Waals contacts between host and guest atoms would be favoured. The α-cyclodextrin cavity is suitable for taking up phenyl derivatives whereas β-cyclodextrin better accommodates the naphthalenes and γ-cyclodextrin prefers anthracene-type derivatives. These modes of complexation will lead to snug fits which allows optimum surface area contact between the atoms of the host and guest molecules and thus maximising the contribution from van der Waals forces. It was therefore expected that the naphthyl unit of ANS will be the included portion in the ANS-β-cyclodextrin complex. It was not expected that the phenyl unit of ANS will be included into the large cavity of γ-cyclodextrin in the ANS-γ-cyclodextrin complex. This mode of complexation will not promote the opportunity for van der Waals contacts between guest and host molecules.

In this study the 2-D ROESY experiment was used to obtain the NOE's between the protons of the ANS molecule and the cyclodextrin molecules. These observed NOE's were then used to model the inclusion geometries of the ANS-β-cyclodextrin and ANS-γ-cyclodextrin complexes. The results of this study are illustrated in figure 1.10 where the NOE's are given in combination with the inclusion geometries of the complexes. The instrumentation available to Schneider et al[36] precluded the accurate integration of the NOE crosspeaks observed in the 2-D ROESY spectra of the ANS-cyclodextrin complexes. The relative intensities are therefore denoted by +

or + + in the structure diagrams (fig 1.10).

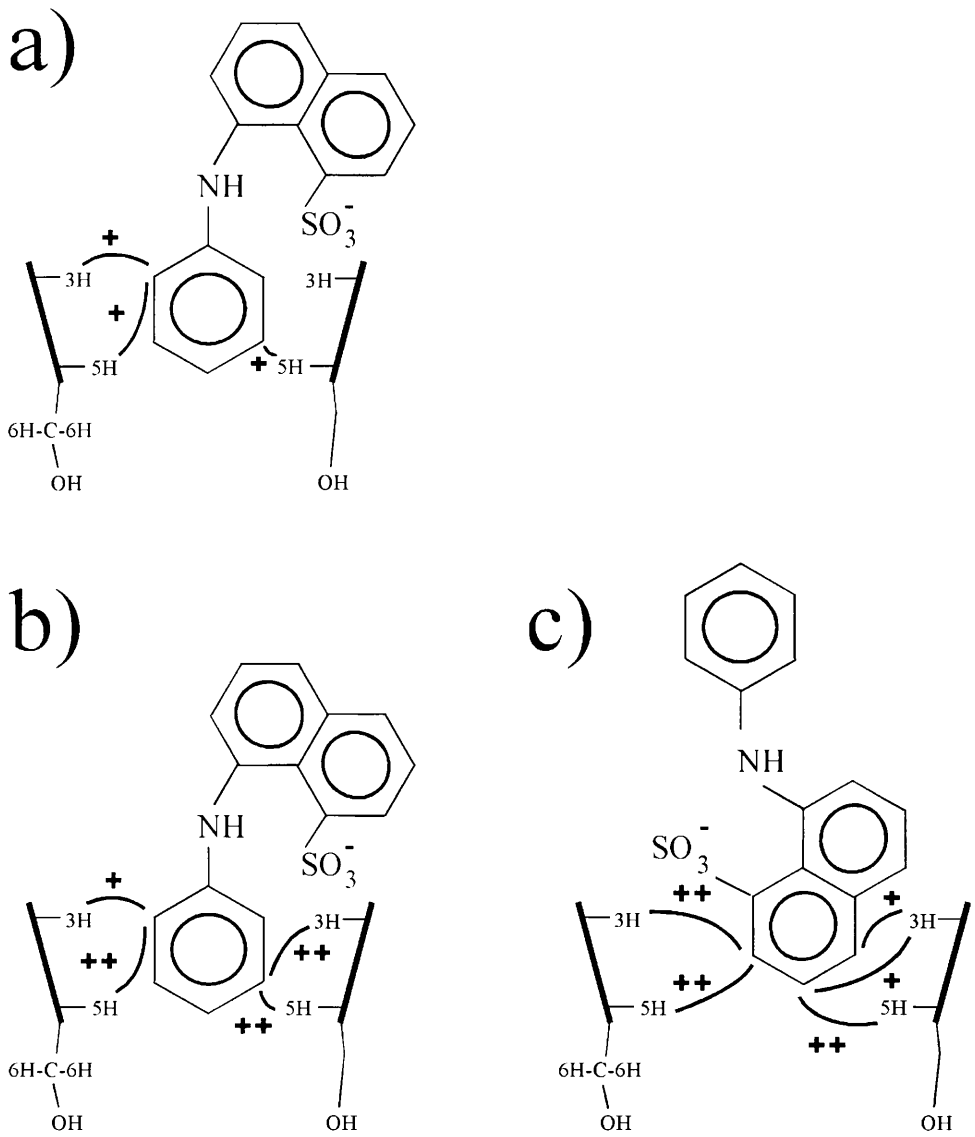

Figure 1.10 a) A representation of the ANS-β-cyclodextrin complex with the phenyl unit inserted into the cavity.
b) The ANS-γ-cyclodextrin complex with the phenyl unit and
c) with the naphthyl unit inserted into the cavity.
The number of + signs at the proton positions denote the increasing intensity of the NOE crosspeaks observed in the 2-D ROESY spectra.

According to the NOE's of the phenyl protons of ANS to the β-cyclodextrin protons 3 and 5, it can be concluded that the phenyl unit and not the naphthyl unit of ANS is included into the β-cyclodextrin cavity. Two modes of complexation were proposed for the ANS-γ-cyclodextrin complex as a result of the NOE's from the protons of both the phenyl and naphthyl units of ANS

to the γ-cyclodextrin protons. This is an example where more than one mode of complexation exists in solution. It is impossible to explain the NOE's of the phenyl and naphthyl units to the γ-cyclodextrin as a result of one inclusion geometry only. There is not enough volume in the cavity to accommodate both units simultaneously.

To lend further weight to the deduced modes of complexation, Schneider et al[36] also made use of the complexation induced shifts of the ANS molecule when complexed to β- and γ-cyclodextrin. In figure 1.11 only the CIS values for the ANS molecule which have a greater absolute magnitude than 0.02ppm are shown. A generalisation is made that the greater the magnitude of the CIS value of a specific guest proton, the greater the proximity of that guest proton to the atoms of the host. For the ANS-β-cyclodextrin complex the presence of significant CIS values of -0.04ppm and -0.11ppm present on the phenyl unit as well as the CIS value of 0.04ppm near the phenyl unit confirm that only the phenyl is complexed to the β-cyclodextrin cavity (see figs 1.10.a and 1.11.a). For the ANS-γ-cyclodextrin complex the presence of CIS values on both the phenyl and naphthyl units confirms that two inclusion geometries exist in solution where either the phenyl or the naphthyl unit is complexed to the γ-cyclodextrin cavity (see figs 1.10.b, 1.10.c and 1.11.b). Furthermore, the presence of CIS values of -0.07ppm, -0.25ppm and -0.35ppm present only on the aromatic ring bearing the sulphonate substituent shows that this aromatic ring is included into the cavity and not the aromatic ring which carries the amine substituent. This is in agreement to the proposed inclusion geometry to explain the NOE's of the naphthyl unit to the γ-cyclodextrin protons (see fig 1.10 c.). The NOE's and CIS values can therefore provide useful complimentary information which can be used to obtain the inclusion geometries of cyclodextrin complexes in solution.

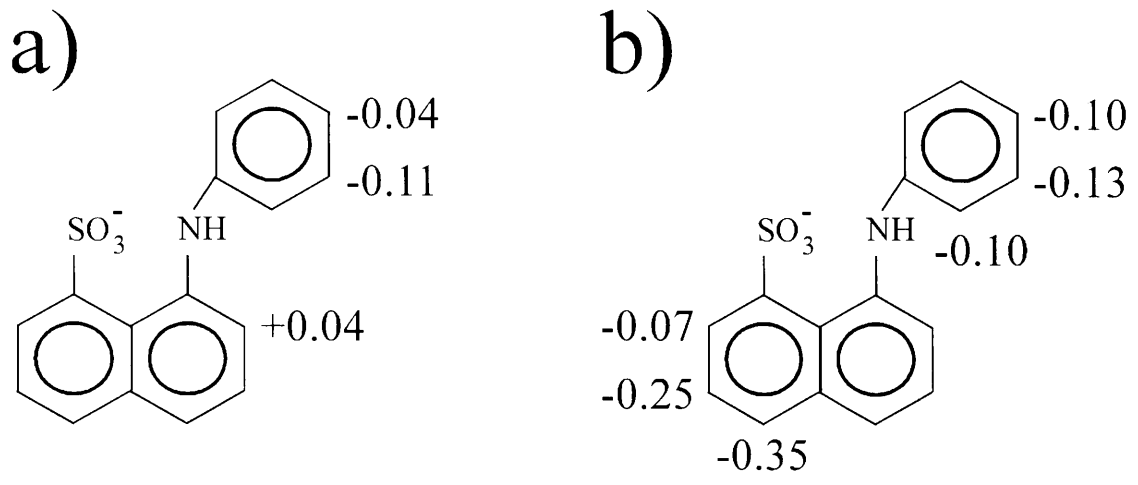

Figure 1.11 The CIS values of naproxen when complexed to a) β-cyclodextrin and to b) γ-cyclodextrin.

The preferred inclusion of the phenyl unit of ANS into the β-cyclodextrin cavity is unexpected. The inclusion of the naphthyl unit would have created more opportunities for van der Waals interactions between the guest and host molecules. However, the insertion of the phenyl unit within the cavity will result in a higher degree of rotational freedom for this included portion. The inclusion of the naphthyl unit and especially the evidence for the inclusion of the phenyl unit into the larger γ-cyclodextrin cavity is also surprising. The popular view of host-guest complexes generally is that a guest molecule will seek the closest contact, or fit, to the host cavity.[36] The results of this study demonstrate that this view is too simplistic for cyclodextrin complexes in water. The obvious trend found with the ANS-β- and γ-cyclodextrin complexes suggests that if a lipophilic molecule has the option of complexing in two or more different orientations it will bind in a manner which favours high mobility of the included moiety.

Entropic contributions, as a result of a high degree of rotational freedom of an included moiety of a guest molecule, must play an important role to hydrophobic binding in these cyclodextrin complexes. The formation of the adamantane carboxylate-γ-cyclodextrin complex discussed previously has also been attributed to entropic factors. Similar arguments based on entropy contributions have been used before to explain the often stronger binding of phenyl derivatives to β-cyclodextrin in comparison to α-cyclodextrin.[50]

1.5.3 The use of computer molecular modelling to determine inclusion geometry

It has been shown that computer-aided molecular modelling can be used to predict the conformation and interaction energy of the salbutamol-β-cyclodextrin complex.[51] However there are limitations to computer modelling since many of these calculations are carried out in vacuo and do not take solvent effects into consideration. As an example the molecular modelling study of the ibuproxam-β-cyclodextrin complex by Mulinacci et al[49] to obtain the inclusion geometry will be discussed. Two types of inclusion geometries can exist in solution (fig 1.12). One type is where the two ibuproxam (IBX) methyl groups are nearer the 2°-OH rim and the other type is where the two IBX methyl groups are closer to the 1°-OH rim of the β-cyclodextrin cavity. The conformations at minimum energies for the two different types of inclusion geometries were

calculated. The calculated formation energies of complexation for complex A and complex B were 209.7kcal/mol and 213.2kcal/mol, respectively.[52,53] The calculated docking energies for complex A and complex B were -30.6kcal/mol and -26.3kcal/mol, respectively. From these calculations it was concluded by Mulinacci et al[49] that complexes A and B have the same probability of existence. In this instance, these molecular modelling calculations were unable to determine the preferred inclusion geometry of the ibuproxam-β-cyclodextrin complex. The research group of Mulinacci et al[49] used the nuclear Overhauser effect between the protons of ibuproxam and β-cyclodextrin to identify the preferred mode of complexation.

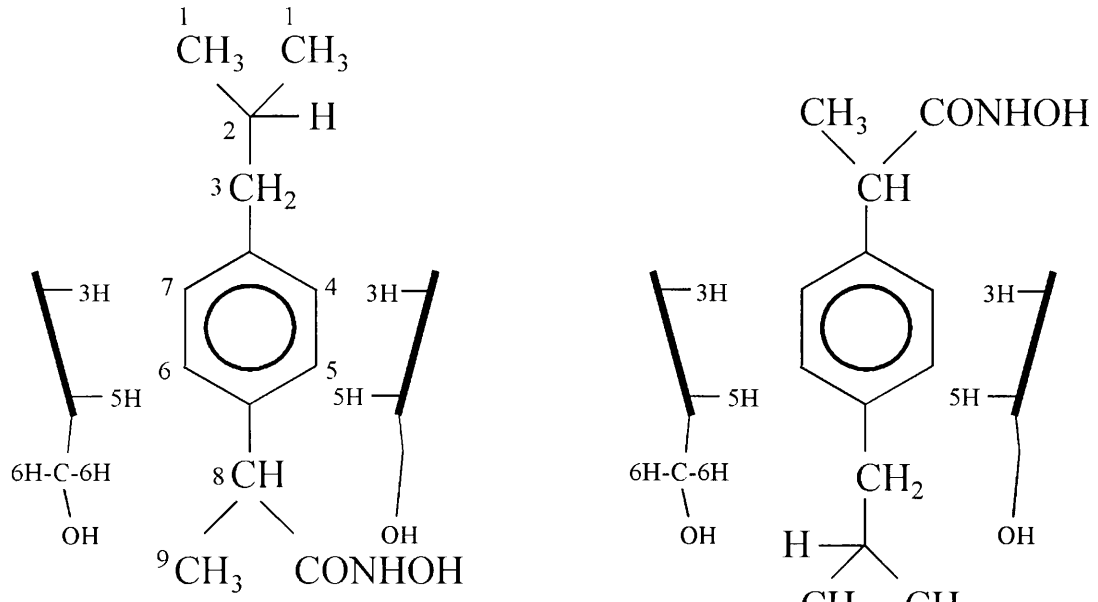

Figure 1.12 A representation of the two possible inclusion geometries of the ibuproxam-β-cyclodextrin complex.

A significant NOE was observed between the ibuproxam 1-H and the β-cyclodextrin proton 3 with a signal increase of 0.8%. Another less intense NOE was recorded between the ibuproxam 1-H and the β-cyclodextrin proton 5 with an increase in the signal of 0.16%. These NOE's position the two ibuproxam methyl groups (1-H ibuproxam) closer to the 2°-OH rim than to the 1°-OH rim of the β-cyclodextrin cavity. The inclusion geometry represented by complex A is therefore preferred above that of complex B. In instances where molecular modelling studies

aimed at determining the preferred inclusion geometries of host-guest complexes are inconclusive, the nuclear Overhauser effect is a valuable complimentary tool.

One of the major concerns confronting molecular modelling studies today is the inclusion of the solvent effects into the calculations. Methods used to possibly simulate water entail the use of distant dependant dielectric constants to shield electrostatic interactions and thereby simulate the effect of water. A more direct appraoch has been addressed by modelling packages such as Molecular Silverware in combination with Molecular Dynamics simulations both of which are available to SYBYL users.[54] The disadvantage of such molecular modelling attempts are for example the large computational times required to obtain minimum energy conformations. This is as a result of the large number of atoms which have to be considered in the calculations. To avoid the need of large computational times many molecular modelling studies only consider the host and guest molecules *in vacuo* as was the case in the previous study of the ibuproxam-β-cyclodextrin complex. This approach mostly considers the electrostaic interactions and van der Waals forces between the host and guest atoms within the cavity which are in close proximity to each other. The recent evidence of Schneider et al[55] suggests that structural parts outside the cavity greatly influence the formation constants of lipophilic guest molecules to cyclophane complexating agents in water. For molecular modelling studies to increase in their predictive ability concerning the stabilities of host-guest complexes they must take more factors into account in particular the shells of solvent which extend far beyond the immediate host-guest complex.

The study of the ibuproxam-β-cyclodextrin complex by Mulinacci et al[49] also reported the CIS values of the included ibuproxam molecule. The CIS values of protons 4-H,7-H and 5-H,6-H which are close to the walls of the β-cyclodextrin cavity are 0.174ppm and 0.040ppm, respectively. The CIS values of the protons 1-H, 2-H, 3-H and 9-H which are situated close to either of the 1°-OH or 2°-OH rims are -0.055ppm, -0.030ppm, -0.021ppm and -0.015ppm, respectively. The CIS value of 8-H could not be determined because it overlapped with the β-cyclodextrin proton 4. The trend found in the naproxen-β-cyclodextrin complex that the protons of naproxen that are close to the walls of the cavity have positive CIS values and the protons of naproxen near either of the two hydroxyl rims of the cavity have negative CIS values

is also present in the ibuproxam-β-cyclodextrin complex.[41]

1.6 The aim and approach for the study of the steroid-cyclodextrin complexes

The steroids cyproterone acetate, ethynyl oestradiol and danazol are biologically active molecules.[56] Cyproterone acetate is both an anti-androgen and a progestagen. Ethynyl oestradiol is a synthetic estrogen which is used in combination with a progestagen as an oral contraceptive. Danazol is an antigonadotropin which is used in the treatment of endometriosis and other endocrine disorders. All three steroids are water-insoluble. The poor absorption of these steroids by membranes as a result of their poor solubility will lower the bioavailability of these drugs when administered orally. The potential of cyclodextrin complexating agents to facilitate the transport of these steroids across biological membranes is very real. A deeper study of the interactions of these steroids with cyclodextrins will lead to an improved predictive ability when choosing a suitable cyclodextrin with which to increase the solubility of steroid molecules.

The determination of the inclusion geometry of the cyproterone acetate-β-cyclodextrin complex might explain the poor solubility of cyproterone acetate in the presence of β-cyclodextrin as determined in the solubility study of Albers and Müller[28]. What effect will the two different cavity sizes of β- and γ-cyclodextrin have on the inclusion geometry of the complexes formed with the three previously mentioned steroid molecules? Will there be a trend in the modes of inclusion for the steroid guest molecules with the cyclodextrin complexating agents since they possess the same steroid-carbon framework? These questions can be answered upon the successful determination of the inclusion geometries of these steroid-cyclodextrin complexes.

The aim of this study is to determine the inclusion geometry of the complexes formed by the three steroids cyproterone acetate, ethynyl oestradiol and danazol with the β- and γ-cyclodextrins with the aid of Nuclear Magnetic Resonance (NMR) spectroscopy. The preceding methodologies which utilise the potential of an NMR spectrometer to study complexes (see 1.5.2) serve as a framework to devise a strategy which can be used to elucidate the inclusion geometry of the

steroid-cyclodextrin complexes.

Two dimensional (2-D) Nuclear Magnetic Resonance Spectroscopy is an important tool which will be used in the study of the steroid-cyclodextrin complexes. The principles of 2-D NMR spectroscopy are discussed in chapter two. The NMR parameters such as the chemical shifts of the proton resonances of the guest molecule and the NOE's between the protons of host and guest molecules can be used to study complexes. It is self evident that a complete assignment of the steroid proton resonances in the ^{1}H NMR spectrum must be achieved before a thorough investigation of the complexes can commence. The strategy used to assign the proton resonances of cyproterone acetate, ethynyl oestradiol and danazol is described in chapter three. The complete assignment of the proton resonances of cyproterone acetate is used as an example to illustrate the effectiveness of this strategy. In chapter four the results of the NMR investigation of the steroid-cyclodextrin complexes are given. The first part of this chapter deals with the solubilising powers of the β- and γ-cyclodextrins with respect to the three steroids. This is followed by the method used to determine the chemical shifts of the proton resonances in the ^{1}H NMR spectra of these steroid-cyclodextrin complexes. The final section of chapter four communicates the results of the 2-D ROESY spectra of all the steroid-cyclodextrin complexes. The interpretation of the NOE crosspeaks observed in the 2-D ROESY spectra is discussed in chapter five. These NOE crosspeaks are used to propose inclusion geometries for the steroid-cyclodextrin complexes. Chapter five also contains a discussion concerning the origin of the chemical shift differences between the steroid proton resonances when complexed to β- and to γ-cyclodextrin. This chapter ends with concluding remarks which deals with the insights gained from the obtained inclusion geometries of the steroid-cyclodextrin complexes.

2 Principles of two-dimensional NMR spectroscopy

2.1 Introduction

Chemists and biochemists have used NMR for many years to characterise molecular systems in combination with other physical techniques such as infrared and mass spectroscopic measurements. In this context, an NMR spectrum is normally obtained under standard conditions so that the observed chemical shifts and coupling constants can be compared with those of model compounds. As molecular complexity increased, the only way of improving the 1-D NMR measurements has been to run the experiment at higher magnetic field strength. This higher magnetic field strength will spread and resolve overlapping resonances in a ^{1}H NMR spectrum and thus facilitate the assignments of the spectrum. However, for complex molecules, even spectra obtained at the highest available magnetic field strength it is found that proton resonances are still obscured by extensive signal overlap.

The fundamental groundwork for two-dimensional NMR was laid by the work of Ernst and Anderson[57]. In its infancy 2-D NMR was more a curiosity than an analytical method, requiring the expertise and patience that only the pioneers in the field could muster. Two-dimensional J-resolved spectroscopy which was one of the earlier 2-D NMR experiments offered a new way to resolve highly overlapping resonances into readily interpretable multiplets and permitted the chemical shift assignments to be made in a simple and direct manner. When the potential of 2-D NMR spectroscopy to overcome many of the problems encountered by 1-D NMR such as signal overlap was realised, much effort to make 2-D NMR spectroscopy accessible to all chemists was made.

At present there are a multitude of various 2-D NMR experiments available to the chemist. To utilise the potential of 2-D NMR spectroscopic experiments to solve the chemical problems particular to this study an understanding of the principles of 2-D NMR spectroscopy must be

acquired. First the mechanism which is common to all 2-D experiments is introduced. This is followed by a short discussion of the principles of a few exemplary 2-D NMR experiments. The chemical information which can be obtained from each of these experiments will also be mentioned.

2.2 The mechanism of the 2-D NMR experiment

The pulse sequences of 2-D NMR experiments can be divided into three main phases. These phases are the preparation phase, the evolution phase where mixing can occur and finally the detection phase which is also known as the data acquisition phase. To illustrate the workings of a two-dimensional experiment use is made of chloroform. $^{13}CHCl_3$ gives rise to a two-spin AX system where the A = proton nucleus, and X = carbon-13 nucleus. The normal procedure of accumulating a ^{13}C NMR spectrum consists of a $90°_{x'}$ excitation pulse on the carbon-13 nuclei which is immediately followed by the detection phase in which the FID is recorded. In contrast to the normal procedure of accumulating a ^{13}C NMR spectrum a variable time delay t_1 is now inserted between the excitation pulse and the recording of the FID (fig 2.1).

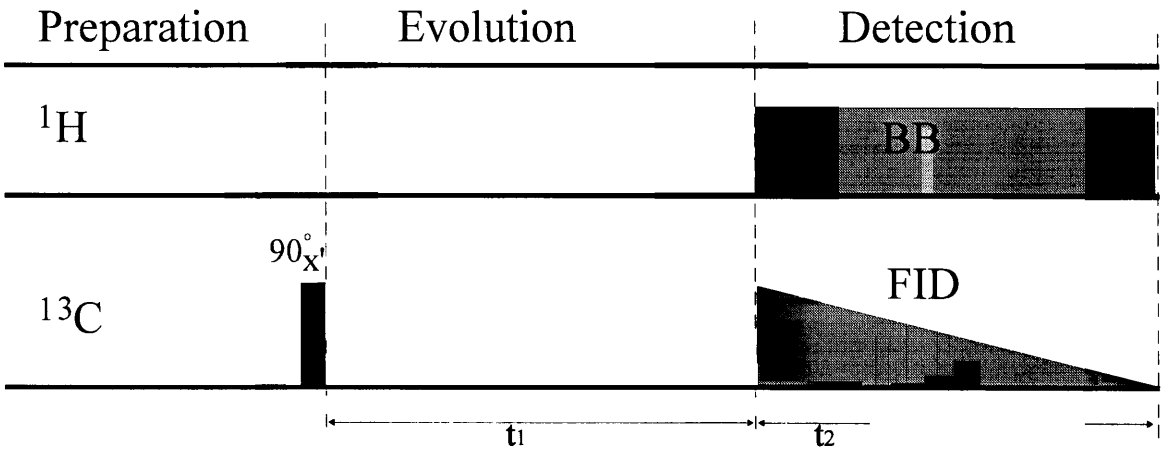

Figure 2.1 The three phases of a two-dimensional NMR expriment.

A number of n experiments are run with different values of t_1, starting with $t_1 = 0$ then increasing the value by constant increments of a few milliseconds from one experiment to the next. If the

FID of each of these n experiments which were accumulated during the data acquisition phase of time t_2 are Fourier transformed it is said that the n interferograms undergo Fourier transformation with respect to t_2 to obtain n frequency domain spectra F_2. Each of these fourier transformed spectra are identical to the normal 1-D ^{13}C NMR spectrum of $^{13}CHCl_3$ with the exception that the intensity of the carbon-13 signal in each spectra will vary from one spectrum to the next. The introduction of the variable time delay t_1 to the experiment has therefore resulted in the observation of a modulation to the intensity of the carbon-13 signal. The signal modulation is caused by the scalar coupling, present during the evolution phase, between the carbon-13 nucleus to its directly bonded proton (C,H coupling).

To aid in the understanding of the mechanics of this experiment use is made of vector diagrams in a rotating coordinate system.[37] Immediately after the $90°_{x'}$ excitation pulse the macroscopic magnetisation M_C of the carbon-13 nuclei lies along the y' direction (fig 2.2). The macroscopic magnetisation M_C consists of two vectors $M_C^{H\alpha}$ and $M_C^{H\beta}$ which arise as a result of the proton in the chloroform molecule being in the α- or the β-state. The vectors $M_C^{H\alpha}$ and $M_C^{H\beta}$ precess with different frequencies (eqn 2.1 and 2.2) where ν_C is the Larmor frequency of the carbon-13 nuclei and J is the coupling constant between the proton and the carbon-13 nucleus.

$$\nu\,(M_C^{H\alpha}) = \nu_C - \tfrac{1}{2}\,J \qquad [2.1]$$

$$\nu\,(M_C^{H\beta}) = \nu_C + \tfrac{1}{2}\,J \qquad [2.2]$$

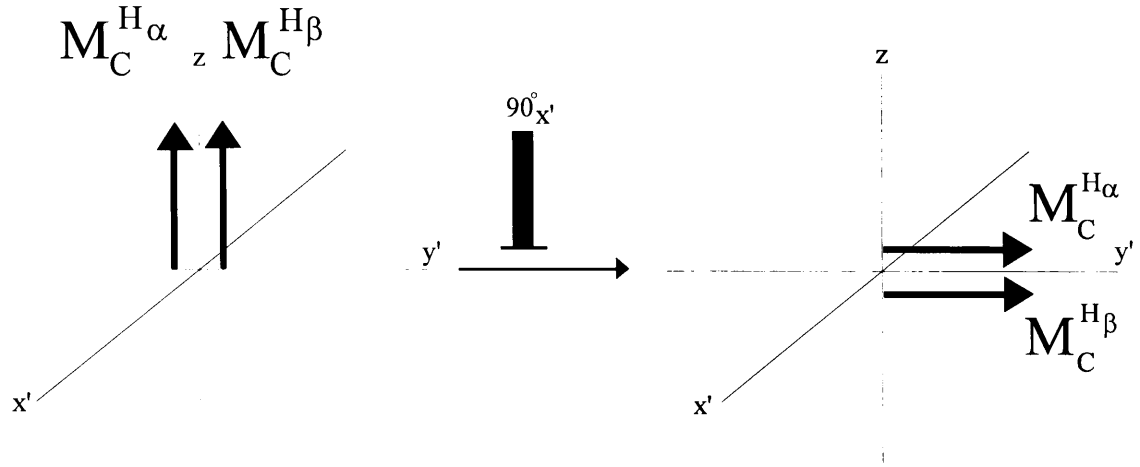

Figure 2.2 A $90°_{x'}$ excitation pulse is given to M_C of the carbon-13 nuclei. The x' and y' are the rotating frame axes. These axes rotate about the z-axis at the same rate as the Larmor frequency of the carbon-13 nuclei.

The coordinate system x', y' shown in figure 2.2 rotates with the Larmor frequency υ_C which is also the average of the two frequencies $M_C^{H\alpha}$ and $M_C^{H\beta}$. The vector $M_C^{H\beta}$ rotates faster than the coordinate system by an amount of ½ J and $M_C^{H\alpha}$ is rotates slower by the same amount. The rotation of the vectors $M_C^{H\alpha}$ and $M_C^{H\beta}$ during the time t_1 is illustrated in figure 2.3. The two vectors $M_C^{H\alpha}$ and $M_C^{H\beta}$ rotate through the angles φ_α and φ_β during the time t_1. The magnitudes of the angles through which the vectors $M_C^{H\alpha}$ and $M_C^{H\beta}$ rotate during the time t_1 are given by:

$$\varphi_\alpha = 2\pi (\upsilon_C - ½ J) t_1 \qquad [2.3]$$

$$\varphi_\beta = 2\pi (\upsilon_C + ½ J) t_1 \qquad [2.4]$$

It is therefore possible to calculate the phase difference Θ of the two vectors.

$$\Theta = \varphi_\beta - \varphi_\alpha = 2\pi J . t_1 \qquad [2.5]$$

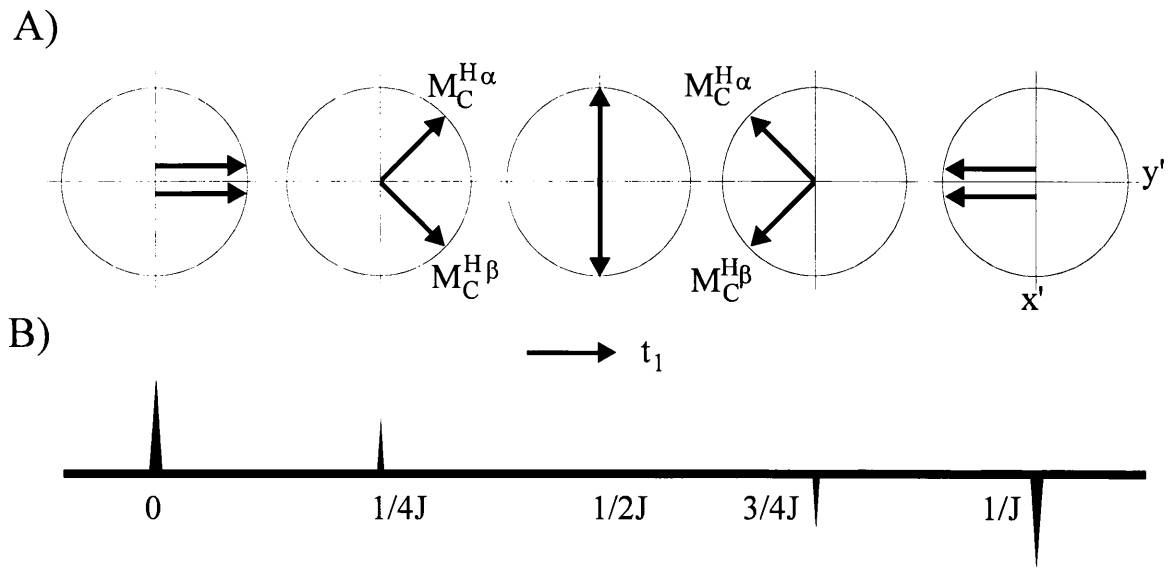

Figure 2.3 A) The evolution of the two vectors $M_C^{H\alpha}$ and $M_C^{H\beta}$ as a function of t_1.
B) Fourier transform of the FIDs with respect to t_2 gives the chemical shift of the carbon-13 nuclei where its amplitude is a function of the evolution time t_1.

The two vectors $M_C^{H\alpha}$ and $M_C^{H\beta}$ only precess at different frequencies whilst the broadband decoupler on the proton nuclei is off. During the data acquisition phase once the broadband decoupler in the proton nuclei is switched on, the C,H coupling is removed and the

fourier transforms with respect to t_2 of all n experiments with different t_1 will consist of singlets. Consider, for example the situation after a time t_1 of 1/4J when according to equation 2.5 the phase difference between the vectors $M_C^{H\alpha}$ and $M_C^{H\beta}$ is 90°. By switching on the broadband decoupler during the data acquisition phase the C,H coupling is removed and the two vectors $M_C^{H\alpha}$ and $M_C^{H\beta}$ now both rotate at the Larmor frequency ν_C. The amplitude induced in the reciever coil is proportional to the vector sum of $M_C^{H\alpha}$ and $M_C^{H\beta}$ along the y'-axis. At $t_1 = 0$ the two vectors are parallel and the vector sum is at its greatest, the carbon-13 signal is therefore at its maximum. At $t_1 = 1/2J$ the sum of the vector components of $M_C^{H\alpha}$ and $M_C^{H\beta}$ is exactly zero so no signal is observed. At $t_1 = 1/J$ the magnitude of the signal is as large as at the beginning but its amplitude is now negative. In figure 2.3 the signals are represented under their corresponding vector diagrams.

If the interferograms collected for n different t_1 values are fourier transformed only with respect to t_2, n F_2 frequency spectra will be obtained. Each spectra will contain one peak at the chemical shift of the carbon-13 nuclues. The signal intensity of this peak will be amplitude-modulated by the C,H coupling constant (J). A second fourier transform of these n F_2 spectra with respect to t_1 will yield two frequencies whose difference corresponds exactly to the C,H coupling constant J.

In conlusion, the F_2 projection contains the chemical shifts and the F_1 projection contains the coupling constants and this information can be represented as a contour plot (fig 2.4). In summary the mathematical transformation is as follows:

$$S(t_1, t_2) \rightarrow S(t_1, F_2) \rightarrow S(F_1, F_2) \qquad [2.6]$$

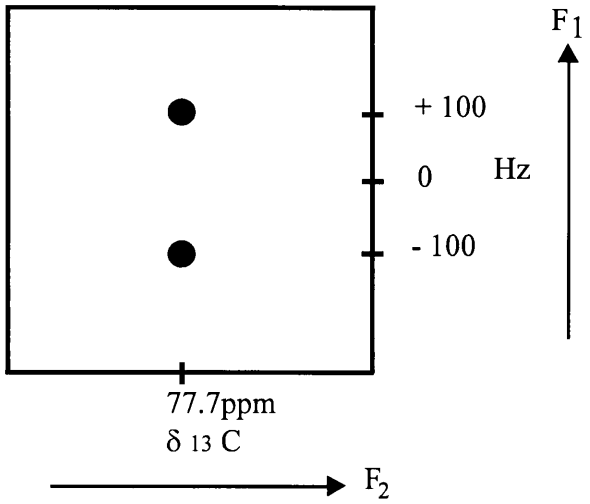

Figure 2.4 The function S (F_1, F_2) represented as a contour plot.

Since the coupling is between nuclei of different species, that is between a proton and a carbon-13 nucleus, this is an example of an heteronuclear two-dimensional J-resolved NMR spectroscopic experiment.

2.3 Heteronuclear shift-correlated NMR spectroscopy

Two-dimensional NMR in the form of ***het***eronuclear shift-***cor***related (HETCOR) NMR spectroscopy offers a way to identify all the directly bonded carbon-proton pairs in a molecule. The AX two-spin system of chloroform where A = proton nucleus and X = carbon-13 nucleus is reused to explain the HETCOR experiment. The NMR pulse sequence of this experiment is given in figure 2.5. The vector representaion of the macroscopic magnetisation of the proton nuclei of chloroform is the model used to explain the rationale behind the HETCOR pulse sequence (fig 2.6).[37] $M_H^{C\alpha}$ and $M_H^{C\beta}$ represent the macroscopic magnetisation vectors of the protons in the chloroform molecules whose carbon-13 nuclei are in the α- and the β-states respectively.

The first $90°_{x'}$ pulse on the proton nuclei turns both vectors $M_H^{C\alpha}$ and $M_H^{C\beta}$ into the y'-direction (fig 2.6.i). As a result of the C,H scalar coupling, J, these vectors rotate at different frequencies

and they therefore move apart (fig 2.6.ii). The frequencies of the two vectors are given by equations 2.7 and 2.8 where υ_H is the Larmor frequency of the proton nuclei and J is the coupling constant between the proton and the carbon-13 nucleus. Equations 2.7 and 2.8 are analogous to equations 2.1 and 2.2, the only difference being that the attention is on the proton nuclei. φ_α and φ_β are the angles between the y'-axis and the vectors $M_H^{C\alpha}$ and $M_H^{C\beta}$ respectively (eqns 2.9, 2.10). The phase difference Θ between these two vectors is given by equation 2.11.

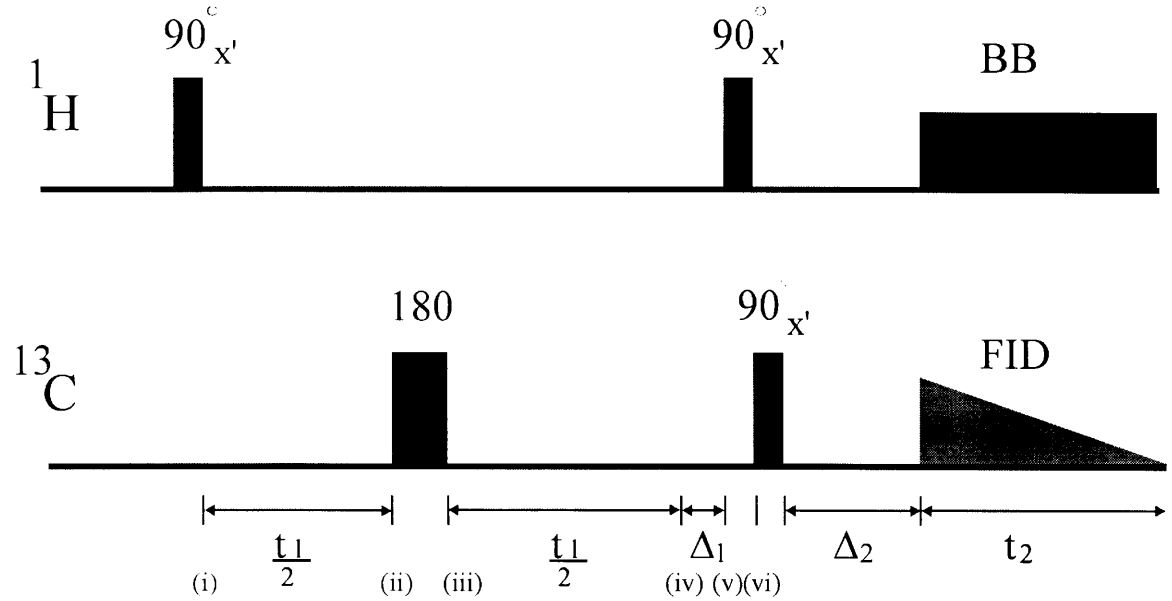

Figure 2.5 A pulse sequence of a HETCOR experiment.

$$\nu\,(M_H^{C\alpha}) = \nu_H - \tfrac{1}{2}\,J \qquad [2.7]$$

$$\nu\,(M_H^{C\beta}) = \nu_H + \tfrac{1}{2}\,J \qquad [2.8]$$

$$\varphi_\alpha = 2\pi\,(\upsilon_H - \tfrac{1}{2}\,J)\,t_1 \qquad [2.9]$$

$$\varphi_\beta = 2\pi\,(\upsilon_H + \tfrac{1}{2}\,J)\,t_1 \qquad [2.10]$$

$$\Theta = \varphi_\beta - \varphi_\alpha = 2\pi\,J\,t_1 \qquad [2.11]$$

After a time period $t_1/2$ the phase difference between the two vectors is $\Theta = \pi\,J\,t_1$ (fig 2.6.ii) and at this stage a 180° pulse to the carbon-13 nuclei inverts the α- and the β-states of these nuclei.

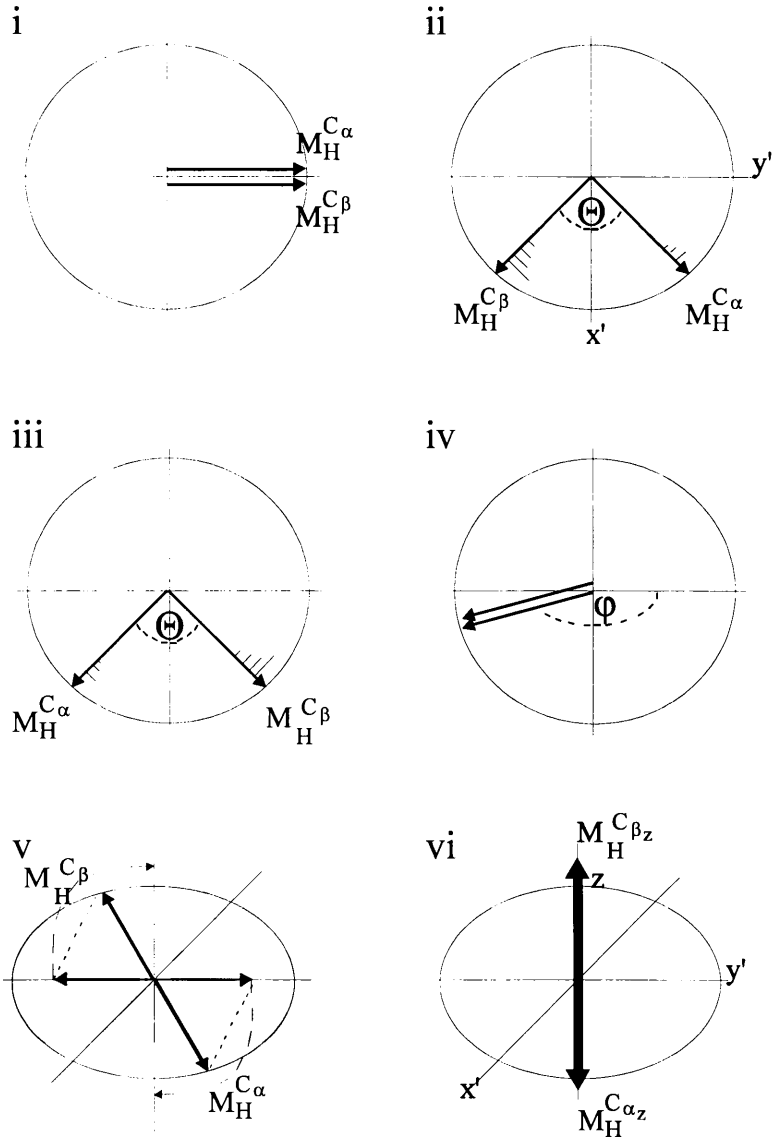

Figure 2.6 A vector representation of the proton macroscopic magnetisation vectors during a HETCOR pulse sequence.

For example the carbon-13 nuclei of the chloroform molecules which were initially in the α-state are now in the β-state. The identity of the slower rotating macroscopic magnetisation $M_H^{C\alpha}$ is changed to that of the faster vector $M_H^{C\beta}$. In the same manner the identity of $M_H^{C\beta}$ is changed to that of $M_H^{C\alpha}$. In figure 2.6.iii it is shown that the vector which is rotating fastest is now following the slower one. After a further interval of $t_1/2$ the vector $M_H^{C\beta}$ has caught up with $M_H^{C\alpha}$ and the two are again in phase. The desired effect of the 180° pulse on the carbon-13 nuclei is to allow the vectors $M_H^{C\alpha}$ and $M_H^{C\beta}$ to coincide after a time t_1 (fig 2.6.iv).

Notice that the total angle φ traveled by the two vectors is only a function of the Larmor

frequency of the proton nuclei and not of the C,H coupling J. If a second $90°_{x'}$ pulse is applied immediately after the period t_1, the vector sum of the $M_H^{C\alpha}$ and $M_H^{C\beta}$ which are in phase will be projected onto the z-axes with no amplitude modulation to the carbon-13 NMR signal due to the absence of polarisation transfer. To introduce this amplitude modulation to the carbon-13 NMR signal an additional delay of Δ_1 is added to the second $t_1/2$ time delay (fig 2.5). This added delay allows the two vectors $M_H^{C\alpha}$ and $M_H^{C\beta}$ to transfer polarisation to the carbon-13 nuclei. The Δ_1 is constant throughout all the pulse sequences of the n interferograms collected. If an arbitrary time of $\Delta_1 = 1/2J$ is used, then the phase difference between the two vectors according to equation 2.11 will be 180° (fig 2.6.v). After the second $90°_{x'}$ pulse the y' components of these two vectors are reflected onto the -z and +z axes, this step changes the population distribution of the energy levels of the proton nuclei. This step is therefore the polarisation step which in turn leads to the amplitude modulation of the macroscopic magnetisation of the carbon-13 nuclei vectors $M_C^{H\alpha}$ and $M_C^{H\beta}$.

It is important to realise that the magnitude of this polarisation step is a function of the angle φ which is governed only by the Larmor frequency of the proton nuclei υ_H. Even though Δ_1 is expressed as a function of the C,H coupling J, it must not be forgotten that Δ_1 is kept constant throughout all the experiments of the n interferograms. This time delay therefore has no varying influence on the carbon-13 signal intensities present in the n interferograms.

After the $90°_{x'}$ pulse on the carbon-13 nuclei reflects the vectors $M_C^{H\alpha}$ and $M_C^{H\beta}$ onto the +y' and -y' axes a time delay of $\Delta_2 = 1/2J$ is inserted before the data acquisition phase (fig 2.5). During this time Δ_2 the angle Θ swept through by the faster vector $M_C^{H\beta}$ is exactly 180° greater than that for $M_C^{H\alpha}$ (eqn 2.5) and these vectors are now in phase. The broadband band pulse on the proton nuclei is switched on which decouples the C,H scalar coupling during the data acquisition period (see fig 2.5).

By fourier transforming the n interferograms with respect to t_2, spectra with only a single carbon-13 resonance are obtained, since the C,H coupling has been removed due to the broadband decoupling on the proton nuclei during the data acquisition phase. The amplitude of the carbon-13 signal present in each of these n spectra is only modulated by the Larmor

frequency of the proton nuclei ν_H as a result of the polarisation step mentioned earlier. Another fourier transformation of all these spectra with respect to t_1 will deliver the chemical shift of the proton nuclei. These fourier transformations can be represented as a contour plot with both the F_1 and F_2 axes being chemical shifts and containing one point (ν_C, ν_H) (fig 2.7).

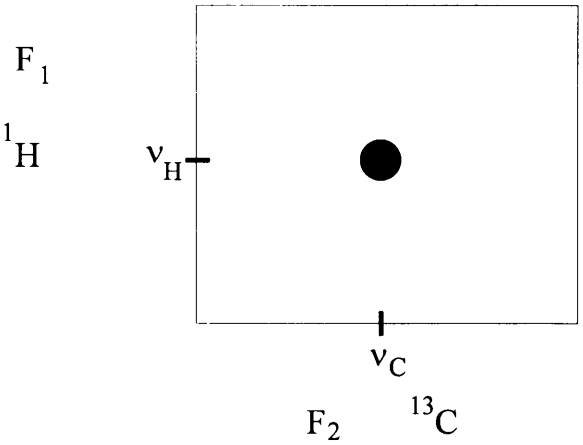

Figure 2.7 A HETCOR spectrum containing the point (ν_C, ν_H).

The HETCOR experiment, like all two-dimensional NMR experiments, describes the environment of the nuclei during the evolution phase. The reflection of a peak found in a HETCOR spectrum onto the F_2-axis corresponds to a chemical shift of a carbon-13 nucleus, the reflection of the same peak onto the F_1-axis will correspond to the chemical shift of a proton nucleus which is directly bonded to the carbon-13 nucleus. The HETCOR experiment can allow the chemist to assign carbon chemical shifts based on known proton chemical shifts or protons based on known carbon shifts. For example, protons that yield a crowded spectrum may be attached to carbons whose spectrum is well resolved, or the converse may occur, where the carbon chemical shifts are very close but the protons are well assigned. This complimentarity makes the HETCOR extremely useful in assigning the proton and carbon spectra of larger molecules.

2.4 Homonuclear shift-correlated NMR spectroscopy

Homonuclear (H,H) shift-*co*rrelated NMR *s*pectroscop*y* (COSY) is a two-dimensional experiment which is capable of identifying protons which are scalar coupled to each other, in so doing the protons within spin systems may be assigned. The COSY experiment is based on the pulse sequence $90°_{x'}$ - $90°_{x'}$ which is applied to the proton nuclei (fig 2.8). The effects this pulse sequence will have on an AX spin system where A and X are both protons with a scalar-coupling constant J is discussed to illustrate the mechanism of the COSY experiment.

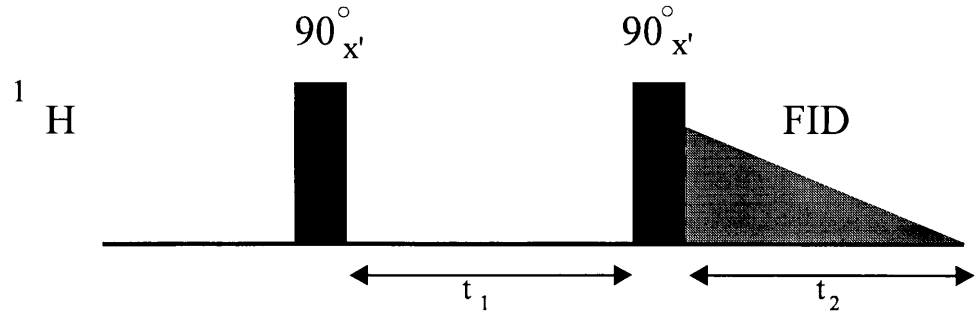

Figure 2.8 The pulse sequence for a (H,H)-COSY experiment.

Due to the J coupling both the A and X nuclei have two macroscopic magnetisation vectors each. For example, the two vectors of the proton nucleus A arise as a result of the X nucleus being in the α- or the β-state. The $90°_{x'}$ pulse on the proton nuclei rotates all the macroscopic magnetisation vectors of both the A and X nuclei onto the y'-axis. These four vectors will rotate in the x',y'-plane with the following frequencies where ν_A and ν_X are the Larmor frequencies of the A and the X protons respectively and J is the coupling constant between A and X:

$$M_A^{X\alpha} = \nu_A - J/2 \qquad [2.12]$$

$$M_A^{X\beta} = \nu_A + J/2 \qquad [2.13]$$

$$M_X^{A\alpha} = \nu_X - J/2 \qquad [2.14]$$

$$M_X^{A\beta} = \nu_X + J/2 \qquad [2.15]$$

After the first $90°_{x'}$ pulse these four magnetisation vectors fan out in the x', y'-plane as a result

of their different frequencies. After the time t_1 each of these vectors have components in the x'- and y'-directions and the second $90°_{x'}$ pulse which follows turns each of the y' components onto the positive and negative z direction. During this step there is a transfer of polarisation. This arises because in a coupled system the second $90°_{x'}$ pulse causes the magnetisation which arose from one transition during t_1 to be redistributed amongst all the others with which it is associated.

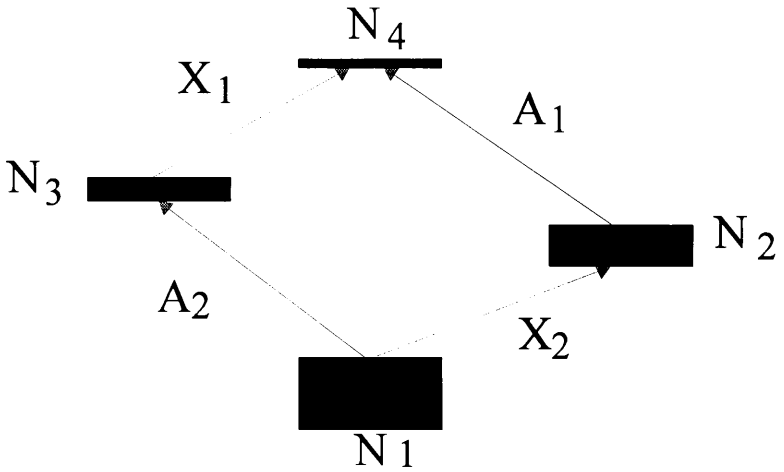

Figure 2.9 The energy leveldiagram for an AX sysytem.

To clarify what is meant by 'all the transitions with which it is associated' refer to the energy diagram of an AX system (fig 2.9). This system has four energy transitions A_1, A_2, X_1 and X_2 and as a result four lines will appear in the ^{1}H NMR spectrum. After the second $90°_{x'}$ pulse, the initial population difference between the energy levels N_2 and N_4, which are resposible for the amplitude of the A_1 line in the ^{1}H NMR spectrum, is changed. In the same manner the population differences between the energy levels responsible for the amplitudes of the lines A_2, X_1 and X_2 also undergo redistribution. The final result is that the amplitudes of each of the four lines in the n F_2 interferograms will be modulated as a function of the amplitudes of one another. The further fourier transform of all the n F_2 interferograms with respect to t_1 can be represented as a two-dimensional plot. This plot is known as a two-dimensional COSY spectrum in which each transition will show crosspeaks to all the other transitions which modulate its amplitude (fig 2.10).

A property of a phase sensitive COSY spectrum is that the coupling constant J can be obtained from the crosspeaks as shown in figure 2.10. This is useful in cases where the overlap of proton

resonances in the ^{1}H NMR spectrum would otherwise prevent a coupling constant from being obtained. Examples of such cases can be found in the ^{1}H NMR spectrum of steroid molecules where in the small region of 1-3ppm as many as twenty proton resonances can be found and the possibility that proton overlap will occur is high.

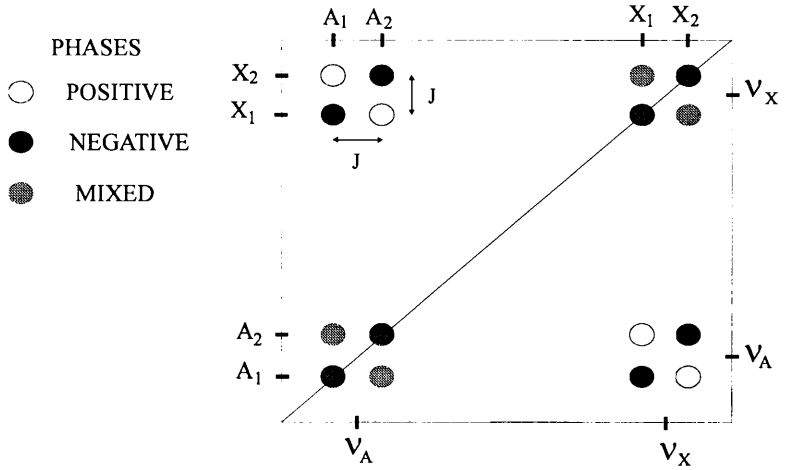

Figure 2.10 An (H, H)- phase sensitive COSY contour plot of a two-spin proton AX system.

At this stage, two very important NMR experiments have been introduced which can lead to the complete assignment of the ^{1}H NMR spectra of complex molecules. The COSY experiment coupled with the use of the HETCOR experiment is a powerful approach to assign the proton chemical shifts of a crowded ^{1}H NMR spectrum. Suppose that a certain C-H bond is established by using the HETCOR experiment. The proton involved in that bond may be coupled to another proton or protons, as indicated by the COSY spectrum. If this other proton is on the same carbon, it will be apparent in the HETCOR spectrum. If not, this other proton must be three or more bonds away. The chemical shift of the coupled proton can be verified by a COSY experiment. The coupled proton may in turn have a correlation that appears in the HETCOR spectrum, thus identifying the carbon atom bound to this proton. In most instances, this procedure will define an HCCH unit. These identified units can then be superimposed on the predicted units derived from a consideration of the complex molecule's structure. Upon reconciling the identified and predicted units, the proton chemical shifts can be assigned.

2.5 The nuclear Overhauser effect

Up till now, the NMR experiments discussed in this chapter have been based on the observation of the through bond coupling (scalar coupling) between nuclei that are covalently linked through one or more bonds. In this section, NMR experiments based on the observation of the through space coupling (dipolar coupling) are examined. These NMR experiments are not dependant on the presence of scalar coupling. Dipolar coupling only occurs between nuclei which are in close spatial proximity to each other. This dipolar coupling is the direct cause of the nuclear Overhauser effect (NOE). This NOE can be observed as a change in the signal intensity of a proton resonance in a one-dimensional NOE experiment or as a crosspeak in the spectrum of a two-dimensional NOE experiment. The observation and quantification of the NOE has turned out to be the most informative sources for the determination of molecular conformation in solution. The relevance of the nuclear Overhauser effect to the study of the conformation of the steroid-cyclodextrin complexes in solution is therefore self-evident. The discussions that follow explain the NOE experiments as well as their possible potential towards the study of the steroid-cyclodextrin complexes.

2.5.1 A 1-D NOE experiment

Consider a two spin system, both are protons, *i* and *s*. Let I_0 be the equilibrium intensity of the resonance of proton *i*. If the intensity of the resonance of proton *i*, while saturating proton *s,* is I, the observed NOE is defined as:

$$\%NOE = \frac{I - I_0}{I_0} \times 100 \qquad [2.16]$$

That is the nuclear Overhauser effect changes the signal intensity of the resonance of proton *i* and this change in intensity can be expressed as a percentage NOE with the use of equation 2.16. From equation 2.16 it can be deduced that the %NOE will be positive if I is greater than I_0 and negative if I is smaller than I_0.

To begin to explain the origins of the nuclear Overhauser effect it must be said that the intensity of an NMR signal is proportional to the difference in the populations of the two energy levels between which the nuclear resonance transition occurs. Consider the energy levels of an AX homonuclear system where A = proton *i* and X = proton *s*. The protons *i* and *s* are not scalar coupled. The absence of scalar coupling is a simplifying assumption and it is not essential in principle, but it makes it easier to explain the nuclear Overhauser effect. The energy levels of this AX spin system is illustrated in figure 2.11. This system has four energy levels, corresponding with the nuclei being in the states αα, αβ, βα and ββ. The transitions between the energy levels 1 and 3 and between 2 and 4 are transitions of the *i* nucleus, while those between 1 and 2 and between 3 and 4 are transitions of the *s* nucleus.

The chemical shift differences between the protons *i* and *s* are very small in comparison with the Larmor frequencies this makes the energy levels of 2 (βα) and 3 (αβ) nearly degenerate in energy. In figure 2.11 the difference in energy between the levels 2 and 3 has only been exaggerated for clarity sake. Due to the absence of scalar-coupling the two transitions of nucleus *i* will be identical as will the two transitions of nucleus *s*. The ^{1}H NMR spectrum of this system at equilibrium will therefore consist of two singlets corresponding to the *i* and *s* nuclei, respectively.

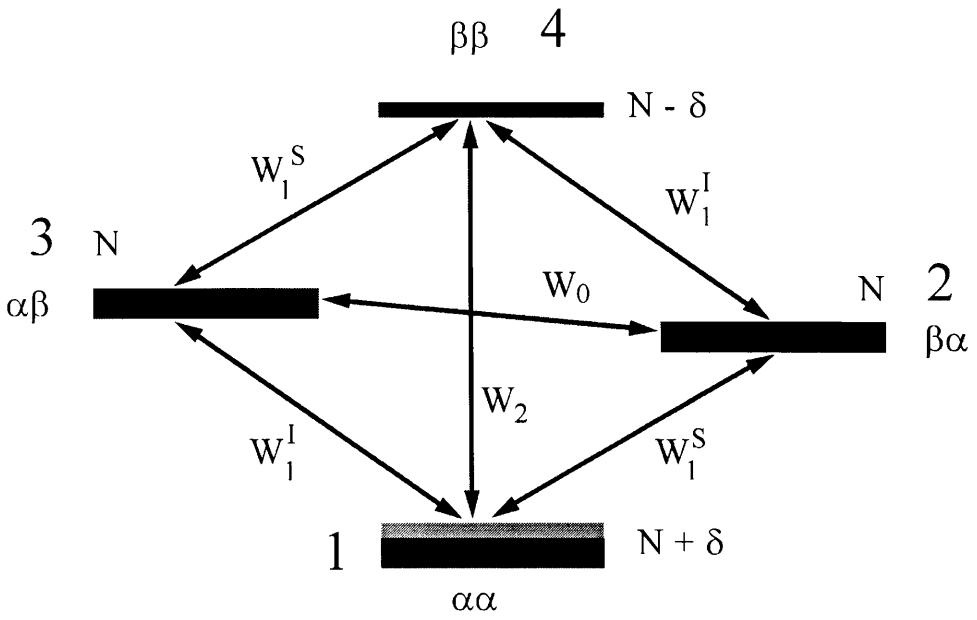

Figure 2.11 AX homonuclear spin system.

Assuming that this system has a total of 4N nuclei, due to the Boltzmann distribution at thermal equilibrium the population distribution will be as in figure 2.11. The αα state, that is energy level 1, being of lower energy will contain an excess of δ nuclei, the high ββ state, level 4, will have a deficiency of δ nuclei. The αβ and βα states due to their energy difference being negligible will both contain an equal amount of N nuclei each.

The population differences between the energy levels at equilibrium can be summarised as follows:

i transitions	αα-αβ	δ	$\Delta M = \pm 1$
	βα-ββ	δ	
s transitions	αα-βα	δ	$\Delta M = \pm 1$
	αβ-ββ	δ	
	αβ-βα	0	$\Delta M = 0$
	αα-ββ	2δ	$\Delta M = \pm 2$

The first four transitions correspond to the single quantum transitions where $\Delta M = \pm 1$. These transitions are quantum mechanically allowed transitions which give rise to the observed NMR signals. The transitions where the change in the quantum number M is zero or two cannot be observed in the NMR spectrum. However these transitions are allowed in the relaxation of the spin system. Therefore all the transitions mentioned above can be used as relaxation pathways for the AX spin system. The rate constant of a relaxation pathway is denoted by W, with a subscript to indicate the change in quantum number M and a superscript to indicate which nucleus the transition belongs to (see fig 2.11).

In performing the NOE experiment, the population differences across some transitions belonging to a nucleus are forced to change. The population differences of other transitions belonging to other nuclei will in turn also change in the attempt to obtain equilibrium for the spin system in question. These changes in population are then observed as changes in the signal intensity of

these other nuclei. For example, both trasitions of the *s* nucleus may be irradiated and the changes in intensity of the signals due to nucleus *i* after the new equilibrium has been established are observed. By considering the population differences after saturation of the *s* nucleus the contribution of each relaxation pathway to re-establish an equilibrium can be qualitatively accessed. The new population differences are:

i transitions	αα-αβ	δ	}
	βα-ββ	δ	} $\Delta M = \pm 1$
s transitions	αα-βα	0	}
	αβ-ββ	0	} $\Delta M = \pm 1$
	αβ-βα	0	
	αα-ββ	2δ	$\Delta M = 0$
			$\Delta M = \pm 2$

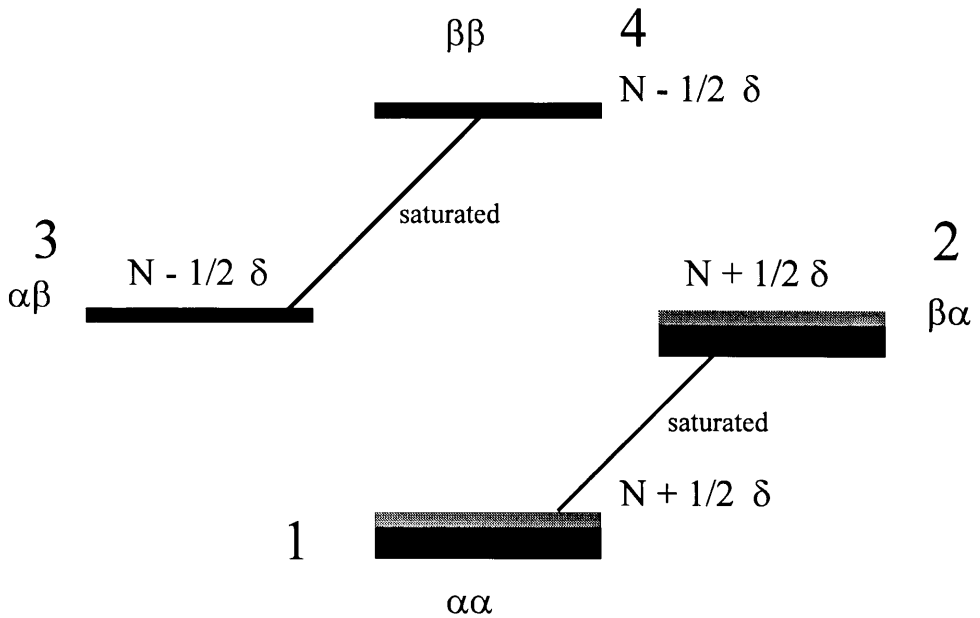

Figure 2.12 Population distribution immediately after saturation of the proton s signal.

These population differences have been obtained with the aid of figure 2.12, where it can been seen that the saturation of the signal of the *s* nucleus causes the populations between energy levels 1 and 2 to be equal as well as the populations between levels 3 and 4 to be equal. This system is clearly no longer at equilibrium and it is up to the relaxation pathways to reobtain the equilibrium population differences. Obviously the relaxation pathway which has the rate W_1^S cannot be used to transfer populations because the population differences are fixed as a result of the saturation of the signal of the *s* nucleus. The population difference across each *i* transition, that is between levels 1 and 3 and between levels 2 and 4, at thermal equilibrium was δ, and during the saturation of the signal of the *s* nucleus this difference is still δ. As far as the relaxation pathway with the rate W_1^I is concerned no change in the populations is necessary. In summary, if single quantum transitions, where $\Delta M = \pm 1$, were the only relaxation pathways allowed in the relaxation mechanism of the spin system, the saturation of the transitions of the *s* nucleus will not affect the signal intensity of the *i* nucleus.

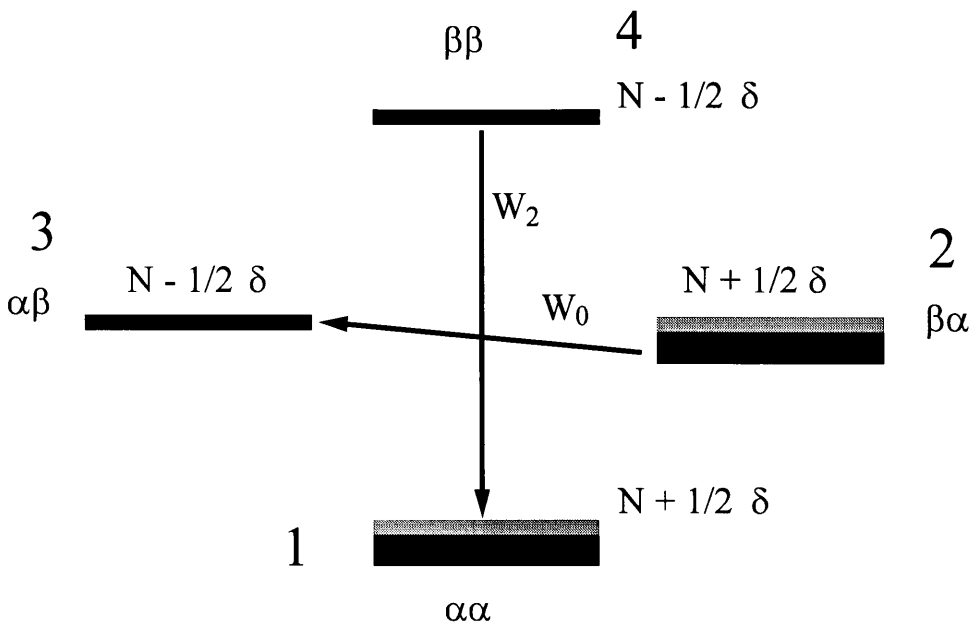

Figure 2.13 The initial direction of the attempt of the relaxation pathways to restore equilibrium after saturation of the proton s signal.

It is left to the relaxation pathways with the rates W_0 and W_2 to produce a nuclear Overhauser effect to nucleus *i* which will change the signal intensity of this nucleus. As shown in figure 2.13,

W_0 acts to transfer population from the state $\beta\alpha$ (level 2) to the state $\alpha\beta$ (level 3) in an effort to return the present population difference between these state of δ to its original equilibrium state of 0. This results in an increase to the population of energy level 3 and a decrease to the population of energy level 2. W_0 therefore causes the population differences between the levels 1 and 3 and between the levels 2 and 4 to decrease. These population decreases are between the energy levels used for the transitions of the *i* nucleus. The decreases in population difference therefore causes a decrease in the signal intensity of the *i* nucleus.

The relaxation pathway with the rate W_2 acts to transfer population from the energy level 4 to level 1 to restore the original equilibrium difference of 2δ. This attempt to restore equilibrium results in a decrease in the population of level 4 and an increase in the population of level 1. W_2 therefore allows the population differences between levels 1 and 3 and between levels 2 and 4 to increase. These increased population differences will result in an increase to the signal of the *i* nucleus.

To conclude, if the pathway with the rate W_0 is the dominant relaxation pathway then saturating the signals of the *s* nuclei will cause a decrease in the signals of the *i* nucleus. In other words, there is a negative NOE at nucleus *i* due to saturating the transitions of nucleus *s*. If the pathway with the rate W_2 is the dominant relaxation pathway then saturating the signals of the *s* nucleus result in a positive NOE at the nucleus *i*.

When is the relaxation pathway with the rate W_2 predominant, and when W_0? The magnitude of the contribution from the dipolar relaxation mechanism is not only a function of the distance between nuclei. This magnitude is also a function of the orientation of the magnetic dipoles of the nuclei with respect to each other as well as the time they spend in that particular orientation. In other words, the dipolar relaxation mechanism is a function of the motion of nuclei in solution. For the sake of simplicity, a single parameter known as the molecular correlation time (τ_C) is defined which approximates the time required for a molecule to change from one orientation to another. The parameter τ_C therefore incorporates the influences of molecular weight, solution viscosity, temperature and so forth into one single parameter. There is a general trend between the molecular weight and the molecular correlation time τ_C. Small molecules will have short

correlation times τ_C and the relaxation pathway with the rate W_2 will dominate. This will result in a positive nuclear Overhauser effect. Larger molecules such as macromolecules will have long correlation times τ_C and the pathway with the rate W_0 will dominate. In this instance a negative nuclear Overhauser effect will be observed.

2.5.2 The 2-D NOESY experiment

In the 1-D NOE experiment only the resonances of one proton can be saturated at a time and in this way the NOE to the other protons can be determined as a result of a decrease or increase in their signal intensities.Unlike the 1-D NOE experiment the two-dimensional nuclear Overhauser effect spectroscopy (NOESY) experiment is able to detect all the NOE's between all the protons in one experiment. In the 2-D NOESY spectrum the diagonal contains all the proton resonances found in the corresponding ^{1}H NMR spectrum, as is the case for the diagonal found in the COSY spectrum. The manner of interpreting the 2-D NOESY spectrum is similar to that of the COSY spectrum except that the crosspeaks are the result of the nuclear Overhauser effect whereas in the COSY spectrum the crosspeaks are the result of scalar coupling.

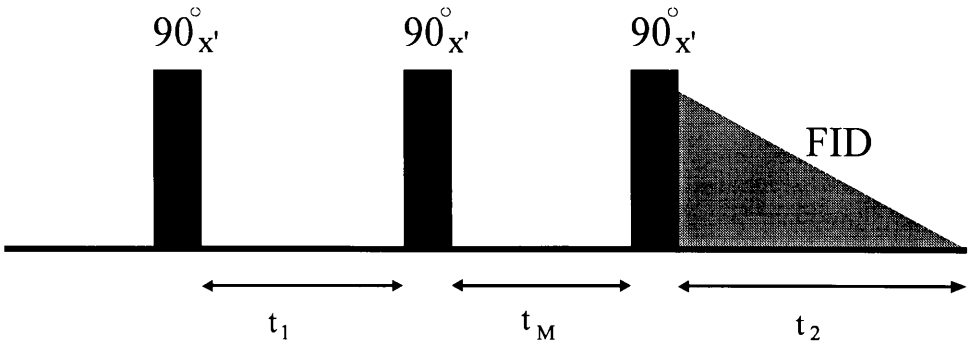

Figure 2.14 A pulse sequence for a 2-D NOESY experiment.

The pulse sequence of the 2-D NOESY experiment is illustrated in figure 2.14. The first part of this pulse sequence, $90°_{x'} - t_1 - 90°_{x'}$, corresponds to the pulse sequence of the COSY experiment illustrated in figure 2.8. From a consideration of an homonuclear AX system which is not scalar coupled, the A nucleus will be in a polarised state immediately after the second $90°_{x'}$ pulse. During the following interval t_M, polarisation is transferred from the A nucleus to the X by the

dipolar relaxation mechanism and this interval is known as the mixing stage. After this mixing interval a further $90°_{x'}$ pulse is applied to the proton nuclei which rotates portions of the macrscopic magnetisation vectors of the A and the X nuclei onto the y'-axis to record the FID during the time t_2. This pulse sequence is repeated for a series of different values of t_1 whilst keeping the mixing time t_M constant. The accumulated FIDs then undergo a second Fourier transformation with respect to t_1. This Fourier transformation can be represented as a two-dimensional chemical shift spectrum with crosspeaks at the positions (ν_A, ν_X) and (ν_X, ν_A). These crosspeaks are as a result of a nuclear Overhauser effect between the two nuclei.

2.5.3 The 2-D ROESY experiment

The use of two-dimensional ***r***otating frame nuclear ***O***verhauser ***e***ffect ***s***pectroscop***y*** (2-D ROESY) was favoured above that of the 2-D NOESY experiment for the observation of NOE crosspeaks between the protons of the steroid and cyclodextrin molecules of this study. The reasons for prefering the 2-D ROESY experiment will be explained. From the study by Schneider et al[36] (see 1.5.2.3) the molecular weights of the complexes investigated ranged between 1400-1600g/mol (1100g/mol and 1300g/mol for β- and γ-cyclodextrin respectively, 298g/mol for the 1-anilino-8-naphthalenesulphonate (ANS) guest molecule). In this study of steroid-cyclodextrin complexes the average molecular weight of a steroid was 300g/mol. Therefore the molecular weights of the complexes of this study also varied between 1400-1600g/mol. On the grounds that both the study by Schneider et al[36] and this study used host-guest complexes of similar molecular weights it is expectd that these complexes will have approximately the same correlation times τ_C. This group observed that the 2-D ROESY experiment circumvented the problem of extremely small NOE crosspeaks found in the 2-D NOESY experiment which result from unfavourable correlation times τ_C. The 2-D ROESY is to be favoured over the 2-D NOESY experiment when unfavourable correlation times τ_C lead to a situation where $W_2 - W_0 = 0$, and hence to a situation where the cross-relaxation rate vanishes and as a result no nuclear Overhauser effect.[58] The study of Schneider et al[36] used a 400MHz- and in this study a 500MHz- NMR spectrometer was used to record the 2-D ROESY experiments of the host-guest complexes. Not only are the correlation times τ_C of the complexes of the two studies similar, both studies also used high field NMR spectrometers to record the 2-D ROESY experiment.

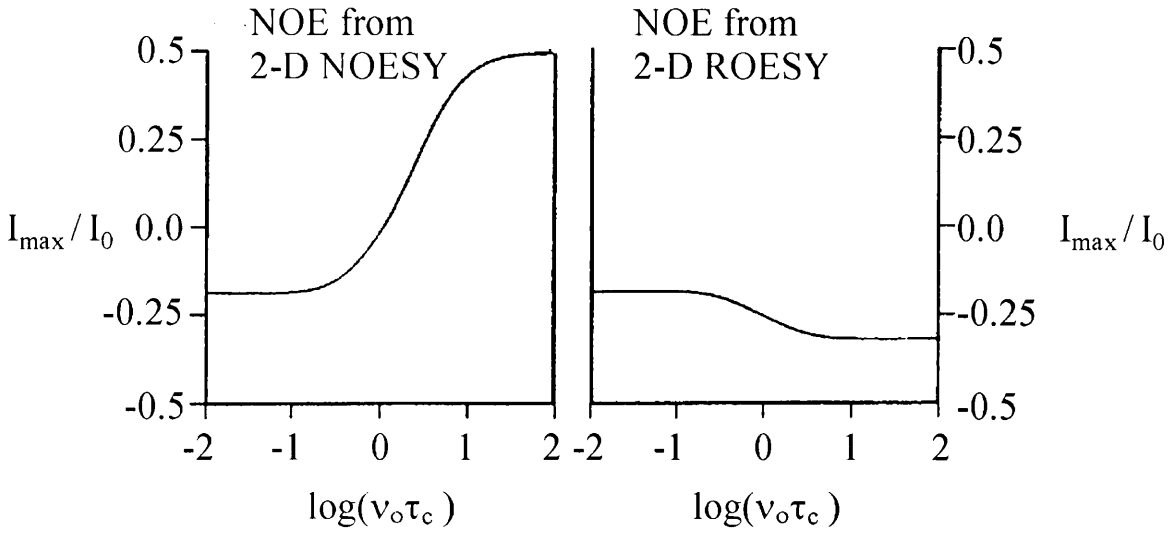

Figure 2.15 A representation of the relationship between the correlation time and the signal intensity of a crosspeak in a 2-D NOESY and ROESY experiment.

It is apparent that there is an important relationship between the correlation times τ_C of the molecular system under study and the choice of two-dimensional experiment to observe NOE crosspeaks. Figure 2.15 illustrates the relationship between τ_C and the NOE crosspeak intensity found in 2-D NOESY and 2-D ROESY spectra of a two spin system.[58] The x-axes is the logarithmic scale of $\nu_0 \times \tau_C$. The constant ν_0 is the Larmor frequency of a proton nucleus. The y-axes is the ratio I_{max} / I_0. The value I_0 is the normalised intensity of a diagonal signal and I_{max} is the maximum intensity of a crosspeak in the 2-D NOESY or 2-D ROESY spectra. Per definition, I_{max} / I_0 will be positive if the NOE crosspeak has the same phase as the diagonal signal and I_{max} / I_0 will be negative if the crosspeak is of opposite phase to the diagonal signal. From the graphs, the cross signal intensity of the 2-D NOESY experiment is ca. 20% at $\tau_C \rightarrow 0$ which can be the case for molecules of small molecular weight. At $\tau_C \rightarrow \infty$ the signal intensity for the 2-D NOESY spectrum is ca. 50% which can be the case for macromolecules such as proteins. But for $\upsilon_0 \times \tau_C = 1$, that is $\log (\nu_0 \times \tau_C) = 0$, the cross signal vanishes and to circumvent this problem use can be made of the 2-D ROESY experiment. The vanishing of the cross signal can arise for molecules of intermediate molecular weight. In the 2-D ROESY experiment the cross signal intensity is ca. 20% for $\tau_C \rightarrow 0$ and ca. 34% for $\tau_C \rightarrow \infty$. Notice that for no value of τ_C does

the NOE cross signal vanish in the 2-D ROESY spectrum. And what is more, the instance where log ($\nu_0 \times \tau_C$) = 0 the cross signal intensity will not be less than ca. 20%.

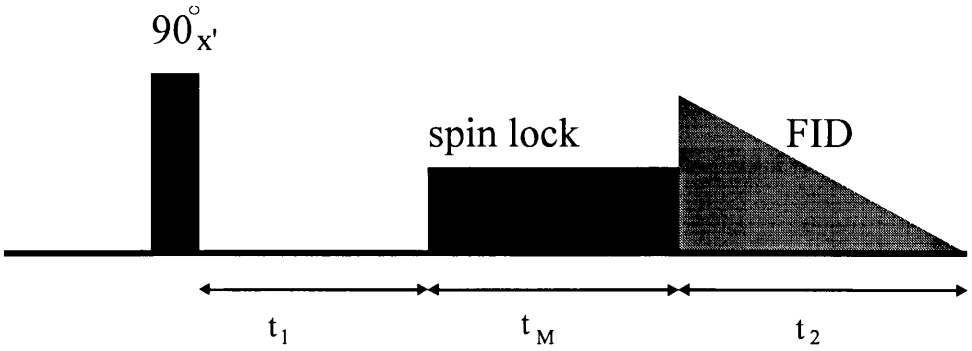

Figure 2.16 A pulse sequence for a 2-D ROESY experiment.

The pulse sequence of the 2-D ROESY experiment is illustrated in figure 2.16. A distinguishing difference between the pulse sequences of the 2-D NOESY and 2-D ROESY experiments is that during the mixing stage of the 2-D ROESY experiment there is a spin lock for the duration t_M. This spin lock keeps the transverse components of the macroscopic magnetisation of the proton nuclei in the x',y'-plane. These transverse components therefore cross-relax whilst remaining locked in the x',y'-plane. This causes the relaxation rates W_0, W_1 and W_2 always to be positive and $W_2 - W_0 \neq 0$.[58] The NOE crosspeaks obtained from 2-D ROESY spectra will always be of opposite phase with respect to the phase of the diagonal signal (see fig 2.15).

The NOE buildup rate in a 2-D ROESY experiment is faster than the NOE buildup rates found in a 2-D NOESY experiment.[58] As a consequence, the time for which the linear approximation of the NOE with respect to distance is valid for the ROESY experiment is shorter than in the NOESY experiment. In cases where t_M is short the linear approximation can be valid for the ROESY experiment and a quantitative evaluation of these NOE's can be made. This evaluation is made on the theoretical basis that the intensity of a measured NOE is proportional to $1/r^6$ where r is the distance between the two protons in question. The previous statement may be true for some isolated examples but in many cases it is an oversimplification and should be used with caution since distance is not the only factor which can determine the magnitude of the NOE.[58]

An extremely important consideration must be made when evaluating the intensities of the NOE crosspeaks of a 2-D ROESY spectrum. *Coherent transfer between scalar-coupled spins* can arise during the 2-D ROESY experiment.[59] This coherent transfer causes crosspeaks, which have the same phase as the diagonal, to appear in the 2-D ROESY spectrum between protons which are scalar coupled. These crosspeaks, also known as Hartmann-Hahn type crosspeaks, are to be avoided since their presence will diminish and they might even quench the underlying NOE crosspeaks which are of opposite phase to the diagonal. When coherent transfer between scalar-coupled spins is present quantitative evaluations of NOE crosspeaks cannot be made.

A strong spin-lock field applied far off from the mid-point of the ^{1}H NMR spectrum is the most widely used strategy to try and minimse the contribution from these Hartmann-Hahn type crosspeaks.[60] But in this study there are not expected to be any contribution from Hartmann-Hahn type crosspeaks to the intermolecular NOE crosspeaks of the steroid and cyclodextrin protons. There is no possibility for scalar coupling between the protons of the steroid and cyclodextrin since these protons are not covalently bonded. The opportunity for coherent transfer between these non-scalar coupled protons does not exist.

3 The assignments of the steroid protons

3.1 Introduction

The proton resonances of both the steroid and the cyclodextrin in the ^{1}H NMR spectrum must be assigned if any conformational sense is to be made from data obtained from NOE experiments. The assignment of the ^{1}H NMR spectra of β- and γ-cyclodextrins is straightforward since these spectra only consist of six proton resonances. These protons are all part of one spin-system and a single two-dimensional COSY spectrum of the cyclodextrin in question is sufficient to unambiguously assign the resonances of all the cyclodextrin protons 1, 2, 3, 4, 5 and 6. The focus of this chapter is the complete assignment of the challenging complex proton spectra of the steroids cyproterone acetate, ethynyl oestradiol and danazol. To facilitate the study of the steroid-cyclodextrin complexes in water it will be more advantageous to initially assign the proton resonances of the pure steroid in D_2O. The three steroids are totally water-insoluble and no steroid proton resonances were observed from a steroid sample prepared in D_2O. All three steroids are soluble in $CDCl_3$. As an alternative, the complete assignment of the proton resonances of a steroid sample prepared in $CDCl_3$ can be used to help assign the steroid proton resonances found in a ^{1}H NMR spectrum of a steroid-cyclodextrin complex prepared in an aqueous medium.

The proton spectra of steroids are usually extremely crowded and many proton resonances can be concealed in the so-called steroid hump or methylene envelope between 0.5ppm and 2.0ppm. To simplify the steroid proton spectrum somewhat, a high-field NMR spectrometer is needed to provide some deconvolution to the overlapping proton resonances. Hall and Sanders[61] have concluded from their steroid NMR studies that the ratio of the chemical shift in hertz between two coupled resonances, $\Delta\delta$, and their scalar coupling, J, must be greater than 3 to provide first-order mutiplets that is $\Delta\delta/J \geq 3$. Two chemical shifts which have a shift difference of 0.01ppm will be 20Hz apart if the proton spectrum is accumulated on a 200MHz NMR spectrometer. If these two protons have a scalar-coupling of 10Hz there will be higher order effects according to the criteria of Hall and Sanders. If this same proton spectrum is run on a 500MHz NMR

spectrometer the chemical shift difference between these two protons will be 50Hz. This shift difference satisfies the criteria that $\Delta\delta/J \geq 3$ and the coupling pattern between these two protons will be first order. Obviously the higher the magnetic field strength the lower the presence of higher order effects in the 1-D ^{1}H NMR spectrum. The steroid proton NMR spectra of this study were recorded with a 500MHz Bruker NMR spectrometer. The assignment of the steroid proton resonances fortunately began with the advantages associated with a high magnetic field NMR spectrometer.

3.2 The assignment strategy

When devising a strategy which will economically and unambiguously assign the steroid proton resonances two important considerations must be kept in mind. The strategy must first correlate the proton resonances to the two-dimensional carbon-steroid framework. Secondly, the three-dimensional orientation of the steroid protons, whether axial or equatorial and whether α- or β-facing, must be determined. The assignment strategy, illustrated in figure 3.1, incorporates these two considerations. The 2-D heteronuclear-correlation experiments, the HMQC and HMBC, and the 2-D homonuclear-correlation experiment, the phase sensitive DQF-COSY, aid in correlating the proton resonances to the carbon-steroid framework. The two NMR parameters, the coupling constants and the nuclear Overhauser effects between steroid protons, help in assigning the stereochemistry of these steroids. More is said about each step involved in the assignment strategy below the headings that follow.

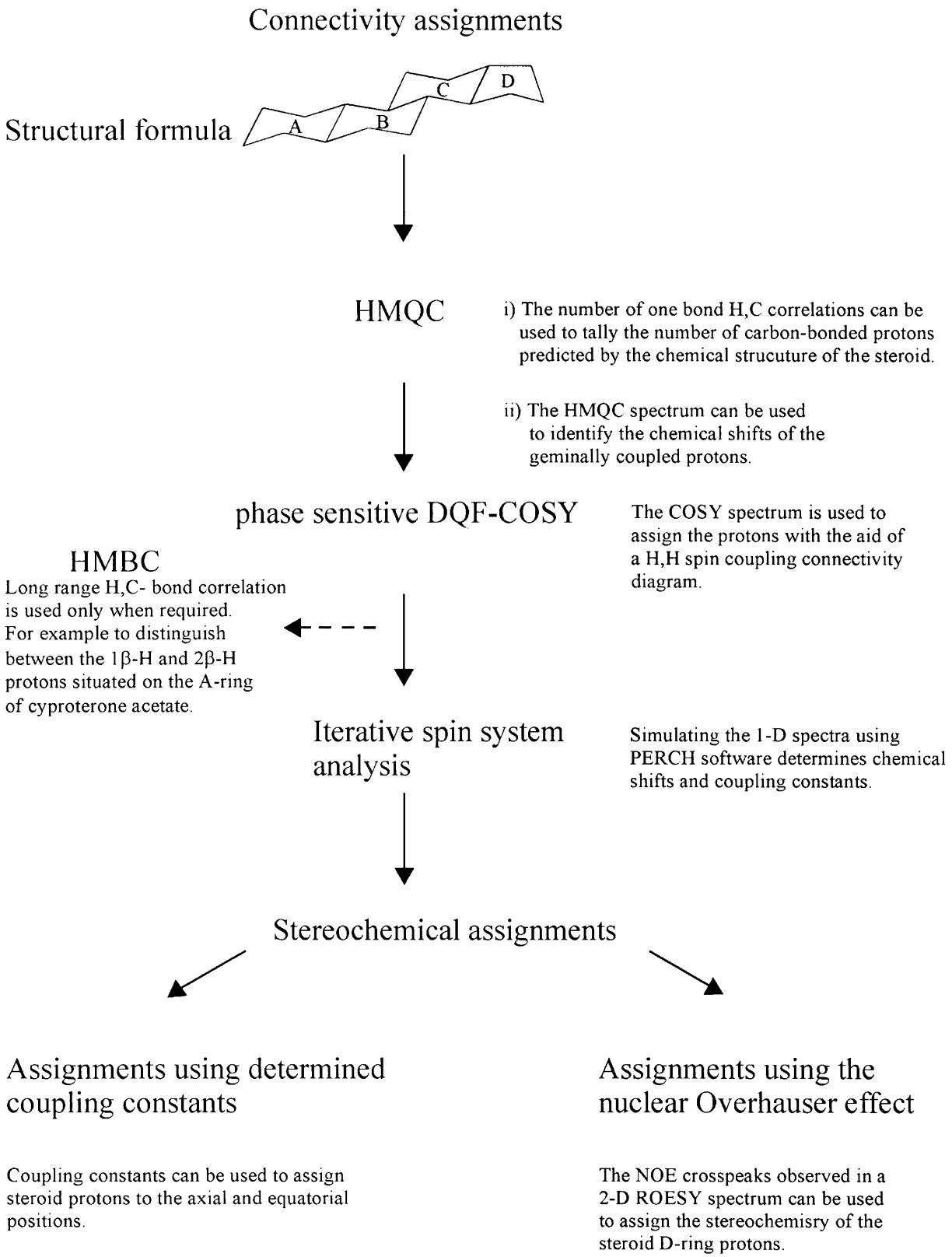

Figure 3.1 The strategy used to completely assign the proton resonances of the steroids cyproterone acetate, ethynyl oestradiol and danazol.

3.2.1 The Heteronuclear Multiple-Quantum Correlation (HMQC) experiment

The HMQC experiment is analogous to the HETCOR experiment in the respect that both experiments reveal the proton and carbon-13 atoms that are connected through a one-bond C,H coupling. The HETCOR experiment, introduced in chapter two, is the classical H,C correlation experiment and it is based on accumulating the FIDs of the carbon-13 nuclei, where the amplitudes of the carbon-13 resonances in the fourier transformed spectra of these FIDs have been modulated by the chemical shifts of the coupled protons (see fig 2.5). An example of a HETCOR spectrum is shown in figure 2.7 where a coupled H,C-pair is represented by a point (ν_C, ν_H) . The chemical shift of the carbon-13 nuclei is found by reflecting this point onto the F_2-axis and the chemical shift of the correlated proton is determined by reflecting this point onto the F_1-axis. In contrast to the HETCOR experiment, the methodology of the HMQC experiment is based on detecting the FIDs of the proton nuclei during the detection phase of the pulse sequence. The amplitudes of the proton resonances found in the fourier transformed spectra of these FIDs are amplitude-modulated by the chemical shifts of the coupled carbon-13 nuclei. The HMQC experiment is an example of a two-dimensional inverse-detected experiment. The term 'inverse' refers to the fact that this experiment is based on observing the FIDs of proton nuclei whereas the HETCOR experiment records the FIDs of the carbon-13 nuclei. The HMQC experiment is far more sensitive than the HETCOR.[58,62] In the HMQC spectrum an H,C one-bond correlation will be represented by a point (ν_H, ν_C). Contrary to the interpretation of the HETCOR spectrum, the chemical shift of the proton nuclei can be found by reflecting this point (ν_H, ν_C) onto the F_2-axis and the chemical shift of the coupled carbon-13 nucleus is found by reflecting the point onto the F_1-axis.

This chapter is focussed on the applications of two-dimensional NMR experiments to assign complex ^{1}H NMR spectra. As shown in figure 3.1, one of the primary steps towards the assignment of the ^{1}H NMR spectrum is the acquisition of an HMQC spectrum. This experiment effectively uses the resolution of the carbon axis to separate the proton signals. The HMQC spectrum therefore allows the carbon and proton resonances to be tallied and thus confirm the empirical formula of the steroid. Secondly this spectrum also enables the sorting of the methyl-,

methylene- and methine-carbon atoms because these atoms will be correlated to three-, two- and one-proton atom, respectively. The HMQC spectrum also allows the identification of the chemical shifts of the geminal proton pairs. The two protons that are correlated to the same methylene carbon are defined to be a geminal pair. At a later stage it will become apparent how the knowledge of the chemical shifts of these geminal proton pairs can simplify the interpretation of the corresponding COSY spectrum.

The first step in interpreting a steroid ^{1}H NMR spectrum is to determine the number and chemical shift of the proton resonances. To check that all the proton resonances from the methine- (CH), methylene- (CH_2) and methyl-groups (CH_3) that are predicted from the chemical structure of the steroid can be accounted for. A single HMQC spectrum is therefore capable of completing the first step towards the analysis of a steroid ^{1}H NMR spectrum.

An example of another inverse detected two-dimensional experiment is the ***H***eteronuclear ***M***ultiple-***B***ond ***C***orrelation (HMBC) experiment. The distinguishing difference between the HMBC spectrum and the HMQC spectrum is that the former shows crosspeaks between proton and carbon-13 nuclei which are scalar-coupled through two or more bonds whereas the latter spectrum shows crosspeaks between proton and carbon-13 nuclei which are scalar-coupled through one bond only.

Heteronuclear experiments therefore allows the sharing of assignment information between carbon and proton data, not only via coupling between the protons attached to carbons as in the HMQC spectrum, but also through the couplings between a carbon and the protons of nearby carbons as in the HMBC experiment. The HMBC experiment was only required for the assignment of the 1β-H and 2β-H protons situated on the A-ring of cyproterone acetate. This instance will be discussed during the second-half of this chapter.

3.2.2 The phase sensitive DQF-COSY experiment

An important advantage in the assignments of the steroid proton resonances is that the chemical structures of all three steroids are known. This allows a H,H spin coupling connectivity diagram

to be predicted without any prior inspection of the corresponding COSY spectrum. This spin coupling connectivity diagram represents the complex connectivities that can be revealed by a COSY spectrum. In this study, as a result of the complexity which is present in the COSY spectra of the steroids, the connectivity diagrams are used as 'road maps' to aid in the interpretation of the COSY spectra.

The strategy for analysing a steroid's COSY spectrum is straightforward. For many steroids the entire spin system is interconnected. For such a spin-coupled network it is logical to consider the molecule ring by ring with the aid of the connectivity diagram as well as the knowledge of the chemical shifts of the geminal pairs. In interpreting the COSY spectrum in this fashion, a starting point must be established by assigning at least one proton. In the ideal case the rest of the spin system structure may be developed by scalar-connectivities displayed in the COSY spectrum. In practice some connectivities are obscured by crosspeak overlap, so several starting points might be needed to complete the assignment of the spectrum. On the other hand, if the obscured connectivity is a crosspeak connecting the two protons of a geminal pair, the crosspeak's presence can be indirectly confirmed from the chemical shifts of this geminal pair as determined from the HMQC spectrum.

When the COSY experiment is used in the magnitude calculation mode the fine structure of the crosspeaks are distorted. This distortion allows for the possibility that the exact location of the mid-point of a crosspeak cannot be determined when there is cross-peak overlap. The importance of the mid-point of a crosspeak lies in the fact that the chemical shifts of the two scalar-coupled protons responsible for the crosspeak can be obtained from the reflection of the mid-point onto the F_1 and F_2 axes, respectively. The phase sensitive COSY experiment preserves the fine structure of the crosspeaks. By taking the fine structure into account it may be possible to identify the mid-points of these overlapping crosspeaks. An example of such an occasion is found in the phase sensitive COSY spectrum of cyproterone acetate in $CDCl_3$ (fig 3.8). If this spectrum were accumulated in the magnitude mode the mid-points of the two slightly overlapping crosspeaks of 16α-15β and 15α-15β would not have been obvious. Whereas in the phase sensitive COSY spectrum these mid-points are apparent as can be seen in figure 3.8. Furthermore, in this study use is made of the phase sensitve double-quantum filtered (DQF)

COSY experiment which removes the intense methyl singlets and therefore yields a cleaner COSY spectrum.[63,64]

3.2.3 Iterative spin-system analysis

It is necessary to include an iterative spin-system analysis into the assignment strategy since a successful simulation of the 1-D ^{1}H NMR spectrum is conclusive evidence that the assignments of the proton resonances are reliable. The coupling constants obtained from the simulation can be used to assign the spatial orientation of protons whenever possible. The iterative spin-system analysis was carried out on PERCH software for a desktop computer.[65]

The procedure used to simulate the proton spectra was as follows:

i) An experimental proton spectra of the respective steroid was accumulated.

ii) The chemical shifts and approximate coupling constants obtained from a 1st order analysis were used as initial parameters with which to simulate an initial approximate proton spectrum

iii) A line-frequency fitting approach was applied where the frequencies of the tops of peaks from the experimental proton spectrum were used to assign by inspection the peak-tops of the initial calculated proton spectrum.

iv) After completion of these assignments, the LAOCOON3 type iteration which was developed by R. Laatikainen[66], available within the PERCH software package, was used to deliver a converged simulated proton spectra with the resulting calculated chemical shifts and coupling constants.

Examples of PERCH simulations can be found in this chapter where a visual comparison between the experimental and simulated spectra is convincing of a successful convergence.

3.2.4 The stereochemical assignments

Two aspects of the stereochemistry of steroid protons must be determined, these are whether the protons are axial or equatorial and secondly whether the protons are on the α- or the β-face of

the steroid. Consider a plane which passes through as many of the carbon atoms of the steroid A-, B-, C- and D-rings as possible. The β-face of this steroid-plane will be that face in which the methyl protons CH_3-18 and CH_3-19 are found. The α-face is the opposite face.

3.2.4.1 Stereochemical assignments using coupling constants

An important contribution to the understanding of vicinal couplings in saturated systems was made by Karplus[67]. It was discovered that the vicinal coupling constant, ^3J, is a function of the dihedral angle, Φ, between the C-H bonds under consideration. From a consideration of the vicinal coupling constants of a number of conformationally rigid saturated systems of which the dihedral angles are known, Karplus was able to derive a theoretical relationship between the vicinal coupling and the dihedral angle. An example of such a relation is given as equation 3.1 and this function is plotted in figure 3.2.

$$^3J = 4.22 - 0.5 \cos \Phi + 4.5 \cos 2\Phi \qquad [3.1]$$

Reparameterisation of the Karplus equation is carried out by various research groups in order to obtain the smallest deviation between prediction and experiment. One of the most recent reparameterisations was published by C. Altona et al[68].

An important application of the Karplus relationship is in determining the conformations and configurations of ethane derivatives and saturated six-membered rings. It can be predicted from the Karplus relationship that if saturated six-membered cyclohexane or carbohydrate derivatives are in the chair conformation, the vicinal coupling constant between axial-axial protons, with a dihedral angle of 180°, will be larger than the coupling constant between axial-equatorial and equatorial-equatorial protons, where the dihedral angles are approximately 60° (i.e. $J_{aa} > J_{ae} \simeq J_{ee}$). Characteristic values found for the vicinal couplings of steroid protons in the A-, B- and C-rings can be placed into three catogories which are 10.5-14Hz, 3.5-5.0Hz and 2.5-4.0Hz.[63] According to the Karplus equation the large couplings 10.5-14Hz can arise when the dihedral angle of the vicinal protons is 180°. For vicinal protons which are part of a six-membered ring this can only arise when these protons are consistently in an axial-axial spatial

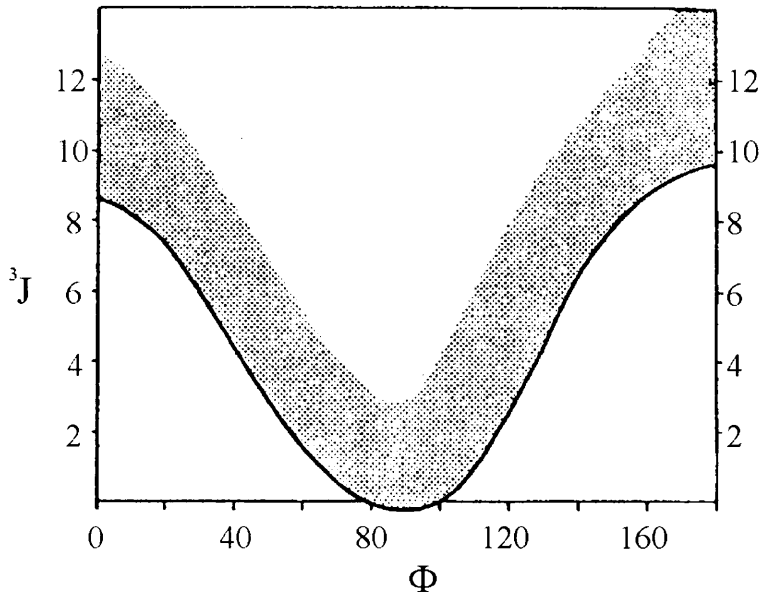

Figure 3.2 The Karplus curve showing the dependance of the vicinal coupling to the dihedral angle Φ. The solid line is derived From equation 3.1 and the shaded region is the range of empirical results.

relationship with respect to each other. This is proof that the six-membered ring is a rigid system.

According to the Karplus equation the couplings of 3.5-5.0Hz and 2.5-4.0Hz can arise as a result of axial-equatorial and equatorial-equatorial couplings, respectively. This is evidence that the rigid six-membered ring system is in the chair conformation.The consistent pattern $J_{aa} > J_{ae} \simeq J_{ee}$ has been incorporated into the construction of the spin-spin coupling connectivity diagram shown in figure 3.5. This pattern enables the assignment of a steroid proton into the axial or equatorial position by virtue of its vicinal coupling constants.

3.2.4.2 Stereochemical assignments using the nuclear Overhauser effect

There are occasions where arguments based on coupling constants cannot reliably be employed to unambiguously assign the spatial orientation of steroid protons. The steroid five-membered D-ring is more flexible than the six-membered A-, B- and C-ring. Furthermore, the conformation of the five-membered ring is also perturbed by D-ring substitutions, particularly those situated at carbon-17.[63] The comparison of the coupling constants of the protons on the D-ring with those

of steroids in the literature with identical substitutions at carbon-17 is an acceptable method of assigning the spatial orientation of these protons. It is still advantageous to exploit an alternative method which is not dependant on the use of vicinal coupling constant values to assign the orientations of these protons. This alternative method should be able to assign the orientation of the D-ring protons in cases where the coupling constants of a literature steroid, with the same D-ring substitutions as the one at hand, is not available for comparative purposes. A possible alternative method worthy of exploitation is the use of the nuclear Overhauser effect between protons within the steroid-framework.

Although the largest NOE's are generally observed between geminal and vicinal protons, these relationships have already been established through scalar-coupling obtained from the phase sensitive DQF-COSY experiment. The most useful relationships to establish will be those where there is spatial proximity but no scalar coupling. In the case of assigning the orientation of the D-ring protons it will be of interest to determine whether there will be any differences in intensity between the NOE's of the methyl protons CH_3-18 to the D-ring protons. The protons on the β-face of the D-ring are closer than the protons on the α-face to the methyl protons CH_3-18. It is expected that the intensity of the NOE's between CH_3-18 and the protons 15β-H and 16β-H will be larger than the intensity of the NOE's between CH_3-18 and the protons 15α-H and 16α-H. This expectation has been confirmed by the literature, where the 1-D NOE difference experiment was employed by irradiating the methyl protons CH_3-18 and observing the possible NOE's to the D-ring protons.[61, 63, 69, 70] NOE's to the protons 15β-H and 16β-H were always observed. Furthermore, during these experiments the protons 15α-H and 16α-H experienced extremely weak NOE's or they were not detected at all.

The disadvantage of the 1-D difference NOE experiment applied to steroids where proton overlap is frequent is that selective irradiation of a single proton resonance is impossible. The utility of two-dimensional NOE experiments were therefore considered. Applications of the 2-D NOESY experiments to steroids have not proved very successful due to the low intensity of the NOE crosspeaks as a result of the unfavourable correlation times, τ_C.[63] To overcome the obstacle of low intensity NOE crosspeaks during this study, the 2-D ROESY experiment was employed for observing the intramolecular NOE's between steroid protons.

The knowledge of the previously mentioned trend found in the literature can be used in combination with the NOE crosspeaks found in a 2-D ROESY spectrum to assign the D-ring protons to the α- or to the β-face. It is expected that both the crosspeaks of CH_3-18 to the protons 15β-H and 16β-H will be more intense than the crosspeaks of CH_3-18 to the protons 15α-H and 16α-H.

3.3 A complete assignment of the proton resonances of cyproterone acetate

Amongst the three steroids whose proton resonances have been assigned with the use of two-dimensional NMR spectroscopy, only the results of the assignment strategy of the cyproterone acetate proton resonances will be discussed in detail. Cyproterone acetate was chosen because of the added complexity introduced to the assignment strategy due to the presence of the methylene bridge in the A-ring. The exact nature of this complexity will become apparent during the course of the following discussions. Since the assignments of the protons of cyproterone acetate were the most involved, their successful assignment should be assurance that the remaining two steroids, ethynyl oestradiol and danazol, enjoyed the same rigorous and thorough attention. The crosspeaks found in the two-dimensional spectra, illustrated in this chapter, as well as the resonances in the one-dimensional and along the axes of the two-dimensional spectra have been labelled using the final assignment. The following discussions describe the rationale used to obtain these assignments.

3.3.1 The connectivity assignments

The ^1H NMR spectrum of cyproterone acetate in $CDCl_3$ is shown in figure 3.3. One of the first steps in assigning this proton spectrum is to identify the methylene protons. From the known chemical structure of cyproterone acetate illustrated in figure 3.4 it is predicted that there must be five pairs of CH_2 groups. The HMQC spectrum of cyproterone acetate illustrated in figure 3.6

is used to locate the chemical shifts of the proton pairs which are attached to the methylene carbons. For convenience, the geminal proton pairs are assigned in the proton spectrum found along the F_2-axis of the HMQC spectrum (fig 3.6). The chemical shifts of these proton pairs are δ1.817 and δ2.968, δ1.875 and δ1.425, δ2.019 and δ1.604, δ1.938 and δ1.542, δ0.851 and δ1.245. The five proton pairs responsible for these resonances are 11α-11β, 12α-12β, 15α-15β, 16α-16β and 22a-22b. The next logical step will be to correlate the chemical shifts of the geminal proton pairs to the carbon-skeletal framework of the steroid. This is accomplished with the aid of a spin-spin coupling connectivity diagram of cyproterone acetate adapted from Sedee et al[71,72] (fig 3.5) and a phase sensitive DQF-COSY spectrum (fig 3.7 and 3.8). In fact, with the use of the connectivity diagram and COSY spectrum all the steroid proton resonances will be assigned to the steroid-carbon framework.

To begin the interpretation of the phase sensitive DQF-COSY spectrum of cyproterone acetate illustrated in figure 3.7 and 3.8, a few proton resonances must be assigned so that they can be regarded as anchor points. There are two olephinic resonances present at δ6.188 and δ6.146 in the ^{1}H NMR spectrum of cyproterone acetate (fig 3.3). From a consideration of the chemical structure of cyproterone acetate (fig 3.4), the olephinic protons responsible for these resonances are 4-H and 7-H. From the COSY spectrum there is a coupling between δ6.146 and δ1.989. The proton resonance at δ1.989 is further coupled to three other protons with resonances at δ1.691, δ1.245 and δ0.851 (fig 3.7). This spin-system corresponds to the coupling pattern predicted for the protons 4-H, 1β-H, 2β-H, 22a-H and 22b-H which is illustrated in the connectivity diagram (fig 3.5). The olephinic resonance at δ6.146 is therefore unambiguously assigned to 4-H. This leaves the resonance at δ6.188 to be assigned to 7-H.

The presence of a coupling between 4-H at δ6.146 and the proton resonance at δ1.989 cannot as yet assign δ1.989 to either of the protons 1β-H and 2β-H. Notice that a possible scalar-coupling between 4-H and 2β-H can arise from two coupling paths, a four-bond and a six-bond coupling path, a possible coupling between 4-H and 1β-H can also arise from two coupling paths, both of which are five-bond coupling paths. More conclusive data is therefore required to unambiguously correlate the protons, with resonances at δ1.691 and δ1.919, to carbon-1 and carbon-2.

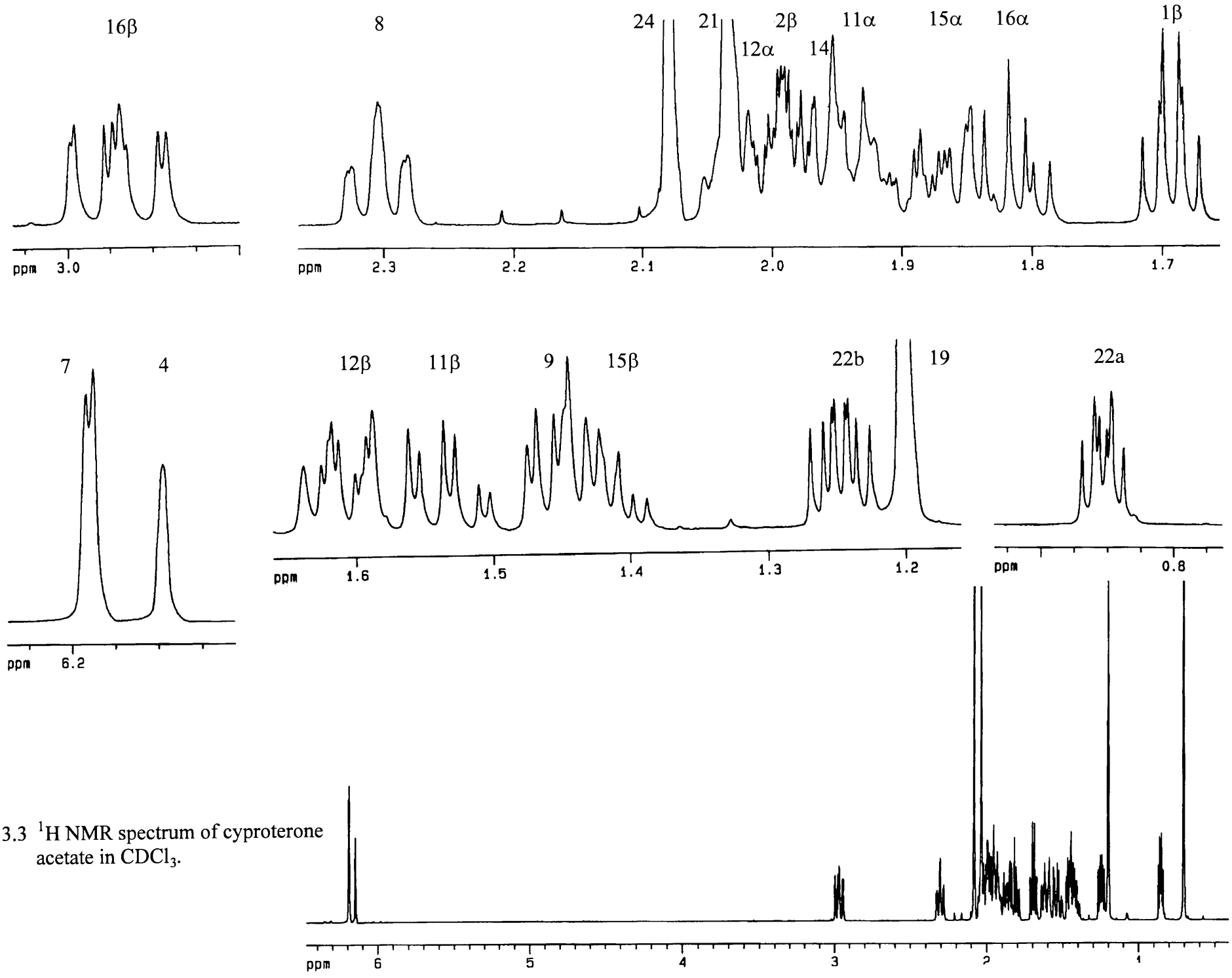

Figure 3.3 ^{1}H NMR spectrum of cyproterone acetate in $CDCl_3$.

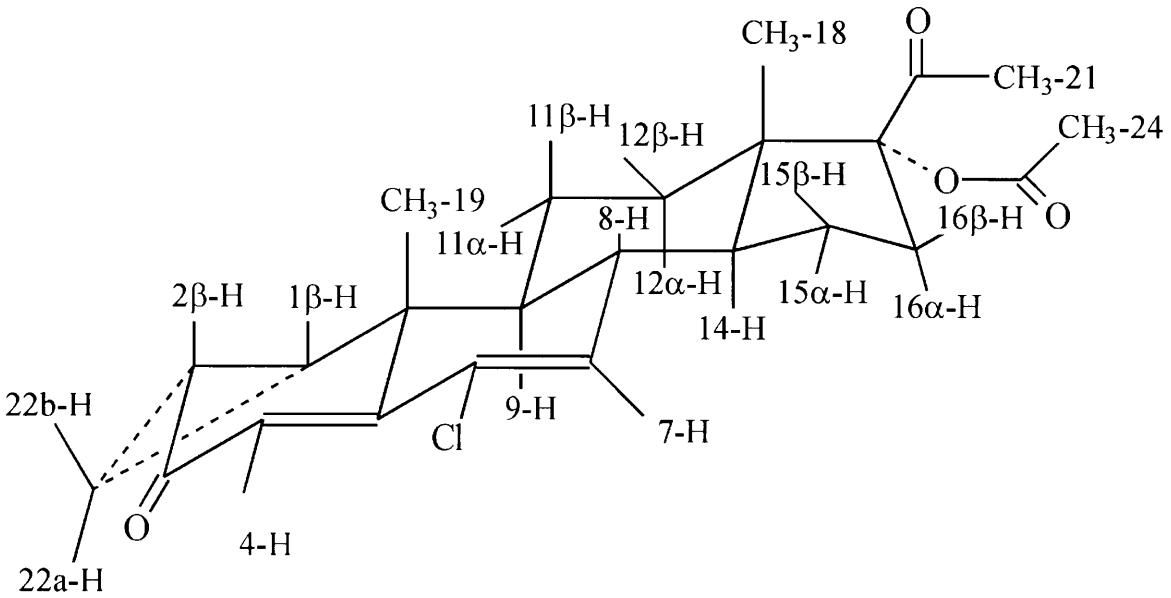

Figure 3.4 Chemical structure of cyproterone acetate showing the α- and the β-orientations of the steroid protons.

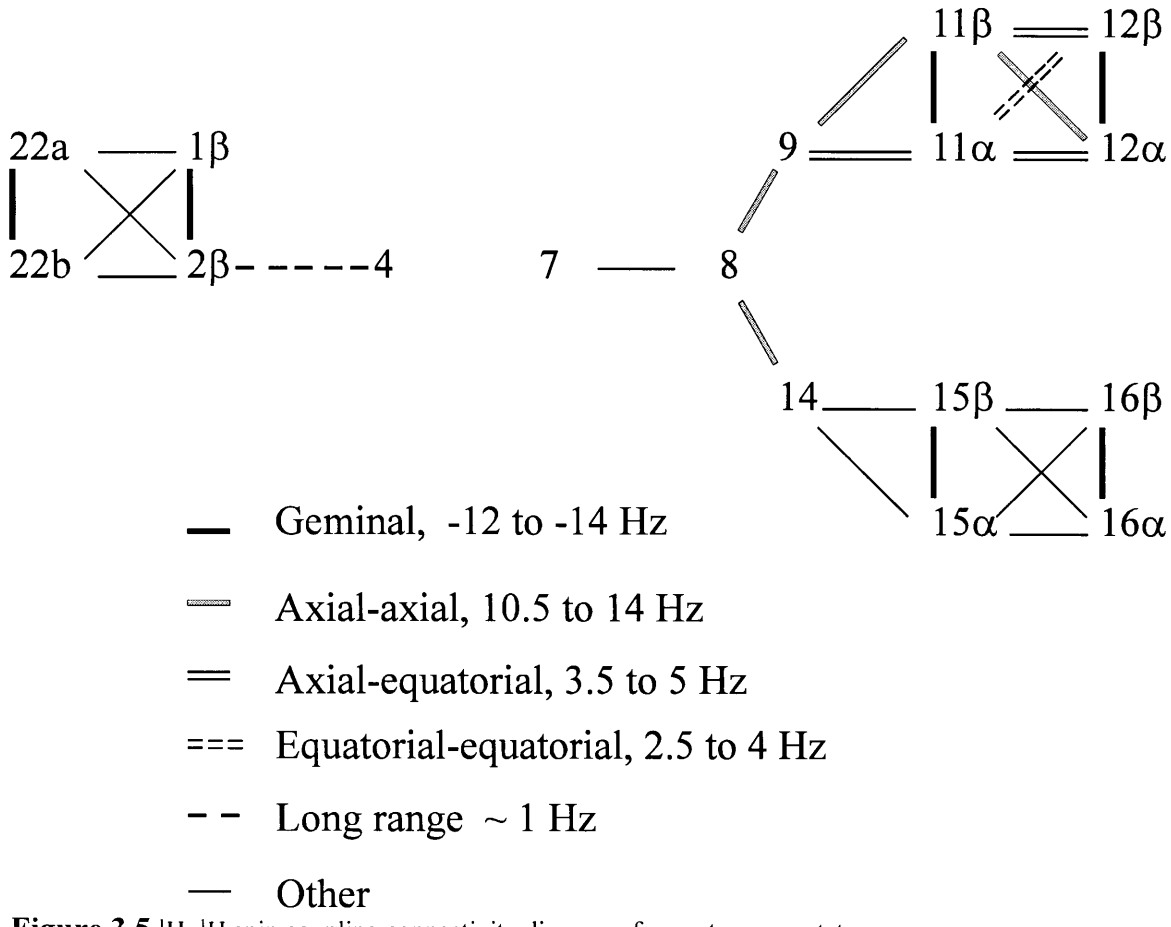

Figure 3.5 ^{1}H, ^{1}H spin coupling connectivity diagram of cyproterone acetate.

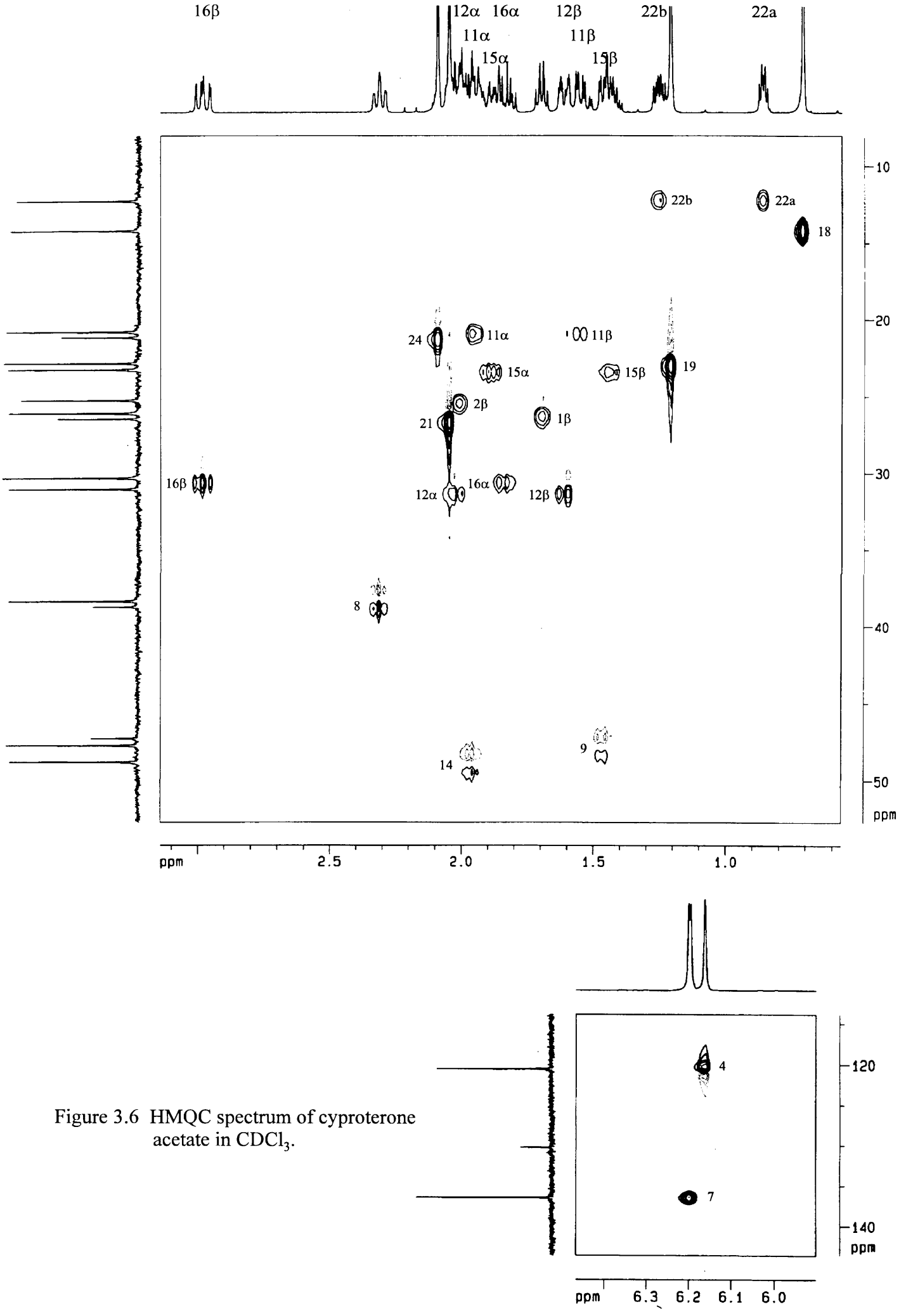

Figure 3.6 HMQC spectrum of cyproterone acetate in $CDCl_3$.

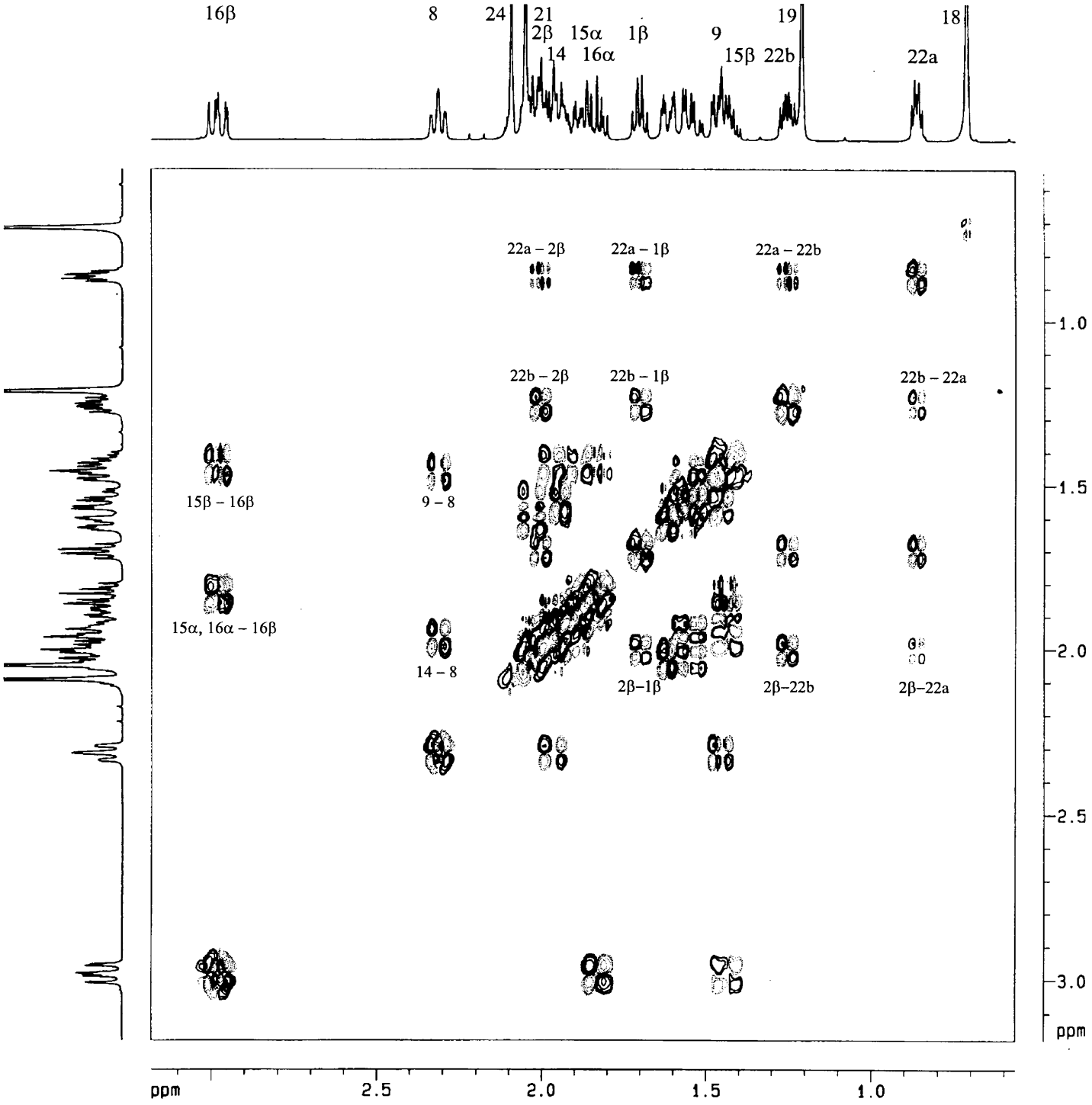

Figure 3.7 Phase sensitive DQF-COSY spectrum of cyproterone acetate in $CDCl_3$.

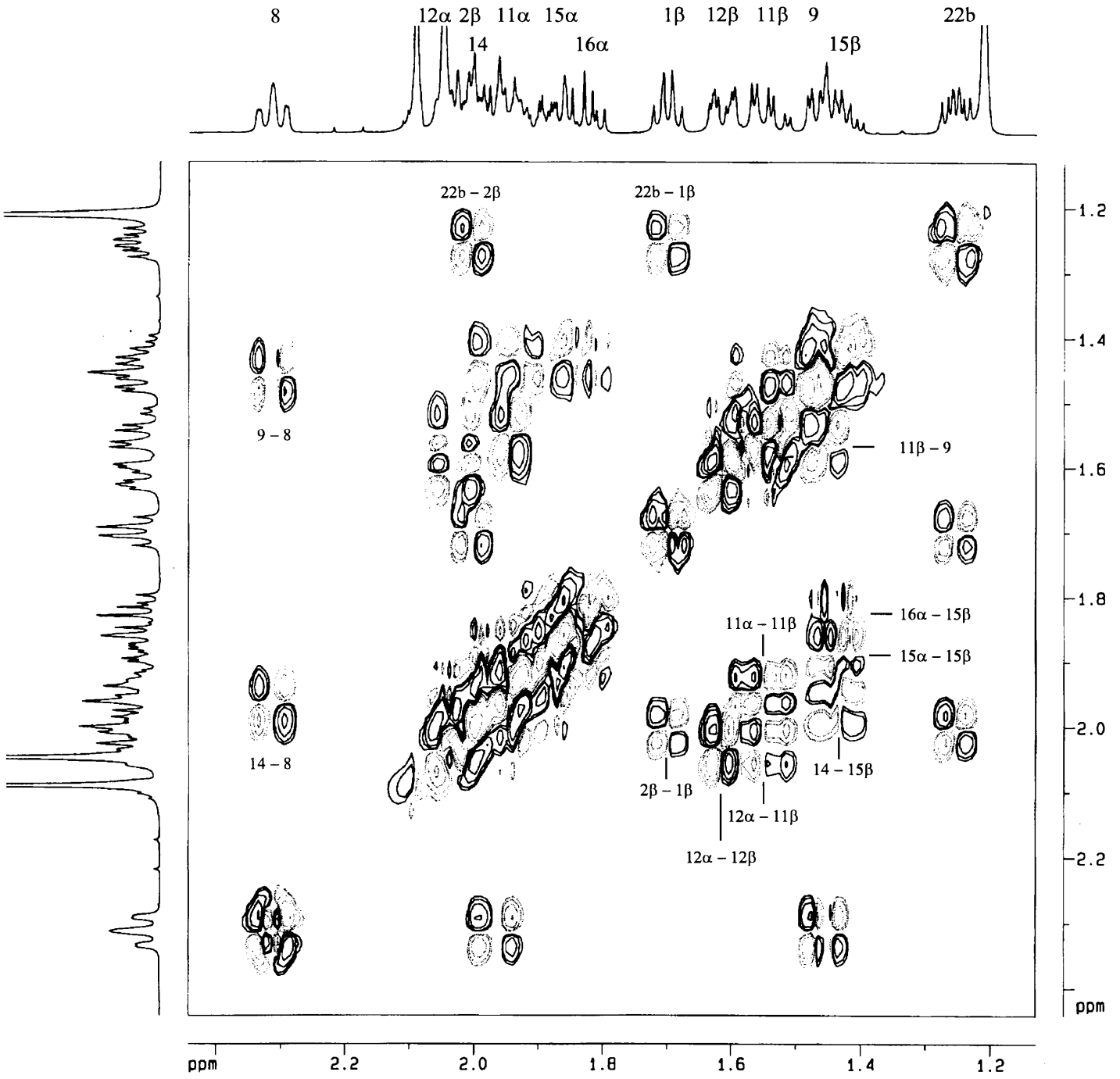

Figure 3.8 Expanded region of the phase sensitive DQF-COSY spectrum of cyproterone acetate in $CDCl_3$.

From the HMQC spectrum (fig 3.6), the resonances δ1.245 and δ0.851 are both correlated to the same methylene carbon. From the connectivity diagram it can be deduced that the geminal protons 22a-H and 22b-H are responsible for these two resonances. The correlation of the proton resonances δ1.691 and δ1.919 to carbon-1 and carbon-2 and the assignment of the resonances δ1.245 and δ0.851 to the spatially different protons 22a-H and 22b-H will be discussed under the heading '3.3.3 The assignment of the resonances to the protons of the methylene bridge'.

In the COSY spectrum there is a coupling between the olephinic 7-H at δ6.188 to the resonance at δ2.302. From consulting the connectivity diagram (fig 3.7), δ2.302 is unambiguously assigned to 8-H. The proton 8-H at δ2.302 further couples to two other resonances at δ1.448 and δ1.957 (fig 3.7). The only protons which can be responsible for the latter two resonances are 9-H and 14-H. The strategy used to assign the resonances δ1.448 and δ1.957 was to follow the couplings of both these two protons. According to the connectivity diagram (fig 3.5), the protons that couple to 9-H and 14-H will be correlated to carbon-11 and carbon-15, respectively. The protons correlated to carbon-15 have coupling constants characteristic of a steroid D-ring and the protons correlated to carbon-11 possess coupling constants characteristic of a proton within a six-membered steroid-ring. From the enlarged portion of the phase sensitive DQF-COSY spectrum (fig 3.8), δ1.957 is coupled to δ1.425. The resonancs δ1.425 and δ1.875 are both correlated to the same carbon resonance as deduced from the HMQC spectrum (fig 3.6). Both these resonances δ1.425 and δ1.875 have coupling constants which are characteristic of D-ring protons (see Table 3.1). These two resonances are therefore both correlated to carbon-15. In retrospect, the resonance δ1.957 must be correlated to 14-H. The proton on carbon-15 with a resonance of δ1.425 further couples to δ2.968 (fig 3.7) and to δ1.817 (fig 3.8). These resonances δ2.968 and δ1.817 therefore belong to the two geminal protons correlated to carbon-16.

Since 14-H is responsible for the resonance at δ1.957, this leaves the resonance at δ1.448 to be assigned to 9-H. The proton 9-H further couples to a proton with a resonance at δ1.542. From the HMQC spectrum (fig 3.6) it can be deduced that the proton with the resonance δ1.542 is geminally coupled to a proton which resonates at δ1.938. From the connectivity diagram (fig 3.5) it is concluded that both resonances δ1.542 and δ1.938 belong to protons which are attached to carbon-11. The proton, attached to carbon-11, with the resonance δ1.542 is further coupled to

the proton with resonance δ2.019 (fig 3.8). This latter proton with the resonance δ2.019 has the proton with resonance δ1.604 for a geminal proton (fig 3.6). Both protons with resonances δ2.019 and δ1.604 are therefore correlated to carbon-12.

Until now, most of the proton resonances of cyproterone acetate have been correlated to their respective carbons which comprise the steroid-skeletal framework. The only exceptions being the methyl proton resonances, but these resonances will be assigned with the use of the nuclear Overhauser effect during the course of the next discussion.

3.3.2 The stereochemical assignments

Now that the connectivities of most of the proton resonances have been established, all that remains is to determine the stereochemical orientations of the protons responsible for these resonances. An important distinction must be made at this stage between protons which do not need any further clarification concerning their stereochemistry and those protons especially geminally paired protons where their spatial orientation must still be defined as being either axial or equatorial and α- or β-facing. For example, for the protons 1β-H, 2β-H, 4-H, 7-H, 8-H, 9-H, 14-H, CH_3-18, CH_3-19, CH_3-21 and CH_3-24, as a result of structural considerations obtained from the cyproterone acetate molecule, it is only necessary to determine their connectivity to a steroid carbon to achieve an unambiguous assignment. But for geminally coupled protons such as 11α-H, 11β-H, 12α-H, 12β-H, 15α-H, 15β-H, 16α-H, 16β-H, 22a-H and 22b-H a simple correlation of their proton resonances to their respective steroid carbons will not result in an unambiguous assignment. The assignment of the stereochemistry of these latter protons is the purpose of the following arguments.

The spatial orientations of the protons responsible for the proton resonances correlated to carbon-11 and carbon-12 were determined with the complimentary use of vicinal coupling constants and the connectivity diagram shown in figure 3.5. A PERCH simulation of two proton resonances, one resonance at δ1.542 correlated to carbon-11 and the other resonance at δ1.604

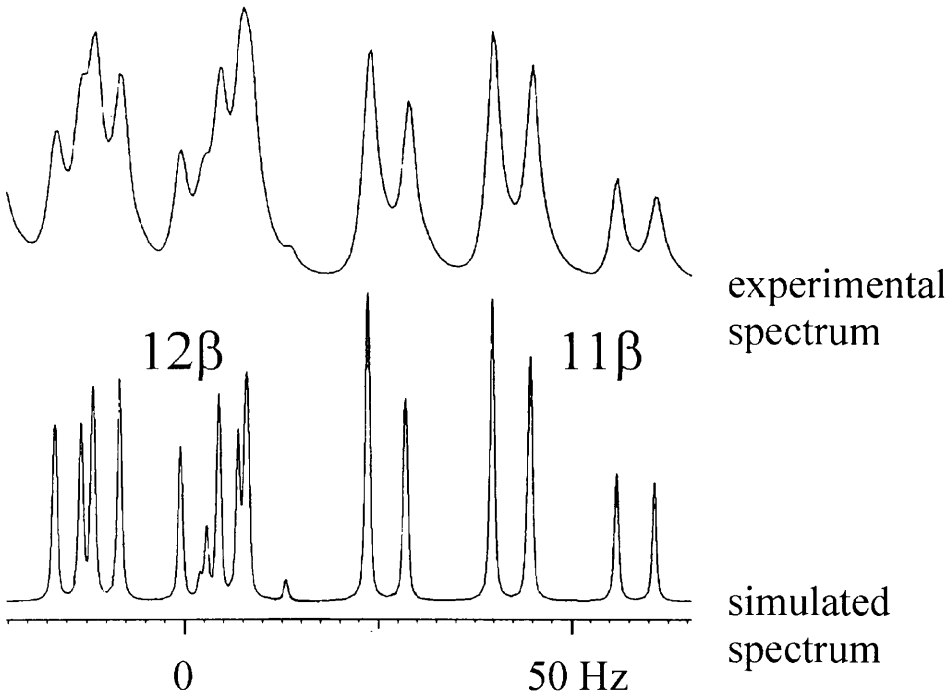

Figure 3.9 PERCH simulated spectrum of protons 11β-H and 12β-H which are situated on the C-ring of cyproterone acetate.

correlated to carbon-12, can be seen in figure 3.9. From this simulation the following couplings could be obtained for the proton which resonates at δ1.542: -13.3Hz, 13.2Hz, 13.2Hz, 4.0Hz. The -13.3Hz coupling is a geminal coupling. The smaller coupling is an axial-equatorial coupling. The other two larger couplings both of which are 13.2Hz can only arise as a result of two axial-axial couplings. If structural considerations are taken into account the proton with the resonance at δ1.542 would have to be in an axial position to allow for the two axial-axial couplings from the axial protons 9-H and 12α-H. The resonance at δ1.542 is therefore assigned to 11β-H which is in an axial position, and it's geminal proton which resonates at δ1.938 is assigned to the equatorial position 11α-H.

From the same simulation illustrated in figure 3.9, the following coupling constants could be obtained for the proton which resonates at δ1.604: -12.9Hz, 4.0Hz, 2.8Hz. The -12.9Hz coupling arises from a geminal coupling. The two smaller couplings of 4.0Hz and 2.8Hz are as a result of an axial-equatorial and an equatorial-equatorial coupling respectively. This proton, with the resonance at δ1.604 which is correlated to carbon-12, would have to be in an equatorial position to be able to allow for both the axial-equatorial coupling from the axial 11β-H and the equatorial-

equatorial coupling from the equatorial 11α-H. The resonance at δ1.604 is therefore assigned to the equatorial position 12β-H, and it's geminal proton which resonates at δ2.619 will then be assigned by default to the axial position 12α-H.

The stereochemistry of the protons responsible for the resonances which have been correlated to the carbon-15 and carbon-16 were determined with vicinal coupling constants. These coupling constants were obtained from the PERCH simulation illustrated in figure 3.10. The chemical

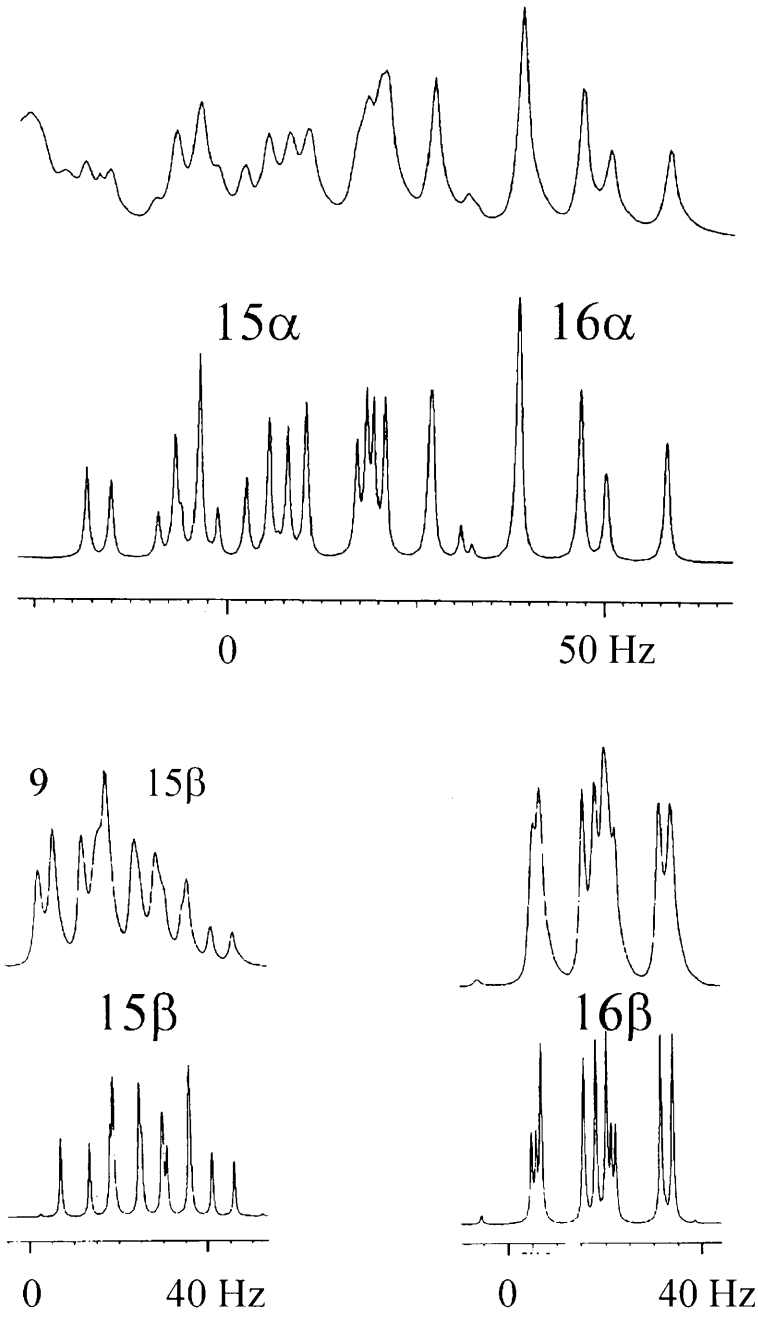

Figure 3.10 PERCH simulation of the protons on the D-ring of cyproterone acetate.

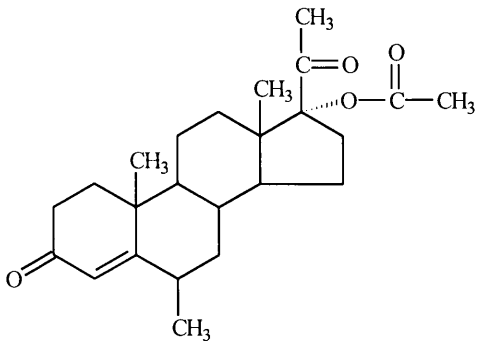

Figure 3.11 The chemical structure of medroxy progesterone.

structure of medroxy progesterone illustrated in figure 3.11 is similar to the structure of cyproterone acetate. Furthermore, both medroxy progesterone and cyproterone acetate have identical substitutions at the carbon-17 position. The coupling constants of the protons attached to the D-ring of medroxy progesterone have been determined by Kirk et al[73]. By comparing these coupling constants with the coupling constants of the protons of the D-ring of cyproterone acetate the stereochemistry of these cyproterone acetate protons can be assigned. From this comparison, which can be found in table 3.1, the proton resonances δ1.875, δ1.425, δ1.817 and δ2.968 were assigned to the protons 15α-H, 15β-H, 16α-H and 16β-H, respectively.

Table 3.1 A comparison of the coupling constants of the D-ring protons of Medroxy Progesterone (Med.P)[73] and Cyproterone Acetate (Cyp.A)

	Med.P.	Cyp.A.		Med.P.	Cyp.A.
14-15α	7.1	7.4	15α-16β	2.6	2.8
14-15β	12.1	11.6	15β-16α	6.7	6.8
15α-15β	-12.2	-12.7	15β-16β	11.3	11.5
15α-16α	9.3	9.4	16α-16β	-16.1	-16.2

The methyl proton resonances were assigned with the use of the nuclear Overhauser effect. In the phase sensitive 2-D ROESY spectrum of cyproterone acetate illustrated in figure 3.12 an NOE crosspeak is observed between the methyl proton resonances at δ0.703 to 16β-H. The presence of this NOE crosspeak assigns the resonance at δ0.703 to the methyl protons CH_3-18. Only CH_3-18, and not CH_3-19, can be responsible for this NOE effect to 16β-H. The methyl protons CH_3-19 are relatively spatially remote from a proton that is attached to carbon-16. This leaves the methyl resonance at δ1.200 to be assigned to CH_3-19.

The methyl ketone protons CH_3-21 and the acetate protons CH_3-24 are responsible for the methyl proton resonances at δ2.034 and δ2.079. The NOE crosspeak between CH_3-18 and the methyl resonance at δ2.034 positions the methyl protons responsible for this resonance in the β-face of the D-ring (see fig 3.12). Since the methyl ketone protons are found in the β-face and the acetate

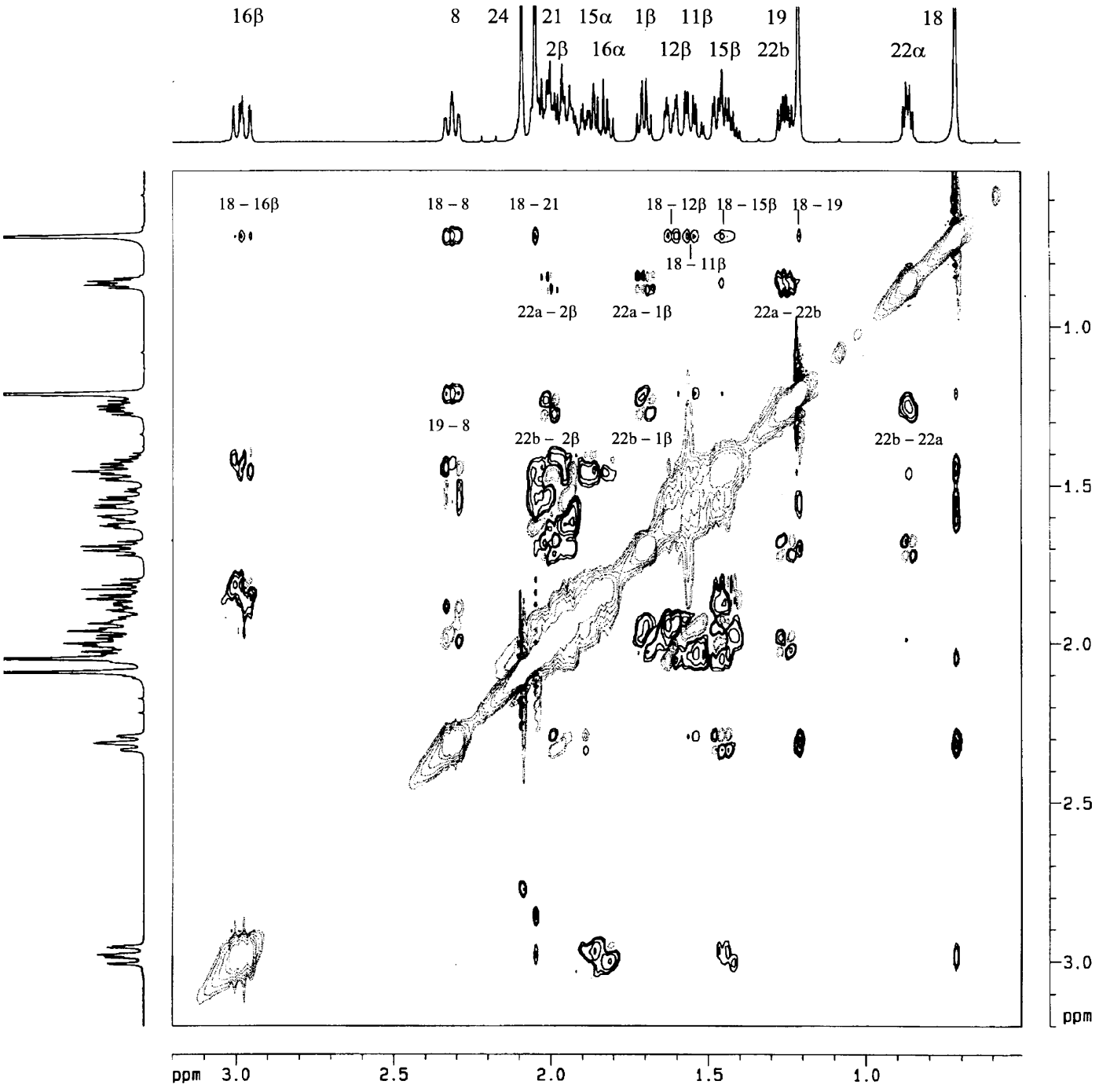

Figure 3.12 2-D ROESY spectrum of cyproterone acetate in $CDCl_3$.

protons are in the α-face of the steroid, the presence of this NOE crosspeak assigns the resonance at δ2.034 to CH_3-21. This leaves the resonance at δ2.079 to be assigned to CH_3-24.

The detection of the NOE crosspeak in a 2-D ROESY spectrum between the methyl protons CH_3-18 and the protons of the D-ring was exploited as an alternative method to determine the stereochemistry of the D-ring protons of cyproterone acetate. In the 2-D ROESY spectrum crosspeaks were observed from the methyl protons CH_3-18 to the resonances δ1.425 and δ2.968, these resonances are correlated to carbon-15 and carbon-16, respectively (fig 3.12). No crosspeaks were observed from the methyl protons CH_3-18 to the resonances δ1.875 and δ1.817 which are also correlated to carbon-15 and carbon-16, respectively. These differences in intensity of the NOE crosspeaks assigns δ1.425 and δ2.968 to the β-faced protons 15β-H and 16β-H, respectively. The resonances at δ1.875 and δ1.817 are assigned to the α-faced protons 15α-H and 16α-H, respectively. The use of vicinal couplings and the nuclear Overhauser effect led to identical assignment of the stereochemistry of the D-ring protons.

3.3.3 The assignment of the resonances to the protons of the methylene bridge

The two proton resonances δ1.691 and δ1.989 have yet to be correlated to carbon-1 and carbon-2 which are situated on the A-ring of cyproterone acetate. From the HMQC spectrum (fig 3.6) it was determined that the two resonances δ1.691 and δ1.989 are correlated through a one-bond coupling to the carbon resonances δ_C26.08 and δ_C25.24, respectively (when referring to a carbon resonance the subscript δ_C will be used). In the NMR literature dealing with the assignment of steroid protons, the HMBC spectrum provided the clearest connectivity information for carbons within two or three bonds of the methyl singlets (CH_3-18 and CH_3-19).[74] For example, with the use of the HMBC experiment it was possible to observe the heteronuclear three-bond coupling between the methyl protons CH_3-19 and the carbon-1 nucleus of androstane.[62] It is expected that the HMBC spectrum of cyproterone acetate should also be able to correlate the methyl protons CH_3-19 to the carbon-1 nucleus. A portion of the HMBC spectrum of cyproterone acetate is illustrated in figure 3.13 which successfully reveals the crosspeak between CH_3-19 and the carbon resonance at δ_C26.08. This crosspeak is caused by a three-bond coupling which assigns δ_C26.08 to carbon-1. This crosspeak is not as a result of a four-bond coupling to carbon-2 since

a four bond coupling would not have resulted in an intense crosspeak as the one shown in figure 3.13.[75] Since δc26.08 is assigned to carbon-1 the proton resonance at δ1.691, which is correlated by a one-bond coupling to δc26.08, is assigned to 1β-H. This leaves the proton resonance at δ1.989 to be assigned to 2β-H.

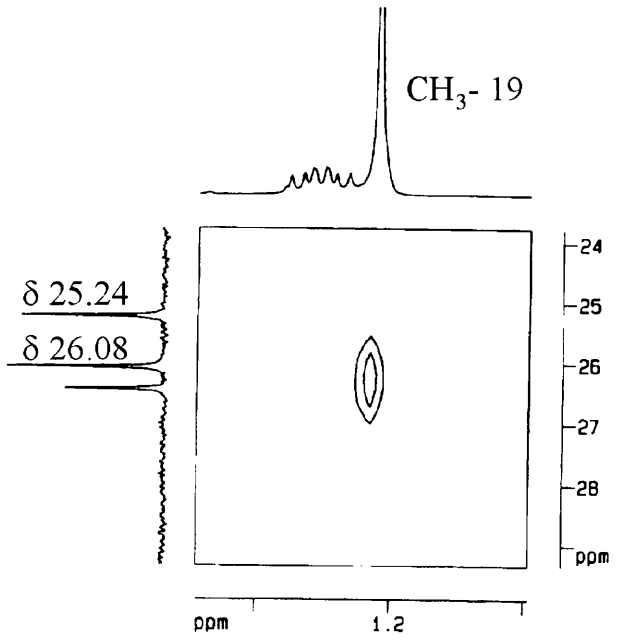

Figure 3.13 HMBC spectrum showing the long range H,C correlation between the methyl protons CH_3-19 and the carbon at δ26.08.

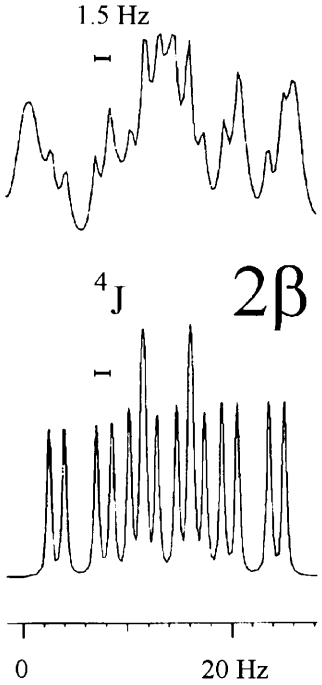

Figure 3.14 PERCH simulation of proton 2β-H showing the calculated 1.5Hz coupling to proton 4-H.

The coupling between 4-H and the proton which resonates at δ1.989 could not initially be used to assign δ1.989 to a steroid proton. Since the HMBC spectrum has successfully been used to make this assignment possible it is now known that this is a long-range four-bond coupling between 4-H and 2β-H. From the PERCH simulation of the proton resonance of 2β-H which is illustrated in figure 3.14, the magnitude of this four-bond coupling was determined to be 1.5Hz. From a consideration of the energy minimised molecular structure of cyproterone acetate, built using SYBYL molecular modelling software, shown in figure 3.15, it is apparent that this four-bond coupling is an example of a stereospecific 'W-coupling'. The path of this W-coupling lies in the plane of the A-ring of cyproterone acetate. The magnitude of long-range four-bond couplings are usually in the order of ~0.5Hz, for example the four-bond W-coupling found in medroxy progesterone between CH_3-19 and 1α-H of 0.4Hz.[73]

The spatial orientations of the protons attached to carbon-22 which are responsible for the proton resonances δ0.851 and δ1.245 are now determined. The dihedral angles between the protons 1β-H and 2β-H to the protons 22a-H and 22b-H were obtained from a molecular model of cyproterone acetate. These dihedral angles were then used to predict vicinal coupling constants using an improved Karplus relation available within the PERCH software package.[65] These predicted coupling constants did not coincide to an acceptable degree to the experimentally determined coupling constants. Arguments based on the values of vicinal coupling constants

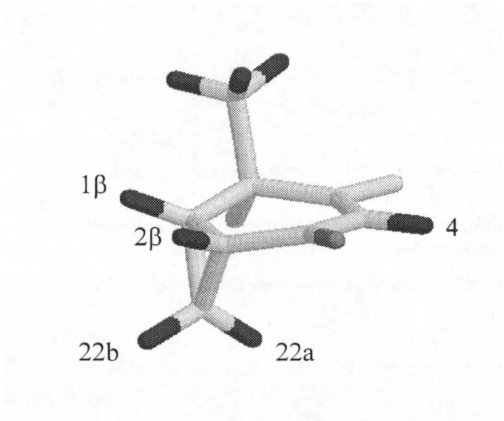

Figure 3.15 Only the A-ring of the energy minimised model of cyproterone acetate is shown.

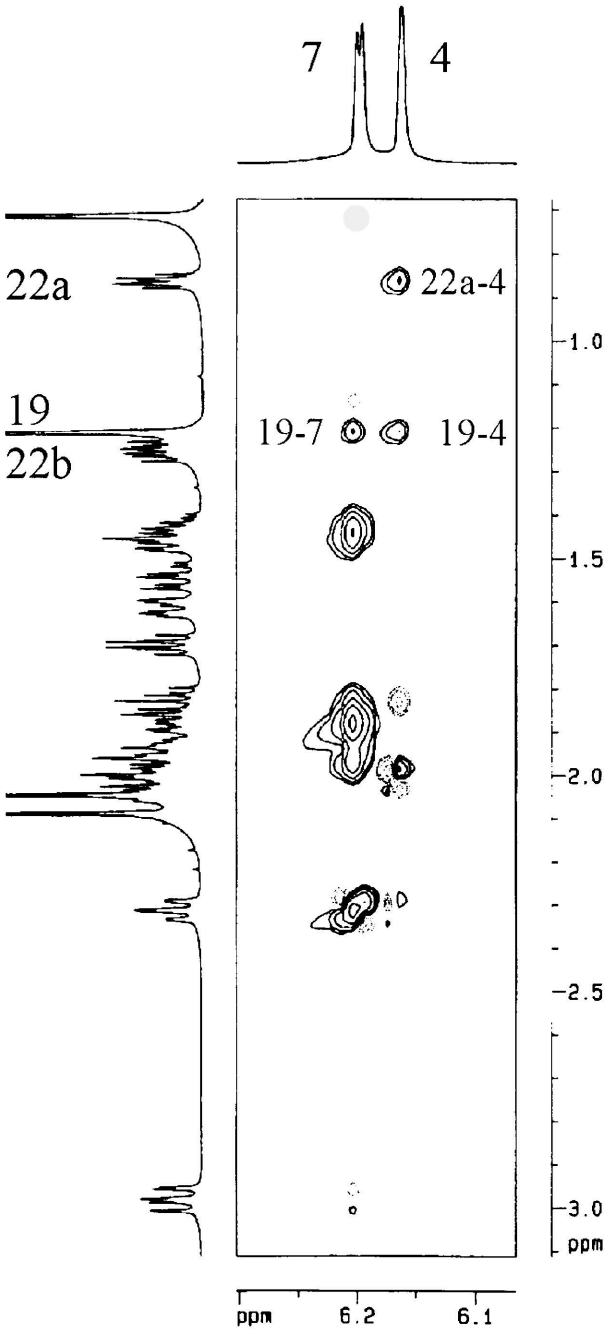

Figure 3.16 A different portion of the 2-D ROESY spectrum of cyproterone acetate that was illustrated in figure 3.12.

could not be used to unambiguously assign the spatial orientation of the protons responsible for the two resonances correlated to carbon-22. Alternatively, the potential use of the intensities of NOE crosspeaks found in the 2-D ROESY spectrum to assign the spatial orientation of these protons was exploited. From the molecular model of cyproterone acetate (fig 3.15), it is apparent that 22b-H is closer than 22a-H to the protons 1β-H and 2β-H. It is expected that 1β-H will have a larger NOE crosspeak to 22b-H than to 22a-H. In the same fashion, it is expected that 2β-H will also have a larger NOE crosspeak to 22b-H than to 22a-H. From the 2-D ROESY spectrum illustrated in figure 3.12, the intensities of the two NOE crosspeaks from 1β-H and 2β-H to the proton resonance at δ1.245 are larger than the NOE crosspeaks from 1β-H and 2β-H to the proton resonance at δ0.851. These results strongly suggest that the proton resonance at δ1.245 should be assigned to 22b-H. Unfortunately these results are not very conclusive since there is an adverse effect to the intensity of these NOE crosspeaks due to a contribution from *coherent transfer through scalar coupled protons*. The crosspeaks which arise as a result of this coherent transfer have an opposite phase to that of the NOE crosspeaks as can be seen in figure 3.12. This prevents a reliable quantification of the intensities of these NOE crosspeaks.

A number of attempts were made to minimise the coherent transfer through scalar coupling by placing the carrier frequency 4-8KHz from the centre of the steroid proton spectrum. Unfortunately, the crosspeaks due to coherent transfer were not minimised to a satisfactory degree to justify an unambiguous assignment based on NOE crosspeak intensities.

The next logical step is to consider the nuclear Overhauser effects between a different combination of protons to facilitate an unambiguous spatial assignment for the proton resonances correlated to carbon-22. From the SYBYL model of cyproterone acetate, the measured distance from 4-H to 22a-H is 3.5Å and the distance from 4-H to 22b-H is 5.0Å. It is predicted that the intensity of the NOE crosspeak of 4-H to 22a-H will be larger than the NOE crosspeak of 4-H to 22b-H. Secondly, there is expected to be no contribution from coherent transfer through scalar coupling since there is no scalar coupling from 4-H to any of the two geminal protons attached to carbon-22. From the 2-D ROESY spectrum illustrated in figure 3.16, an NOE crosspeak between 4-H and the proton resonance at δ0.851 was observed. No NOE crosspeak between 4-H and δ1.245 could be seen from this spectrum. These observations unambiguously assign δ0.851

and δ1.245 to the protons 22a-H and 22b-H respectively.

3.4 A summary

A summary of the coupling constants and chemical shifts of the proton resonances of cyproterone acetate can be found in table 3.2. The results of the application of the assignment strategy to the proton resonances of the other steroids, ethynyl oestradiol and danazol, are given in tables 3.3 and 3.4. The assigned ^{1}H NMR spectra of these steroids in $CDCl_3$ are illustrated in figures 3.17 and 3.18.

Table 3.2 Proton chemical shifts and coupling constants for cyproterone acetate in $CDCl_3$

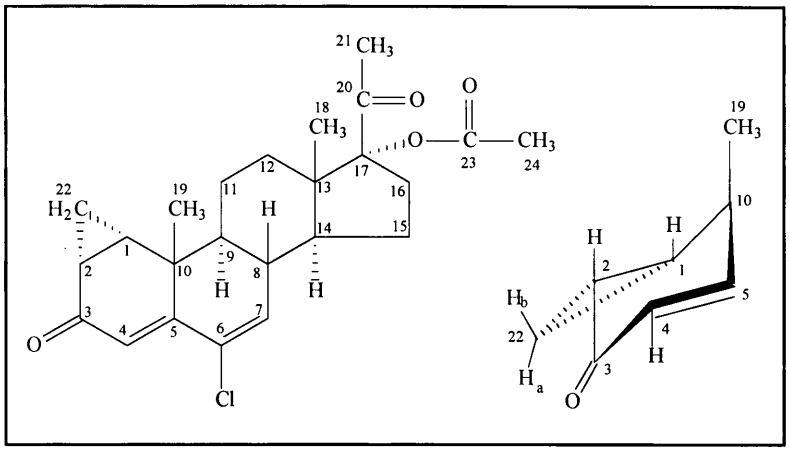

chemical shifts		coupling constants (Hz)				
proton	δ (ppm)	^2J	Ax-Ax	Ax-Eq	Eq-Eq	other
1β	1.691					7.7(2β) 6.4(22a) 7.8(22b)
2β	1.989					1.5(4) 4.6(22a) 8.9(22b)
4	6.146					
7	6.188					2.1(8)
8	2.302		9.9(9) 11.9(14)			
9	1.448		13.2(11β)	3.6(11α)		
11α	1.938	-13.3(11β)		4.4(12α)	2.8(12β)	
11β	1.542		13.2(12α)	4.0(12β)		
12α	2.019	-12.9(12β)				
12β	1.604					
14	1.957					7.4(15α) 11.6(15β)
15α	1.875	-12.7(15β)				9.4(16α) 2.8(16β)
15β	1.425					6.8(16α) 11.5(16β)
16α	1.817	-16.2(16β)				

proton	δ (ppm)	^2J	Ax-Ax	Ax-Eq	Eq-Eq	other
16β	2.968					
18	0.703					
19	1.200					
21	2.034					
22a	0.851	-14.7(22b)				
22b	1.245					
24	2.079					

Table 3.3 Proton chemical shifts and coupling constants for ethinyl oestradiol in $CDCl_3$

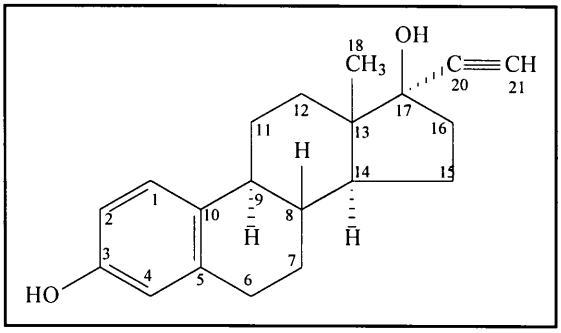

chemical shifts		coupling constants (Hz)				
proton	δ (ppm)	^2J	Ax-Ax	Ax-Eq	Eq-Eq	other
1	7.132					8.2(2)
2	6.597					2.8(4)
4	6.532					
6α	2.79	-14.6(6β)		6.5(7α)	2.8(7β)	
6β	2.79		11.9(7α)	5.5(7β)		
7α	1.334	-13.3(7β)	11.7(8)			
7β	1.841			3.7(8β)		
8	1.399		10.0(9) 11.0(14)			
9	2.184		13.39(11β)	4.4(11α)		
11α	2.325	-12.2(11β)		4.4(12α)	2.6(12β)	
11β	1.454		13.3(12α)	4.0(12β)		
12α	1.885	-13.1(12β)				
12β	1.702					
14	1.678					7.6(15α) 11.6(15β)
15α	1.763	-12.4(15β)				9.7(16α) 4.0(16β)
15β	1.379					5.7(16α) 12.1(16β)
16α	2.309	-13.8(16β)				
16β	1.997					
18	0.859					

proton	δ (ppm)	^2J	Ax-Ax	Ax-Eq	Eq-Eq	other
21	2.572					

Table 3.4 Proton chemical shifts and coupling constants for danazol in $CDCl_3$

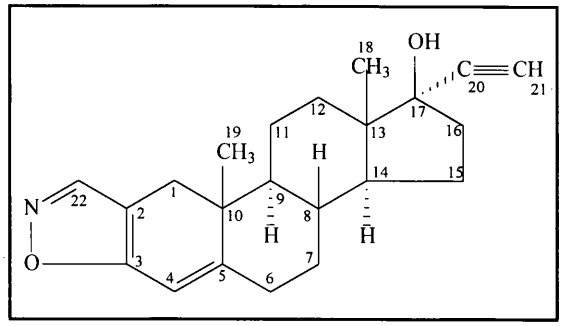

chemical shifts		coupling constants (Hz)				
proton	δ (ppm)	^2J	Ax-Ax	Ax-Eq	Eq-Eq	other
1α	2.476	15.8(1β)				
1β	2.691					
4	6.144					2.5(6β)
6α	2.348	-15.7(6β)		3.8(7α)	2.4(7β)	
6β	2.407		13.8(7α)	5.0(7β)		
7α	1.030	-12.8(7β)	11.0(8)			
7β	1.765			2.6(8)		
8	1.49		10.2(9) 12.3(14)			
9	1.159		12.6(11β)	3.9(11α)		
11α	1.604	-13.4(11β)		4.2(12α)	3.0(12β)	
11β	1.448		13.3(12α)	4.1(12β)		
12α	1.710	-12.9(12β)				
12β	1.629					
14	1.49					7.4(15α) 12.0(15β)
15α	1.714	-12.2(15β)				9.7(16α) 4.1(16β)
15β	1.337					5.6(16α) 12.1(16β)
16α	2.274	-13.8(16β)				
16β	1.981					
18	0.871					
19	0.993					

proton	δ (ppm)	^2J	Ax-Ax	Ax-Eq	Eq-Eq	other
21	2.545					
22	7.967					

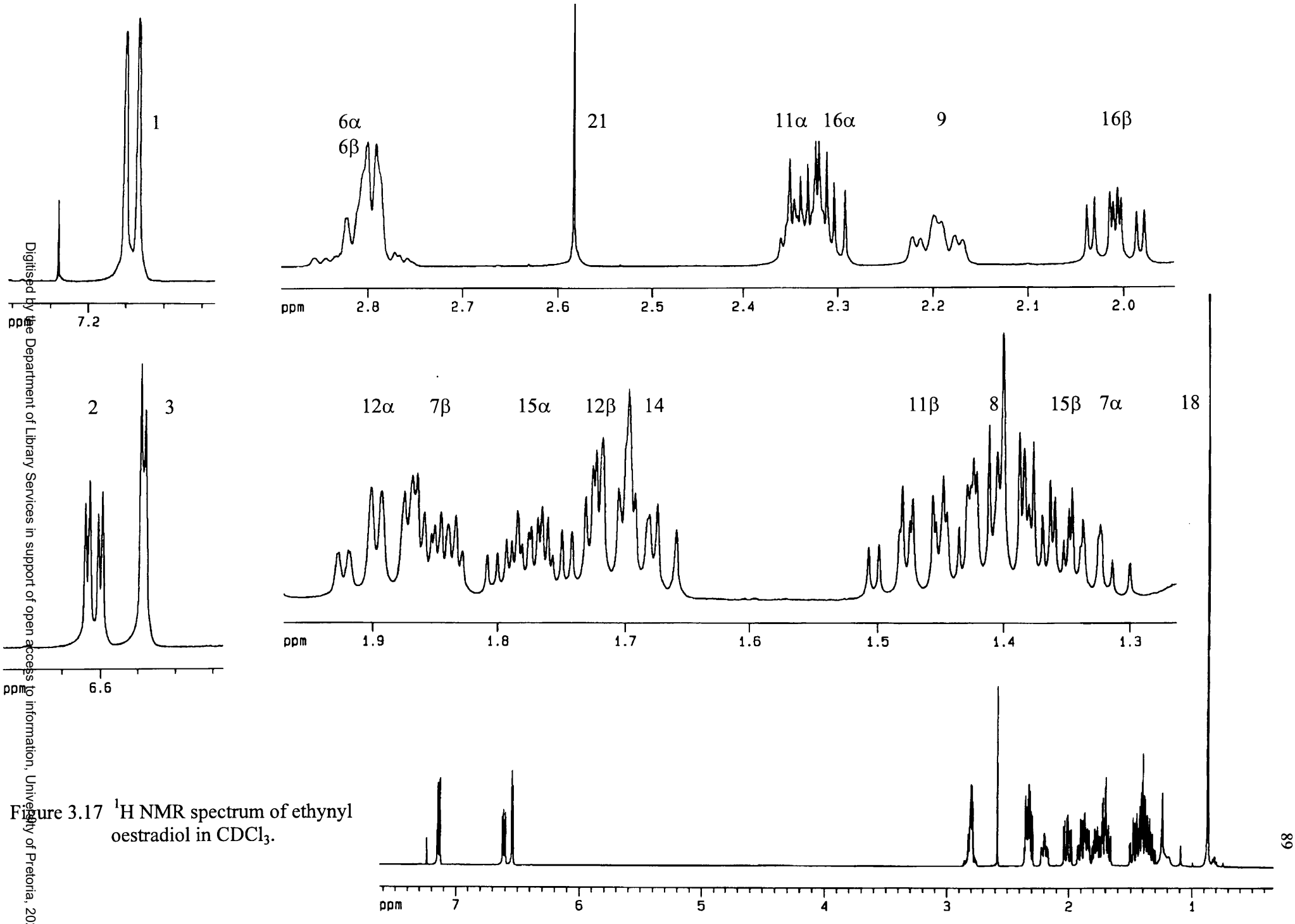

Figure 3.17 ^{1}H NMR spectrum of ethynyl oestradiol in $CDCl_3$.

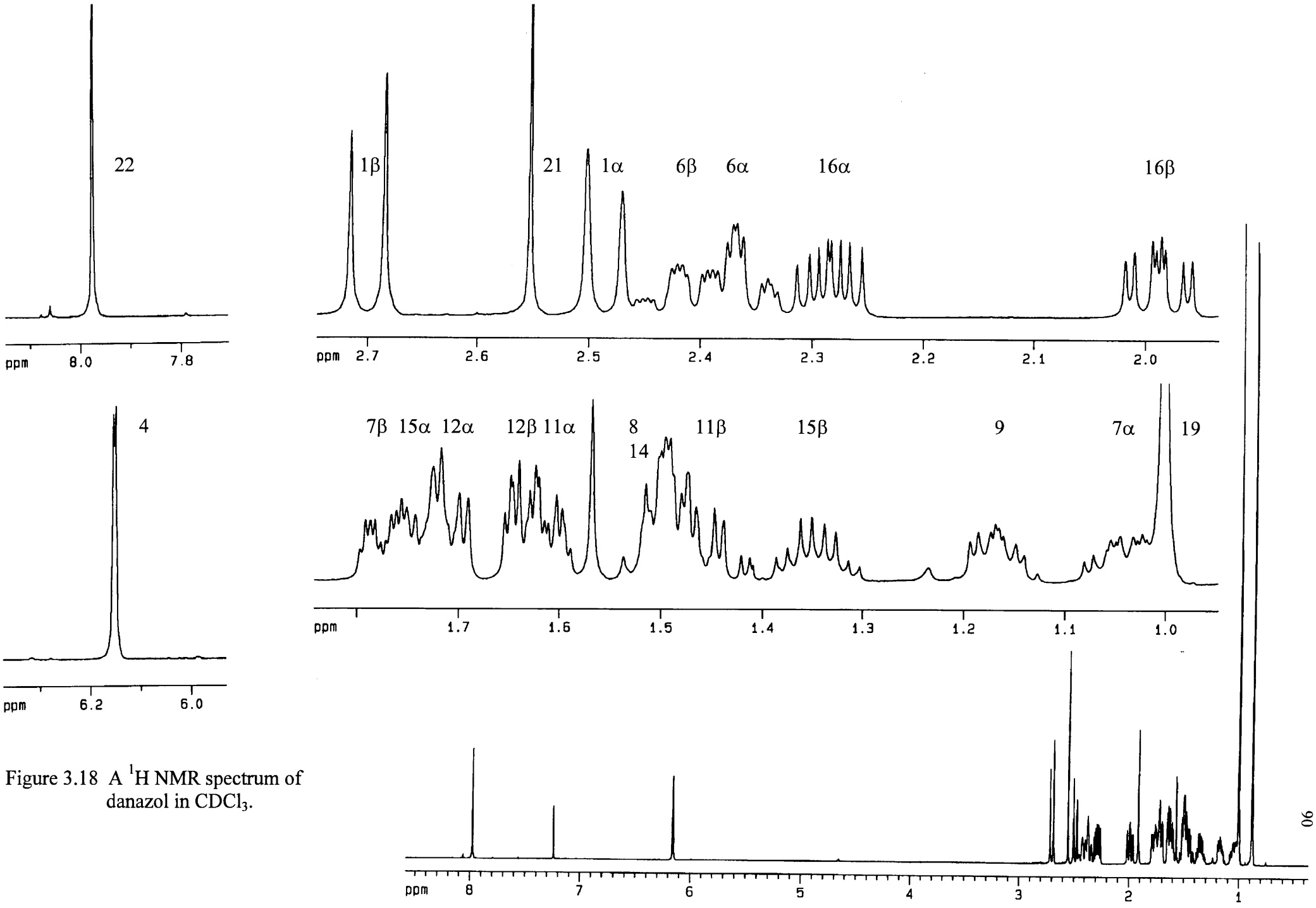

Figure 3.18 A ^{1}H NMR spectrum of danazol in $CDCl_3$.

4 The results of the NMR study of the steroid-cyclodextrin complexes

4.1 Introduction

The approach used to study the samples containing steroid and cyclodextrin consisted of three stages. During the first stage the cyclodextrin's ability to increase the amount of dissolved steroid in an aqueous medium was determined. Increases to the amount of dissolved steroid will improve the signal to noise ratio of the steroid proton resonances observed in the ^{1}H NMR spectrum. These increases will in turn facilitate an NMR investigation of the steroid-cyclodextrin complexes. A low concentration of steroid will hinder an NMR investigation since the steroid proton resonances recorded in the ^{1}H NMR spectrum will have a poor signal to noise ratio. The second stage dealt with the complete assignment and chemical shift determination of all the proton resonances in the ^{1}H NMR spectra of the samples containing dissolved steroid and cyclodextrin. The final stage involved the accumulation and quantification of the intermolecular Overhauser effects between the protons of the steroid and cyclodextrin.

4.2 A solubility study of the steroid-cyclodextrin complexes

The three steroids cyproterone acetate, ethynyl oestradiol and danazol are highly water insoluble. Any steroid proton resonances observed in the ^{1}H NMR spectra of the samples containing steroid and cyclodextrin prepared in D_2O resulted from complexed steroid only. The amount of dissolved steroid present in these samples was therefore proportional to the amount of dissolved steroid-cyclodextrin complex. The steroid and cyclodextrin proton resonances in the ^{1}H NMR spectra of these complexes were integrated. The values of these integrations could be used to calculate the ratio of steroid to cyclodextrin molecules present in solution. This ratio, known as the molecular ratio, could be used to determine the amount of dissolved steroid in the steroid-cyclodextrin sample provided the amount of dissolved cyclodextrin is known.

The solubilities of the steroid-cyclodextrin complexes prepared by two different methods were investigated. These were the kneading and the sonication methods.

The kneading method involved the kneading of 1:1 molar quantities of steroid and cyclodextrin together with a mortar and pestle in the presence of trace amounts of water to form a paste. Due to the small amount of water the free cyclodextrin concentration is high and according to Le Chateliers principle, the reaction is driven towards complex formation to restore equilibrium. When the paste was left in the open a dried steroid-cyclodextrin complex was obtained. The ^1H NMR spectra of 15mg of each of the dried steroid-cyclodextrin complexes were recorded in 0.5ml D_2O. The steroid and cyclodextrin proton resonances in these spectra were integrated and the values were used to calculate the molecular ratio of steroid to cyclodextrin present in solution.

The sonication method involved the preparation of samples which contain steroid and cyclodextrin in an aqueous medium. The advantage of placing these samples in a sonic bath is that the equilibrium of steroid-cyclodextrin complex formation is obtained at a faster rate. The phase solubility diagrams of Albers et al[28] confirms that for many steroids in the presence of β-cyclodextrin, an increase in the concentration of β-cyclodextrin will increase the amount of steroid in solution. In the preparation of the steroid-β-cyclodextrin complexes a quantity of 1mg of steroid was added to 0.5ml of D_2O which contained 15mg of dissolved β-cyclodextrin. This resulted in a saturated β-cyclodextrin solution which would dissolve the maximum amount of steroid. Though γ-cyclodextrin is far more soluble than β-cyclodextrin,[11] only 20mg of γ-cyclodextrin was dissolved in 0.5ml D_2O in the preparation of the steroid-γ-cyclodextrin complexes. A larger amount usually resulted in the eventual crystallisation of some γ-cyclodextrin from solution.

Using 1mg of the water-insoluble steroid in the preparation of all the steroid-β- and -γ-cyclodextrin complexes ensured that the sonicated samples were saturated with respect to the steroid. This was confirmed by an amount of undissolved steroid still present in each sonicated sample that was prepared in D_2O.

For the purposes of this study two conditions must be met for a steroid-cyclodextrin complex to be defined as *water-insoluble*. The isolation procedure, as described in chapter one (see 1.5.2.1), must successfully isolate a complex and the ^{1}H NMR spectrum of the sample prepared by the addition of the steroid and cyclodextrin to D_2O must not contain steroid proton resonances. The complex is defined as *poorly water-soluble* if the isolation procedure obtains the complex and the ^{1}H NMR spectrum of the steroid-cyclodextrin sample in D_2O does contain steroid proton resonances. A successful isolation of a complex reveals that the complex does have water-insoluble properties, but the detection of the proton resonances of a water-insoluble steroid indicates that the steroid is also present in solution in the complexed state. The complex is *water soluble* if the isolation procedure fails to obtain the complex and the ^{1}H NMR spectrum of the steroid-cyclodextrin sample in D_2O detects steroid proton resonances.

4.2.1 Cyproterone acetate-β-cyclodextrin complex

The ^{1}H NMR spectrum recorded in D_2O of the dried cyproterone acetate-β-cyclodextrin complex prepared by the kneading method gave proton resonances belonging to cyproterone acetate and β-cyclodextrin. The cyproterone acetate methyl resonances CH_3-18 and CH_3-19 and the β-cyclodextrin 1-H protons were integrated. From these values a molecular ratio of one steroid molecule to every eighty β-cyclodextrin molecules could be determined. During the preparation of the sample used to record the ^{1}H NMR spectrum (i.e. the addition of 0.5ml D_2O to 15mg of the dried complex) all of the complex did not dissolve and a precipitate remained. This precipitate could be free insoluble cyproterone acetate or an insoluble cyproterone acetate-β-cyclodextrin complex. The identity of this precipitate could be indirectly deduced from the results of the isolation procedure, introduced in section 1.5.2.1, on 200mg of the dried complex. For example, if no solid remains after the isolation procedure then it can be indirectly deduced that the precipitate which remained after the addition of 0.5ml D_2O to the dried complex is only insoluble cyproterone acetate. If a solid is isolated by the procedure then it can be deduced that the precipitate which remained after the addition of 0.5ml D_2O is a water-insoluble cyproterone acetate-β-cyclodextrin complex.

No complex was obtained by the isolation procedure on 200mg of the dried cyproterone acetate-

β-cyclodextrin complex therefore this complex is water soluble. The precipitate that formed during the preparation of the sample was only water insoluble cyproterone acetate. The detection of cyproterone acetate proton resonances in the ^1H NMR spectrum of the dried complex in D_2O proves that there was cyproterone acetate-β-cyclodextrin complex present in solution. These proton resonances cannot belong to uncomplexed steroid since cyproterone acetate is water insoluble.

The integrated proton spectrum of the cyproterone acetate-β-cyclodextrin complex prepared in D_2O by the sonication method also revealed a molecular ratio of 1:80. All of the complexed β-cyclodextrin was in solution since the cyproterone acetate-β-cycylodextrin complex is water soluble. Uncomplexed β-cyclodextrin was also in solution because it is water-soluble. All of the 15mg of β-cyclodextrin used to prepare the sample was in solution. Since the amount of β-cyclodextrin in solution was known, the molecular ratio could be used to calculate the amount of cyproterone acetate in solution. The following steps reveal the method used to obtain this amount:

i) The number of moles of β-cyclodextrin present in 0.5ml D_2O are :

MW (β-cyclodextrin) = 1135g/mol

number of moles $= \frac{0.0150g}{1135g/mol} = 1.32 \times 10^{-5}$ mol

ii) The molecular ratio of 1:80 is used in combination with the number of moles of β-cyclodextrin to calculate the number of moles of cyproterone acetate present in 0.5ml D_2O :

number of moles (cyproterone acetate) $= \frac{1.32 \times 10^{-5} \text{ mol}}{80.0} = 1.65 \times 10^{-7}$ mol

iii) The amount in grams of cyproterone acetate present in 0.5ml D_2O is :

mass (cyproterone acetate) $= 1.65 \times 10^{-7}$ mol $\times$ 416.9g/mol $= 6.88 \times 10^{-5}$ g $\simeq$ 0.07mg

In the sonicated sample of 15mg of β-cyclodextrin in 0.5ml D_2O there was approximately 0.07mg of dissolved cyproterone acetate present.

4.2.2 Cyproterone acetate-γ-cyclodextrin complex

A proton spectrum of the cyproterone acetate-γ-cyclodextrin complex prepared by the kneading method was recorded in D_2O. The integration values of the steroid and γ-cyclodextrin resonances gave a molecular ratio of 1:25. During the preparation of the sample, a precipitate remained after the addition of 0.5ml of D_2O to 15mg of dried cyproterone acetate-γ-cyclodextrin complex. The isolation procedure on 200mg of dried complex failed to isolate a complex. It can therefore be deduced that the cyproterone acetate-γ-cyclodextrin complex is water soluble and that the precipitate which formed during the preparation of the sample is only uncomplexed insoluble cyproterone acetate.

A sample of the cyproterone acetate-γ-cyclodextrin complex was also prepared by the sonication method. From the integrals of the cyproterone acetate and γ-cyclodextrin proton resonances found in the ^1H NMR spectrum of this sample a molecular ratio of 1:25 was calculated. The total amount of 20mg of γ-cyclodextrin used in the preparation of this sample dissolved since both γ-cyclodextrin and the cyproterone acetate-γ-cyclodextrin are water-soluble. The molecular ratio could be used to calculate that there was 0.3mg of dissolved cyproterone acetate in 0.5ml of D_2O.

4.2.3 Ethynyl oestradiol-β-cyclodextrin complex

A volume of 0.5ml D_2O was added to 15mg of the dried ethynyl oestradiol-β-cyclodextrin complex prepared by the kneading method. A steroid-cyclodextrin molecular ratio of 1:45-55 was obtained using the integrals of the proton resonances found in the ^1H NMR spectrum of this sample. Again, a precipitate remained after the addition of D_2O to the dried complex. A complex was obtained from the isolation procedure on 200mg of the dried ethynyl oestradiol-β-cyclodextrin complex. It can be deduced that the precipitate which remained after addition of D_2O to the dried complex is the water insoluble ethynyl oestradiol-β-cyclodextrin complex.

There is also a possibility that some uncomplexed insoluble ethynyl oestradiol was also present in the precipitate.

The successful isolation of a complex initially suggested that the ethynyl oestradiol-β-cyclodextrin complex is water-insoluble. The detection of ethynyl oestradiol proton resonances in the ^{1}H NMR spectrum of this complex proved that there is still ethynyl oestradiol present in solution. These observed steroid proton resonances cannot belong to uncomplexed ethynyl oestradiol since this steroid is water-insoluble. Taking these factors into consideration the ethynyl oestradiol-β-cyclodextrin complex is considered to be a poorly water-soluble complex.

The stoichiometry of complexation (see 1.4.2.1) of an isolated complex can be deduced from the proton resonances found in the ^{1}H NMR spectrum of this complex dissolved in DMSO-d_6. Steroids are expelled from the cavities of cyclodextrins upon addition of isolated steroid-β- or γ-cyclodextrin complexes to dimethyl sulphoxide.[39] Most steroids as well as both β- and γ-cyclodextrin are soluble in dimethyl sulphoxide. Therefore, upon the addition of 5mg of an isolated steroid-cyclodextrin complex to 0.5ml DMSO-d_6 all steroid and cyclodextrin should dissolve. The steroid and cyclodextrin proton resonances recorded from the ^{1}H NMR spectrum of this sample can be integrated and these values can be used to calculate the molecular ratio. Since the isolation procedure ensures the removal of free uncomplexed-steroid and -cyclodextrin the molecular ratio will be equivalent to the stoichiometry of complexation of the isolated steroid-cyclodextrin complex.

An amount of 5mg of the isolated ethynyl oestradiol-β-cyclodextrin complex completely dissolved in 0.5ml DMSO-d_6. The calculated molecular ratio of the ethynyl oestradiol-β-cyclodextrin complex, which is equivalent to the stoichiometry of complexation, was 1:2. The isolation of the complex as well as the determined molecular ratio of 1:2 in DMSO-d_6 were reproducible. The 1:2 stoichiometry is evidence that the isolated poorly water soluble ethynyl oestradiol-β-cyclodextrin consists of one ethynyl oestradiol molecule which is complexed to two β-cyclodextrin molecules.

The molecular ratio of ethynyl oestradiol to β-cyclodextrin of 1:45-55 was obtained after an amount of β-cyclodextrin had already precipitated as insoluble complex. The amount of ethynyl oestradiol present in the sonicated sample can therefore not be established using the molecular ratio. For an equal number of scans the proton spectrum of the cyproterone acetate-β-cyclodextrin sample prepared by the sonication method had a better signal to noise ratio for the observed steroid proton resonances than the ethynyl oestradiol-β-cyclodextrin sample. The ethynyl oestradiol-β-cylodextrin sonicated sample therefore has an even smaller amount of dissolved steroid than the cyproterone acetate-β-cyclodextrin sample.

The small amount of dissolved ethynyl oestradiol indicates that there is a low concentration of ethynyl oestradiol-β-cyclodextrin complex present in the sonicated sample. This low concentration of ethynyl oestradiol-β-cyclodextrin complex is expected to give a poor signal to noise ratio for any observed intermolecular NOE's. Any increase in the complex concentration may improve the signal to noise ratio in the NOE experiment. A way to increase the concentration of the ethynyl oestradiol-β-cyclodextrin complex was sought so that reliable intermolecular NOE values could be obtained.

The ethynyl oestradiol-β-cyclodextrin complex is poorly soluble in D_2O. Steroids are expelled from the β-cyclodextrin cavity upon addition of dimethyl sulphoxide to a steroid-β-cyclodextrin complex.[39] Dimethyl sulphoxide is capable of dissolving both ethynyl oestradiol and β-cyclodextrin. A mixture of dimethyl sulphoxide and deuterium oxide may have the ability to increase the concentration of the ethynyl oestradiol-β-cyclodextrin complex with a minimum loss of complex due to expulsion of the steroid.

Sonicated samples, each containing 1mg ethynyl oestradiol and 15mg β-cyclodextrin, were prepared in solutions consisiting of various DMSO-d_6:D_2O volume ratios. These solutions were prepared with DMSO-d_6 volumes of 0.1, 0.2, 0.3, 0.4 and 0.5cm^3 and D_2O was added to each sample to a final volume of 0.6cm^3. The ethynyl oestradiol and β-cyclodextrin were totally dissolved in the samples which contained DMSO-d_6 volumes of 0.2cm^3 or greater.

4.2.4 Ethynyl oestradiol-γ-cyclodextrin complex

A sample was prepared from the addition of 0.5ml D_2O to 15mg of the dried ethynyl oestradiol-γ-cyclodextrin complex that was obtained by the kneading method. The integration values of the steroid and γ-cyclodextrin proton resonances in the ^1H NMR spectrum of this sample gave a molecular ratio of 1:5. Upon addition of D_2O to the dried complex a precipitate remained. No complex could be obtained by the isolation procedure on 200mg of the dried complex which was prepared by the kneading method. The ethynyl oestradiol-γ-cyclodextrin complex is therefore water soluble and the precipitate which formed after addition of D_2O is uncomplexed insoluble ethynyl oestradiol.

The proton spectrum of the ethynyl oestradiol-γ-cyclodextrin complex prepared by the sonication method also revealed a molecular ratio of 1:5. All of the 20mg of γ-cyclodextrin used to prepare this sample was in solution, either in the uncomplexed state or in the water soluble ethynyl oestradiol-γ-cyclodextrin complexed state. The molecular ratio was used to calculate an amount of 0.9mg of ethynyl oestradiol present in 0.5ml D_2O.

4.2.5 Danazol-β-cyclodextrin complex

An amount of 15mg of the dried danazol-β-cyclodextrin prepared by the kneading method was added to 0.5ml D_2O. This sample was used to record a ^1H NMR spectrum. A molecular ratio of 1:8 was calculated from the integration values of the danazol and β-cyclodextrin proton resonances. A precipitate resulted upon addition of 0.5ml D_2O to the dried complex. The isolation procedure, on the dried complex that was prepared by the kneading method, did not obtain a complex. The danazol-β-cyclodextrin is therefore a water soluble complex and the precipitate that formed upon addition of 0.5ml D_2O to the dried complex was only uncomplexed insoluble danazol.

The preparation of the danazol-β-cyclodextrin complex by the sonication method gave a molecular ratio of 1:8 from the integration of the danazol and cyclodextrin resonances in the recorded proton spectrum. β-Cyclodextrin and the danazol-β-cyclodextrin complex are both

water soluble therefore all of the 15mg of β-cyclodextrin was dissolved and the molecular ratio could be used to calculate an amount of 0.6mg of dissolved danazol present in this sample of 0.5ml D_2O.

A further sample was prepared by adding quantities of 1mg danazol and 15mg of β-cyclodextrin to a mixture of 0.2ml DMSO-d_6 and 0.4ml D_2O. A precipitate resulted in the preparation of this sample. The ^1H NMR spectrum from a sample prepared by only adding an amount of 1mg of danazol to a mixture of 0.2ml DMSO-d_6 and 0.4ml D_2O detected no danazol proton resonances. Danazol is therefore insoluble in this solvent mixture. If it is assumed that the precipitate which formed was insoluble danazol and not the danazol-β-cyclodextrin complex it could be concluded that all of the 15mg of β-cyclodextrin was in solution. The molecular ratio of 1:120 could be used to calculate an amount of 0.04mg of dissolved danazol present in this sample.

The above assumption was confirmed by the results of the following experiment. Quantities of 10.0mg of danazol and 150.0mg of β-cyclodextrin were added to a mixture containing 2.0ml of DMSO-d_6 and 4.0ml D_2O. This sample was then sonicated for two hours. The precipitate which formed was isolated by filtration and washed twice by 3.0ml of solvent which was a mixture of 1ml DMSO-d_6 and 2ml D_2O. An amount of 5mg of the washed filtrate was then dissolved in 0.5ml DMSO-d_6. The ^1H NMR spectrum of this sample only recorded danazol proton resonances. The precipitate did not contain any β-cyclodextrin.

4.2.6 Danazol-γ-cyclodextrin complex

The ^1H NMR spectrum was recorded from a sample of 15mg of the dried danazol-γ-cyclodextrin complex in 0.5ml D_2O. Only the proton resonances belonging to γ-cyclodextrin could be recorded, no proton resonances belonging to danazol were detected. The isolation procedure on the dried danazol-γ-cyclodextrin complex obtained a complex. The danazol-γ-cyclodextrin complex is water-insoluble. The isolation of the danazol-γ-cyclodextrin complex was reproducible but the stoichiometry of the complex could not be determined. The molecular ratios determined in DMSO-d_6 from a number of isolated danazol-γ-cyclodextrin complexes did not converge to any value. A possible explanation is that the danazol-γ-cyclodextrin complex is

slightly soluble in diethyl ether. Upon dissolution of the complex in diethyl ether danazol is expelled from the γ-cyclodextrin cavity allowing the free γ-cyclodextrin to precipitate in the organic medium. During the isolation procedure on the danazol-γ-cyclodextrin complex, the steroid to cyclodextrin ratio changed each time this complex came into contact with diethyl ether.

An amount of 1mg of danazol and 20mg of γ-cyclodextrin was added to 0.5ml D_2O. This sample was then placed in a sonic bath. No danazol proton resonances were observed in the ^1H NMR spectrum. The absence of danazol proton resonances proves that there is no or extremely little dissolved danazol-γ-cyclodextrin complex. To increase the concentration of the danazol-γ-cyclodextrin complex, these complexes were prepared in various DMSO-d_6: D_2O volume ratios. Amounts of 1mg danazol and 20mg γ-cyclodextrin were added to the identical volume ratios that were previously used in the preparation of the ethynyl oestradiol-β-cyclodextrin samples (see 4.2.3).

4.2.7 A comparison of the kneading and sonication methods

The inclusion reaction can take place in various mediums. It can take place in aqueous medium, organo-aqueous medium (coprecipitation), in a paste (kneading method) or by simple grinding. Throughout all these methods at least trace amounts of water must be present because the complex formation occurs in an aqueous environment. The inclusion reaction occurs when both the steroid and cyclodextrin are in the aqueous phase so that an equilibrium can be established with a characteristic equilibrium constant K (fig 4.1). The constant K, also known as the stability constant, is a measure of the tendency of the complex to dissociate in the presence of water.

Whether the kneading method or the sonication method is used to prepare the 0.5ml D_2O samples, the steroid-cyclodextrin complexes will still have the same tendency to dissociate in the presence of water. This is reflected by a consistent molecular ratio for a steroid-cyclodextrin complex irrespective of which method is used to prepare this complex.

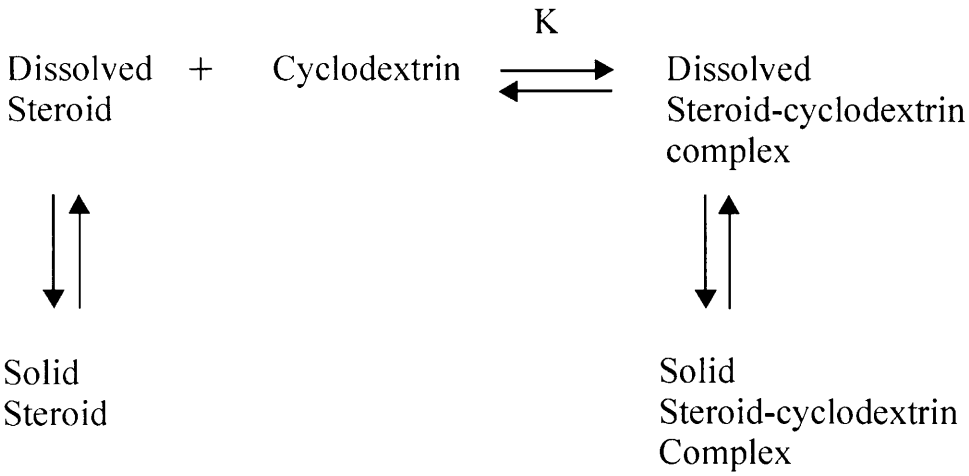

Figure 4.1 Equilibria for inclusion formation in aqueous medium.

The ability of the cyclodextrin to increase the solubility of a steroid in the 0.5ml D_2O sample is dependant only on the stability constant K and not on the method used to prepare the complexes. The sonication method was chosen to prepare the samples for further NMR investigations because the amount of dissolved steroid in the samples could easily be calculated for water soluble complexes and all the complexes of this study could be directly prepared in the NMR sample tube.

4.3 The chemical shift determination of the steroid-cyclodextrin complexes

The assigned phase sensitive DQF-COSY spectra of the steroids in $CDCl_3$ were used as templates to aid the assignments of the steroid proton resonances of the COSY spectra of the steroid-cyclodextrin complexes. The fine structure of the crosspeaks and the number of protons within each spin system of the steroid are preserved in both the phase sensitive DQF-COSY spectra recorded from the steroid in $CDCl_3$ and the steroid in an aqueous solution of β- or γ-cyclodextrin.

The phase sensitive DQF-COSY spectrum of the cyproterone acetate-β-cyclodextrin complex prepared by the sonication method in D_2O is used as an example to illustrate how the chemical

shifts of all the steroid-cyclodextrin complexes were obtained (fig 4.2). Most of the chemical shifts of the steroid proton resonances were determined directly from the proton spectrum but when overlap occurred the midpoints of the scalar crosspeaks in the phase sensitive DQF-COSY spectrum were used. The chemical shift determination of 12α-H which is overlapped by methyl proton resonances is used to illustrate the method.

The chemical shift frequencies of two scalar coupled protons can be obtained from the (F_1, F_2) frequencies of the midpoint of the corresponding crosspeak in the phase sensitive DQF-COSY spectrum. The chemical shift frequency of 12α-H was determined from the average of the two relevant frequencies of the midpoints of the two scalar crosspeaks of 11β-H to 12α-H situated on either side of the diagonal of the phase sensitive DQF-COSY spectrum as can be seen in figure 4.2.

By comparing the chemical shifts of proton resonances that could be obtained from the ^{1}H NMR spectrum and the phase sensitive DQF-COSY spectrum, such as proton 11β-H (fig 4.2), the chemical shift frequencies did not differ by more than 5Hz. It can be concluded that the chemical shift frequencies of steroid protons determined using the phase sensitive DQF-COSY spectrum are accurate to ±5Hz for a 500 MHz NMR spectrometer. This is equivalent to an accuracy for the chemical shift of ±0.01ppm.

There are significant differences between the chemical shifts of the steroid protons when complexed to β- and to γ-cyclodextrin. This difference is defined as Δ :

$$\Delta = \text{chemical shift of steroid protons in steroid-}\gamma\text{-cyclodextrin complex} - \text{chemical shift of steroid protons in steroid-}\beta\text{-cyclodextrin complex} \quad [4.1]$$

For example the chemical shift of the cyproterone acetate proton 7-H when complexed to β-cyclodextrin in deuterium oxide is 6.590ppm and when complexed to γ-cyclodextrin is 6.419ppm. Giving a Δ = -0.171ppm. The chemical shifts of the proton 7-H in both complexes have been determined from their respective proton spectra. The chemical shift differences for protons whose chemical shifts have been determined from the midpoints of the crosspeaks in the

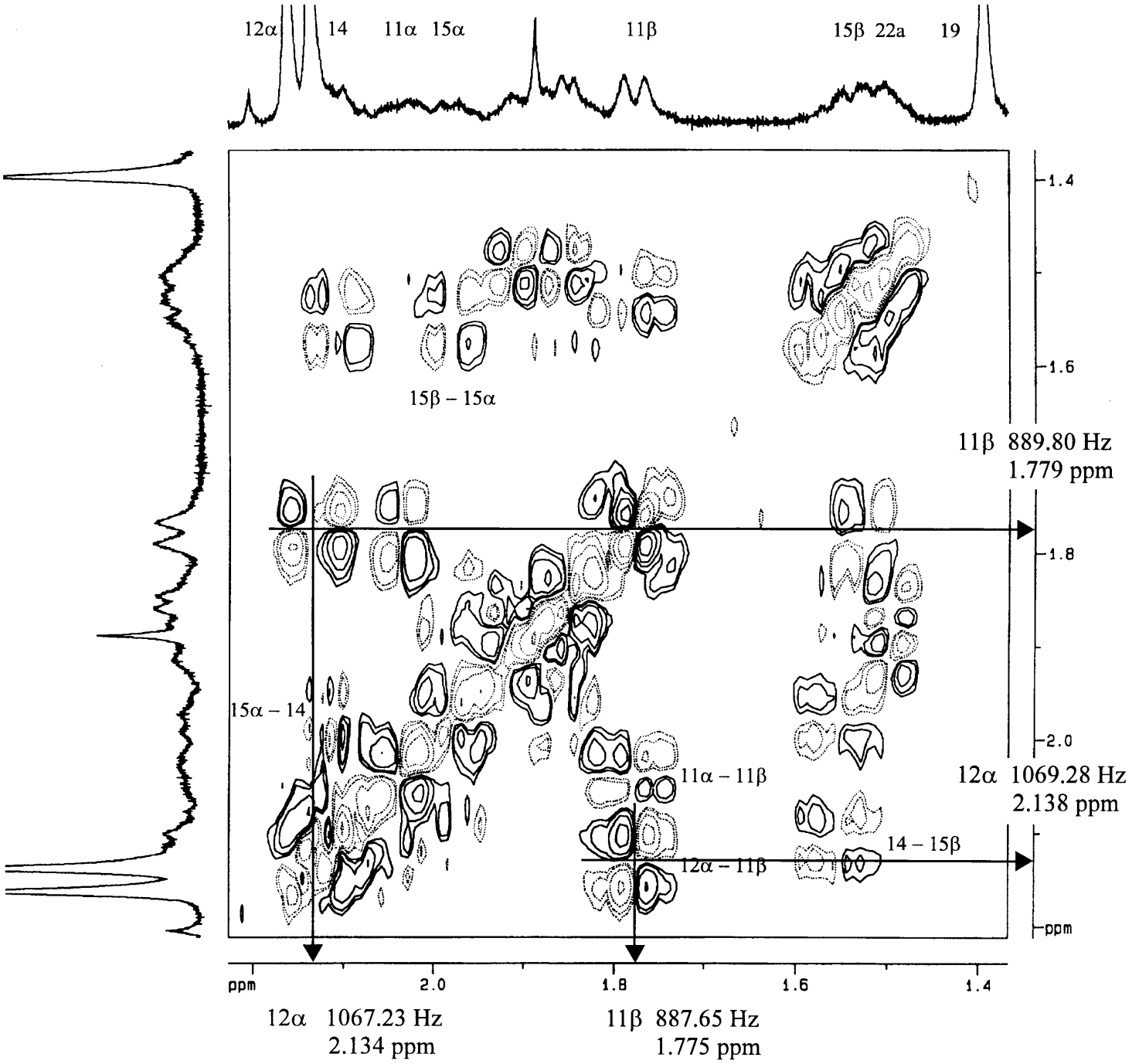

Figure 4.2 Expanded region of the phase sensitive DQF-COSY spectrum of the cyproterone acetate-β-cyclodextrin complex in deuterium oxide. The chemical shift determinations of the protons 11β-H and 12α-H are illustrated.

phase sensitive DQF-COSY spectra are only significant if the absolute Δ values are greater than 0.04ppm. The reason being that the chemical shifts of these overlapping protons were determined to an accuracy of ± 0.01ppm, giving an accuracy for Δ of ±0.02ppm.

4.4 The intermolecular NOE values of the steroid-cyclodextrin complexes

The host-guest inclusion geometry of the steroid-cyclodextrin complexes can be deduced from the nuclear Overhauser effect. Due to the reasons discussed in section 2.5.3 the 2-D ROESY experiment was exclusively used in this study.[36,76]

All the 2-D ROESY experiments were accumulated by placing the carrier frequency in the centre of the proton spectrum which is between 4ppm and 5ppm. Fortunately, when the 2-D ROESY experiment was used to study host-guest complexes, there was no contribution to the magnitudes of the intermolecular NOE crosspeaks as a result of *coherent-transfer through scalar coupling* simply because the steroid is not covalently bonded to the cyclodextrin.

A spin locking field of 2.0kHz was used to record all the 2D-ROESY spectra. The duration of the mixing time which would ensure an optimum NOE buildup between protons of the steroid and cyclodextrin had to be found. The danazol-β-cyclodextrin sonicated sample prepared in D_2O was chosen for the initial study to determine a favourable mixing time. This sample had a high concentration of danazol-β-cyclodextrin complex (see 4.2.5).

Two 2-D ROESY experiments were recorded for each of the mixing times 75, 150, 225 and 300ms. For every processed 2-D ROESY spectrum the intermolecular NOE crosspeaks between the danazol protons 22-H and 4-H and the β-cyclodextrin proton 3 and the overlapping protons 5 and 6 were integrated as shown in figure 4.3. As an example, only the values of the integrations of the crosspeaks of the danazol 22-H to the overlapping cyclodextrin protons 5 and 6 are found in table 4.1. The single proton resonances of 22-H of danazol found on the diagonal of every 2-D ROESY spectrum were also integrated and are given in table 4.2.

Table 4.1 Integrated NOE magnitudes of danazol 22-H to the overlapping β-cyclodextrin protons 5 and 6

	mixing times			
	75ms	150ms	225ms	300ms
Exp 1	3.2322	4.9286	5.3032	5.3423
Exp 2	3.3092	4.4318	5.2131	5.5262
Average	3.2707	4.6802	5.2582	5.4343

Table 4.2 Integrated magnitudes of the diagonal proton resonances of danazol 22-H

	mixing times			
	75ms	150ms	225ms	300ms
Exp 1	55.791	51.381	47.464	42.759
Exp 2	56.359	49.939	46.919	43.055
Average	56.075	50.660	47.192	42.907

The averages of all the integrated NOE magnitudes obtained from the two 2-D ROESY experiments recorded with a mixing time of 75ms were converted to percentages. The average of the integrated diagonal danazol 22-H resonance obtained from these same two experiments was defined as unity. This same procedure was followed for the conversion of the averages obtained at mixing times 150, 225 and 300ms. These percentages will be referred to as NOE percentages (%NOE). The following example illustrates the conversion of an integral of an NOE crosspeak to an NOE percentage. The NOE percentage of the danazol 22-H to the overlapping β-cyclodextrin protons 5 and 6 is calculated from the 2-D ROESY experiments recorded with a mixing time of 75ms :

$$\%NOE = (3.2707 / 56.075) \times 100 = 5.8327\ \% \qquad [4.2]$$

From equation 4.2, the value of 5.8327% shows that the instrumental facility of the Bruker ARX-500 spectrometer allows the NOE percentages to be calculated to four decimals. The value

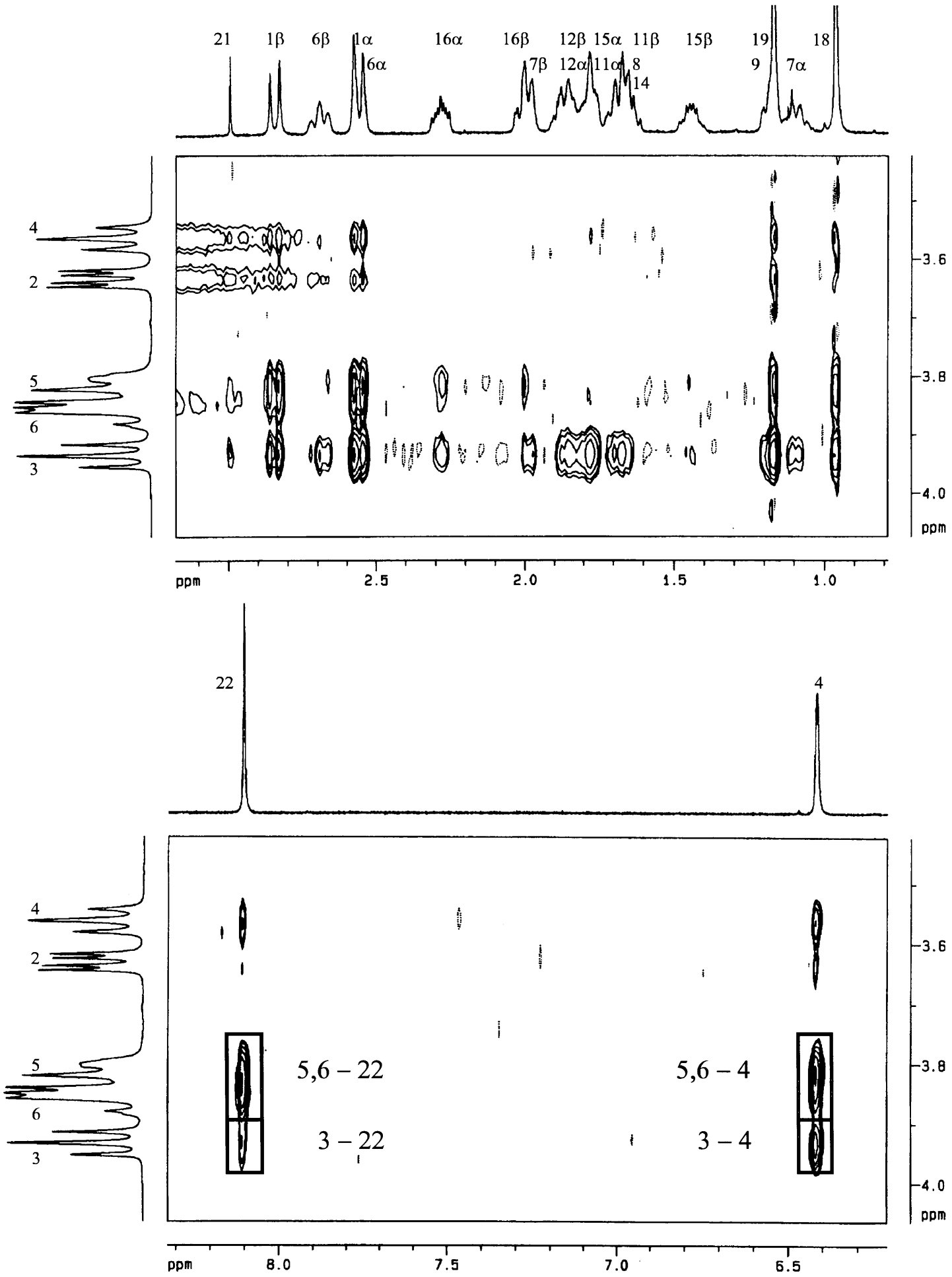

Figure 4.3 The 2-D ROESY spectrum of the danazol-β-cyclodextrin complex in deuterium oxide. The regions that were integrated to obtain the magnitudes of the NOE crosspeaks of the danazol protons 4-H and 22-H to the β-cyclodextrin protons are shown.

of the calculated NOE percentages can be influenced by the processing procedures of the 2-D ROESY spectra such as the manual phasing and the automatic baseline corrections of the spectra. The accumulation parameters such as the number of experiments, 256 or 512, the number of scans for each experiment, the length of the mixing time and the magnitude of the spin locking field can introduce variation to the integrated values. If all these factors which can influence the calculated NOE percentages are taken into consideration, it can be argued that these NOE percentages are only significant to one decimal place. The complete results of these conversions are found in tables 4.3 and 4.4.

Table 4.3 The %NOE of the danazol protons 22-H and 4-H to the β-cyclodextrin proton 3

	mixing times			
	75ms	150ms	225ms	300ms
22-H	0.6	0.9	1.0	1.6
4-H	2.3	4.2	5.5	7.1

Table 4.4 The %NOE of the danazol protons 22-H and 4-H to the overlapping β-cyclodextrin protons 5 and 6

	mixing times			
	75ms	150ms	225ms	300ms
22-H	5.8	9.2	11.1	12.7
4-H	5.6	10.3	12.8	15.0

The NOE percentages have been normalised with respect to the single proton diagonal resonance 22-H found in all the processed 2-D ROESY spectra. This normalisation allows the %NOE listed in table 4.3 and 4.4 to be compared with each other. The NOE buildup can therefore be followed by graphing the %NOE given in the two previous tables as a function of the mixing time as shown in figures 4.4 and 4.5.

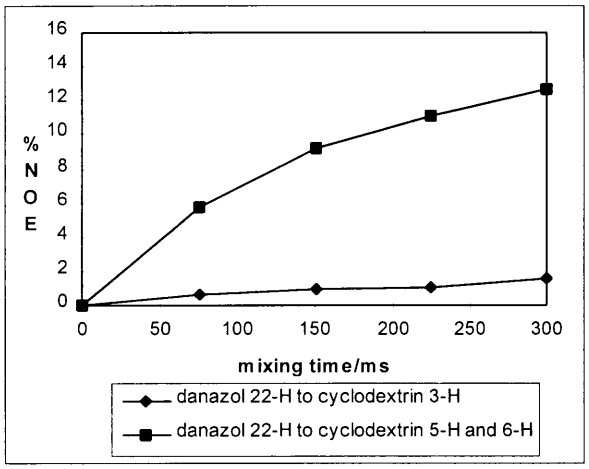

Figure 4.4 The NOE buildup between the danazol 22-H and the β-cyclodextrin protons.

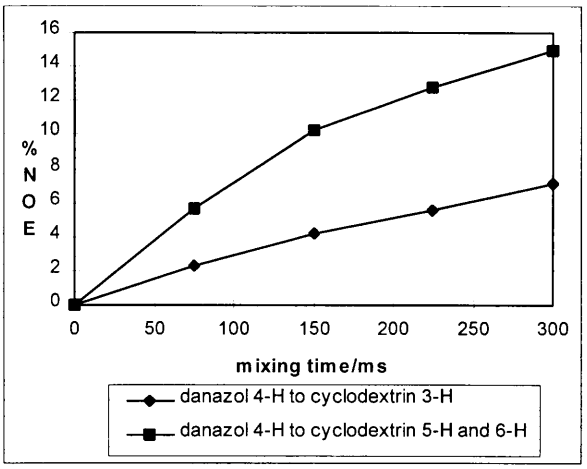

Figure 4.5 The NOE buildup between the danazol 4-H and the β-cyclodextrin protons.

The NOE percentages of danazol 4-H to the overlapping β-cyclodextrin protons 5 and 6 for the mixing times 75ms and 150ms are 5.6% and 10.3% respectively(table 4.4). This is almost a 100% increase to the %NOE. The increases taken from table 4.4 of 10.3% to 12.8% and 12.8% to 15.0% are consecutive increases to the NOE perentage of 24% and 17% respectively. The mixing time periods of 150ms to 225ms and 225ms to 300ms do not lead to the 100% increase in the NOE percentage previously obtained during the mixing time period of 75ms to 150ms. After a mixing time of 150ms, during the accumulation of a 2-D ROESY experiment, the rate of the NOE buildup decreases considerably.

The rate of the NOE buildup between the danazol 4-H and the β-cyclodextrin protons 5 and 6 is a trend which is followed by all the NOE buildups illustrated in figures 4.4 and 4.5. The following deductions can be made for these NOE buildups. A mixing time of 250ms will allow the two-fold increase in the %NOE which occurs between 75ms and 150ms. The mixing time of 250ms will also ensure a further ~24% increase in the %NOE which occurs during the mixing time period of 150ms and 225ms.

If it is assumed that all the intermolecular NOE buildups between the steroid and cyclodextrin protons of the complexes of this study follow the same trend as those which are illustrated in figures 4.4 and 4.5, a mixing time of 250ms will ensure a reasonable NOE buildup. A chosen

mixing time of 250ms should therefore promote the detection of sufficient NOE crosspeaks to be used to successfully model the inclusion geometry of the various steroid-cyclodextrin complexes.

The results of the 2-D ROESY experiments recorded with a mixing time of 250ms on all the sonicated samples containing steroid and cyclodextrin are now presented.

4.4.1 Cyproterone acetate-β-cyclodextrin

Two 2-D ROESY experiments were run on the sample containing cyproterone acetate and β-cyclodextrin. It was deduced from the small amount of 0.07mg of dissolved cyproterone acetate in 0.5ml D_2O that there was a low concentration of complex. Both 2-D ROESY experiments were recorded with 128 scans for the 256 experiments to obtain a reasonable signal to noise ratio (fig 4.4). Even with 128 scans per experiment only a few intermolecular NOE crosspeaks between cyproterone acetate and β-cyclodextrin protons were detected. The magnitudes of these intermolecular NOE crosspeaks could still be used to model the inclusion geometry of the cyproterone acetate-β-cyclodextrin complex. To enhance the accuracy of the NOE values the crosspeaks in the 2-D ROESY spectra were integrated. These integrated values were then converted to NOE percentages. The integrated intermolecular NOE values of the cyproterone acetate 4-H to the β-cyclodextrin protons is used as an example to illustrate this conversion.

The magnitudes of the integrated NOE crosspeaks, as shown in figure 4.4, between cyproterone acetate 4-H and β-cyclodextrin proton 3, the overlapping protons 5 and 6, proton 2 and proton 4 obtained from the two consecutive 2-D ROESY experiments, are given in table 4.5. The single proton resonances of 7-H, 4-H, 16β-H and 8-H of cyproterone acetate found on the diagonals of both 2-D ROESY spectra were also integrated (table 4.6).

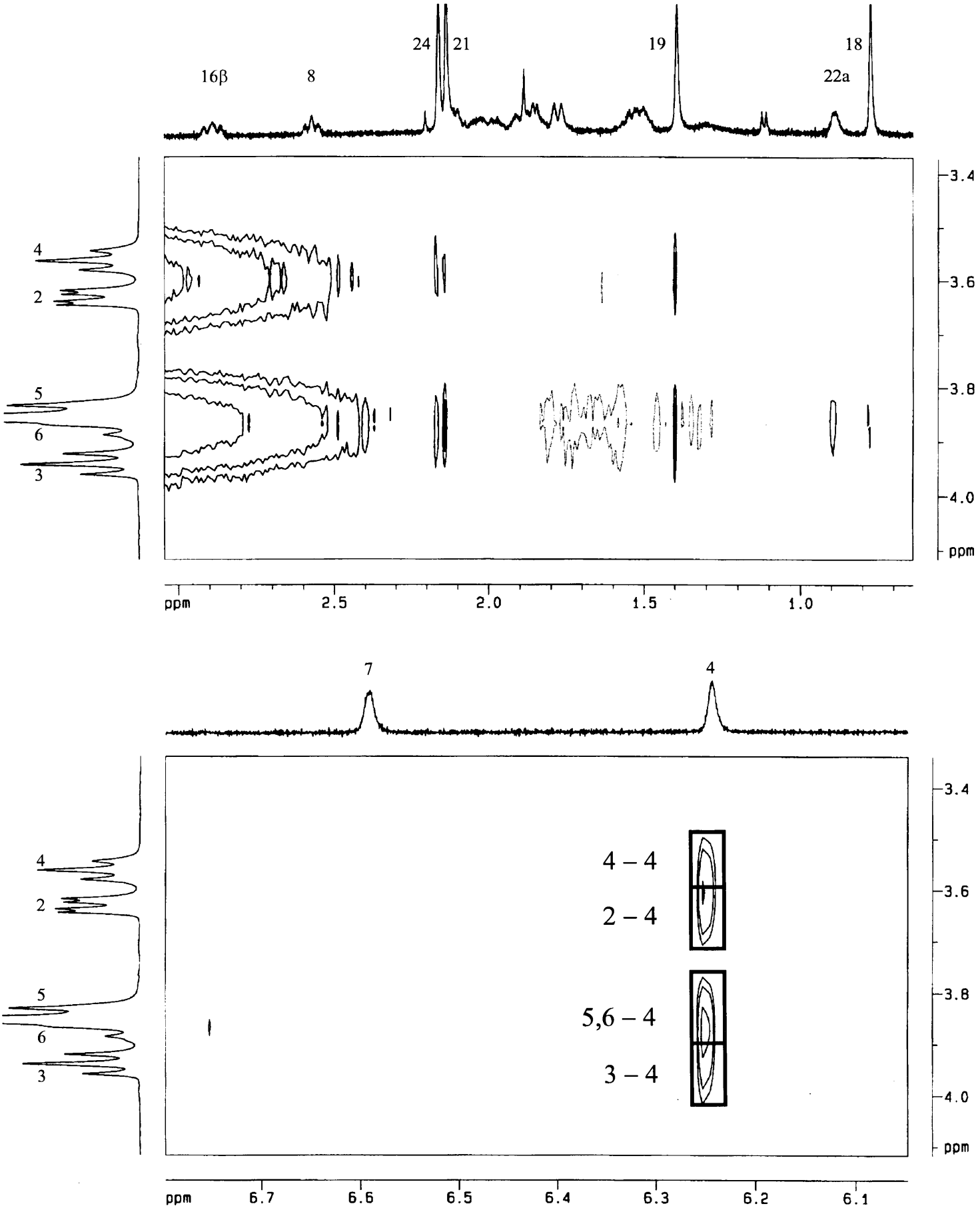

Figure 4.4 The 2-D ROESY spectrum of the cyproterone acetate-β-cyclodextrin complex in deuterium oxide. The regions that were integrated to obtain the magnitudes of the NOE crosspeaks of the cyproterone acetate proton 4-H to the β-cyclodextrin protons are shown.

Table 4.5 Integrated NOE magnitudes of cyproterone acetate 4-H to the β-cyclodextrin protons

	3	5/6	2	4
Exp 1	3.3144	4.0747	2.7934	2.8365
Exp 2	4.0112	5.4524	3.2899	3.1171
Average	3.6628	4.7636	3.0417	2.9768

Table 4.6 Integrated NOE magnitudes of diagonal protons

	7-H	4-H	16β-H	8-H
Expt 1	95.29	102.06	88.72	103.32
Expt 2	82.84	88.66	82.25	92.77

As was expected all the resonances of these single steroid protons found on the diagonal had integration values of a similar magnitude. The average value of these integrations was equal to 91.99. The average values found in table 4.5 were then converted to NOE percentages where the average value of the single diagonal proton resonances of 91.99 was defined as unity (table 4.7).

Table 4.7 Intermolecular NOE percentages of proton 4-H

	3	5/6	2	4
4-H	3.982	5.178	3.307	3.236

The only difference between the conversion of these integrated magnitudes to NOE percentages and the conversion of the previous magnitudes given in tables 4.3 and 4.4, was the fact that more than one diagonal proton resonance was used in defining the integrated magnitude which was to be equivalent to unity.

The fact that the NOE percentages in table 4.7 have been calculated to four figures can convey the incorrect impression that they have four significant figures. As mentioned earlier, the

processing and accumulation factors of the 2-D ROESY experiment can influence the values of the final NOE percentages. The calculated NOE percentages should rather be interpreted as having only one significant figure, though they may be listed in tables 4.8 to 4.16 to one or at most to two decimal places. This interpretation of the significance of the calculated NOE percentages does not prevent the use of these percentages to model the inclusion geometries of the steroid-cyclodextrin complexes. In the past, the even simpler categorisation of intermolecular NOE crosspeak magnitudes into the three classes of small, medium and large has been successfully used to model the inclusion geometry of guest-host complexes.[36] All the NOE percentages found in the tables 4.8 to 4.16 have been obtained with the same procedure used to obtain the NOE percentages of the cyproterone acetate proton 4-H to the β-cyclodextrin protons. To summarise, this procedure involved the integration of the intermolecular NOE crosspeaks and then converting these values to NOE percentages. The value of an integrated single steroid proton resonance found on the diagonal of each 2-D ROESY spectrum was defined as unity.

Table 4.8 contains the chemical shifts and the NOE percentages obtained from the phase sensitive DQF-COSY and the 2-D ROESY experiments run on the sample containing cyproterone acetate and β-cyclodextrin dissolved in D_2O. This table contains the chemical shifts of the β-cyclodextrin proton 3, the overlapping protons 5 and 6, proton 2 and proton 4. For the overlapping protons 5 and 6 only the chemical shift of proton 5 was determined since it could be obtained from the midpoint of the scalar crosspeak of proton 4 to proton 5 found in the phase sensitive DQF-COSY spectra. The first two columns of Table 4.8 contain the proton chemical shifts and the corresponding assignments of the cyproterone acetate proton resonances. The last four columns contain the intermolecular NOE percentages between the steroid protons listed in the rows to the cyclodextrin protons heading the columns. The blank spaces present in all the tables represent the instances where the intermolecular NOE crosspeaks could not be accurately integrated or where they were not observed. For example, the intermolecular NOE percentages for steroid protons 16β-H and 8-H to the β-cyclodextrin protons could not be determined due to severe baseline noise present in the 2-D ROESY spectrum in the region where these possible NOE crosspeaks were expected (fig 4.4).

Table 4.8 Chemical shifts and intermolecular %NOE's between cyproterone acetate and β-cyclodextrin in deuterium oxide

steroid chemical shifts		%NOE			
δ in decreasing order	proton	3 3.940ppm	5/6 3.845ppm(5)	2 3.630ppm	4 3.561ppm
6.590	7	1.0	2.0	1.0	1.0
6.244	4	4.0	5.0	3.0	3.0
2.891	16β				
2.572	8				
2.162	24	0.5	1.0	1.0	1.0
2.138	21	0.5	2.0	1.0	1.0
2.136	12α				
2.110	14				
2.042	11α				
1.909	2β	0.5	1.0	0.5	0.5
1.86	15α	0.5	0.3	0.3	0.3
1.86	16α				
1.856	1β				
1.81	12β				
1.777	11β				
1.553	15β				
1.524	9				
1.498	22b	1.0	1.5	0.2	0.5
1.396	19	1.5	2.5	1.5	1.0
0.886	22a	2.0	3.0	1.0	1.0
0.775	18	1.5	2.5	1.0	1.0

There appears to be a contradiction between table 4.8 and the corresponding 2-D ROESY spectrum illustrated in figure 4.4. The NOE percentages in table 4.8 of cyproterone acetate 7-H to the β-cyclodextrin proton 3, the overlapping 5 and 6, 2 and 4 of 1.0%, 2.0%, 1.0% and 1.0%, respectively are calculated from the magnitudes of the corresponding NOE crosspeaks. In figure 4.4 these crosspeaks are absent. All the NOE percentages found in table 4.8 have been calculated from the spectra of two 2-D ROESY experiments. Both these 2-D ROESY spectra had a poor signal to noise ratio. The processing parameters, such as the manual phasing and the automatic baseline corrections, can prevent the observation of weak intensity NOE crosspeaks where there is a poor signal to noise ratio. The one 2-D ROESY spectrum illustrated in figure 4.4 had poor success in detecting the NOE crosspeaks of cyproterone acetate 7-H to the β-cyclodextrin protons. The other processed 2-D ROESY experiment had better success in detecting these weak NOE crosspeaks. The NOE percentages of 7-H to the β-cyclodextrin protons are calculated from the average of the results of the spectra obtained from both 2-D ROESY experiments. These results showed that the accumulation of two 2-D ROESY experiments for each of the samples containing steroid and cyclodextrin could increase the probability of detecting the weaker intermolecular NOE crosspeaks.

There were occasions when the steroid proton signals overlapped and the identitiy of the steroid proton or protons responsible for the intermolecular NOE crosspeak to the cyclodextrin protons could not be identified, these crosspeaks were still integrated but in the table 4.8 they are represented as a joined cell encompassing all the steroid protons which could possibly contribute to the observed NOE crosspeak. The tables 4.9 to 4.16 have the same layout as table 4.8. The tables 4.9,4.11,4.13 and 4.16 of the steroid-γ-cyclodextrin complexes contain an additional column with the Δ values.

4.4.2 Cyproterone acetate-γ-cyclodextrin

The processed 2-D ROESY experiment run on the sample containing cyproterone acetate and γ-cyclodextrin was recorded with 64 scans per experiment and is shown in figure 4.5. This spectrum had a better signal to noise ratio for the intermolecular NOE crosspeaks than the processed 2-D ROESY experiment run on the sample containing cyproterone acetate and

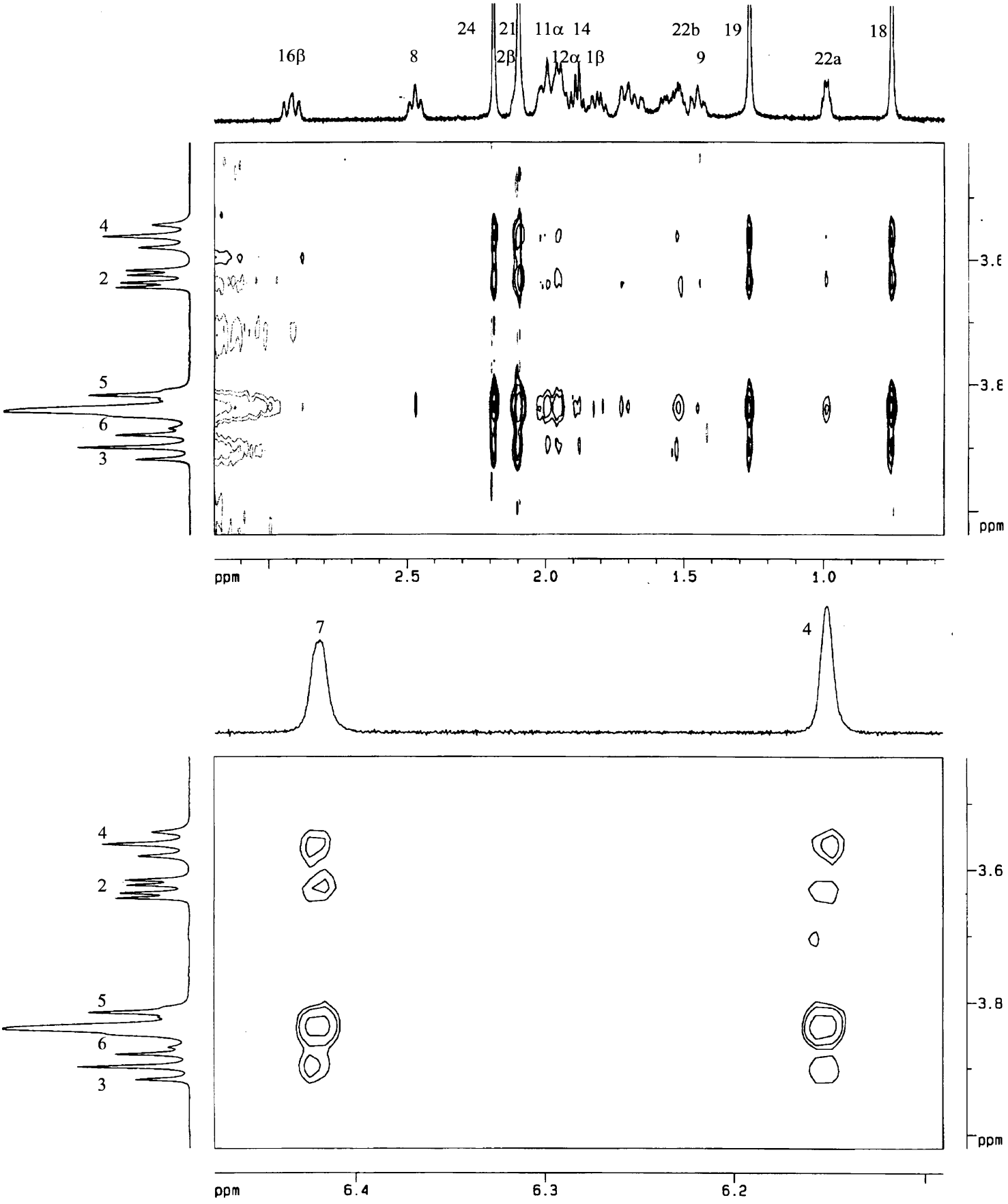

Figure 4.5 The 2-D ROESY spectrum of the cyproterone acetate-γ-cyclodextrin complex in deuterium oxide.

β-cyclodextrin. Increases to the concentration of the steroid-cyclodextrin complex resulted in improvements to the signal to noise ratio of the intermolecular NOE crosspeaks. The higher concentration of the cyproterone acetate-γ-cyclodextrin complex could be deduced from the amount of 0.3mg of dissolved cyproterone acetate in comparison to the cyproterone acetate-β-cyclodextrin complex which only had 0.07mg of dissolved cyproterone acetate (see 4.2.1 and 4.2.2).

The 2-D ROESY experiment run on the sample containing cyproterone acetate and γ-cyclodextrin was recorded using 512 experiments and the 2-D ROESY run on the sample of cyproterone acetate and β-cyclodextrin was recorded using 256 experiments. The NOE crosspeaks of cyproterone acetate 4-H to the β- and γ-cyclodextrin protons, shown in figures 4.4 and 4.5, respectively can be compared to illustrate the increase in resolution accompanied by an increase in the number of experiments used to record the 2-D ROESY experiment. Unless stated otherwise, all of the 2-D ROESY experiments that were run on the samples of this study were recorded using 512 experiments. This ensured that a reasonable degree of resolution would be present in the spectra.

The NOE percentages that were calculated from the crosspeaks found in the 2-D ROESY spectrum of the cyproterone acetate-γ-cyclodextrin complex can be found in table 4.9.

4.4.3 Ethynyl oestradiol-β-cyclodextrin complex

Two 2-D ROESY experiments were run on the sample containing ethynyl oestradiol and β-cyclodextrin in D_2O prepared by the sonication method. Each of the 2-D ROESY experiments were accumulated with 128 scans for each of the 256 experiments. The calculated intermolecular NOE percentages obtained from the 2-D ROESY spectrum are given in table 4.10. This 2-D ROESY spectrum had a poor signal to noise ratio for the observed intermolecular NOE crosspeaks. As mentioned before, in an attempt to increase the concentration of the ethynyl oestradiol-β-cyclodextrin complex in the sample, quantities of 1mg of ethynyl oestradiol and 15mg of β-cyclodextrin were dissolved in different DMSO-d_6: D_2O volume ratios. 2-D ROESY experiments were recorded for each of the newly prepared samples. The sample with 0.2ml of

DMSO-d_6 and 0.4ml D_2O gave the best signal to noise ratio for the observed intermolecular NOE crosspeaks (see fig 4.6). On the grounds that a higher complex concentration would deliver an improved signal to noise ratio, it could be deduced this sample had the highest concentration of ethynyl oestradiol-β-cyclodextrin complex. The intermolecular NOE percentages calculated from the 2-D ROESY spectra of this sample are given in table 4.11.

4.4.4 Ethynyl oestradiol-γ-cyclodextrin complex

The sample containing ethynyl oestradiol and γ-cyclodextrin had an amount of 0.9mg of dissolved ethynyl oestradiol in 0.5ml D_2O. This large amount of dissolved steroid could be used to deduce that there was a high concentration of ethynyl oestradiol-γ-cyclodextrin in this sample. As was expected, the recorded 2-D ROESY experiments of this sample of 32 scans per experiment resulted in a good signal to noise ratio for the observed intermolecular NOE crosspeaks (fig 4.6).

Further 2-D ROESY experiments were run on a sample containing 1mg of ethynyl oestradiol and 20mg of γ-cyclodextrin prepared in a mixture of 0.2ml DMSO-d_6 and 0.4ml D_2O (fig 4.7). A difference of the 2-D ROESY spectra of this sample when compared to the previous 2-D ROESY spectra of ethynyl oestradiol and γ-cyclodextrin in D_2O, was the observation of more intermolecular NOE crosspeaks from the ethynyl oestradiol protons to the γ-cyclodextrin protons 2 and 4.

The calculated intermolecular NOE percentages obtained from the 2-D ROESY spectra of the ethynyl oestradiol-γ-cyclodextrin complex in D_2O and in DMSO-d_6: D_2O are listed in table 4.12 and 4.13 respectively.

4.4.5 Danazol-β-cyclodextrin complex

The sonicated sample prepared by adding 1mg of danazol and 15mg of β-cyclodextrin to 0.5ml D_2O resulted in an amount of 0.6mg of dissolved danazol. The spectra of the 2-D ROESY experiments of 32 scans for each experiment had a good signal to noise ratio for the

intermolecular NOE crosspeaks (fig 4.3).

The spectra of the 2-D ROESY experiments run on the sample containing danazol and β-cyclodextrin in a mixture of 0.2ml DMSO-d_6 and 0.4ml D_2O (see 4.2.5) had a poor signal to noise ratio for the intermolecular NOE crosspeaks. The amount of 0.04mg of dissolved danazol in this sample is complexed steroid only. Danazol in the free uncomplexed state has been determined to be insoluble in this solvent mixture. The small amount of dissolved danazol is used to deduce that there is also a low concentration of danazol-β-cyclodextrin complex. A low concentration of complex will account for the poor signal to noise ratio for the intermolecular NOE crosspeaks obtained from the 2-D ROESY spectra.

The preparation of the ethynyl oestradiol-β-cyclodextrin and ethynyl oestradiol-γ-cyclodextrin complexes in a mixture of 0.2ml DMSO-d_6 and 0.4ml D_2O led to 2-D ROESY spectra which had good signal to noise ratios. The same could not be said for the 2-D ROESY spectrum of the danazol-β-cyclodextrin complex prepared in the same mixture.

The intermolecular NOE percentages obtained from the 2-D ROESY spectra of the danazol-β-cyclodextrin complexes prepared in D_2O and in DMSO-d_6: D_2O can be found in tables 4.14 and 4.15, respectively.

4.4.6 Danazol-γ-cyclodextrin complex

The danazol-γ-cyclodextrin complex is a water insoluble complex. Amounts of 1mg of danazol and 20mg of γ-cyclodextrin were added to different DMSO-d_6: D_2O volume ratios to find the optimum sample conditions which would result in the best signal to noise ratio for the detected intermolecular NOE crosspeaks from the 2D-ROESY experiment. The sample prepared in a mixture of 0.2ml DMSO-d_6 and 0.4ml D_2O gave the best signal to noise ratio (fig 4.9). The intermolecular NOE percentages obtained from the 2-D ROESY spectra run on this sample can be found in table 4.16.

Table 4.9 Chemical shifts and intermolecular %NOE's between cyproterone acetate and γ-cyclodextrin in deuterium oxide

steroid chemical shifts		Δ	%NOE			
δ in decreasing order	proton		3 3.901ppm	5/6 3.832ppm(5)	2 3.627ppm	4 3.556ppm
6.419	7	-0.171	1.5	2.0	0.5	1.0
6.152	4	-0.092	1.0	2.0	0.5	1.0
2.915	16β	0.024				
2.471	8	-0.101				
2.186	24	0.024	4.0	6.0	2.0	2.5
2.096	21	-0.042	5.0	8.0	3.0	3.0
2.103	2β	0.194				
2.012	11α	-0.030	3.0	3.0	1.0	1.0
1.98	12α	-0.156				
1.944	14	-0.166				
1.885	1β	0.029	0.3	0.3		
1.82	15α	-0.04				
1.82	16α	-0.04				
1.712	12β	-0.10				
1.674	11β	-0.103				
1.56	15β	0.007				
1.521	22b	0.023	0.5	0.2	0.2	0.1
1.448	9	-0.076				
1.265	19	-0.131	3.0	4.0	1.5	1.5
0.992	22a	0.106	0.5	0.5	0.2	0.2
0.756	18	-0.019	3.0	4.0	2.0	2.0

Table 4.10 Chemical shifts and intermolecular %NOE's between ethynyl oestradiol and β-cyclodextrin in deuterium oxide

steroid chemical shifts		%NOE			
δ in decreasing order	proton	3 3.942ppm	5/6 3.836ppm(5)	2 3.622ppm	4 3.560ppm
7.154	1	4.0	10.0	2.0	2.0
6.538	2	5.0	15.0	2.5	3.0
6.531	4				
3.131	21				
2.86	6α				
2.86	6β				
2.496	11α				
2.331	16α	3.0	10.0	3.0	4.0
2.162	9	2.5	7.0	2.0	3.0
2.127	16β				
2.034	7β	1.5	4.0	1.0	3.0
2.019	12α				
1.920	15α				
1.882	12β				
1.840	14				
1.574	11β				
1.474	15β				
1.398	7α				
1.310	8				
1.030	18	2.0	4.0	2.5	3.0

Table 4.11 Chemical shifts and %NOE's between ethynyl oestradiol and β-cyclodextrin in DMSO-d_6 :deuterium oxide

steroid chemical shifts		%NOE			
δ in decreasing order	proton	3/6 3.914 (3) 3.877 (6)	5 3.796ppm	2 3.670ppm	4 3.616ppm
7.170	1	7.0	6.0	2.0	3.0
6.664	2	10.0	4.0	1.0	1.5
6.650	4				
3.197	21	1.5	0.5	0.3	0.3
2.82	6α	10.0	6.5	3.0	4.0
2.82	6β				
2.580	11α	4.0	2.0	1.5	1.5
2.427	16α	0.6	0.3	0.1	0.1
2.174	9	6.0	4.0	2.0	2.0
2.162	16β				
2.099	7β	7.0	3.5	2.5	2.5
2.049	12α				
1.962	15α	5.0	1.5	2.0	1.5
1.909	12β				
1.827	14	1.6	0.8	0.5	0.3
1.548	15β	5.5	2.5	2.0	2.0
1.524	11β				
1.428	7α	7.0	4.0	2.0	2.5
1.377	8				
1.024	18	6.0	2.0	3.0	2.0

Table 4.12 Chemical shifts and intermolecular %NOE's between ethynyl oestradiol and γ-cyclodextrin in deuterium oxide

steroid chemical shifts		Δ	%NOE			
δ in decreasing order	proton		3 3.879ppm	5/6 3.799ppm(5)	2 3.624ppm	4 3.559ppm
7.090	1	-0.064	2.5	5.0	0.0	0.0
6.709	2	0.171	2.0	3.5	0.0	0.0
6.672	4	0.141	0.5	1.5	0.0	0.0
3.074	21	-0.057	2.4	2.0		
2.81	6α	-0.05	5.0	5.5		
2.81	6β	-0.05				
2.355	11α	-0.141	3.5	5.0	0.0	0.0
2.309	16α	-0.022				
2.017	9	-0.145	2.0	4.0	0.0	0.0
1.959	16β	-0.168				
1.842	12α	-0.177	4.0	7.0	0.0	0.0
1.842	7β	-0.192				
1.777	15α	-0.143				
1.732	12β	-0.150				
1.647	14	-0.193				
1.410	11β	-0.164	2.0	3.0	0.0	0.0
1.351	15β	-0.123				
1.329	8	0.019				
1.271	7α	-0.127				
0.849	18	-0.181	4.0	5.0	0.1	0.1

Table 4.13 Chemical shifts and NOEs between ethynyl oestradiol and γ-cyclodextrin in DMSO-d_6 :deuterium oxide

steroid chemical shifts		Δ	%NOE			
δ in decreasing order	proton		3/6 3.900(3) 3.894(6)	5 3.822ppm	2 3.675ppm	4 3.610ppm
7.194	1	0.024	2.4	1.0	0.8	0.8
6.774	2	0.110	2.0	0.4	0.15	0.20
6.727	4	0.077	1.0	0.3	0.20	0.3
3.211	21	0.014	3.0	1.2	1.0	0.8
2.90	6α	0.08	4.0	1.5	1.5	1.0
2.90	6β	0.08				
2.447	11α	-0.133	2.5	1.5	1.0	1.0
2.350	16α	-0.077	1.5	0.5	0.2	0.2
2.083	9	-0.091	5.0	2.5	1.0	1.5
2.024	16β	-0.138				
1.930	7β	-0.169	4.0	2.0	1.0	1.0
1.890	12α	-0.159				
1.819	15α	-0.143	4.5	2.5	1.0	1.5
1.793	12β	-0.116				
1693	14	-0.134	1.5	1.0	0.1	0.2
1.420	11β	-0.104	7.0	4.0	1.5	2.0
1.397	15β	-0.151				
1.345	8	-0.032				
1.333	7α	-0.095				
0.897	18	-0.127	7.0	4.0	2.0	2.5

Table 4.14 Chemical shifts and intermolecular %NOE's between danazol and β-cyclodextrin in deuterium oxide

steroid chemical shifts		%NOE			
δ in decreasing order	proton	3 3.935ppm	5/6 3.809ppm(5)	2 3.633ppm	4 3.564ppm
8.104	22	1.0	14.0	0.1	1.0
6.415	4	7.0	14.5	0.4	1.8
3.004	21	0.5	0.5		
2.848	1β	4.0	6.0	1.0	1.5
2.698	6β	2.5	1.2	0.5	0.5
2.563	1α	10.0	8.0	1.5	1.5
2.556	6α				
2.285	16β	1.5	1.5	0.0	0.0
2.003	16α	1.5	0.3	0.0	0.0
1.985	7β				
1.95-1.75	12β	14.0	1.0	0.0	0.0
1.882	12α				
1.844	15α				
1.781	11α				
1.75-1.60	11β	5.0	0.0	0.0	0.0
1.675	8				
1.655	14				
1.438	15β	0.5	0.1	0.0	0.0
1.182	9	12.0	5.0	0.8	0.8
1.171	19				
1.095	7α	2.0	0.0	0.0	0.0
0.967	18	5.5	5.5	0.5	0.5

Table 4.15 Chemical shifts and %NOE's between danazol and β-cyclodextrin in DMSO-d_6 : deuterium oxide

steroid chemical shifts		%NOE			
δ in decreasing order	proton	3/6 3.904(3)	5 3.815ppm	2 3.677ppm	4 3.614ppm
8.231	22	6.0	4.5	0.2	1.0
6.520	4	11.0	7.5	0.8	1.2
3.060	21				
2.919	1β				
2.636	1α				
2.63	6α				
2.63	6β				
2.317	16α				
2.067	16β				
2.022	7β				
1.842	15α	8.0	0.0	0.0	0.0
1.90-1.60	12α				
1.90-1.60	12β				
1.90-1.60	11α				
1.697	8				
1.636	14				
1.75-1.45	11β				
1.500	15β				
1.216	9	10.0	1.8	0.0	0.0
1.197	19				
1.131	7α				
0.998	18	1.0	0.8	0.0	0.0

Table 4.16 Chemical shifts and %NOE's between danazol and γ-cyclodextrin in DMSO-d_6 :deuterium oxide

steroid chemical shifts		Δ	%NOE			
δ in decreasing order	proton		3/6 3.888(3)	5 3.809ppm	2 3.672ppm	4 3.606ppm
8.352	22	0.121	2.0	0.5	0.05	0.25
6.446	4	-0.074	2.5	0.8	0.15	0.25
3.176	21	0.116	5.0	1.4	0.5	0.3
2.877	1β	-0.042	3.0	1.0	0.4	0.3
2.559	1α	-0.077	7.0	2.4	0.6	0.8
2.55	6α	-0.08				
2.55	6β	-0.08				
2.307	16α	-0.010	1.0	0.5	0.0	0.0
2.006	16β	-0.061	1.3	0.9	0.0	0.0
1.875	7β	-0.147	2.0	1.2	0.0	0.0
1.749	15α	-0.093	9.5	6.0	0.3	1.2
1.694	11α					
1.80-1.65	12α					
1.80-1.65	12β					
1.561	8	-0.136	4.5	3.0	0.1	0.4
1.509	14	-0.127				
1.60-1.45	11β					
1.358	15β	-0.142	1.7	1.0	0.0	0.0
1.114	19	-0.083	4.2	2.0	0.2	0.5
1.042	9	-0.174	4.7	2.8	0.0	0.5
0.999	7α	-0.132				
0.914	18	-0.084	6.7	3.8	0.5	0.9

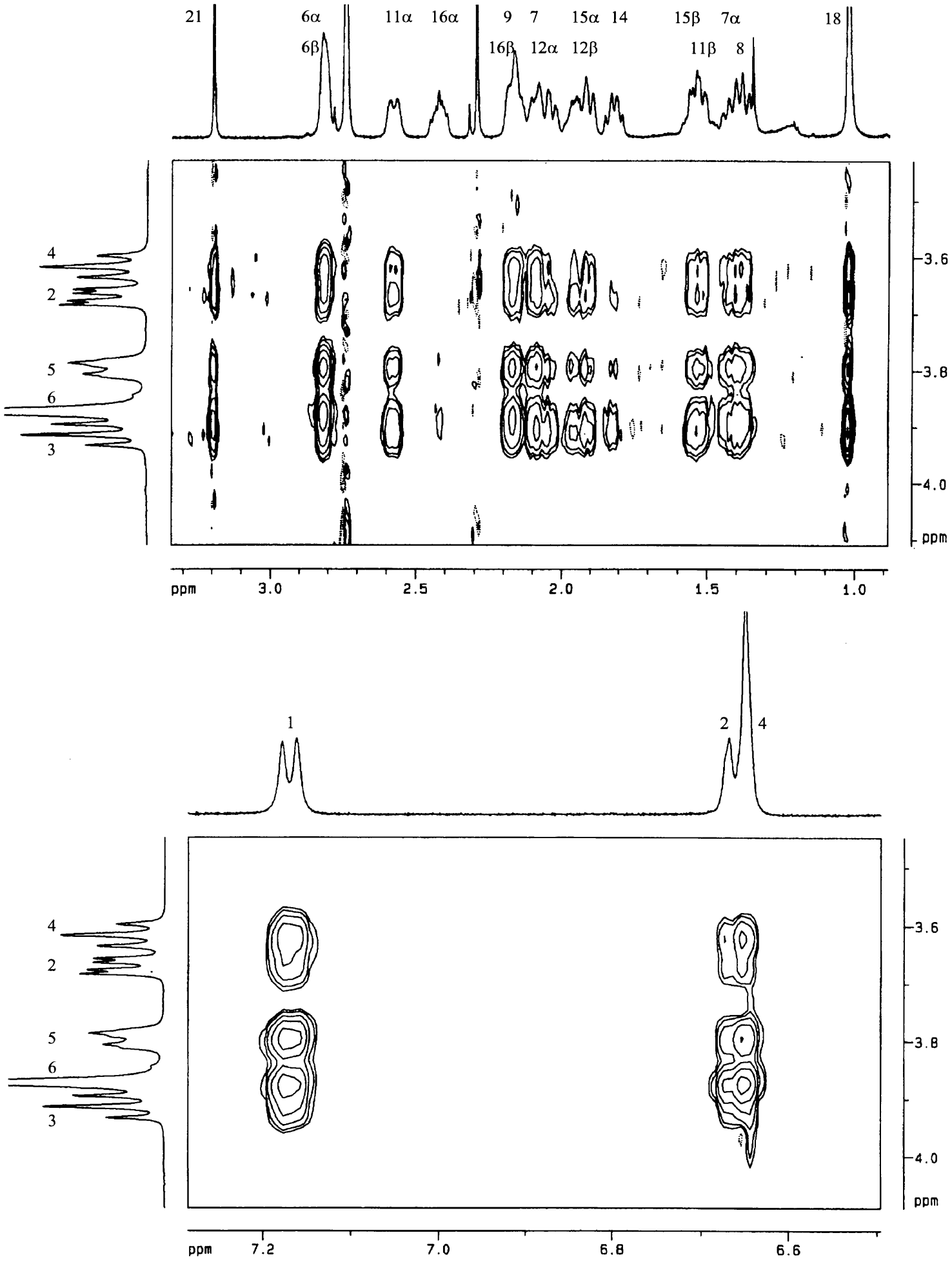

Figure 4.6 The 2-D ROESY spectrum of the ethynyl oestradiol-β-cyclodextrin complex in DMSO-d_6 :deuterium oxide.

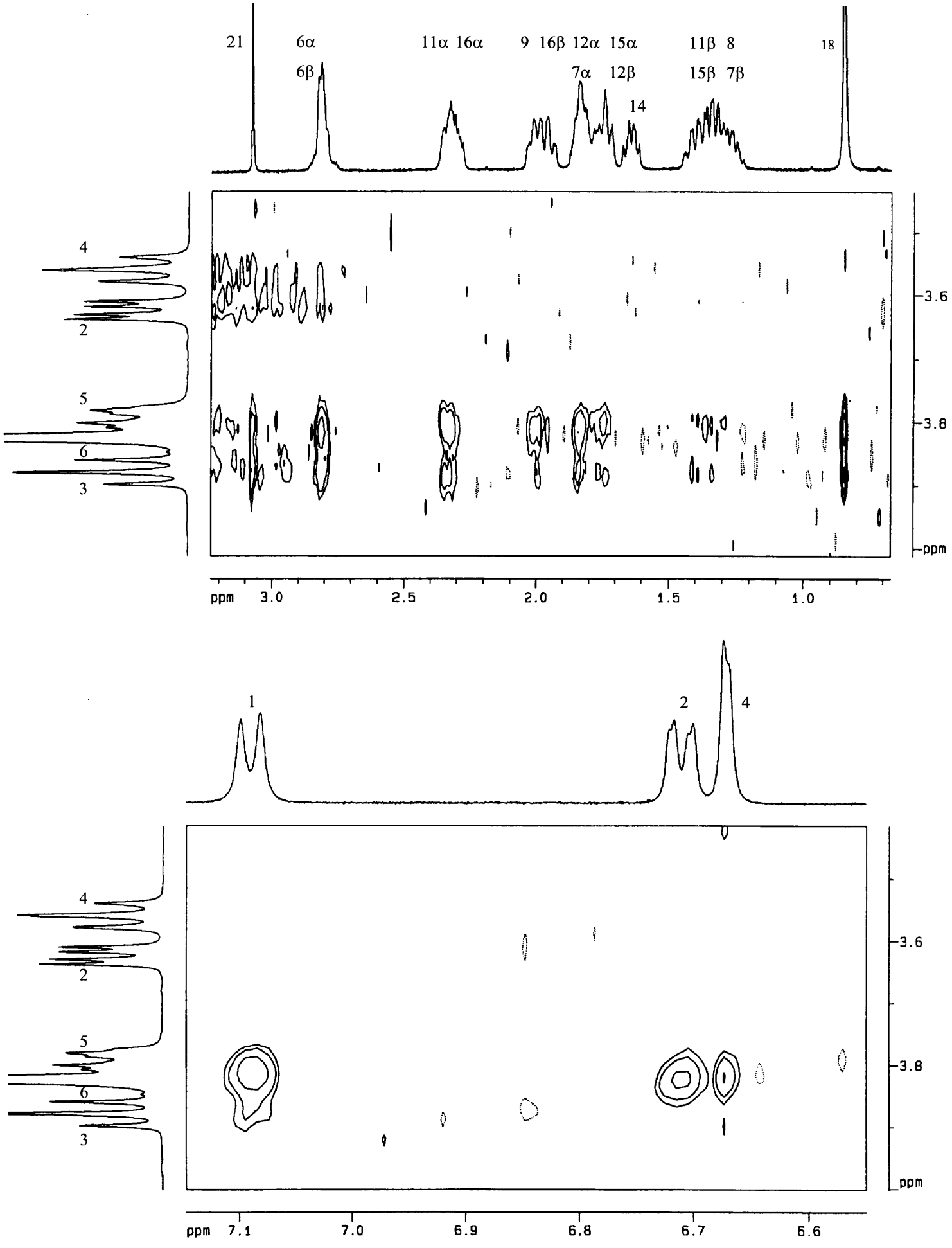

Figure 4.7 The 2-D ROESY spectrum of the ethynyl oestradiol-γ-cyclodextrin complex in deuterium oxide.

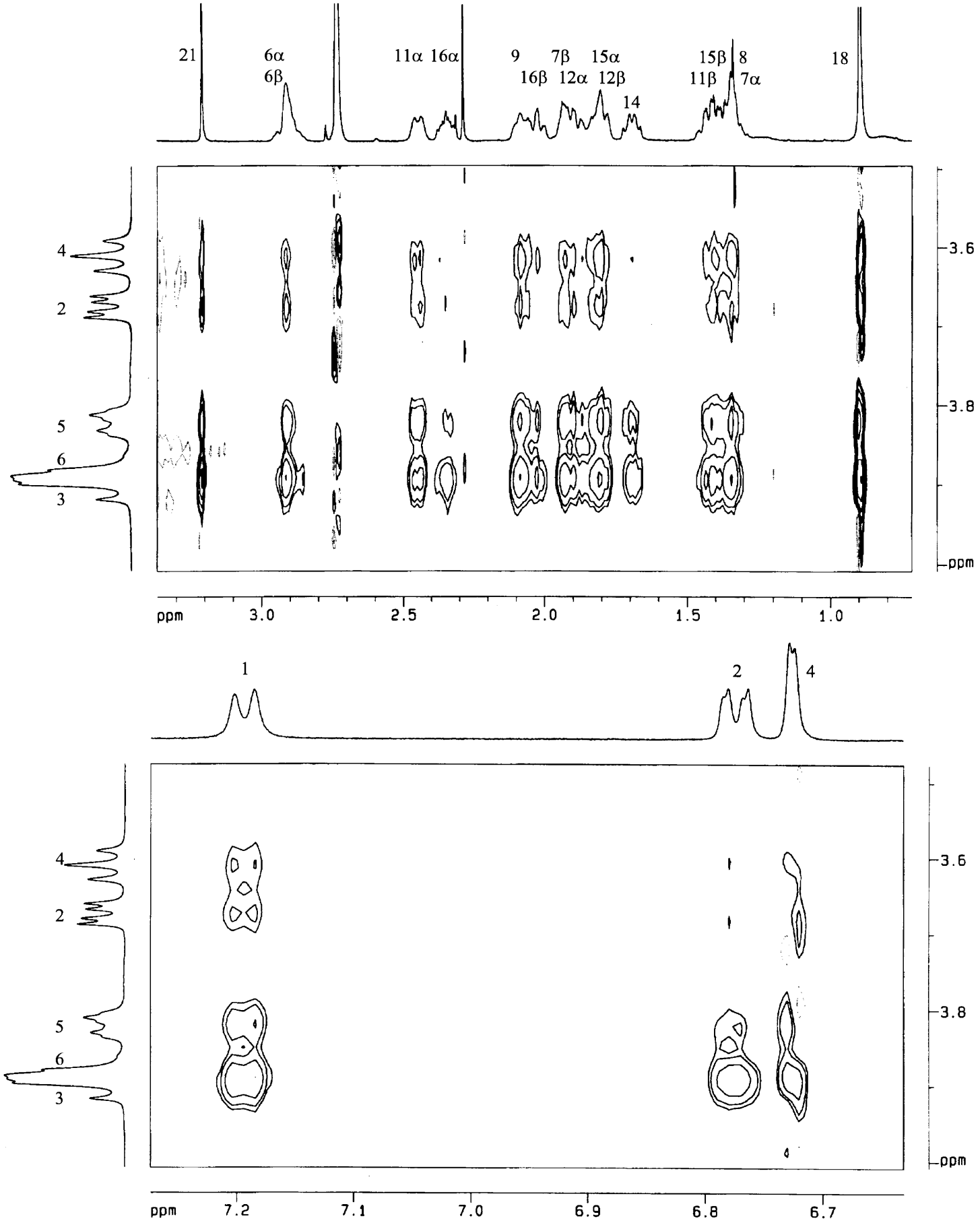

Figure 4.8 The 2-D ROESY spectrum of the ethynyl oestradiol-γ-cyclodextrin complex in DMSO-d_6 :deuterium oxide.

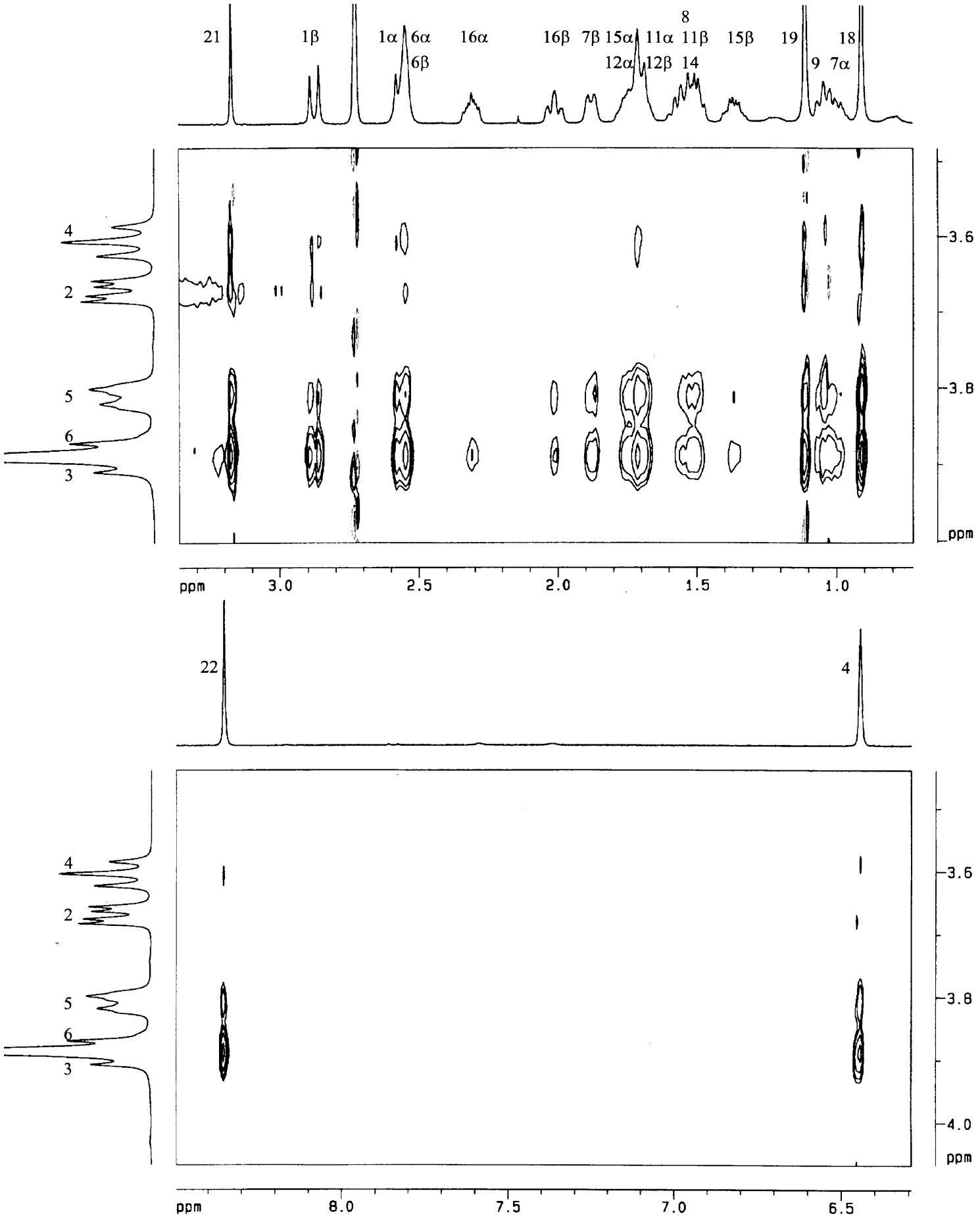

Figure 4.9 The 2-D ROESY spectrum of the danazol-γ-cyclodextrin complex in DMSO-d_6 :deuterium oxide.

4.5 Summary

The water solubilities of the steroid-cyclodextrin complexes are given in table 4.17. The calculated molecular ratios as well as the deduced amounts of dissolved steroid are also summarised in table 4.17. The larger the amount of dissolved steroid the better the signal to noise ratio of the NOE crosspeaks. Since the magnitude of the amount of dissolved steroid is proportional to the concentration of steroid-cyclodextrin complex for the samples prepared in D_2O it follows that the higher the concentration of complex the better the signal to noise ratio for an intermolecular NOE crosspeak.

Table 4.17 Sonicated samples prepared in 0.5ml D_2O

Complex	Solubility of complexes	Mol. ratio	Dissolved steroid/ mg	ROESY	%NOE
cyproterone acetate-β-CD	soluble	1:80	0.07	Fig 4.4	Table 4.8
cyproterone acetate-γ-CD	soluble	1:25	0.3	Fig 4.5	Table 4.9
ethynyl oestra-diol-β-CD	poorly soluble	1:45-55	unable to determine	-	Table 4.10
ethynyl oestra-diol-γ-CD	soluble	1:5	0.9	Fig 4.7	Table 4.12
danazol-β-CD	soluble	1:8	0.6	Fig 4.3	Table 4.14
danazol-γ-CD	insoluble	-	0.0	-	-

The molecular ratios and the amounts of dissolved steroid for the steroid-cyclodextrin complexes prepared in a mixture of 0.2ml DMSO-d_6 and 0.4ml D_2O are given in table 4.18. Three of the prepared samples listed in table 4.18 were clear solutions with both steroid and cyclodextrin dissolved. In these samples the total amount of 1mg steroid, which was added during the preparation of these complexes, was in solution. The molecular ratios obtained from the ^1H NMR spectrum of these samples could be independantly used to confirm that there was indeed 1mg of dissolved steroid. Only the sample that was prepared by adding amounts of 1mg of danazol and

15mg of β-cyclodextrin to a mixture of 0.2ml DMSO-d_6 and 0.4ml D_2O resulted in the formation of a precipitate. The molecular ratio of 1:120 gave an amount of 0.04mg of dissolved danazol present in this sample.

Table 4.18 Sonicated samples prepared in 0.2ml DMSO-d_6 : 0.4ml D_2O

Complex	Mol. ratio	Dissolved steroid/ mg	ROESY	%NOE
ethynyl oestra-diol-β-CD	1:3.9	1.0	Fig 4.6	Table 4.11
ethynyl oestra-diol-γ-CD	1:4.5	1.0	Fig 4.8	Table 4.13
danazol-β-CD	1:120	0.04	-	Table 4.15
danazol-γ-CD	1:4.5	1.0	Fig 4.9	Table 4.16

In all the water soluble steroid-cyclodextrin complexes it was possible to detect the nuclear Overhauser effects between the protons of the steroid and cyclodextrin in the 2-D ROESY spectra recorded from the samples prepared in D_2 O. These intermolecular NOE crosspeaks were then converted to NOE percentages which were used to model the inclusion geometry of the steroid-cyclodextrin complexes.

No danazol proton resonances were observed in the ^{1}H NMR spectrum of the danazol-γ-cyclodextrin complex in D_2O. This negated the possibility of observing intermolecular NOE crosspeaks in a 2-D ROESY spectrum of this complex in D_2O. The spectra of the 2-D ROESY experiments run on the poorly soluble ethynyl oestradiol-β-cyclodextrin complex prepared in D_2O resulted in a poor signal to noise ratio for the intermolecular NOE crosspeaks. To improve the signal to noise ratio of the intermolecular NOE crosspeaks the steroid and cyclodextrin were dissolved in various volume ratios of DMSO-d_6 and D_2O. For both the ethynyl oestradiol-β-cyclodextrin and danazol-γ-cyclodextrin complexes the best signal to noise ratios of the

intermolecular NOE crosspeaks were obtained from the 2-D ROESY spectra of these complexes that were prepared in a mixture of 0.2ml DMSO-d_6 and 0.4ml D_2O. The accumulated NOE data in these 2-D ROESY spectra could be used to model the inclusion geometry of the complexes whereas previously no reliable NOE data could be obtained.

Though dimethyl sulphoxide causes expulsion of the steroids from the cavities of β- and γ-cyclodextrin.[39] The detection of the intermolecular NOE crosspeaks for all the complexes listed in Table 4.17 proves that these steroid-cyclodextrin complexes can exist in a mixture of DMSO-d_6 and D_2O.

To avoid false deductions to be made from the magnitudes of the tabulated NOE percentages of tables 4.8 to 4.16 a discussion concerning the margins of errors is warranted. From table 4.8, the NOE percentages of cyproterone acetate 7-H to β-cyclodextrin proton 3 and proton 2 are both equal to 1.0%. These percentages may lead to the unrealistic conclusion that the distances of 7-H to proton 3 and to proton 2 are equivalent. Since proton 3 is situated inside the cavity and proton 2 is found on the outside, on average an included cyproterone acetate 7-H will always be closer to proton 3 than to proton 2. It is therefore expected that the NOE percentage of 7-H to proton 3 should be larger than the NOE percentage of 7-H to proton 2. The discrepency in the magnitudes of these NOE percentages is attributed to a large margin of error for the calculated NOE percentages of table 4.8. The margin of error for the percentages found in table 4.8 can be expected to be in the region of ± 1.0% which can be attributed to the poor signal to noise ratio of the intermolecular NOE crosspeaks found in the 2-D ROESY spectrum of the cyproterone acetate-β-cyclodextrin complex. The same margin of error of ± 1.0% is expected for tables 4.9, 4.10 and 4.15.

For tables 4.11, 4.12, 4.13, 4.14 and 4.16 the margin of error is expected to be in the region of ± 0.5%. The lower margin of error can be attributed to the improved signal to noise ratios of the intermolecular NOE crosspeaks found in the 2-D ROESY spectra of the steroid-cyclodextrin complexes represented by these tables.

5 Modelling of the steroid-cyclodextrin complexes

5.1 Introduction

Both the stoichiometry of complexation and the inclusion geometry of host-guest complexes can be determined with methods which involve NMR spectroscopy (see 1.5.2). The determination of the stoichiometry of complexation involves the use of the Job Plot method (see 1.5.2.1).[36,41,76] Cyproterone acetate, ethynyl oestradiol and danazol are water insoluble steroids. All the samples that were required by the Job Plot method could not be prepared (see 1.5.2.1). This method could not be applied to the steroid-cyclodextrin complexes.

Only the stoichiometry of complexation for the ethynyl oestradiol-β-cyclodextrin complex could be obtained. In this instance the poorly water soluble ethynyl oestradiol-β-cyclodextrin complex was isolated and a 1:2 stoichiometry was determined (see 1.5.2.1 and 4.2.3). Unfortunately though the danazol-γ-cyclodextrin complex is water insoluble the isolation procedure could not be used to determine the stoichiometry. The steroid to cyclodextrin ratio of the danazol-γ-cyclodextrin complex did not remain constant throughout the isolation procedure (see 4.2.5). In conclusion, the stoichiometries of these steroid-cyclodextrin complexes, with the exception of one, could not be determined with the aid of NMR spectroscopic methods. Though the stoichiometry is an important property the objective of this study is rather the elucidation of the inclusion geometries of the steroid-cyclodextrin complexes. However, by taking the inclusion geometries into consideration it will be possible to propose realistic stoichiometries for these steroid-cyclodextrin complexes.

Two NMR spectroscopic methods can be used to determine the inclusion geometries of host-guest complexes. These methods depend on the use of the complexation induced shift (CIS) values (see 1.5.2.2) and the nuclear Overhauser effects (see 1.5.2.3) to model the inclusion geometries. The Benesi-Hildebrand method was used to obtain the CIS values of the protons of

naproxen when it was complexed to β-cyclodextrin.[42] These CIS values were used to obtain the inclusion geometry of the naproxen-β-cyclodextrin complex (see 1.5.2.2). The calculation used by the Benesi-Hildebrand method to obtain the CIS value requires the chemical shift values of the free guest molecule dissolved in water (see eqn 1.1). As a result of the water insolubility of the three steroids, the chemical shifts of the uncomplexed protons of cyproterone acetate, ethynyl oestradiol and danazol in D_2O could not be obtained. The CIS values of the guest molecules of the steroid-cyclodextrin complexes of this study could therefore not be obtained.

Fortunately, use can be made of the nuclear Overhauser effect to model the inclusion geometries of these complexes. The 2-D ROESY spectra obtained during the NMR investigation proved that steroid-cyclodextrin samples could be prepared which would deliver a reasonable signal to noise ratio for the intermolecular NOE crosspeaks (see figs 4.3 to 4.9). In the same fashion that the NOE crosspeaks observed in the 2-D ROESY spectra of the 1-anilino-8-naphthalenesulphonate-cyclodextrin complexes were used to model the inclusion geometries (see 1.5.2.3)[36], the NOE crosspeaks found in figures 4.3 to 4.9 are used to obtain the geometries of the steroid-cyclodextrin complexes. To refine the inclusion geometries deduced from the intensities of the NOE crosspeaks use is made of SYBYL molecular modelling software. The advantage of using this software is that it incorporates factors such as electrostatic forces, van der Waals interactions and steric contributions which are used to guide the interpretation of the NOE values so that realistic orientations of the guest molecule within the cyclodextrin cavity can be obtained.

The first part of this chapter contains the inclusion geometries of the steroid-cyclodextrin complexes which are obtained by the interpretation of the NOE values in combination with the use of molecular models. The second part discusses the possible origins for the chemical shift differences (Δ as defined in eqn 4.1) of the steroid protons when complexed to β- and γ-cyclodextrin.

5.2 Modelling of the complexes using the intermolecular nuclear Overhauser effects

The approach used to determine the inclusion geometries of the steroid-cyclodextrin complexes initially consists of the consideration of the theoretically possible geometries. This is followed by the interpretation of the NOE values which then enables the distinction to be made between the inclusion geometries which do exist in solution and those geometries which are purely theoretical.

A number of different theoretical inclusion geometries can be proposed from the use of the chemical structures of the steroid and cyclodextrin (fig 5.1). The steroid can be thought of as a long cylindrical molecule with the steroid A and D rings positioned at opposite ends with the methyl CH_3-18 closer to the D-ring and CH_3-19 closer to the A-ring. The cyclodextrin molecule has a cavity with dimensions which may accommodate the cylindrical steroid. The A-ring of the steroid can approach the cavity from the 2°-OH (complex I) or from the 1°-OH rim (complex II).

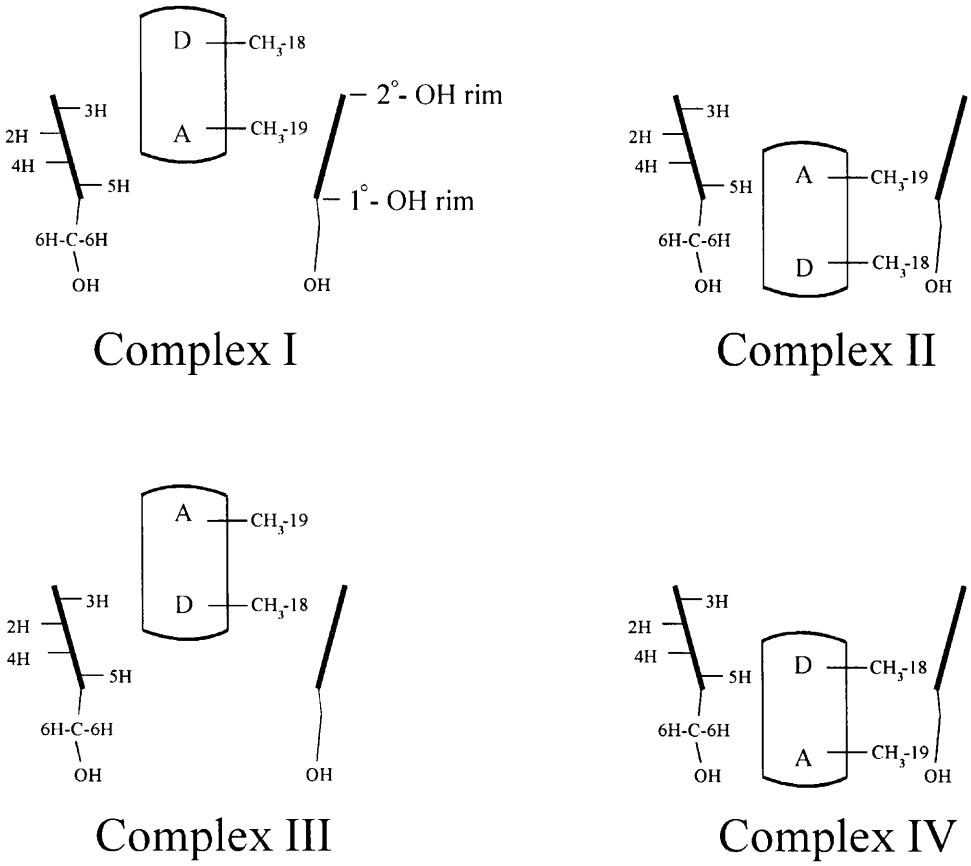

Figure 5.1 Possible inclusion geometries for steroid-cyclodextrin complexes.

The same two approaches for the D-ring of the steroid towards the cyclodextrin cavity are also possible (see complexes III and IV).

The magnitudes of the intermolecular NOE crosspeaks in the 2-D ROESY spectra of the steroid-cyclodextrin complexes have been converted to NOE percentages, where the magnitude of a single proton resonance on the diagonal of each 2-D ROESY spectrum is defined as unity. The values of these NOE percentages represent the average of the contributions from a number of possible conformations. These different conformations arise from the dynamics of the steroid within the cavity. As a consequence these NOE percentages only give qualitative distance constraints between the protons of the steroid and cyclodextrin. These qualitative distance constraints can be used to access the position of a steroid proton within the cyclodextrin cavity. For example it is possible to use these constraints to determine to which rim of the cyclodextrin cavity a steroid proton is closest to.

Ideally, use should be made of the NOE percentages to the cyclodextrin protons 3 and 5 when determining the relative proximities of the steroid protons to the rims of the cyclodextrin cavity. The cyclodextrin protons 3 and 5 are situated within the cavity therefore any steroid protons that are included will have the largest intensity NOE crosspeaks to these cyclodextrin protons. The proximity of the steroid protons to the rims will be easily determined since the cyclodextrin protons 3 and 5 are positioned at the 2°-OH and 1°-OH rims, respectively. Unfortunately, it is not always practically possible to obtain the NOE percentages to the cyclodextrin protons 3 and 5. In this study overlap between proton 5 and proton 6 occured frequently and overlap of proton 3 and proton 6 was also observed. During the present study the steroid-cyclodextrin complexes were prepared in two different solvent mediums, that of pure D_2O and a mixture of DMSO-d_6 :D_2O. In the ^1H NMR spectra of the complexes prepared in both mediums there was always the occasion that the resonance of either the cyclodextrin proton 3 or 5 was overlapping with another cyclodextrin proton. Caution must therefore be exercised when interpreting the intensities of NOE crosspeaks from the steroid protons to the cyclodextrin protons that overlapped.

In all the steroid-cyclodextrin samples that were prepared in D_2O the resonances of the cyclodextrin protons 5 and 6 were overlapping in the ^1H NMR spectra. It should be realised that the intensity of an NOE crosspeak from a steroid proton to the overlapping cyclodextrin protons 5 and 6 can be contributed by the NOE of three protons (one proton 5 and two proton 6's) per amylose monomer of cyclodextrin to the steroid proton. The intensity of an NOE crosspeak from a steroid proton to a cyclodextrin proton 3 is contributed by the NOE of only one proton per amylose monomer of cyclodextrin to the steroid proton. The cyclodextrin proton 3 is close to the 2°-OH rim and the cyclodextrin protons 5 and 6 are close to the 1°-OH rim. If a steroid proton has a more intense NOE crosspeak to the cyclodextrin proton 3 than to the overlapping cyclodextrin protons 5 and 6 it will be positioned closer to the 2°-OH rim than to the 1°-OH rim of the cyclodextrin cavity. But a steroid proton with a more intense NOE crosspeak to the cyclodextrin proton 5 and 6 than to the cyclodextrin proton 3 will not necessarily position this steroid proton closer to the 1°-OH rim than to the 2°-OH rim of the cyclodextrin cavity. A larger intensity crosspeak can be a result of more protons per amylose monomer of cyclodextrin contributing to the crosspeaks and not caused by a closer proximity of the steroid proton to the 1°-OH rim of the cyclodextrin cavity.

The resonances of the cyclodextrin protons 3 and 6 were overlapping in the ^1H NMR spectra of the steroid-cyclodextrin complexes prepared in a mixture of 0.2ml DMSO-d_6 and 0.4ml D_2O. Any possible NOE crosspeaks in the 2-D ROESY spectra from a steroid to the cyclodextrin proton 3 and to the cyclodextrin proton 6 will overlap. The intensity of an NOE crosspeak from a steroid proton to the cyclodextrin protons 3 and 6 cannot be used to position the steroid proton closer to any of the two rims. Fortunately, in the ^1H NMR spectra of the steroid-cyclodextrin complexes prepared in the mixture of DMSO-d_6 :D_2O the resonances of the cyclodextrin protons 2 and 4 did not overlap with each other or with any other proton resonances. In the 2-D ROESY spectra of these samples, except for the spectra of the danazol-β-cyclodextrin complex, the signal to noise ratio for all the NOE crosspeaks improved in comparison to the signal to noise ratios obtained from the 2-D ROESY spectra of these same complexes prepared in D_2O. The cyclodextrin proton 2 is close to the 2°-OH rim and the cyclodextrin proton 4 is close to the 1°-OH rim. The proximity of a steroid proton to the rims of the cyclodextrin cavity can be deduced from a comparison of the intensities of the NOE crosspeaks of the steroid proton to the

cyclodextrin proton 2 and to the cyclodextrin proton 4.

The method of determining the inclusion geometry can now be summarised as follows. The NOE percentages derived from the intensities of the NOE crosspeaks are used to determine the positions of more than one steroid proton relative to the rims of the cyclodextrin cavity. The inclusion geometries, represented in figure 5.1, which exist in solution will be the geometries which can account for the relative positions of the steroid protons as deduced from the NOE percentages. Or in other words, the steroid-cyclodextrin inclusion geometries are obtained by placing the steroid protons in the positions dictated by the NOE percentages.

Arguments based on steric hindrances between steroid and cyclodextrin which arise when the proposed complexes I-IV are modelled with SYBYL 6.1 software can also be used to determine the likelihood of certain inclusion geometries existing in solution. This approach is useful in the instances where the interpretation of the NOE percentages can be ambiguous or when there is insufficient NOE data to support a proposed inclusion geometry. The SYBYL 6.1 computer generated molecular models of the steroid-cyclodextrin complexes illustrated in this chapter are obtained by manually docking the steroid into the cyclodextrin cavity in accordance with the intermolecualr NOE percentages. The resulting geometry of inclusion is further refined by minimising the docked host-guest conformation using the default values of the TRIPOS force field with the atomic charges calculated by the Gasteiger and Marsili method and the local minimum is obtained with the MAXIMIN2 minimiser.[54]

The main purpose of the molecular modelling is to provide a space-filling model to access whether there is enough space within the cyclodextrin cavity to accomodate the steroid for all the proposed modes of inclusion. All the complexes shown in the figures have been minimised until a local energy minimum conformation has been reached. A transverse cross-sectional view of the final result of each of the modelled complexes are illustrated in the ensuing discussions. The orientation of the cyclodextrin relative to the steroid is conveyed by two amylose monomers of cyclodextrin which are situated on either side of the steroid. The included steroid molecule is drawn in stick mode and the amylose monomers are shown in space-filling mode. Accompanying the illustrated complexes, some of the intermolecular NOE percentages which are used to model

the inclusion geometry are given.

5.2.1 Cyproterone acetate-β-cyclodextrin complex

The intermolecular NOE percentages, used to model the mode of inclusion, recorded from the cyproterone acetate-β-cyclodextrin complex prepared in D_2O can be found in table 4.8. The largest NOE percentages are for the cyproterone acetate protons 4-H and 7-H to the β-cyclodextrin protons 3 and 5/6. Since the protons 4-H and 7-H are situated close to the A-ring of cyproterone acetate it can be deduced that the A-ring is complexed to the β-cyclodextrin cavity. The inclusion geometries that allow the A-ring to be complexed are those depicted by complexes I and II (see fig 5.1). Molecular modelling was used in this occasion to determine the preferred inclusion geometry. Molecular models of cyproterone acetate and β-cyclodextrin showed that the A-ring of cyproterone acetate could not be manually docked into the narrower entrance of the cavity (1°-OH rim) without being sterically hindered. These hindrances were the result of unfavourable van der Waals contacts between the atoms of the methylene bridge, situated on the A-ring of cyproterone acetate, and the atoms of β-cyclodextrin. However, the A-ring of cyproterone acetate was able to approach the wider entrance to the β-cyclodextrin cavity without being sterically hindered. Taking only steric hindrances into consideration, complex I as shown in figure 5.1 is the only mode of complexation possible for the approach of the A-ring of cyproterone acetate towards the β-cyclodextrin cavity.

From the use of the values of the NOE percentages of the cyproterone acetate protons 4-H and 7-H to the β-cyclodextrin protons insight into the depth of insertion of the A-ring into the β-cyclodextrin cavity can be obtained. The NOE percentages of 4-H to the β-cyclodextrin protons 3 and 5/6 of 4.0% and 5.0%, respectively are larger than those of 7-H to the β-cyclodextrin protons 3 and 5/6 of 1.0% and 2.0%, respectively. The cyproterone acetate 4-H is thus closer to the inner cavity protons 3 and 5 of β-cyclodextrin than 7-H. The NOE percentages from 4-H to the β-cyclodextrin protons 3 and 5/6 are of comparable magnitudes suggesting that 4-H is situated within the β-cyclodextrin cavity. The insertion of 4-H into the cavity such that it is situated between the cyclodextrin protons 3 and 5 could explain the lower NOE percentages of 7-H to the inner cavity protons relative to 4-H, because 7-H is now situated

outside the β-cyclodextrin cavity (see fig 5.2). Furthermore, the comparison of the magnitudes of the NOE percentages of the cyproterone acetate protons 4-H and 7-H to the β-cyclodextrin proton 3 of 4.0% and 1.0%, respectively supports the previous qualitative distance constraint that proton 4-H is closer than 7-H to the β-cyclodextrin proton 3.

Further evidence for the inclusion of the A-ring of cyproterone acetate into the β-cyclodextrin cavity is obtained from the NOE percentages of protons 22b-H and 2β-H to the β-cyclodextrin protons (see table 4.8). The NOE percentages of 1.0% from 22b-H and 0.5% from 2β-H to the β-cyclodextrin proton 3 indicates that the steroid proton 22b-H is closer than 2β-H to the β-cyclodextrin proton 3. This observation supports the proposed mode of inclusion depicted in figure 5.2. From this proposed molecular model of inclusion the steroid proton 22b-H is situated approximately equidistant to the two rims of the β-cyclodextrin. This is reflected by the comparable NOE percentages from 22b-H to the β-cyclodextrin protons 3 and 5/6 of 1.0% and 1.5%, respectively, with the NOE percentage to the protons 5/6 being slightly larger due to the possible extra contribution to the NOE effect from the β-cyclodextrin proton 6's.

The proposed model shown in figure 5.2 has the cyproterone acetate protons 4-H, 22b-H and 2β-H situated within the β-cyclodextrin cavity. It is therefore expected that the NOE percentages of these protons 4-H, 22b-H and 2β-H to the β-cyclodextrin protons should be comparable in magnitude. The lower NOE percentages of 22b-H and 2β-H to the β-cyclodextrin protons compared to the NOE percentages arising from 4-H can be attributed to a poorer signal to noise ratio of the NOE crosspeaks of 22b-H and 2β-H to the β-cyclodextrin protons. This poor ratio was caused by the presence of baseline noise in the 2-D ROESY spectrum of the cyproterone acetate-β-cyclodextrin complex.

The depth of insertion of cyproterone acetate into the β-cyclodextrin cavity modelled using the NOE percentages is supported by the molecular models. A deeper insertion of the cyproterone acetate into the cavity than shown in figure 5.2 will cause unfavourable van der Waals contacts to arise as deduced from the use of the TRIPOS force field. These unfavourable van der Waals contacts are between the chlorine atom of cyproterone acetate, with its large atomic radius, with the atoms in the immediate vicinity of the 2°-OH rim as well as between the atoms of the

methylene bridge and the β-cyclodextrin protons 3 and 5 situated within the cavity.

Further information concerning the inclusion geometries can be obtained from the NOE percentages of the methyl protons of cyproterone acetate to the β-cyclodextrin protons. The cyproterone acetate methyl CH_3-19 is closer to the A-ring than to the D-ring of the steroid carbon-framework. Any NOE's from CH_3-19 to the β-cyclodextrin protons are most likely to originate from an inclusion mode where the A-ring is complexed to the β-cyclodextrin cavity. The complexation mode depicted by complex II (see fig 5.1) need not be considered for steric reasons. The origins of the NOE percentages of CH_3-19 to the β-cyclodextrin protons 3 and 5/6 of 1.5% and 2.5%, respectively can only be accounted for by a complexation mode such as complex I as shown in figure 5.2. On the other hand, the cyproterone acetate methyl CH_3-18 is positioned closer to the D-ring than to the A-ring of the steroid carbon-framework. The NOE percentages of CH_3-18 to the β-cyclodextrin protons 3 and 5/6 of 1.5% and 2.5%, respectively are most likely caused by a complexation mode where the D-ring is complexed to the β-cyclodextrin cavity. It could be argued that the NOE percentages of CH_3-18 could still be accounted for by an inclusion geometry depicted by complex I. Yet, to explain the origin of the NOE percentages of the methyl protons CH_3-24 of the acetate substituent of cyproterone acetate to the β-cyclodextrin protons 3 and 5/6 of 0.5% and 1.0%, respectively another mode of complexation, other than the one where the A-ring is complexed, must be proposed. The CH_3-24 methyl group and the A-ring are positioned at opposite ends of the cyproterone acetate molecule. Only inclusion geometries depicted by complexes III and IV, where the D-ring is complexed to the β-cyclodextrin cavity, will be able to account for the NOE effects of the protons of both methyl groups CH_3-24 and CH_3-18 to the β-cyclodextrin protons.

The molecular models showed that the CH_3-24 methyl group of cyproterone acetate can approach the β-cyclodextrin cavity from both the 1°-OH as well as the 2°-OH rim without steric hindrance. From these steric considerations the preferred approach of CH_3-24 towards the cavity which would lead to either one of the inclusion geometries depicted by complexes III and IV could not be determined. An attempt to interpret the values of the NOE percentages of the protons CH_3-18 and CH_3-24 to the β-cyclodextrin protons to distinguish the preferred mode of complexation was also unsuccessful. Both modes of complexation depicted by complex III

and IV can account for these NOE percentages. Since the arguments derived from the use of NOE percentages could not identify the preferred mode of inclusion a possible distinction can be based on the following argument. Firstly, from the use of CPK models it was shown that the 1°-OH rim is the narrower entrance to the β-cyclodextrin cavity. The two diameters of the rims of β-cyclodextrin are 6.0Å and 6.4Å where the smaller value is for the ring which passes through the β-cyclodextrin proton 5's and the larger value is for the ring which passes through the β-cyclodextrin proton 3's.[11] Secondly, the freely rotating 1°-OH groups will further impede the entrance of a guest molecule to the cavity from the 1°-OH rim. Taking these two factors into account the probability of a guest molecule entering the β-cyclodextrin cavity from the 1°-OH rim is less than entering from the 2°-OH rim. Though the inclusion modes depicted by complexes III and IV are both sterically possible, due to the differences in accessibility to the two entrances of the β-cyclodextrin cavity it can be concluded that the inclusion geometry depicted by complex III will be in higher concentration relative to complex IV. The mode of complexation illustrated in figure 5.4 is therefore the preferred mode which will account for the NOE percentages of CH_3-24 and CH_3-18 to the β-cyclodextrin protons.

The presence of an NOE crosspeak from the CH_3-21 protons to the β-cyclodextrin protons could not be unambiguously established. It was impossible to distinguish between the individual NOE crosspeaks of the cyproterone acetate protons CH_3-21, 12α-H and 14-H to the β-cyclodextrin protons because these NOE crosspeaks overlapped. The sum total of the NOE percentages of the protons CH_3-21, 12α-H and 14-H to the β-cyclodextrin protons 3 and 5/6 are 0.5% and 2.0%, respectively (see table 4.8). The possibility that the methyl protons CH_3-21 do contribute to these NOE percentages cannot be ignored. The complexation of CH_3-21 to the β-cyclodextrin cavity must also be considered as a possible cyproterone acetate-β-cyclodextrin complex which can exist in solution. Due to the difference in accessibility to the entrances of the β-cyclodextrin cavity only the complex obtained from the approach of CH_3-21 towards the 2°-OH rim has to be modelled. Steric considerations deduced from the molecular models indicate that both methyl groups CH_3-21 and CH_3-24 are unable to occupy the β-cyclodextrin cavity simultaneously. Whilst one of these methyl groups occupy the cavity the other methyl is situated near the 2°-OH rim of the cavity (see figures 5.4 and 5.5). The complexation mode shown in figure 5.5 will account for the NOE's which can possibly arise from the CH_3-21 methyl protons

to the β-cyclodextrin protons.

5.2.2 Cyproterone acetate-γ-cyclodextrin complex

The observation of NOE crosspeaks between the cyproterone acetate protons 4-H and 7-H to the γ-cyclodextrin protons 3 and 5/6 (see fig 4.5) proves that the A-ring is inserted into the cavity of γ-cyclodextrin. Though the γ-cyclodextrin cavity has a larger radius than the β-cyclodextrin cavity, molecular models proved that steric hindrances still arise for the mode of complexation depicted by complex II (fig 5.1). These hindrances arose from unfavourable van der Waals contacts between the atoms of the methylene bridge of cyproterone acetate and the γ-cyclodextrin protons 3 and 5. No steric hindrances arose from the approach of the A-ring towards the 2°-OH rim. Complex I is the only mode of inclusion that is sterically allowed for the complexation of the A-ring to the cavity of γ-cyclodextrin.

The NOE percentages of the cyproterone acetate protons 4-H and 7-H to the γ-cyclodextrin protons found in table 4.9 are used to model the depth of insertion of the A-ring when complexed to the cavity of γ-cyclodextrin. The NOE percentages of 4-H to γ-cyclodextrin protons 3 and 5/6 are 1.0% and 2.0%, respectively. The NOE percentaes of 7-H to γ-cyclodextrin protons 3 and 5/6 are 1.5% and 2.0%, respectively. Since these percentages are of similar magnitudes it can be deduced that protons 4-H and 7-H are of comparable distances to these γ-cyclodextrin protons.

More specifically, from the NOE percentages of the cyproterone acetate protons 4-H and 7-H to the γ-cyclodextrin proton 3 of 1.0% and 1.5%, respectively it can be deduced that protons 4-H and 7-H are approximately equidistant to the γ-cyclodextrin proton 3. Perhaps 7-H, with the slightly larger NOE percentage, is slightly closer than 4-H to the γ-cyclodextrin proton 3.

The proposed mode of incluson was obtained by an initial manual docking of cyproterone acetate and γ-cyclodextrin in accordance with the intermolecular NOE percentages of 4-H and 7-H to the γ-cyclodextrin protons followed by energy minimisation. The resulting conformation, which is the one illustrated in figure 5.3, is in a local minimum energy conformation and there are no unfavourable van der Waals contacts present. The molecular model of γ-cyclodextrin has enough

space within it's cavity to accommodate the chlorine as well as the bulky methylene bridge for this deduced depth of insertion for the cyproterone acetate guest. This result shows that the cyproterone acetate-γ-cyclodextrin complex has a deeper insertion of the cyproterone acetate molecule into the cyclodextrin cavity in comparison to the depth of inclusion for the cyproterone acetate-β-cyclodextrin complex (compare figures 5.2 and 5.3).

The intermolecular NOE percentages of the cyproterone acetate protons 1β-H of 0.3% and 0.3% and 22b-H of 0.5% and 0.5% to the γ-cyclodextrin protons 3 and 5/6, respectively places the depth of insertion of the cyclopropane ring somewhere between the two rims of the γ-cyclodextrin cavity (table 4.9). This is still accounted for by the proposed depth of insertion of the cyproterone acetate molecule illustrated in figure 5.3. The NOE percentages of CH_3-19 to the γ-cyclodextrin protons 3 and 5/6 of 3.0% and 4.0%, respectively are also accounted for by a complexation mode depicted by complex I as illustrated in figure 5.3.

Since the CH_3-18 methyl group is positioned close to the D-ring the NOE percentages of CH_3-18 to the γ-cyclodextrin protons 3 and 5/6 of 3.0% and 4.0% are most likely to arise from modes of complexation of the type illustrated by complex III and complex IV. The NOE percentages of cyproterone acetate CH_3-24 to the γ-cyclodextrin protons 3 and 5/6 of 4.0% and 6.0% proves that an inclusion geometry where the CH_3-24 methyl group is complexed to the γ-cyclodextrin cavity exists in soluton. The molecular models of cyproterone acetate and γ-cyclodextrin showed that the approach of CH_3-24 towards the 2°-OH rim and towards the 1°-OH rim are both possible. Using the previous arguments concerning the differences in accessibility between the two entrances of the cyclodextrin cavity (see 5.2.1), it can be concluded that the D-ring of cyproterone acetate will approach the γ-cyclodextrin cavity from the 2°-OH rim to form an inclusion geometry represented by complex III (fig 5.1). The NOE percentages of the methyl protons of CH_3-18 and CH_3-24 can therefore be accounted for by a similar mode of complexation as represented by figure 5.4.

The NOE crosspeaks from CH_3-21 and 2β-H to the γ-cyclodextrin protons, observed in the 2-D ROESY spectrum in D_2O overlapped (see fig 4.5). The NOE percentages of CH_3-21 and 2β-H to the γ-cyclodextrin protons 3 and 5/6 are 5.0% and 8.0%, respectively. These NOE

percentages are much bigger than what would have been expected from 2β-H alone. Especially when the known NOE percentages of 1β-H to the γ-cyclodextrin protons 3 and 5/6 of 0.3% and 0.3% are taken into consideration. The possibility that the CH_3-21 protons do contribute to the NOE percentages to the γ-cyclodextrin protons 3 and 5/6 must be considered. Based on this deduction the inclusion geometries arising from the complexation of the CH_3-21 methyl group to the γ-cyclodextrin cavity must be taken into account. Though the γ-cyclodextrin cavity is larger than that of β-cyclodextrin, from the use of the molecular models it is still unlikely that both methyl groups CH_3-21 and CH_3-24 are able to occupy the γ-cyclodextrin cavity simultaneously without steric hindrances arising. The most likely mode of complexation which can explain the NOE percentages of the CH_3-21 to the γ-cyclodextrin protons is similar to that of the cyproterone acetate-β-cyclodextrin complex shown in figure 5.5.

5.2.3 Ethynyl oestradiol-β-cyclodextrin complex

The ethynyl oestradiol-β-cyclodextrin complex prepared in a 1:2 mixture of DMSO-d_6 and D_2O gave a good signal to noise ratio for the intermolecular NOE crosspeaks. The NOE percentages obtained from this complex are used to model the inclusion geometry. These percentages can be found in table 4.11.

The NOE percentages of 1-H to the β-cyclodextrin protons 3/6 and 5 of 7.0% and 6.0%, respectively indicate that the aromatic ring of ethynyl oestradiol is included into the β-cyclodextrin cavity. Unfortunately, for the ethynyl oestradiol-β-cyclodextrin complex prepared in this mixture the NOE crosspeaks to the β-cyclodextrin protons 3 and 6 overlapped (see fig 4.6). Since the β-cyclodextrin protons 2 and 4 are close to the 2°-OH and the 1°-OH rims respectively, the relative proximity of a steroid proton to the rims of the β-cyclodextrin cavity can be determined with the use of the NOE percentages of the steroid proton to the β-cyclodextrin protons 2 and 4. The intermolecular NOE percentages of 1-H, 2-H and 4-H to the β-cyclodextrin protons 2 and 4 are used to determine the favoured mode of complexation, whether complex I or II.

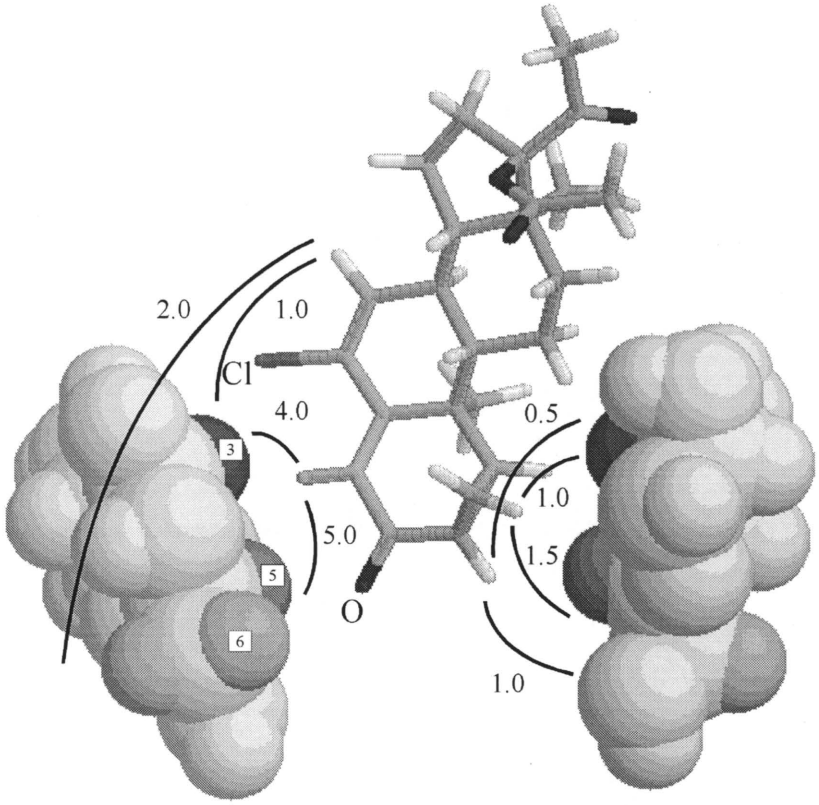

Figure 5.2 The A-ring of Cyproterone acetate complexed to β-cyclodextrin. The intermolecular NOE percentages to the β-cyclodextrin protons 3 and 5/6 are shown.

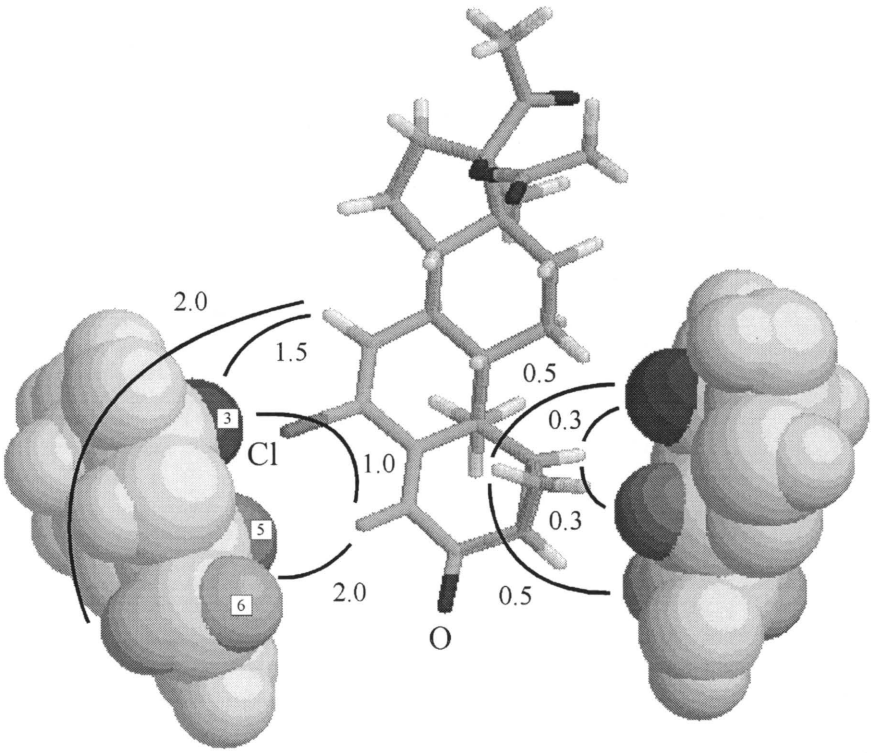

Figure 5.3 The A-ring of Cyproterone acetate complexed to γ-cyclodextrin. The intermolecular NOE percentages to the γ-cyclodextrin protons 3 and 5/6 are shown.

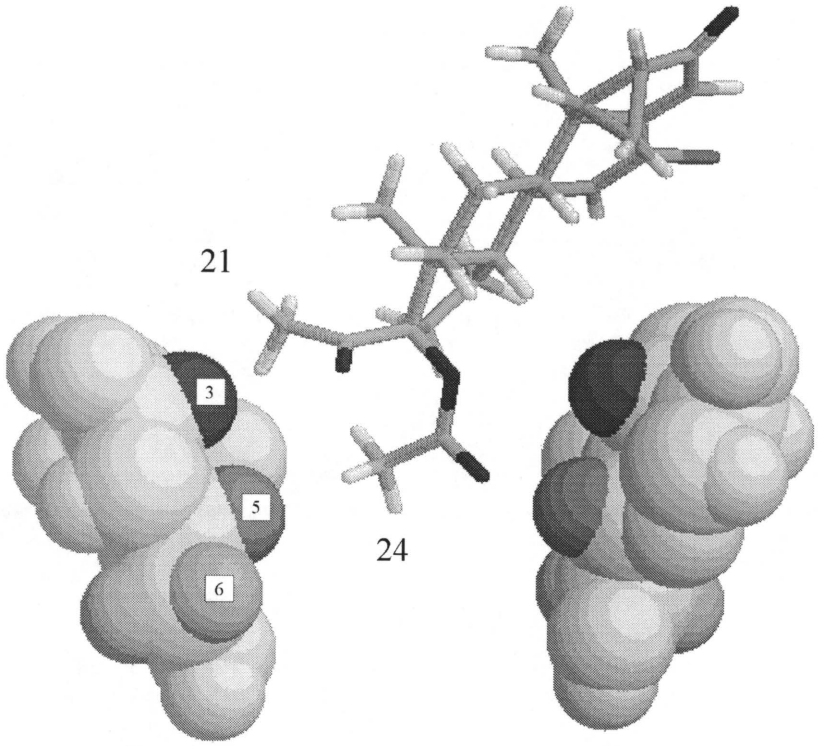

Figure 5.4 The CH_3-24 acetate protons of Cyproterone acetate complexed to β-cyclodextrin.

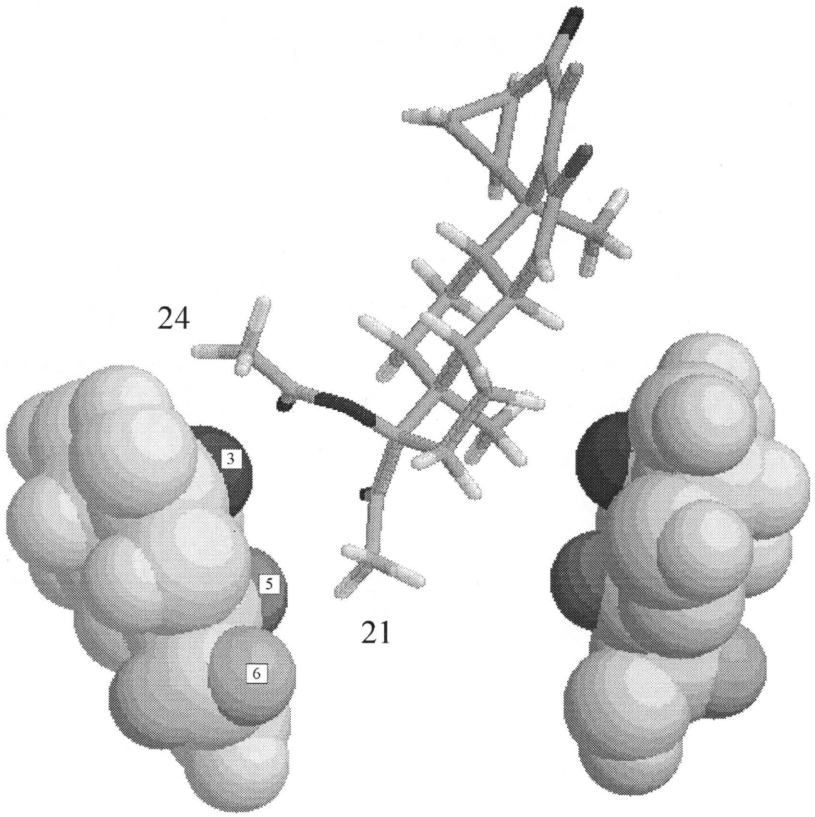

Figure 5.5 The CH_3-21 methyl ketone protons of Cyproterone acetate complexed to β-cyclodextrin.

The resonances of the two ethynyl oestradiol protons 2-H and 4-H overlapped in the ^{1}H NMR spectrum of the ethynyl oestradiol-β-cyclodextrin complex prepared in the 1:2 mixture of DMSO-d_6 and D_2O. The sum of the NOE percentages of the overlapping protons 2-H and 4-H to the β-cyclodextrin proton 2 is 1.0%. This NOE percentage is still smaller than the NOE percentage of 1-H to the β-cyclodextrin proton 2 of 2.0%. This proves that the ethynyl oestradiol 1-H is closer than both the protons 2-H and 4-H to the β-cyclodextrin proton 2. The NOE percentage of 2-H/4-H to the β-cyclodextrin proton 4 of 1.5% compared to the NOE percentage of 1-H to the β-cyclodextrin proton 4 of 3.0% proves that 1-H is closer than both 2-H and 4-H to the β-cyclodextrin proton 4. Two modes of inclusion for the A-ring of ethynyl oestradiol into the β-cyclodextrin cavity can be proposed which can satisfy the above deduced distance constraints (see mode 1 and 2 shown in fig 5.6).

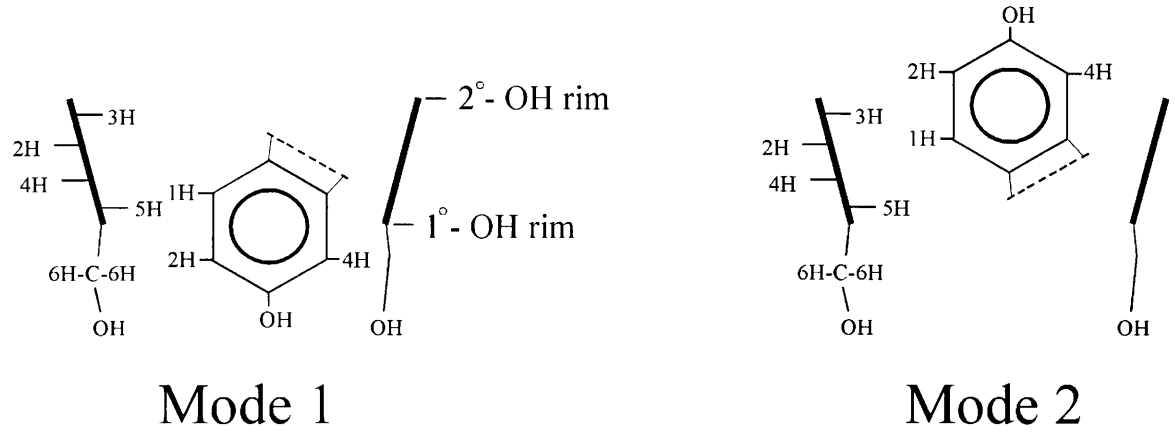

Figure 5.6 The two proposed modes of inclusion for the A-ring of Ethynyl oestradiol to the β-cyclodextrin cavity.

For mode 1, the average of the seven distances between 2-H to each of the β-cyclodextrin proton 4's is smaller than the average of the distances between 2-H to each of the β-cyclodextrin proton 2's. The average of the distances of 4-H to each of the β-cyclodextrin proton 4's is also smaller than the average of the distances between 4-H to each of the β-cyclodextrin proton 2's. These distances forms the basis for the prediction that the NOE percentage of 2-H/4-H to the β-cyclodextrin proton 4 will be larger than the NOE percentage of 2-H/4-H to the β-cyclodextrin proton 2 if mode 1 is preferred. If mode 2 is preferred it can be predicted that the NOE percentages of 2-H/4-H to the β-cyclodextrin proton 2 will be larger than the NOE percentage of 2-H/4-H to the β-cyclodextrin proton 4.

The NOE percentages of 2-H/4-H to the β-cyclodextrin protons 2 and 4 of 1.0% and 1.5%, respectively support the mode of inclusion represented by mode 1. The A-ring of ethynyl oestradiol therefore favours the approach of the β-cyclodextrin cavity from the 2°-OH rim. The molecular model shown in figure 5.7 is deduced from qualitative distance constraints obtained from the previous discussion of the NOE percentages of ethynyl oestradiol protons 1-H and the overlapping 2-H and 4-H to the β-cyclodextrin protons 2 and 4.

The proposed model illustrated in figure 5.7 has both the ethynyl oestradiol protons 6α-H and 6β-H closer to the β-cyclodextrin proton 4 than to 2. The proposed model predicts that the NOE percentage of 6α-H/6β-H to the β-cyclodextrin proton 4 will be larger than the NOE percentage of 6α-H/6β-H to the β-cyclodextrin proton 2. The NOE percentages of 6α-H/6β-H to the β-cyclodextrin protons 4 and 2 of 4.0% and 3.0%, respectively are in agreement with this prediction.

The NOE percentages of 7α-H/8-H to the β-cyclodextrin protons 2 and 4 are 2.0% and 2.5% respectively. The different orientations of the ethynyl oestradiol protons 7α-H and 8-H on the steroid carbon-framework make it difficult to predict with the use of the molecular model illustrated in figure 5.7 the relative magnitudes of the NOE percentages of these protons to the β-cyclodextrin protons 2 and 4. The NOE percentages do imply that both the protons 7α-H and 8-H are situated within the β-cyclodextrin cavity. This deduction supports the proposed model illustrated in figure 5.7.

It can be deduced from the identical molecular models shown in figures 5.7 and 5.8 that the protons 6α-H and 6β-H are closer than all the protons 2-H, 4-H, 7α-H and 8-H to the β-cyclodextrin proton 5. The NOE percentage of 6α-H/6β-H to the β-cyclodextrin proton 5 should be larger than the NOE percentages of 2-H/4-H and 7α-H/8-H to the β-cyclodextrin proton 5. The NOE percentages of 6α-H/6β-H to β-cyclodextrin proton 5 of 6.5% and 2-H/4-H and 7α-H/8-H to proton 5 of 4.0% and 4.0%, respectively are in agreement with the predictions deduced from the model (see fig 5.8).

The NOE percentages of the ethynyl oestradiol 21-H to the β-cyclodextrin protons 5 and 3/6 of 0.5% and 1.5%, respectively prove that the ethynyl group is complexed to the cavity. It can be deduced from the molecular models of ethynyl oestradiol and β-cyclodextrin that the ethynyl group can approach the cavity from both rims. The two complexes that can result from these approaches are represented by complexes III and IV shown in figure 5.1. The relative proximity of the CH_3-18 group to the rims of the β-cyclodextrin cavity will determine the mode of complexation, whether complex III or IV, is favoured. The NOE percentages of the CH_3-18 protons to the β-cyclodextrin protons 2 and 4 are 3.0% and 2.0%, respectively. The CH_3-18 group is therefore closer to the 2°-OH rim which means that complex III is preferred. This preference is not contrary to what would have been expected if the difference in the accessibility between the two entrances of the cavity were to be considered. A molecular model of the ethynyl oestradiol-β-cyclodextrin complex which depicts an inclusion geometry represented by complex III is illustrated in figure 5.9.

5.2.4 Ethynyl oestradiol-γ-cyclodextrin complex

Many NOE crosspeaks of the ethynyl oestradiol protons to the γ-cyclodextrin protons 3 and the overlapping 5 and 6 could be observed in the 2-D ROESY spectrum in D_2O. Unfortunately, the signal to noise ratio of this 2-D ROESY spectrum did not facilitate the detection of any possible intermolecular NOE crosspeaks to the γ-cyclodextrin protons 2 and 4 (see fig 4.7). In the 2-D ROESY spectrum of the ethynyl oestradiol-γ-cyclodextrin complex prepared in a 1:2 mixture of DMSO-d_6 and D_2O many NOE crosspeaks between the ethynyl oestradiol protons to the γ-cyclodextrin protons 2 and 4 were observed (see fig 4.8).Unless stated otherwise, the NOE percentages that were calculated from the spectrum of the ethynyl oestradiol-γ-cyclodextrin complex prepared in the mixture of DMSO-d_6 and D_2O are used to model the inclusion geometries of this complex. These NOE percentages can be found in table 4.13.

The NOE percentages of the ethynyl oestradiol protons 1-H, 2-H and 4-H to the γ-cyclodextrin protons 5 and to the overlapping protons 3 and 6 indicate that the A-ring of ethynyl oestradiol is complexed to the γ-cyclodextrin cavity. The NOE percentages of these ethynyl oestradiol protons to the γ-cyclodextrin protons 2 and 4 are used to model this inclusion geometry. The

same argument that was used to determine the favoured mode of complexation (whether mode 1 or 2, see fig 5.6) of the ethynyl oestradiol-β-cyclodextrin complex is used here for the ethynyl oestradiol-γ-cyclodextrin complex.

The NOE percentages of the γ-cyclodextrin proton 2 to the ethynyl oestradiol protons 1-H, 2-H and 4-H are 0.8%, 0.15% and 0.2%, respectively. These percentages show that the 1-H is closer than 2-H and 4-H to the γ-cyclodextrin proton 2. The NOE percentages of γ-cyclodextrin proton 2 to the ethynyl oestradiol protons 1-H, 2-H and 4-H are 0.8%, 0.2% and 0.3%, respectively. Ethynyl oestradiol 1-H is therefore closer than 2-H and 4-H to the γ-cyclodextrin proton 4. Two modes of complexation (complexes 1 and 2 as shown in fig. 5.6) can satisfy these deduced distance constraints.

The NOE percentages of 2-H to γ-cyclodextrin protons 2 and 4 are 0.15% and 0.2%, respectively. Ethynyl oestradiol 2-H is closer to proton 4 than to proton 2. NOE percentages of 4-H to γ-cyclodextrin protons 2 and 4 are 0.2% and 0.3% respectively. The ethynyl oestradiol 4-H is therefore also closer to proton 4 than to 2. Only mode 1 and not mode 2 can account for these additional distance constraints. From this further inspection of the NOE percentages, mode 1 was determined to be the favoured mode of complexation.

Since mode 1 is favoured the A-ring approaches the cavity from the 2°-OH rim. The complex which forms is represented by complex I (fig. 5.1) and the NOE percentages of 1-H, 2-H and 4-H to the γ-cyclodextrin protons 2 and 4 are used to obtain the molecular model illustrated in figure 5.10. The NOE percentage of ethynyl 1-H to γ-cyclodextrin protons 2 and 4 of 0.8% and 0.8%, respectively places the depth of insertion of 1-H in the middle of the two rims of the cavity. The NOE percentages of 6α-H/6β-H to γ-cyclodextrin protons 2 and 4 of 1.5% and 1.0%, respectively suggests that both the protons 6α-H and 6β-H are situated somewhere between the two rims of the cavity. These conclusions support the proposed molecular model illustrated in figure 5.10.

The depth of insertion of ethynyl oestradiol initially proposed from the use of intermolecular NOE percentages to the γ-cyclodextrin protons 2 and 4 can be refined from a consideration of

the NOE percentages of the ethynyl oestradiol protons to the γ-cyclodextrin proton 5. The NOE percentage of 1-H to the γ-cyclodextrin proton 5 of 1.0% is larger than both the NOE percentages of protons 2-H and 4-H to the cyclodextrin proton 5 of 0.4% and 0.3%, respectively (fig 5.11). This positions 1-H closer to the cyclodextrin proton 5 than both the protons 2-H and 4-H. The depth of insertion of ethynyl oestradiol is therefore slightly deeper than the initial depth proposed in the identical molecular models illustrated in figures 5.10 and 5.11.

This increase in the depth of insertion is further supported by the NOE percentage of 6α-H/6β-H to the γ-cyclodextrin proton 5 of 1.5%. From the NOE percentage of 1.5% it can be concluded that at least one of the 6α-H or 6β-H protons will have an NOE percentage greater than 0.4%. This will position the specific 6α-H or 6β-H proton with the NOE percentage greater than 0.4% closer to the cyclodextrin proton 5 than any of the 2-H or 4-H protons.

Thus far, the NOE percentages obtained from the ethynyl oestradiol-γ-complex prepared in a mixture of DMSO-d_6 and D_2O have been used to show that the inclusion geometry represented by complex I (fig. 5.1) is favoured above that of complex II. The question arises, what effect do the different solvents have on the preferred modes of complexation? For example, will the ethynyl oestradiol-γ-cyclodextrin complex still prefer the complexation mode of complex I above that of complex II when this complex is prepared in D_2O? The NOE percentages of the ethynyl oestradiol-γ-cyclodextrin complex prepared in D_2O are now used to determine which of the two complexation modes, complex I or II, is preferred in a D_2O solvent (table 4.12).

The NOE percentages of ethynyl oestradiol 1-H to the γ-cyclodextrin protons 3 and 5/6 are 2.5% and 5.0%, respectively. The NOE percentages of 2-H to the protons 3 and 5/6 are 2.0% and 3.5%, respectively and the NOE percentages of 4-H to protons 3 and 5/6 are 0.5% and 1.5%, respectively. All the above percentages prove that the A-ring is complexed to the γ-cyclodextrin cavity when the ethynyl oestradiol-γ-cyclodextrin complex is prepared in D_2O. Unfortunately, both modes of complexation represented by complexes I and II (fig. 5.1) can account for these percentages.

The NOE percentages of 6α-H/6β-H to the γ-cyclodextrin protons 3 and 5/6 of 5.0% and 5.5%, respectively places these two protons 6α-H and 6β-H closer to the 2°-OH rim than to the 1°-OH rim of the cavity. The fact that these NOE percentages are of comparable magnitudes can only be accounted for by complex I and not complex II. The slightly larger NOE percentage of 5.5% is probably due to the extra contribution to the NOE effect from the γ-cyclodextrin proton 6's. If the two protons 6α-H and 6β-H were closer to the 1°-OH rim it could be expected that the NOE percentage of 6α-H/6β-H to the γ-cyclodextrin protons 5/6 would have been much greater than 5.5%. The reasons for this are as follows. In the orientation represented by complex II both the protons 6α-H and 6β-H will be much closer to the γ-cyclodextrin protons 5 and 6 than to the proton 3. The NOE percentage of 6α-H/6β-H to the γ-cyclodextrin protons 5/6 is contributed by three protons (one proton 5 and two proton 6's) per amylose monomer of γ-cyclodextrin. The NOE percentage of 6α-H/6β-H to the γ-cyclodextrin proton 3 is only contributed by one proton (proton 3) per amylose monomer.

In conclusion, complex I was favoured above complex II (see fig 5.1) by both the ethynyl oestradiol-β-cyclodextrin complexes that were prepared in the pure D_2O solvent and in the mixture of DMSO-d_6 and D_2O. This result suggests that the preferred modes of complexation will not change irrespective of the solvent medium used to prepare the steroid-cyclodextrin complexes.

The molecular model of the ethynyl oestradiol-γ-cyclodextrin complex which represents complex I is illustrated in figure 5.10. The NOE percentages of ethynyl oestradiol 4-H to γ-cyclodextrin protons 3 and 5/6 of 0.5% and 1.5%, respectively are smaller than the NOE percentages of 2-H to the protons 3 and 5/6 of 2.0% and 3.5%, respectively (see table 4.12). This is unexpected since from the molecular model illustrated in figure 5.10 it can be deduced that the protons 2-H and 4-H have the same depth of insertion into the γ-cyclodextrin cavity and they should therefore have NOE percentages to the γ-cyclodextrin protons 3 and 5/6 of comparable magnitudes. Further inspection of this molecular model gave a possible explanation for the smaller NOE percentages of 4-H to the protons 3 and 5/6.

The carbon-framework of ethynyl oestradiol ensures that 4-H is always positioned slightly further away than 2-H from the walls of the γ-cyclodextrin cavity for the proposed depth of insertion illustrated in figure 5.10. The protons 6α-H, 6β-H, 7α-H and 7β-H situated on the B-ring of ethynyl oestradiol are in contact with the protons 3 and 5 within the cavity. From steric considerations these contacts prevent 4-H from approaching the protons 3 and 5 whilst at the same time these contacts at one side of the cavity encourages 2-H to approach the protons 3 and 5 at the opposite side of the cavity.

The NOE percentages of ethynyl oestradiol 21-H to the γ-cyclodextrin protons 5 and 3/6 of 1.2% and 3.0% (see table 4.13) proves that the ethynyl group is complexed to the γ-cyclodextrin cavity. By determining the relative proximity of the CH_3-18 methyl group to the two rims of the cyclodextrin cavity the preferred mode of complexation, whether complex III or IV, can be identified. The NOE percentages of CH_3-18 to the γ-cyclodextrin protons 5 and 3/6 are 4.0% and 7.0%, respectively. The relative contributions of the γ-cyclodextrin protons 3 and 6 to the NOE percentage of 7.0% cannot be obtained. This percentage of 7.0% cannot be used to ascertain which rim of the γ-cyclodextrin cavity the CH_3-18 methyl group is closest to.
The NOE percentages taken from table 4.12 of the ethynyl oestradiol CH_3-18 protons to the γ-cyclodextrin protons 3 and 5/6 are 4.0% and 5.0%, respectively. The fact that these NOE percentages are of comparable magnitude suggests that the CH_3-18 methyl group is positioned closer to the 2°-OH rim of the γ-cyclodextrin cavity. If the CH_3-18 methyl group was however positioned closer to the 1°-OH rim the NOE percentage of CH_3-18 to 5/6 would have been greater than 5.0%. Since in this orientation the CH_3-18 methyl protons would be much closer to the γ-cyclodextrin protons 5 and 6 than to the proton 3.

The ethynyl group prefers to approach the γ-cyclodextin cavity from the 2°-OH rim since this will position the CH_3-18 group closer to the 2°-OH rim. The inclusion geometry of the complex obtained from such an approach is represented by complex III and the molecular model of such a complex is similar to the ethynyl oestradiol-β-cyclodextrin complex illustrated in figure 5.9.

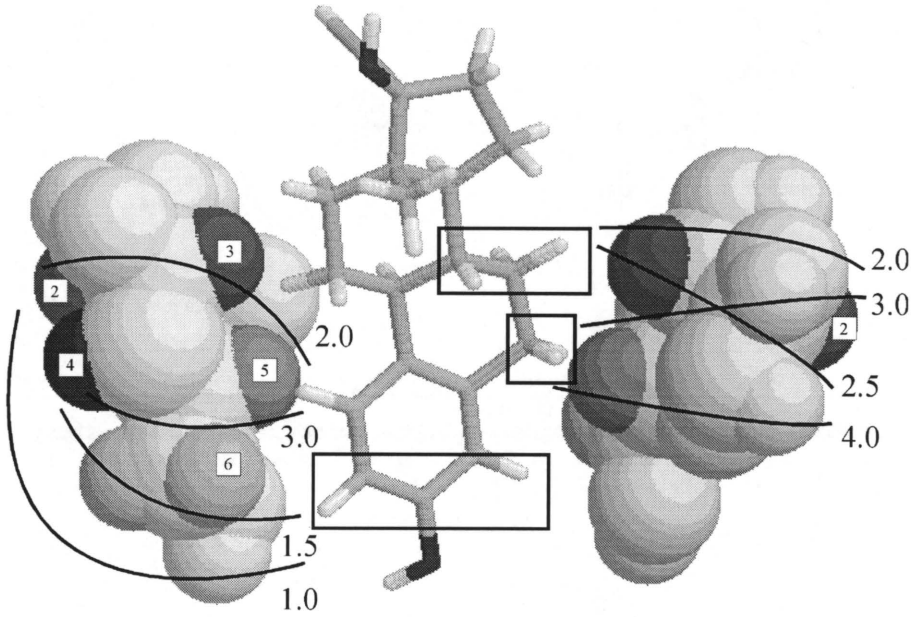

Figure 5.7 The A-ring of Ethynyl oestradiol complexed to β-cyclodextrin. The intermolecular NOE percentages to the β-cyclodextrin protons 2 and 4 are shown.

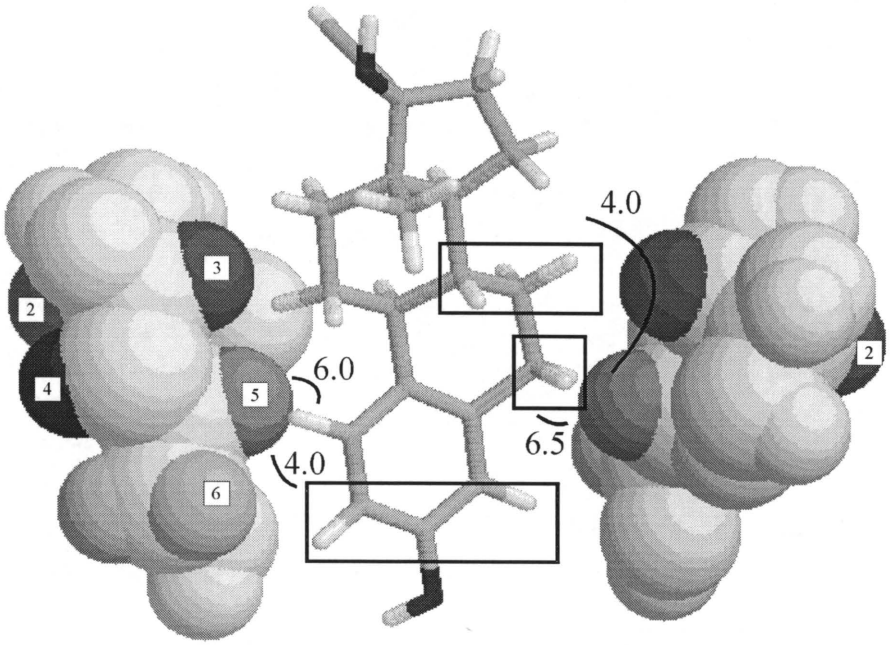

Figure 5.8 The A-ring of Ethynyl oestradiol complexed to β-cyclodextrin. The intermolecular NOE percentages to the β-cyclodextrin proton 5 are shown.

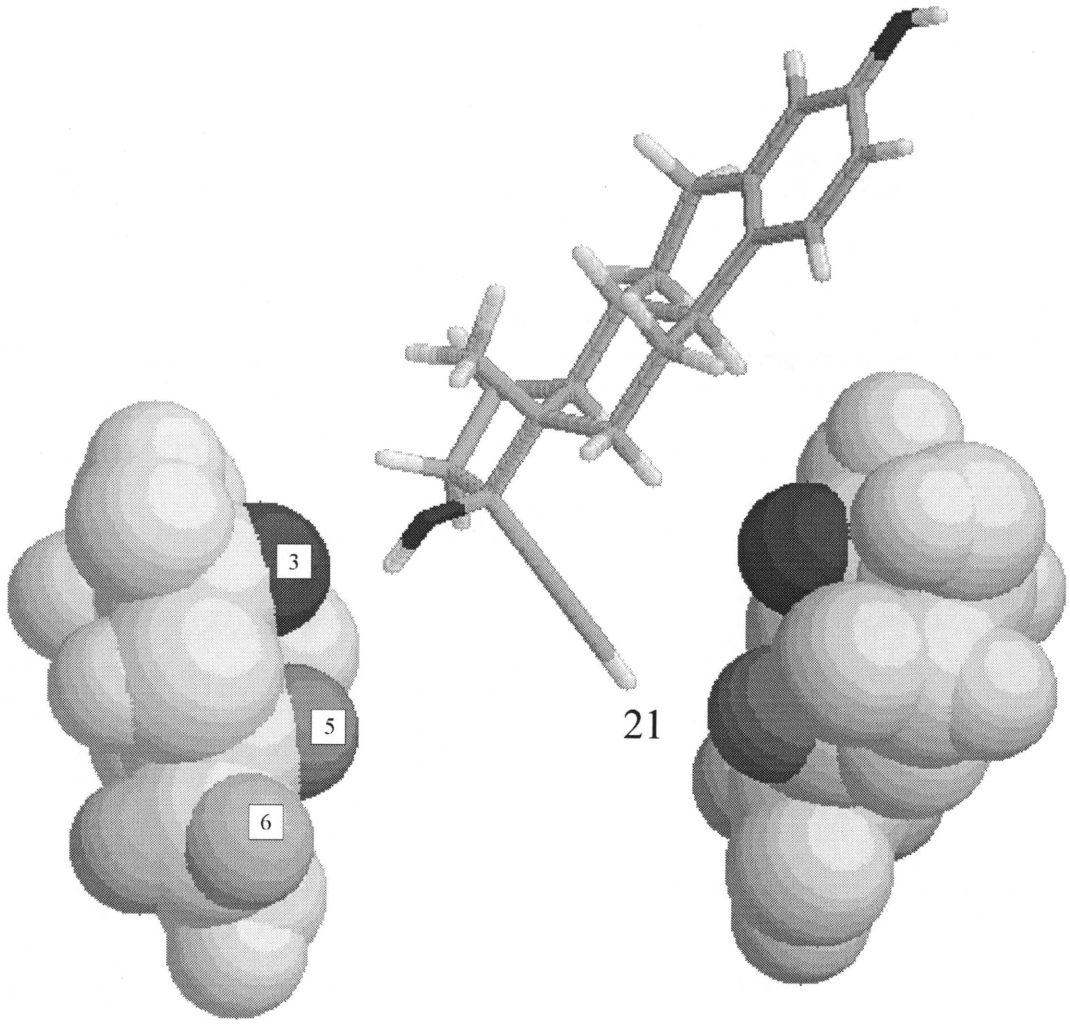

Figure 5.9 The ethynyl group on the D-ring of Ethynyl oestradiol complexed to β-cyclodextrin.

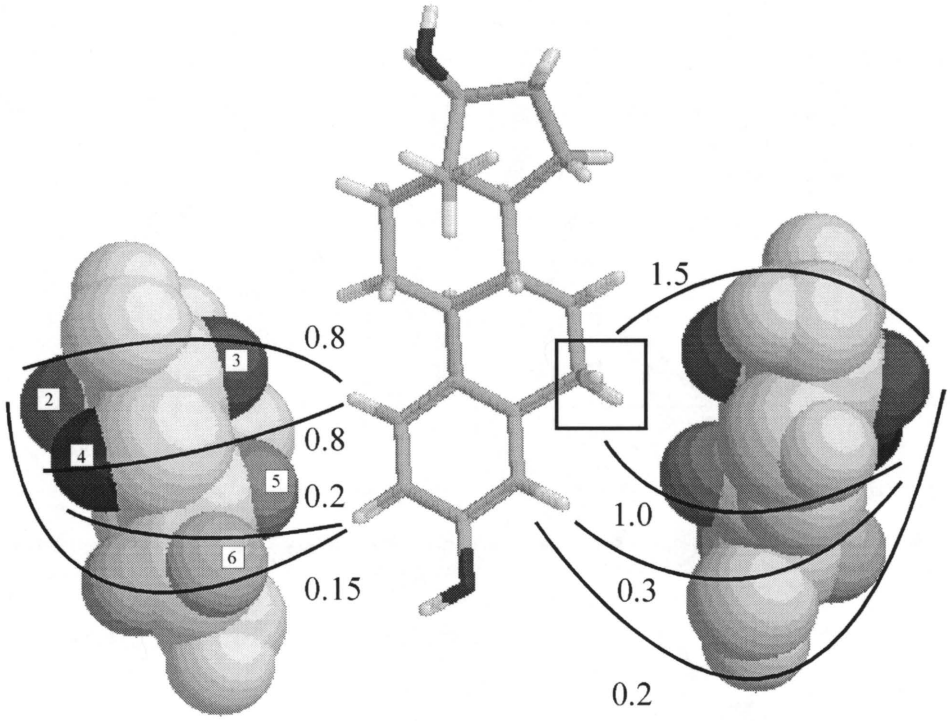

Figure 5.10 The A-ring og Ethynyl oestradiol complexed to γ-cyclodextrin. The intermolecular NOE percentages to the γ-cyclodextrin protons 2 and 4 are shown.

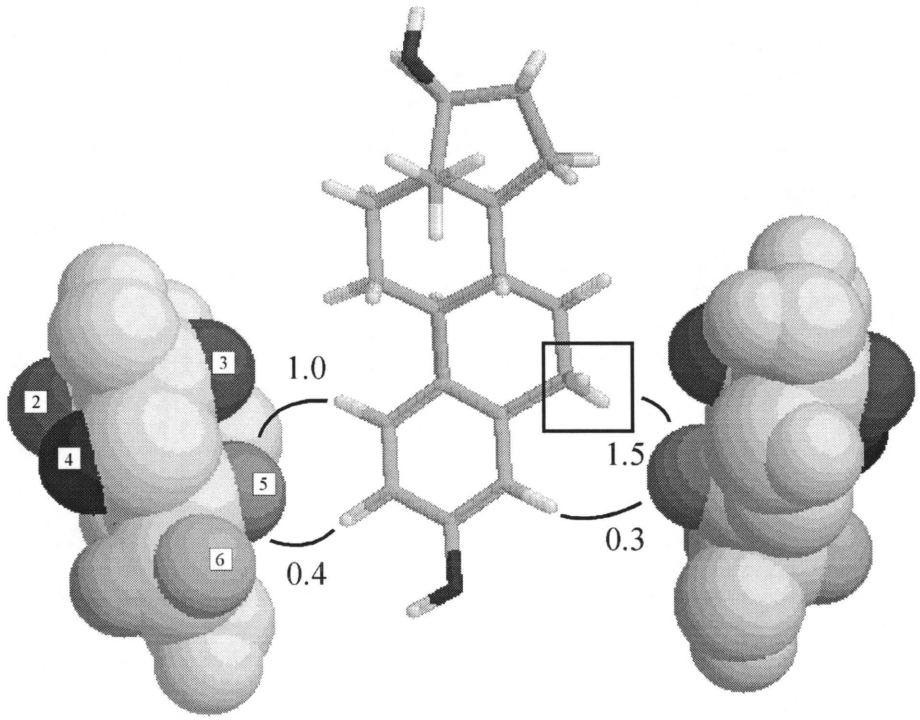

Figure 5.11 The A-ring of Ethynyl oestradiol complexed to γ-cyclodextrin. The intermolecular NOE percentages to the γ-cyclodextrin proton 5 are shown.

5.2.5 Danazol-β-cyclodextrin complex

Many NOE crosspeaks of the danazol protons to the β-cyclodextrin protons 3 and the overlapping 5 and 6 could be observed in the 2-D ROESY spectrum of the danazol-β-cyclodextrin complex prepared in D_2O (see fig 4.3). However, few NOE crosspeaks of the danazol protons to the β-cyclodextrin protons 2 and 4 could be observed in this spectrum. An attempt was made to improve the signal to noise ratio for all the NOE crosspeaks by preparing the danazol-β-cyclodextrin complex in a 1:2 mixture of DMSO-d_6 and D_2O. Since the spectra of both the ethynyl oestradiol-β-cyclodextrin and ethynyl oestradiol-γ-cyclodextrin complexes prepared in the 1:2 mixture of DMSO-d_6 and D_2O had improved signal to noise ratios for all the intermolecular NOE crosspeaks compared to the ratios of these complexes prepared in pure D_2O. Unfortunately, the signal to noise ratio for the intermolecular NOE crosspeaks of the danazol-β-cyclodextrin complex prepared in the 1:2 mixture of DMSO-d_6 and D_2O was much poorer than the ratio for this complex prepared in pure D_2O. The NOE percentages that are used to model the inclusion geometries of the danazol-β-cyclodextrin complex are obtained from the 2-D ROESY spectrum of this complex recorded in D_2O. These percentages are found in table 4.14.

The molecular models of danazol and β-cyclodextrin showed that both inclusion geometries represented by complexes I and II are sterically possible. The NOE percentages of 1β-H to the β-cyclodextrin protons 2 and 4 are 1.0% and 1.5%, respectively. The NOE percentages of 4-H to the β-cyclodextrin protons 2 and 4 are 0.4% and 1.8%, respectively. These NOE percentages positions both protons 1β-H and 4-H closer to 1°-OH rim than to the 2°-OH rim of the β-cyclodextrin cavity. If an inclusion geometry of complex I (fig 5.1) is preferred it can be expected that the NOE percentage of danazol 22-H to β-cyclodextrin proton 4 will be greater than the NOE percentage of 22-H to proton 2. The NOE percentages of danazol 22-H to β-cyclodextrin proton 2 and 4 of 0.1% and 1.0%, respectively are in favour of an inclusion geometry represented by complex I for the danazol-β-cyclodextrin complex. The molecular model of this inclusion geometry for the danazol-β-cyclodextrin complex is illustrated in the identical figures of 5.12 and 5.13. The NOE percentages of the danazol protons to the β-cyclodextrin protons 3 and 5/6 can be used to further substantiate this favoured mode of complexation.

The NOE percentages of the β-cyclodextrin proton 3 to the danazol protons 1β-H, 4-H and 22-H are 4.0%, 7.0% and 1.0%, respectively. These NOE percentages place protons 1β-H and 4-H closer than 22-H to the β-cyclodextrin proton 3. This qualitative distance constraint provides further support for the molecular model illustrated in figure 5.12. If complex II was to be the favoured mode of complexation, this mode would position the danazol proton 22-H closer to the β-cyclodextrin proton 3 than to the protons 5 and 6. An inclusion geometry depicted by complex II would not be able to account for the NOE percentages of danazol 22-H to the β-cyclodextrin protons 3 and 5/6 of 1.0% and 14.0%, respectively. However, a mode of complexation such as complex I as illustrated in figure 5.13 would be able to account for these NOE percentages. A further conclusive result can be obtained from the NOE percentages of the danazol 6β-H to the β-cyclodextrin protons 3 and 5/6 of 2.5% and 1.2%, respectively. These NOE percentages of 6β-H to the β-cyclodextrin protons 3 and 5/6 can only be accounted for if 6β-H is much closer to the β-cyclodextrin proton 3 than to any of the protons 5 and 6. Only an inclusion geometry of complex I (see figure 5.12) and not complex II will allow 6β-H to be positioned closer to β-cyclodextrin proton 3.

The NOE percentages of danazol 21-H to the β-cyclodextrin protons 3 and 5/6 of 0.5% and 0.5% shows that the ethynyl group of danazol is complexed to the β-cyclodextrin cavity. The positioning of the danazol CH_3-18 methyl group relative to the two rims of the β-cyclodextrin cavity will identify the preferred mode of complexation of the included ethynyl group, whether complex III or IV (see fig 5.1). The two equivalent NOE percentages of CH_3-18 to the β-cyclodextrin protons 3 and 5/6 which are equal to 5.5% suggest that the CH_3-18 methyl group is positioned closer to the 2°-OH rim of the β-cyclodextrin cavity. If the CH_3-18 methyl group was positioned closer to the 1°-OH rim it can be expected that the NOE percentage of CH_3-18 to the β-cyclodextron protons 5/6 should be greater than 5.5%. Complex III is the favoured inclusion geometry since this geometry will allow the CH_3-18 methyl group to be positioned closer to the 2°-OH rim of the cavity. The molecular model of this inclusion geometry of the danazol-β-cyclodextrin complex is similar to that which is illustrated in figure 5.9.

5.2.6 Danazol-γ-cyclodextrin complex

Good signal to noise ratios for the intermolecular NOE crosspeaks were obtained from the 2-D ROESY spectrum of the danazol-γ-cyclodextrin complex prepared in a 1:2 mixture of DMSO-d_6 and D_2O. The NOE percentages derived from this spectrum will be used to model the inclusion geometries of the danazol-γ-cyclodextrin complex (see table 4.16).

The molecular models of danazol and γ-cyclodextrin showed that both inclusion geometries illustrated by complexes I and II are sterically feasible. Though the NOE percentages of the danazol protons 22-H, 4-H and 1β-H to the γ-cyclodextrin protons 3/6 and 5 prove that the A-ring of danazol is included into the γ-cyclodextrin cavity, these percentages cannot be interpreted in a manner that will enable the identification of the preferred mode of complexation, whether complex I or II. The NOE percentages of 1β-H to the γ-cyclodextrin protons 2 and 4 of 0.4% and 0.3%, respectively positions 1β-H between the two rims of the γ-cyclodextrin cavity. The NOE percentages of 4-H to protons 2 and 4 of 0.15% and 0.25%, respectively also positions 4-H within the γ-cyclodextrin cavity. The decisive NOE percentages of danazol 22-H to the γ-cyclodextrin protons 2 and 4 of 0.05% and 0.25% respectively positions 22-H closer to proton 4 than to proton 2. Only a complexation mode depicted by complex I and not complex II can account for the distance constraint that 22-H is positioned closer to γ-cyclodextrin proton 4. The molecular model of the danazol-γ-cyclodextrin complex illustrated in the identical figures 5.14 and 5.15 was obtained in accordance to the NOE percentages of the protons 1β-H, 4-H and 22-H to the γ-cyclodextrin protons 2 and 4.

Furthermore, the NOE percentages of 1β-H, 4-H and 22-H to the γ-cyclodextrin proton 5 also position the danazol protons 1β-H and 4-H closer than 22-H to the γ-cyclodextrin proton 5 (see table 4.16). This deduction is in agreement with the molecular model of the danazol-γ-cyclodextrin complex illustrated in figure 5.15.

The NOE percentages of danazol 21-H to the γ-cyclodextrin protons 5 and 3/6 of 1.4% and 5.0%, respectively prove that the ethynyl group of danazol is complexed to the γ-cyclodextrin cavity. These NOE percentages cannot be used to position the 21-H proton closer to any of the

two rims of the γ-cyclodextrin cavity. The different contributions which the γ-cyclodexrin protons 3 and 6 make towards the NOE percentage of 5.0% is not known. For the same reason the NOE percentages of CH_3-18 to the γ-cyclodextrin protons 5 and 3/6 of 3.8% and 6.7%, respectively cannot be used to determine the relative proximity of CH_3-18 to the two rims of the cavity. In this instance, the favoured mode of complexation, whether complex III or IV, cannot be determined from modelling the relative positions of 21-H and CH_3-18 to the rims of the cavity. Furthermore, both possible modes of complexation can account for the NOE percentages of the danazol protons CH_3-18 and 21-H to the γ-cyclodextrin protons 2 and 4 (see table 4.16). In conclusion, a preferred mode of complexation for the danazol-γ-cyclodextrin complex cannot be determined using the NOE percentages of this complex prepared in the mixture of DMSO-d_6 and D_2O. It has been shown that the ethynyl oestradiol-γ-cyclodextrin complex prefers the complexation mode of complex III above that of complex IV (see 5.2.4). Ethynyl oestradiol and danazol both have ethynyl groups situated on their D-rings. On the basis that ethynyl oestradiol and danazol have identical D-ring structures and that the ethynyl oestradiol-γ-cyclodextrin complex prefers the mode depicted by complex III, it is predicted that the danazol-γ-cyclodextrin complex will also prefer the mode depicted by complex III. The molecular model of this preferred mode of the danazol-γ-cyclodextrin complex is similar to the model of the ethynyl oestradiol-β-cyclodextrin complex illustrated in figure 5.9.

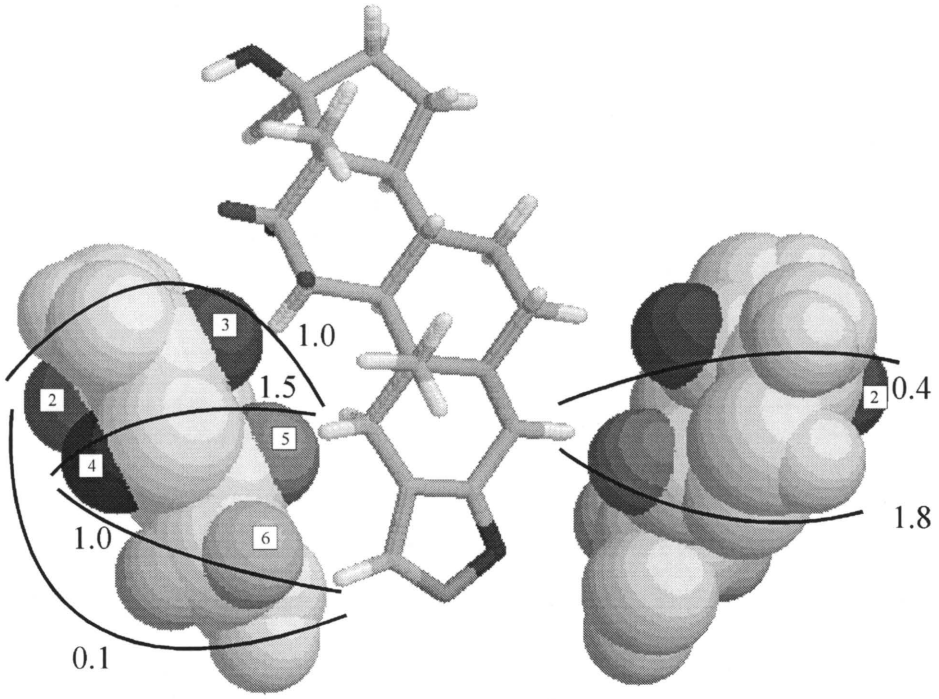

Figure 5.12 The A-ring of Danazol complexed to β-cyclodextrin.
The intermolecular NOE percentages to the β-cyclodextrin protons 2 and 4 are shown.

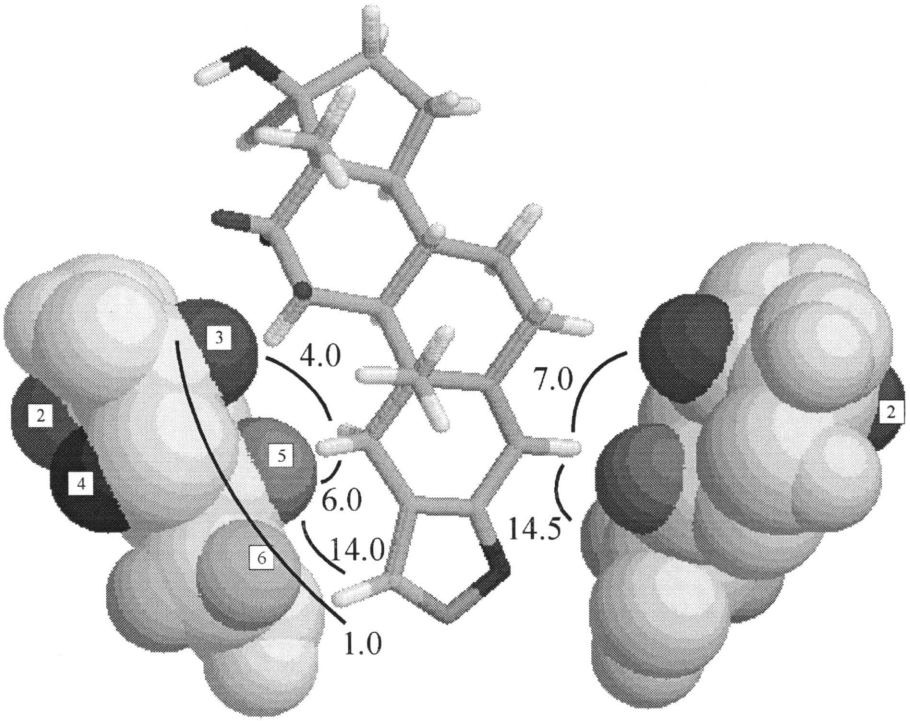

Figure 5.13 The A-ring of Danazol complexed to β-cyclodextrin.
The intermolecular NOE percentages to the β-cyclodextrin protons 3 and 5/6 are shown.

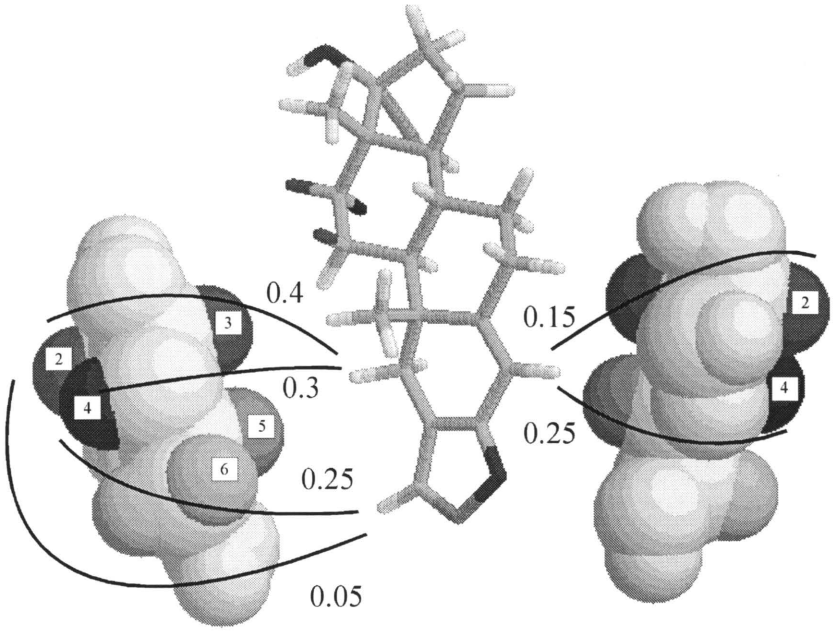

Figure 5.14 The A-ring of Danazol complexed to γ-cyclodextrin.
The intermolecular NOE percentages to the γ-cyclodextrin protons 2 and 4 are shown.

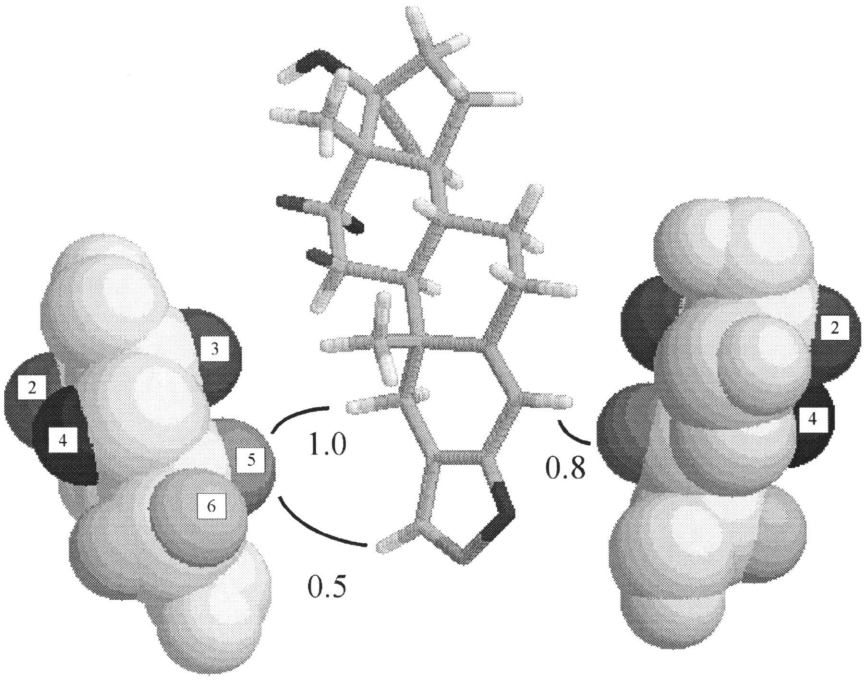

Figure 5.15 The A-ring of Danazol complexed to γ-cyclodextrin.
The intermolecular NOE percentages to the γ-cyclodextrin proton 5 are shown.

5.3 The causes for the Δ chemical shift values

Proton resonances of the water-insoluble steroids detected in the ^1H NMR spectra of the steroid-cyclodextrin complexes prepared in D_2O belong to complexed steroid only (see 4.2). The chemical shifts of these steroid proton resonances are therefore the chemical shifts of these protons when fully complexed to the cyclodextrin host molecule. There are differences in the chemical shifts of the steroid protons of cyproterone acetate, ethynyl oestradiol and danazol, when fully complexed to β-cyclodextrin and γ-cyclodextrin. For example, there were significant differences in the chemical shifts of the protons of cyproterone acetate when complexed to β-cyclodextrin and γ-cyclodextrin in an aqueous medium (see the Δ values in table 4.9). Just as the CIS values are a reflection of the changes in surroundings the guest protons undergo from an aqueous medium to a cyclodextrin complexed state, the chemical shift differences, defined as Δ (see eqn 4.1), are a measure of the changes in the chemical environment the steroid protons experience when going from the β- to the γ-cyclodextrin complexed state.

Unfortunately, the identification of the causes for the signs + or - of the Δ values are not as obvious as the causes for the signs of the CIS values of naproxen when complexed to β-cyclodextrin. For a steroid molecule already complexed to β- or to γ-cyclodextrin the causes for the changes in chemical shift of a steroid proton resonance, such as electric field effects, anisotropic effects and sterically induced polarisations, are already present. A positive Δ value is equivalent to a downfield change in shift which according to the trend found in the literature[41,49] (see 1.5.2.2) can be attributed to an increase in the proximity of the steroid proton to the walls of the cyclodextrin cavity. A positive Δ value of a steroid proton can therefore be caused from further increases in proximity to the walls of the cavity which this steroid proton experiences going from a β- to a γ-cyclodextrin complexed state.

An upfield change in chemical shift is attributed to a gain in proximity of a guest proton to the 1°- and 2°-OH rims. It is a logical deduction that a positive Δ value which is equivalent to a downfield change in chemical shift can be caused by a loss in proximity of a steroid proton to the 1°- or 2°-OH's situated on the rims of the cavity when going from the β- to the γ-cyclodextrin complexed state.

To summarise, a positive Δ value can be caused by either or both an increase in proximity to the cavity walls and/or a decrease in proximity to the 1°- or 2°-OH's situated at the rims of the cavity. It can be further reasoned that a negative Δ value can be caused by either or both a decrease in proximity to the cavity walls and/or an increase in the proximity to the 1°-OH or to the 2°-OH's situated on the rims of the cavity.

From existing predetermined molecular models of the inclusion geometry the most likely cause for the Δ values can be ascertained. In the following discussions, the possible causes for the Δ values of the steroid protons which are close to the A-ring of the steroid carbon-framework are given.

5.3.1 The Δ values of the cyproterone acetate-cyclodextrin complexes

The Δ values found in figure 5.16 are the chemical shift differences of the cyproterone acetate protons when complexed to β- and to γ-cyclodextrin. These values have been taken from table 4.9. The molecular models of the inclusion geometries of the cyproterone acetate-β-cyclodextrin and cyproterone acetate-γ-cyclodextrin complexes illustrated in figures 5.2 and 5.3, respectively are used to identify the causes for the Δ values depicted in figure 5.16.

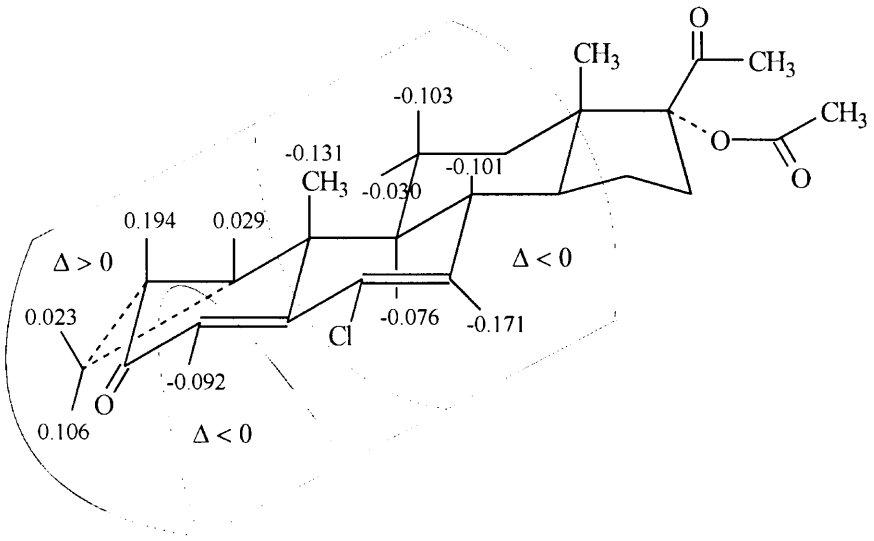

Figure 5.16 The Δ values of the cyproterone acetate-cyclodextrin complexes.

The negative Δ values of the cyproterone acetate protons 7-H, 8-H, 9-H, CH_3-19, 11α-H and 11β-H arise from an increased proximity of these protons to the hydroxyl groups situated on the 2°-OH rim. This increased proximity to the 2°-OH rim occurs upon the increased depth of insertion of cyproterone acetate when going from the β- to the γ-cyclodextrin complexed state. The increased depth of insertion will also place the proton 4-H closer to the hydroxyl groups of the 1°-OH rim when cyproterone acetate goes from the β- to the γ-cyclodextrin complexed state. This increased proximity to the 1°-OH rim can account for the negative Δ value of 4-H of --0.092ppm. When cyproterone acetate is complexed to β-cyclodextrin (see fig 5.2), proton 4-H is situated within the β-cyclodextrin cavity and the bulky chlorine atom is situated at the periphery of the 2°-OH rim of the cavity. However, when cyproterone acetate is complexed to the γ-cyclodextrin cavity it is apparent that more of the bulky chlorine atom is included into the γ-cyclodextrin (see fig 5.3). Since the proton 4-H is situated at the same side of the steroid-carbon framework as the chlorine atom, the increased inclusion of the chlorine atom will decrease the opportunity for 4-H to be in close contact to the walls of the γ-cyclodextrin cavity. This decrease in proximity to the walls of the cavity may also contribute to the negative Δ value of proton 4-H of -0.092ppm. Both an increase in proximity to the 1°-OH rim as well as a decrease in proximity to the walls of the cyclodextrin cavity can be responsible for the negative Δ value of 4-H.

It can be expected that the larger radius of the γ-cyclodextrin cavity should in most circumstances decrease the opportunity of an included steroid molecule to be in close contact with the wall of the γ-cyclodextrin cavity. However, since the cyproterone acetate protons 1β-H, 2β-H, 22a-H and 22b-H of the 'bulky methylene bridge' are immediately opposite to the chlorine atom, the increased inclusion of the large chlorine atom will encourage the protons 1β-H, 2β-H, 22a-H and 22b-H to be in close contact with the walls of the γ-cyclodextrin cavity. The positive Δ values of the protons 1β-H, 2β-H, 22a-H and 22b-H depicted in figure 5.16 suggest that the greater inclusion of the chlorine atom has increased the proximity of the protons of the 'methylene bridge' to the walls of the cavity when cyproterone acetate goes from the β- to the γ-cyclodextrin complexed state. The positive Δ values of the protons 1β-H, 2β-H, 22a-H and 22b-H can also be caused by a decrease in proximity of these protons to the hydroxyl groups situated on the rims of the cavity. From an inspection of figures 5.2 and 5.3 the contribution

which the hydroxyl groups make towards the positive Δ value is not obvious. A decrease in the proximity of the protons 1β-H, 2β-H, 22a-H and 22b-H to the hydroxyl groups on the 2°-OH rim goes hand-in-hand with an increase in proximity of these protons to the hydroxyl groups of the 1°-OH rim.

5.3.2 The Δ values of the ethynyl oestradiol- and danazol-cyclodextrin complexes

The Δ values displayed in figure 5.17, that have been taken from table 4.12, are the chemical shift differences of the ethynyl oestradiol protons when complexed to the β- and to γ-cyclodextrin. Since danazol is insoluble in the 1:2 mixture (read 4.4.5), the danazol proton resonances observed in the ^{1}H NMR spectra of the danazol-β-cyclodextrin and danazol-γ-cyclodextrin complexes prepared in the mixture belong to the resonances of the fully complexed danazol protons. The Δ values shown in figure 5.18 are the chemical shift differences of the danazol protons when complexed to β- and to γ-cyclodextrin (see table 4.16).

The NOE percentages of the cyproterone acetate-cyclodextrin complexes could be used to unambiguously determine that cyproterone acetate is inserted deeper into the γ-cyclodextrin cavity than the β-cyclodextrin cavity. Unfortunately, for the ethynyl oestradiol-cyclodextrin complexes it is not obvious from the inspection of the NOE percentages which complex, whether the ethynyl oestradiol-β-cyclodextrin or the ethynyl oestradiol-γ-cyclodextrin complex, has a deeper insertion of the steroid guest molecule. The same is true for the danazol-cyclodextrin complexes. However, from an inspection of the figures 5.7, 5.10, 5.12 and 5.14 it can be expected that the protons of the ethynyl oestradiol and danazol will undergo similar changes in chemical environment from the β-cyclodextrin to the γ-cycloxtrin complexed state. This expectation is further supported by the fact that the Δ values of both the ethynyl oestradiol-cyclodextrin and danazol-cyclodextrin complexes can both be grouped into two identical regions (see figs 5.17 and 5.18). A positive Δ region which is positioned at the end of the A-rings of both the ethynyl oestradiol and danazol, and a negative Δ region as depicted in figures 5.17 and 5.18.

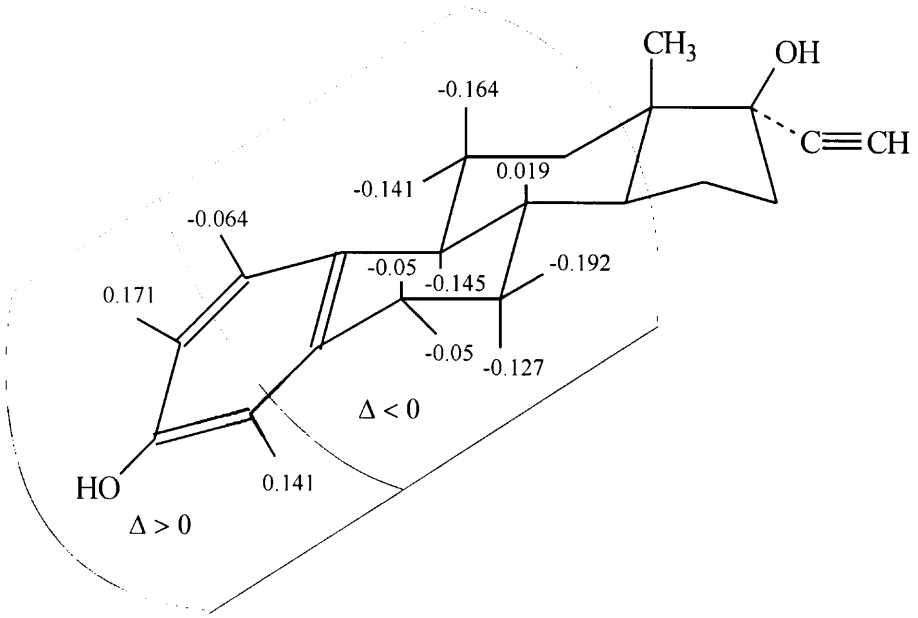

Figure 5.17 The Δ values of the ethynyl oestradiol-cyclodextrin complexes.

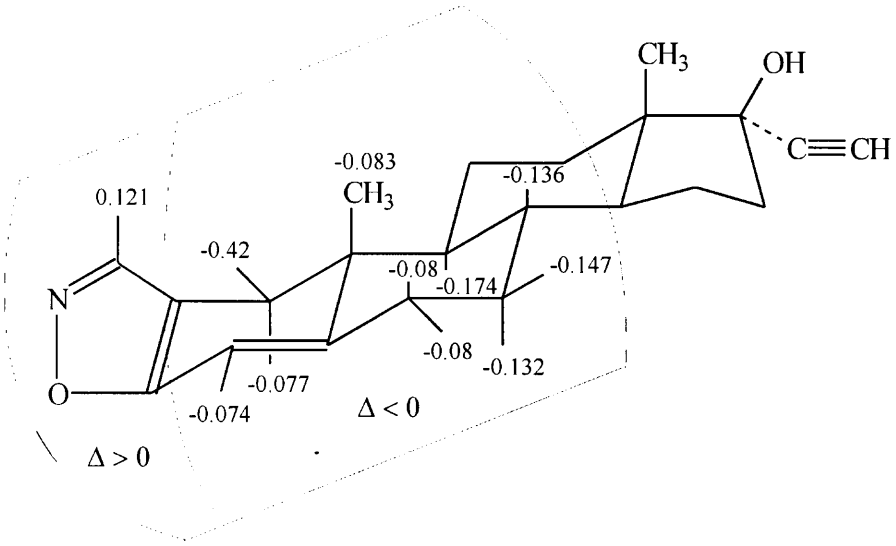

Figure 5.18 The Δ values of the danazol-cyclodextrin complexes.

In all the figures 5.7, 5.10, 5.12 and 5.14 it is apparent that the protons of the ethynyl oestradiol and danazol which are found in the negative Δ regions (see figs 5.17 and 5.18) are either included into the cyclodextrin cavity or they are in the immediate vicinity of either one of the rims of the cyclodextrin cavity. Since the radius of the γ-cyclodextrin cavity is larger than the radius of the β-cyclodextrin cavity, the protons of ethynyl oestradiol and danazol which are part of the negative Δ region will experience a decrease in proximity to the walls of the cavity when going from the β- to the γ-cyclodextrin complexed state. This decrease in proximity to the walls of the

cavity is the most likely cause for all the negative Δ values in the negative Δ regions depicted in figures 5.17 and 5.18.

There are two changes in the chemical environment which can account for the positive Δ regions at the ends of the A-ring of ethynyl oestradiol and danazol illustrated in figures 5.17 and 5.18. The possibility that the positive Δ regions are caused by a decrease in proximity of the ethynyl oestradiol protons 2-H and 4-H and the danazol proton 22-H to the hydroxyl groups of the 1°-OH rim is apparent from a comparison of fig 5.7 with fig 5.10 and fig 5.12 with fig 5.14. The fact that the γ-cyclodextrin cavity has a larger radius than β-cyclodextrin accounts for there being a decrease in proximity to the hydroxyl groups situated on the 1°-OH rim. From an inspection of the molecular models illustrated in figures 5.10 and 5.14, the protons 2-H and 4-H of ethynyl oestradiol and proton 22-H of danazol, which all have positive Δ values, are all close to the γ-cyclodextrin proton 6's. Another likely cause for the observed positive Δ values found in figures 5.17 and 5.18 may involve the cyclodextrin proton 6's. The possibility exists that sterically induced polarisations[45] or the change in the extent of van der Waals contacts41 from the cyclodextrin proton 6's to the steroid protons in the positive Δ regions also contribute to their positive CIS values.

5.4 Conclusion

The NOE percentages proved that two modes of complexation exist in solution, one where the A-ring and one where the D-ring of the steroid is complexed to the cavity of the cyclodextrin molecule. All the illustrated molecular models in this chapter consist of only one steroid and one cyclodextrin molecule. These illustrated complexes therefore all have 1:1 stoichiometries and are binary complexes. A binary complex is a complex which consists of two molecular units, a complex with one steroid and one cyclodextrin unit. Unfortunately, the NOE's cannot determine whether these effects originate from binary or from ternary complexes. A ternary complex is defined as a complex which has three molecular units. The most likely ternary complexes which will account for the NOE percentages are those which consist of one steroid and two cyclodextrin units. In other words, they will be those complexes with 1:2 stoichiometries where the one cyclodextrin caps the A-ring and the other cyclodextrin caps the D-ring of the steroid. It is still

possible to predict the most likely types of complex which are responsible for the NOE percentages, whether they be binary or ternary complexes. These predictions are based on the following assumption: the greater the degree of exposure of the steroid to the aqueous environment when complexed, the less likely this mode of complexation will exist in an aqueous environment.

5.4.1 Cyproterone acetate-cyclodextrin complexes

The binary 1:1 complexes of cyproterone acetate with β-cyclodextrin as illustrated in figures 5.4 and 5.5 are probably water insoluble since a large portion of the water insoluble cyproterone acetate will still be in contact with the aqueous environment. However, β-cyclodextrin does increase the solubility of cyproterone acetate. The most likely mode of complexation which will be water soluble will be the mode where the A-ring of cyproterone acetate is complexed to the β-cyclodextrin cavity as depicted in figure 5.2. This mode will allow a larger portion of the cyproterone acetate to be immersed into the cavity. Less of the water insoluble cyproterone acetate will be exposed to the aqueous environment compared to the mode of complexation illustrated in figures 5.4 and 5.5. It is postulated that the mode of complexation depicted in figure 5.2, which is a binary complex with a 1:1 stoichiometry, is therefore the solubilising step. It is unlikely that the binary complexes illustrated in figures 5.4 and 5.5 can exist in solution. The NOE percentages which are in support of these modes of complexation must still be accounted for. It is therefore deduced that these NOE percentages are caused by ternary complexes which have guest:host stoichiometries of 1:2. It is expected that there will be two types of ternary complexes present in solution. These ternary complexes are the result of the binary complexes, depicted in figure 5.2 which are already present in solution, that are further capped at the exposed D-ring end of the cyptoterone acetate by cyclodextrins. This second complexation will cause two types of ternary complexes to be present in solution. Both types will have the A-ring cyproterone acetate complexed as shown in figure 5.2, the D-ring of cyproterone acetate will be complexed as depicted in figure 5.4 in one of the ternary complexes and the other ternary complex will have its D-ring of cyproterone acetate complexed as depicted in figure 5.5. In conclusion, it is possible that the different cyproterone acetate-β-cyclodextrin complexes co-exist in the form of binary and ternary complexes in solution.

The previous deductions are also applicable to the cyproterone acetate-γ-cyclodextrin complexes. The soluble binary complexes of cyproterone acetate-γ-cyclodextrin are expected to be those where the A-ring of cyproterone acetate is complexed to the cavity as depicted in figure 5.3. The soluble ternary complexes are obtained from a second capping either at the exposed acetate or methyl ketone group of the already complexed cyproterone acetate.

The NOE percentages could be used to unambiguously prove that the A-ring of cyproterone acetate has a deeper insertion into the γ-cyclodextrin cavity then the β-cyclodextrin (see 5.2.1 and 5.2.2). This deeper insertion of the guest molecule will increase the opportunity for van der Waals contacts which can lead to improved stability of the complex. The deeper insertion of cyproterone acetate into the cavity of γ-cyclodextrin relative to β-cyclodextrin occurs alongside an increase in the solubilising capacity of γ-cyclodextrin relative to β-cyclodextrin (see table 4.17). It is postulated that the increased solubilising capacity of γ-cyclodextrin is attributed to the increase in the depth of insertion of cyproterone acetate. It can also be said that the poorer solubilising capacity of β-cyclodextrin for cyproterone acetate can be attributed to the partial inclusion of the A-ring of cyproterone acetate into the cavity of β-cyclodextrin.

5.4.2 Ethynyl oestradiol- and danazol-cyclodextrin complexes

The ethynyl oestradiol-β-cyclodextrin complex depicted in figure 5.7 is a 1:1 binary complex. A large portion of the water insoluble ethynyl oestradiol is immersed into the β-cyclodextrin cavity therefore this complex is expected to exist as a water-soluble binary complex. It is debatable whether the binary ethynyl oestradiol-β-cyclodextrin complex depicted in figure 5.9, which has the ethynyl group complexed to the cavity, will be water soluble. For this binary complex a large portion of the water insoluble ethynyl oestradiol is exposed to the aqueous environment. Furthermore, it is not certain how favourably the exposed hydrophilic hydroxyl situated on the A-ring of ethynyl oestradiol will influence the water solubility of this binary complex. However, the NOE percentages of the ethynyl proton of ethynyl oestradiol to the cavity protons of β-cyclodextrin must still be accounted for. A possible inclusion geometry which can exist in solution which might better account for these NOE percentages will be a ternary complex

where the A-ring of ethynyl oestradiol is included as depicted in figure 5.7 and the D-ring is complexed as depicted in figure 5.9. Such a ternary complex is most likely to arise from an initial solubilising step which is the formation of the complex where the A-ring of ethynyl oestradiol is complexed to the cavity (see fig 5.7). Once this binary complex (depicted in fig 5.7) is in solution the ethynyl group situated on the D-ring of the ethynyl oestradiol is free to further complex with another β-cyclodextrin present in solution. Further evidence for the formation of a ternary complex is the isolation of the poorly water soluble ethynyl oestradiol-β-cyclodextrin complex with a stoichiometry of 1:2 (see 4.2.3).

Two binary complexes can be proposed which will be able to account for the NOE percentages of danazol-β-cyclodextrin. These binary complexes have inclusion geometries where the A-ring and the D-ring are included into the cavity as represented by figures 5.14 and 5.8, respectively. The mode of complexation where the D-ring is complexed is less likely since the large exposed region of the water insoluble danazol will be expected to contribute to the hydrophobic properties of the danazol-β-cyclodextrin complex and therefore make it less likely that this binary complex can remain soluble in an aqueous environment. A ternary complex where the A-ring and D-ring of danazol are both capped by β-cyclodextrin will better explain the NOE percentages of the ethynyl proton of danazol to the β-cyclodextrin cavity protons.

The same conclusions made concerning the complexes responsible for the NOE percentages of the ethynyl oestradiol- and danazol-β-cyclodextrin complexes can be expected for the ethynyl oestradiol- and danazol γ-cyclodextrin complexes. In solution both binary and ternary complexes exist for the ethynyl oestradiol- and danazol-γ-cyclodextrin complexes. The most likely binary complex is where the A-ring of each of these two steroids is complexed to the γ-cyclodextrin cavity as depicted in figures 5.10 and 5.14. The binary complex where the ethynyl group is complexed to the γ-cyclodextrin cavity, if it exists in solution, will be in minor concentration. The ternary complex will have the inclusion geometry where both ends of each of the two steroids are capped by γ-cyclodextrin.

The ethynyl oestradiol-β-cyclodextrin complex is a poorly water soluble complex which was isolated. The danazol-β-cyclodextrin complex, on the other hand, was found to be a water

soluble complex. The ethynyl oestradiol-γ-cyclodextrin complex is water soluble but the danazol-γ-cyclodextrin complex was water insoluble. Ethynyl oestradiol and danazol are similar molecules in the respect that they have identical D-rings and both A-rings have aromatic properties. The ethynyl oestradiol has the aromatic phenyl for an A-ring, and danazol has the aromatic imidazole group attached to its A-ring. However, the structural differences between these two steroids is that ethynyl oestradiol lacks a CH_3-19 methyl group and from a consideration of the dimensions of these steroids, danazol is longer in length as a result of the imidazole substituent. In conclusion, it is an exceptional observation that though there are structural similarities between ethynyl oestradiol and danazol, the differences are enough to cause extreme changes to the water solubilities of the complexes these steroids make with β- and γ-cyclodextrin.

As a result of the bulkiness introduced by the large chlorine atom and methylene bridge to cyproterone acetate, there are many opportunities for van der Waals contacts to be made between cyproterone acetate and the walls of the γ-cyclodextrin cavity. However, from a comparison of figures 5.7 with 5.10 and 5.12 with 5.14 it is apparent that both the A-rings of ethynyl oestradiol and danazol will have less opportunity to make van der Waals contacts in the γ-cyclodextrin complexed state. This loss in van der Waals contacts in the ethynyl oestradiol- and danazol-γ-cyclodextrin complexes will contribute to a loss in stability for these complexes. With this predicted loss in stability, γ-cyclodextrin is still able to solubilise a relatively large amount of ethynyl oestradiol (see 4.2.4) which is proof that there is a high concentration of ethynyl oestradiol-γ-cyclodextrin complex. A high concentration of complex implies that this complex is relatively stable. Though the danazol-γ-cyclodextrin complex is water insoluble, the presence of intermolecular NOE's between the protons of danazol and γ-cyclodextrin of this complex prepared in the mixture of DMSO-d_6 and D_2O is proof that the complex exists in this medium. Yet if there is a loss in van der Waals contacts, which implies that there is a loss in the stability of the complex, why does the danazol-γ-cyclodextrin complex still persist to exist in the mixture? It must be recalled that dimethyl sulphoxide further undermines the stability of cyclodextrin complexes (see 1.4).

To find possible explanations for the stability of the ethynyl oestradiol- and danazol-γ-cyclodextrin complexes it can be expected that since γ-cyclodextrin has a larger cavity than β-cyclodextrin both ethynyl oestradiol and danazol will have a larger degree of rotational freedom when complexed to γ-cyclodextrin compared to when complexed to β-cyclodextrin. The increase in the degree of rotational freedom will make a positive contribution towards the entropy change of complexation which will in turn increase the magnitude of the Gibb's energy of complexation. The stability of the ethynyl oestradiol- and danazol-γ-cyclodextrin complexes can therefore be attributed to the increased mobility these guest molecules have within the cavity. These deductions are based on the observed changes in enthalpy and entropy during the calorimetric study of the complexation of adamantane carboxylate with α-, β- and γ-cyclodextrin (see 1.5.1).[33] Further evidence in support of the stability of the ethynyl oestradiol- and danazol-γ-cyclodextrin complexes can be obtained from the study of the complexes of 1-anilino-8-naphthalenesulphonate (ANS) with β- and γ-cyclodextrin by Schneider et al.[36] From the preferred modes of complexation of the ANS-β-cyclodextrin and ANS-γ-cyclodextrin complexes it was concluded that if a lipophilic molecule has the option of complexing in two or more different orientations it will bind in a manner which favours high mobility of the included portion (see 1.5.2.3). It is therefore a trend present in both the adamantane carboxylate-γ-cyclodextrin and ANS-γ-cyclodextrin complexes that the increased mobility of an included lipophilic guest molecule will contribute towards the stability of the host-guest inclusion complex.

It can be said that the van der Waals forces between the atoms of host and guest play an important role in the stability of the cyproterone acetate-, ethynyl oestradiol- and danazol-β-cyclodextrin complexes since the smaller cavity radius of β-cyclodextrin will promote van der Waals contacts. These same van der Waals forces will also play a large role in the stability of the cyproterone acetate-γ-cyclodextrin complex since the bulkiness present on cyproterone acetate caused by the large chlorine atom and the atoms of the methylene bridge promote the opportunity of van der Waals contacts between the atoms of cyproterone acetate and the cavity of γ-cyclodextrin. It is apparent that van der Waals forces cannot play as large a role to the stability of the ethynyl oestradiol- and danazol-γ-cyclodextrin complexes. The larger radius of γ-cyclodextrin minimises the opportunity for van der Waals contacts to be made between the included guest atoms and the atoms within the γ-cyclodextrin cavity. Other factors such as the

increased mobility of the steroid molecule within the cavity of γ-cyclodextrin contribute to the stability of these steroid-γ-cyclodextrin complexes.

Although a snug fit will create better opportunities for van der Waals contacts which should therefore contribute towards the stability of a complex, the contribution which the mobility of an included guest molecule can make towards the stability of a complex should not be ignored when trying to predict the stability of a steroid-γ-cyclodextrin complex.

5.5 Future prospects

The success of detecting the intermolecular NOE's for the water insoluble danazol-γ-cyclodextrin complex, when this complex was prepared in a mixture of DMSO-d_6 and D_2O allowed the inclusion geometry of this complex to be deduced from the derived NOE percentages. The possibility exists that the inclusion geometries of other water-insoluble complexes, which could not be determined due to the inability to observe the proton resonances of the complex, might now be obtained if these complexes are prepared in a mixture of DMSO-d_6 and D_2O.

It is predicted that the magnitude of the entropy change of complexation of the ethynyl oestradiol-γ-cyclodextrin complex (TΔS) will be greater than the magnitude of TΔS for the ethynyl oestradiol-β-cyclodextrin complex due to the increased mobility the ethynyl oestradiol has within the cavity of γ-cyclodextrin. The same changes in the magnitudes of the TΔS values that are expected for the ethynyl oestradiol-β- and ethynyl oestradiol-γ-cyclodextrin complexes can be expected for the danazol-β- and danazol-γ-cyclodextrin complexes. These predictions are based on the TΔS values of the adamantane carboxylate-γ-cyclodextrin and adamantane carboxylate-β-cyclodextrin complexes of 25.1kJ.mol^{-1} and 4.3kJ.mol^{-1}, respectively which were attributed to the increased mobility the adamantane carboxylate has when complexed to γ-cyclodextrin.[33]

These statements are only speculative since the contributions that other factors might have towards the changes in enthalpy and entropy such as the displacement of water from the cavity

are not taken into account. However, these predictions might provide a frame of reference which can be used to explain the causes for the experimentally determined changes in enthalpy and entropy of these steroid-cyclodextrin complexes. This process will then lead to a further understanding of the mechanism of complexation. It will be beneficial to implement a calorimetric study on the steroid-cyclodextrin complexes to possibly verify the predictions.

If further inclusion geometries of other steroid-β- and γ-cyclodextrin complexes are obtained from the use of NOE percentages, the corresponding Δ values can be recorded into a database. It is expected that if the database contains enough examples, it should be able to relate trends in the Δ values to specific types of inclusion geometries. This will eventually enable the inclusion geometries of steroid-β- and γ-cyclodextrin complexes to be determined from a consideration of the Δ values only. The use of the NOE percentages to determine the inclusion geometry will therefore not be critical. For steroid-β- and γ-cyclodextrin complexes that have low concentrations any observed intermolecular NOE crosspeaks will have poor signal to noise ratios. However, in most of these instances the chemical shifts of the protons of the complexed steroid molecule can be determined. In the cases where the intermolecular NOE's of steroid-cyclodextrin complexes cannot be obtained, it will be advantageous to be able to use the database which relates Δ values to inclusion geometries to afford the inclusion geometries of these poorly soluble steroid-cyclodextrin complexes.

6 Experimental

6.1 Materials

The β- and γ-cyclodextrins as well as the steroids, cyproterone acetate, ethynyl oestradiol and danazol were a gift from South African Druggists (Pty)Ltd. Deuterated chloroform ($CDCl_3$) 99.8%, deuterium oxide (D_2O) 99.8% and hexadeuterio-dimethylsulphoxide (DMSO-d_6) 99.8% were from MERCK (Uvasol®). The β- and γ-cyclodextrins were both lyophilised four times in 99.8% D_2O. The steroids cyproterone acetate, ethynyl oestradiol and danazol were recrystallised from $CHCl_3$. All other materials and solvents were of analytical reagent grade.

6.2 Sample preparation

6.2.1 The preparation of the steroid samples in $CDCl_3$

A weighed amount of 8.0mg of each steroid (cyproterone acetate, ethynyl oestradiol and danazol) was dissolved in 0.5ml $CDCl_3$. The $CDCl_3$ solutions were then degassed by five freeze-pump thaw cycles. These samples were used to record the following NMR experiments to aid in the complete assignment of the steroid proton resonances: 1-D ^1H NMR, 1-D ^{13}C NMR, HMQC, HMBC if required, phase sensitive DQF-COSY and 2-D ROESY.

6.2.2 The preparation of the steroid-cyclodextrin complexes using the kneading method

1:1 steroid:cyclodextrin mole ratios were placed in a mortar and pestle and then kneaded by hand. Whilst kneading, a few drops of D_2O were added to the mixture of steroid and cyclodextrin to maintain a paste. After two hours of kneading, the paste was left to dry at room temperature resulting in the final dried steroid-cyclodextrin complex. The complexes prepared together with the amounts of steroid and cyclodextrin used are given in table 6.1.

Table 6.1 Complexes prepared by the kneading method		
steroid-cyclodextrin complexes	steroid/mg	cyclodextrin /mg
cyproterone acetate-β-cyclodextrin	75.0	200.0
cyproterone acetate-γ-cyclodextrin	65.0	200.0
ethynyl oestradiol-β-cyclodextrin	58.0	200.0
ethynyl oestradiol-γ-cyclodextrin	50.0	200.0
danazol-β-cyclodextrin	60.0	200.0
danazol-γ-cyclodextrin	52.0	200.0

15.0mg of each of the dried steroid-cyclodextrin complexes was added to 0.5ml D_2O and the ^1H NMR spectrum of this sample recorded. The molecular ratios were determined from the integraions of the steroid and cyclodextrin resonances. The complexes prepared by the kneading method were also used as material for the isolation procedure (see 6.2.2.1).

6.2.2.1 The isolation procedure for obtaining a water-insoluble complex

The isolation procedure adapted from the procedure of Djedaïni et al[39] consisted of four cycles. Each cycle comprised of addition of solvent, sonication, centrifugation and removal of supernatant, in that order. The first cycle began with the addition of 10ml of deionised water to 200mg of dried steroid-cyclodextrin complex prepared by the kneading method. This mixture was sonicated for two minutes only resulting in the formation of a suspension. This dispersed mixture was centrifuged for a maximum of 30 minutes until the cloudiness disappeared and a pellet formed. The supernatant was discarded after centrifugation to leave only the pellet behind. A second cycle on the isolated pellet used another 10ml of deionised water as solvent. The third and fourth cycles both used 10ml of diethyl ether as solvent.

If a pellet was isolated after the final cycle, the ^1H NMR spectrum of this pellet dissolved in 0.5ml DMSO-d_6 was recorded. The steroid and cyclodextrin resonances present in this spectrum

were integrated and the steroid:cyclodextrin molecular ratio determined.

6.2.3 The preparation of the steroid-cyclodextrin complexes using sonication

The following steps were used to prepare the steroid-β-cyclodextrin complexes in D_2O.

1. A $CHCl_3$ solution of 2.00mg.ml^{-1} for each steroid (cyproterone acetate, ethynyl oestradiol and danazol) was prepared.
2. 500µl of the micropipetted $CHCl_3$ solution to an NMR tube was allowed to evaporate slowly under a stream of nitrogen leaving 1.00mg of dried steroid in the NMR tube.
3. 15mg of lyophilised β-cyclodextrin was dissolved in 0.5ml D_2O and added to the NMR tube containing the dried steroid.
4. The NMR tube containing both steroid and cyclodextrin was then sonicated for 6 hours.

The procedure for the preparation of the steroid-γ-cyclodextrin complexes in D_2O was identical to the preparation of the steroid-β-cyclodextrin except that in step 3 an amount of 20.0mg of lyophilised γ-cyclodextrin was used.

Steroid-β-cyclodextrin complexes were also prepared in solutions of DMSO-d_6 and D_2O. These solutions were prepared by micropipetting volumes of 100µl, 200µl, 300µl, 400µl and 500µl of DMSO-d_6, D_2O was then micropipetted to each of the dimethyl sulphoxide solutions to a final volume of 600µl. 15.0mg of β-cyclodextrin was dissolved in each solution. These final solutions were placed in an NMR tube containing 1.00mg of dried steroid.

The preparation of the steroid-γ-cyclodextrin complexes in mixtures of DMSO-d_6 and D_2O was identical to the procedure used to prepare the steroid-β-cyclodextrin complexes with the exception being that 20.0mg of lyophilised γ-cyclodextrin was added to each of the five different solutions.

6.3 Nuclear Magnetic Resonance Experiments

The standard accumulation and processing parameters of the NMR experiments of this study are as follows:

All the one- and two dimensional NMR expeiments were run on a Bruker ARX-500 spectrometer interfaced to an ASPECT X-32 computer and a BVT-1000E variable temperature control unit. The NMR spectrometer was operating at 500.13MHz when recording ^{1}H NMR spectra and 125.76MHz when recording ^{13}C NMR spectra. All the 1-D and 2-D NMR expriments were recorded at 303.0 K.

The 1-D ^{1}H NMR experiment used a 90° flip angle (9.1μs) and a relaxation delay of 1.5 s. The spectra were collected using 32 K real data points and a spectral width of 5000 Hz. Gaussian multiplications were applied to the accumulated FID's. Digital integrations of the Fourier transformed FID were performed after polynomial baseline correction. The chemical shifts (δ) were measured relative to external TMS reference at 0.000 ppm.

The 1-D proton noise decoupled ^{13}C NMR experiment used a 90° flip angle (11.8μs) and a relaxation delay of 2 s. The spectra were collected using 64 K real data points and a spectral width of 30 kHz. Exponential multiplication were applied to the accumulated FID's prior to Fourier transformation.

The pulse sequence of Bax, Griffey and Hawkins[77] was used to record the Heteronuclear Multiple-Quantum Correlation (HMQC) experiment.The experiment was recorded in the phase senstive mode using Time Proportional Phase Increments (TPPI)[78] and with decoupling during the acquisition period. A value of 145 Hz for $^{1}J_{C,H}$ was used to calculate the delays in the pulse sequence. 2K data points were collected for t_2 (^{1}H) and 512 points for t_1 (^{13}C). A spectral width of 5000 Hz (10 ppm) for F2 was used which gave a digital resolution of 2.5 Hz (accuracy δ_H ±0.005 ppm). A spectral width of 30 000Hz (240 ppm) for F1 gave a digital resolution of 60 Hz (accuracy δ_C ±0.48 ppm). 64 scans were collected for each of the 512 experiments with a relaxation delay of 1.5 s. FID's were multiplied by a squared sine window function in both the

F1 and F2 dimensions and zero-filled to 1K datapoints in the t_1 dimension prior to Fourier transformation.

The pulse sequence of Bax and Summers[79] was used to record the Heteronuclear Multiple-Bond Correlation (HMBC) experiment.The experiment was recorded in the magnitude mode and no decoupling was used in the data acquisition phase. The pulse sequence contains a low-pass J-filter to suppress one bond correlation.[79,80] A value of 145 Hz for $^1J_{C,H}$ was used to calculate the delays in the pulse sequence with a delay of 50.0 ms to allow for the evolution of long range couplings. 2K data points were collected for t_2 (^1H) and 256 points for t_1 (^{13}C). A spectral width of 5000 Hz for F2 was used which gave a digital resolution of 2.5 Hz (accuracy δ_H ±0.005 ppm). A spectral width of 30 000 Hz (240 ppm) for F1 gave a digital resolution of 120 Hz (accuracy δ_C ±0.96 ppm).32 scans were collected for each of the 256 experiments with a relaxation delay of 1.5 s. FID's were multiplied by a sine window function in both F1 and F2 dimensions and zero-filled to 1K datapoints in the t_1 dimension prior to Fourier transformation.

The double quantum filtered (DQF) COSY experiment was recorded using the modified pulse sequence of Derome and Williamson.[64] The experiment was recorded in the phase sensitive mode using TPPI. 2K data points were collected for t_2 (acquisition time 0.20 s), and 512 points for t_1. Spectral widths of 5000 Hz were used in both dimensions which gave a digital resolution of 2.5 Hz in F2 and 10.0 Hz in F1. 32 scans for each of the 512 experiments were collected with a relaxation delay of 1.5 s was used. FID's were multiplied by a squared sine window function in both the F1 and F2 dimensions and zero-filled to 1K datapoints in the t_1 dimension prior to Fourier transformation. Additive phase correction in F1 and F2 with automatic baseline correction in both dimensions was carried out on the spectra using standard Bruker software.

The 2-D ROESY experiment was recorded using the pulse sequence of Bax and Davis.[59] The experiment was recorded in the phase sensitive mode using TPPI and a mixing time of 250ms was used. A continuous wave spin lock with an rf field strength of 2 kHZ with a carrier frequency positioned at ~4.0 ppm was used for all 2-D ROESY experiments. 2K data points were collected for t_2 (acquisition time 0.20 s), and 512 points for t_1. Spectral widths of 5000 Hz were used in both dimensions. 32 scans for each of the 512 experiments were collected. When required

to improve the signal to noise ratio of the NOE crosspeaks the 2-D ROESY experiment was collected using 2K data points for t_2 and 256 points for t_1 where each of the 256 experiments were accumulated with 128 scans. All 2-D ROESY experiments were recorded with a relaxation delay of 1.5 s. FID's were multiplied by a squared sine window function in both the F1 and F2 dimensions and zero-filled to 1K datapoints in the t_1 dimension prior to Fourier transformation. Additive phase correction followed by automatic baseline correction in the F1 and F2 dimensions were carried out using standard Bruker software before the crosspeaks were integrated.

6.4 The Molecular Modelling methods

All calculations were performed using the molecular modelling software SYBYL version 6.2 (Tripos Associates, St Louis, MO, USA) on an INDIGO 2 Silicon Graphics workstation. The standard Tripos force field[81] was used in all energy calculations; the potential functions included energies arising from bond stretching, angle bending, out-of-plane bending, torsional deviations, van der Waals interactions, hydrogen bonding and electrostatic interactions. For the electrostatic interactions the charges were calculated using the method of Gasteiger and Marsili[82]. Energy minimisatons were executed with MAXIMIN2. The Powell technique of the MAXIMIN2 program was used for the minimisations. The minimisations were terminated when the energy difference between iterations was less than 0.05 kcal/mol.

The steroids cyproterone acetate, ethynyl oestradiol and danazol were built using the Sketch option of SYBYL followed by energy minimisation. The Sketch option allowed three-dimensional interaction whilst building the chemical structure of the steroid. Prior to energy minimisation the D-rings of the steroids were sketched to resemble the puckered envelope conformation and where applicable the steroid rings A, B and C were sketched to resemble the chair conformation.

α 1,4-linked D-glucopyranose residues were joined to form a linear chain of 7 or 8 residues in the case of building β- or γ-cyclodextrin respectively, with the use of the Build Bioploymer option in SYBYL 6.2. The C5-O1 and O1-C1 bonds were then rotated until the linear chain resembled a cone. When rotating these bonds care was taken to ensure that the 1°-OH groups of

the residues were all pointing in one direction whilst the 2°-OH groups were all pointing in the opposite direction. Once a structure which resembled a cone had been obtained the two terminal residues were then also α 1,4 linked. At this stage the cone was not perfectly symmetrical. The cone then underwent an energy minimisation with the constraint that all the torsion angles defined by C4-C5-C1'-O5' are restricted to 0.0° with a force constant of 25kcal.mol^{-1}.degree^{-1}. After the energy minimisation a cone with C_n (n = 7 or 8) symmetry was obtained. The resulting structure was further used as a starting point for the subsequent final optimisation without any constraints. For both the molecular models of β- and γ-cyclodextrin the symmetry of the cone was preserved after the second minimisation. The molecular model of β-cyclodextrin which was obtained from this procedure can be clearly seen in figures 1.2 and 1.3.

The molecular models illustrated throughout chapter 5 were obtained by manually docking the steroid molecule into the cyclodextrin molecule in accordance to the NOE percentages. This docking was then followed by the energy minimisation procedure with the constraint that the coordinates of all the cyclodextrin atoms had to remain stationary. Only the steroid atoms were mobile during the minimisation of the steroid-cyclodextrin complex.

References

1. K. Freudenburg, M. Meyer-Delius, *Ber. Dtsch. Chem. Ges.* 71 (1938) 1596.
2. F. Cramer, *Einschlussverbindungen*, Springer, Berlin (1954).
3. F. Cramer, *Cyclodextrins and their Industrial Uses* (edited by D. Duchêne) Editions de Santé, Paris (1987) 11.
4. A. Villiers, *C.R. Acad. Sci.* 112 (1891) 536.
5. F. Schardinger, *Wien. Klin. Wochenschr.* 17 (1904) 207.
6. K. Freudenburg, F. Cramer, *Z. Naturforsch.* B3 (1948) 464.
7. F. Cramer, F.M. Henglein, *Chem. Ber.* 90 (1957) 2561.
8. a) F. Cramer, *Chem. Ber.* 86 (1953) 1576.
   b) F, Cramer, *Chem. Ber.* 92 (1959) 378.
9. C.J. Pedersen, *J. Am. Chem. Soc.* 89 (1967) 7017.
10. F. Diederich, *Angew. Chem. Int. Ed. Engl.* 27 (1988) 362.
11. W. Saenger, *Angew. Chem. Int. Ed. Engl.* 19 (1980) 344.
12. M. Ennis, W. Lorenz, W. Gerland, *Ag. Actions*, 18 (1986) 235.
13. M. Ennis, W. Lorenz, B. Kapp, L. Luben, A. Schmal, *Ag. Actions*, 16 (1985) 265.
14. W. Davis, C. Washington, P. West, L. Illum, G. Liversidye, L. Sternson, R. Kirsch *Ann. N.Y. Acad. Sci.* 507 (1987) 75.
15. J. Pitha, J. Milecki, H. Fales, L. Panell, K. Uekama, *Int. J. Pharm.* 29 (1986) 73.
16. D. Duchêne, D. Wouessidjewe, *J. Coord. Chem.* 27 (1992) 223.
17. G. Wenz, *Angew. Chem. Int. Ed. Engl.* 33 (1994) 803.
18. P.C. Manor, W. Saenger, *J. Am. Chem. Soc.* 96 (1974) 3630.
19. K. Lindner, W. Saenger, *Angew. Chem. Int. Ed. Engl.* 17 (1978) 694.
20. K. Harata, *Chem. Lett*, (1984) 641.
21. M.E. Amato, G.C. Pappalardo, *Magn. Res. Chem.* 31 (1993) 455
22. H-J. Schneider, *Angew. Chem. Int. Ed. Engl.* 30 (1991) 1417.
23. Y. Inoue, *Ann. Rep. NMR Spec.* 27 (1993) 59
24. R.L. VanEtten, J.F. Sebastian, G.A. Clowes, M.L. Bender, *J. Am. Chem. Soc.* 89 (1967) 3242
25. M. Komiyama, M.L. Bender, *J. Chem. Phys.* 100 (1978) 2259
26. F. Cramer, W. Kampe, *J. Am. Chem. Soc.* 87 (1965) 1115

27. F. Cramer, *Chem. Ber.* 84 (1951) 851.

28. E. Albers, B.W. Müller, *J. Pharm. Sci.* 81 no.8 (1992) 756.

29. B. Siegel, R. Breslow, *J. Am. Chem. Soc.* 97 (1975) 6869.

30. K.A. Connors, M.J. Mulski, A. Paulson, *J. Org. Chem.* 57 (1992) 756.

31. N. Yoshida, A. Seiyama, M. Fujimoto, *J. Phys. Chem.* 94 (1990) 4246.

32. Y. Matsui, T. Nishioka, T. Fujita, *Part I: Top. Curr. Chem.* 128 (1985) 61.

33. W.C. Cromwell. K. Byström, M.R. Eftink, *J. Phys. Chem.* 89 (1985) 326.

34. K. Lindner, W. Saenger, *Carbohydr. Res.* 99 (1982) 103.

35. a) L. Stryer, *Biochemistry 3rd edition*
W.H. Freeman and Company (New York, 1988) 186.
b) A.C. Coxon, W.D. Curtis, D.A. Laidler, J.F. Stoddart,
Carbohydrates, Nucleosides, Nucleotides 6 (1979) 167.

36. H-J. Schneider, T. Blatter, S. Simova, *J. Am. Chem. Soc.* 113 (1991) 1996.

37. H. Friebolin, *Basic One- and Two-Dimensional NMR Spectroscopy*,
VCH Publishers (1991).

38. G. Fronza, A. Mele, E. Redenti, P. Ventura, *J. Pharm. Sci.* 81 (1992) 1162.

39. F. Djedaïni, B. Perly, *J. Pharm. Sci.* 80 (1991) 1157.

40. F. Djedaïni. S.Z. Lin. B. Perly, *J. Pharm. Sci.* 79 (1990) 643.

41. A. Ganza-Gonzalez, J.L. Vila-Jato, S. Anguiano-Igea, F.J. Otero-Espinar,
J. Blanco-Méndez, *Int. J. Pharm.* 106 (1994) 179.

42. H.A. Benesi, J.H. Hildebrand, *J. Am. Chem. Soc.* 71 (1949) 2703.

43. R.J. Begeron, M.A. Channing, K.A. McGovern, *J. Am. Chem. Soc.* 100 (1978) 2878

44. R.J. Bergeron, M.A. Channing, G.J. Gibeily, D.M. Pillor
J. Am. Chem. Soc. 99 (1977) 5146

45. H-J. Schneider, G. Schmidt, *J. Chem. Soc. Perkin Trans. II* (1985) 2027

46. A.D. Buckingham, *Can. J. Chem.* 38 (1960) 300

47. H-J. Schneider, E.F. Weigand, *J. Am. Chem. Soc.* 99 (1977) 8362

48. H-J. Schneider, U. Buchheit, N. Becker, G. Schmidt, U. Siehl,
J. Am. Chem. Soc. 107 (1985) 7027

49. N. Mulinacci, F. Melani, G. Mazzi, F.F. Vincieri, *Int. J. Pharm.* 90 (1993) 35

50. M.L. Bender, M. Komiyama, *Cyclodextrin Chemistry*, Springer publishers, Berlin (1977).

51. H.M. Cabral Marques, J. Hadgraf, I.W. Kellaway, W.J. Pugh
Int. J. Pharm. 63 (1990) 267.

52. All calculations were accomplished using the Discover II program version 2.7.0 and Insight II program version 2.0.0 available from Biosym Technologies, 10065 Barnes Canyon Road San Diego Ca. 92121.

53. See Biosym Technologies Theory manual for a further description of the CVFF force field used to calculate energies.

54. SYBYL Theory Manual. TRIPOS Associates. Inc.,
1699 S. Hanley Road, St. Louis, Missouri 63144-2913.

55. H-J. Schneider, R. Kramer, I. Theis, M. Zhou,
J. Chem. Soc. Chem. Comm. (1990) 276.

56. *The Merck Index 11th edition* (1989), Merck and Co., Inc. Rathway, N.J. U.S.A.

57. R.R. Ernst, W.A. Anderson, *Rev. Sci. Instrum.* 37 (1966) 93.

58. H. Kessler, M. Gerhke, C. Griesinger, *Angew. Chem. Int. Ed. Engl.* 27 (1988) 490.

59. A. Bax, D.G. Davis, *J. Magn. Res.* 63 (1985) 207.

60. H. Desvaux, P. Berthault, N. Birlirakis, M. Goldman M. Piotto
J. Magn. Res. A 113 (1995) 47.

61. L.D. Hall, J.K.M. Sanders, *J. Org. Chem.* 46 (1981) 1132.

62. W.R. Croasmun, R.M.K. Carlson, *Two-Dimensional NMR Spectroscopy-Applications for Chemists and Biochemists 2nd Edition* (1994) VCH Publishers.

63. W.R. Croasmun, R.M.K. Carlson, *Two-Dimensional NMR Spectroscopy-Applications for Chemists and Biochemists:*
Volume 9 Methods in Stereochemical Analysis (1987) VCH Publishers.

64. A.Derome, M. Williamson, *J. Magn. Res.* 88 (1990) 177.

65. R. Laaikainen, *PERCH Peak Research-An integrated software for analysis of NMR spectra on PC*, Kuopio University NMR Research Group, Department of Chemistry University of Kuopio, P.O. Box 1627
S F 70211 Kuopio, Finland.

66. R. Laatikainen, *J. Magn. Res.* 92 (1991) 1.

67. M. Karplus, *J. Am. Chem. Soc.* 85 (1963) 2870.

68. C. Altona, R. Francke, R. De Haan, J.H. Ippel, G.J. Daalmans, A.J.A. Westra Hoekzema J. Van Wijk, *Magn. Res. Chem.* 32 (1994) 670.

69. M.W. Barrett, R.D. Furrant, D.W. Kirk, *J. Chem. Soc. Perkin II* (1982) 105.

70. L.D. Hall, J.K.M. Sanders, *J. Am. Chem. Soc.* 102 (1980) 5703.

71. A.G.J. Sedee, G.M.J. Beijerbergen van Henegouwen. W. Guijt, C.A.G. Haasnoot, *J. Chem. Soc. Perkin II* (1984) 1755.

72. A.G.J. Sedee, G.M.J. Beijerbergen van Henegouwen. W. Guijt, C.A.G. Haasnoot, *J. Org. Chem.* 50 (1985) 4182.

73. D.N. Kirk, M.W. Barrett, R. Duncan Farrant, J.D. Mersh, J.K.M. Sanders, W.L. Duax, *J. Chem. Soc. Perkin II* (1982) 105.

74. S. Isaacs, R. Berman, Y. Kashman, *J. Nat. Prod.* 54 (1991) 83.

75. J.L. Marshall, *Carbon-Carbon and Carbon-Proton NMR Couplings-Applications to Organic Stereochemistry and Conformational Analysis: Volume 2 Methods in Stereochemical Analysis* (1983) VCH Publishers.

76. J. Redondo, J. Frigola, A. Torrens, P. Lupón, *Magn. Res. Chem.* 33 (1995) 104.

77. A.D. Bax, R.H. Griffey, B.L. Hawkins, *J. Magn. Res.* 55 (1983) 301.

78. D. Mario, K. Wüthrich, Biochem. Biophys. *Res. Comm.* 113 (1983) 967.

79. A. Bax, M.F. Summers, *J. Am. Chem. Soc.* 108 (1986) 2093.

80. H. Kogler, O.W. Sørensen, G. Bodenhausen, R.R. Ernst, *J. Magn. Reson.* 55 (1983) 157.

81. M.Clark, R.D. Cramer III, N. van Opdenbosch, *J. Comp. Chem.* 10 (1989) 982.

82. J. Gasteiger, M. Marsili, *Tetrahedron* 36 (1980) 3219.